Global Journal of Researches In Engineering

discovering thoughts and inventing future

Volume 10 Issue 4 Version 1.0

ISSN: 0975-5861

14 Revolutions In Engineering World

The Volume 10

Issue 4 Version 1.0

highlights

Contrast and Brightness in Consumer

Design Consideration of a Low

Replacement for Absorbing Material

Zinc Incorporated Hydroxy apatite as Catalysts

Global Journal of Researches in Engineering

Global Journal of Researches in Engineering

Volume 10 Issue 4 (Ver.1.0)

Global Academy of Research and Development

License No.: 42125/022010/1186
Registration No.: 430374

Global Academy of Research and Development

Publisher's correspondence office

Global Journals Inc., Headquarters Corporate Office, United States

Offset Typesetting

Global Journals Inc., City Center Office, United States

Packaging & Continental Dispatching

Global Journals Inc., India

Find a correspondence nodal officer near you

To find nodal officer of your country, please email us at *local@globaljournals.org*

eContacts

Press Inquiries: *press@globaljournals.org*
Investor Inquiries: *investers@globaljournals.org*
Technical Support: *technology@globaljournals.org*
Media & Releases: *media@globaljournals.org*

Pricing (Including by Air Parcel Charges):

For Authors:
22 USD (B/W) & 50 USD (Color)

Yearly Subscription (Personal & Institutional):
200 USD (B/W) & 500 USD (Color)

Editorial Board Members

Dr. Carlos García Pont
Associate Professor of Marketing
IESE Business School, University of Navarra
Doctor of Philosophy (Management),
Massachusetts Institute of Technology (MIT)
Master in Business Administration, IESE,
University of Navarra
Degree in Industrial Engineering,
Universitat Politècnica de Catalunya

Dr. Fotini Labropulu
Mathematics - Luther College
University of Regina
Ph.D., M.Sc. in Mathematics
B.A. (Honors) in Mathematics
University of Windsor

Dr. Lynn Lim
Reader in Business and Marketing
Roehampton University, London
BCom, PGDip, MBA (Distinction), PhD, FHEA

Dr. Mihaly Mezei
ASSOCIATE PROFESSOR
Department of Structural and Chemical Biology
Mount Sinai School of Medical Center
Ph.D., Etvs Lornd University
Postdoctoral Training, New York University

Dr. Pina C. Sanelli
Associate Professor of Public Health
Weill Cornell Medical College

Dr. Miguel Angel Ariño
Professor of Decision Sciences
IESE Business School
Barcelona, Spain (Universidad de Navarra)
CEIBS (China Europe International Business School).
Beijing, Shanghai and Shenzhen
Ph.D. in Mathematics
University of Barcelona
BA in Mathematics (Licenciatura)
University of Barcelona
Philip G. Moscoso
Technology and Operations Management
IESE Business School, University of Navarra
Ph.D in Industrial Engineering and Management, ETH Zurich
M.Sc. in Chemical Engineering, ETH Zurich

Dr. Sanjay Dixit, M.D.
Director, EP Laboratories, Philadelphia VA Medical Center
Cardiovascular Medicine - Cardiac Arrhythmia
Univ of Penn School of Medicine

Dr. Han-Xiang Deng
MD., Ph.D Associate Professor and Research Department
Division of Neuromuscular Medicine
Davee Department of Neurology and Clinical Neurosciences
Northwestern University Feinberg School of Medicine
Associate Attending Radiologist
New York-Presbyterian Hospital
MRI, MRA, CT, and CTA
Neuroradiology and Diagnostic

Radiology
M.D., State University of New York at Buffalo, School of Medicine and Biomedical Sciences

Dr. Roberto Sanchez
Associate Professor
Department of Structural and Chemical Biology Mount Sinai School of Medicine
Ph.D. The Rockefeller University

Dr. Wen-Yih Sun
Professor of Earth and Atmospheric Sciences Purdue University Director National Center for Typhoon and Flooding Research, Taiwan University
Chair Professor Department of Atmospheric Sciences, National Central University, Chung-Li, TaiwanUniversity
Chair Professor Institute of Environmental Engineering, National Chiao Tung University, Hsin-chu, Taiwan.
Ph.D., MS The University of Chicago, Geophysical Sciences
BS National Taiwan University, Atmospheric Sciences
Associate Professor of Radiology

Dr. Michael R. Rudnick
M.D., FACP
Associate Professor of Medicine
Chief, Renal Electrolyte and Hypertension Division (PMC)
Penn Medicine, University of Pennsylvania
Presbyterian Medical Center, Philadelphia
Nephrology and Internal Medicine
Certified by the American Board of Internal Medicine

Dr. Bassey Benjamin Esu
B.Sc. Marketing; MBA Marketing; Ph.D Marketing
Lecturer, Department of Marketing, University of Calabar
Tourism Consultant, Cross River State Tourism Development Department
Co-ordinator , Sustainable Tourism Initiative, Calabar, Nigeria

Dr. Aziz M. Barbar, Ph.D.
IEEE Senior Member
Chairperson, Department of Computer Science
AUST - American University of Science & Technology
Alfred Naccash Avenue – Ashrafieh

Chief Author

Dr. R.K. Dixit (HON.)
M.Sc., Ph.D., FICCT
Chief Author, India
Email: authorind@computerresearch.org

Dean & Editor-in-Chief (HON.)

Vivek Dubey(HON.)
MS (Industrial Engineering),
MS (Mechanical Engineering)
University of Wisconsin
FICCT
Editor-in-Chief, USA
editorusa@computerresearch.org

Sangita Dixit
M.Sc., FICCT
Dean and Publisher, India
deanind@computerresearch.org

Er. Suyog Dixit
BE (HONS. in Computer Science), FICCT
SAP Certified Consultant
Technical Dean, India
Website: www.suyogdixit.com
Email:suyog@suyogdixit.com,
dean@computerresearch.org

Contents of the Volume

From the Chief Author's Desk

We see a drastic momentum everywhere in all fields now a day. Which in turns, say a lot to everyone to excel with all possible way. The need of the hour is to pick the right key at the right time with all extras. Citing the computer versions, any automobile models, infrastructures, etc. It is not the result of any preplanning but the implementations of planning.

With these, we are constantly seeking to establish more formal links with researchers, scientists, engineers, specialists, technical experts, etc., associations, or other entities, particularly those who are active in the field of research, articles, research paper, etc. by inviting them to become affiliated with the Global Journals.

This Global Journal is like a banyan tree whose branches are many and each branch acts like a strong root itself.

Intentions are very clear to do best in all possible way with all care.

Dr. R. K. Dixit
Chief Author
chiefauthor@globaljournals.org

Improvement of Contrast and Brightness in Consumer Video Using Video Processing Chain

K.Srinivasan[1] Lmi Leo Joseph[2]

GJRE Classification (FOR)
GJRE-F 109999

***Abstract*-The goal of this paper is to review the requirements of color and contrast processing in consumer video, and the key aspects of the processing as it relates to content, video algorithms involved, and display-specific processing. The perceptual objective of color and contrast enhancement is to increase vividness and colorfulness of all objects and detailed structures under different lightness conditions. That objective must be met for a variety of content formats and qualities which, in the age of DTV and HDTV have increased dramatically and put increasing pressure on the display processing engine performance.**

Keywords- color enhancement, contrast enhancement, video processing.

I. INTRODUCTION

To review the requirements of color and contrast processing in consumer video we need an understanding of the processing objectives, e.g. color and contrast enhancement, the input source characteristics, e.g. format and content type, and the processing algorithms needed to match the display technology involved. Color and contrast enhancement in consumer video mainly focuses on improving the liveliness and fullness of color, enhancing details and visibility of the content of interest. Taking this one step further, all the enhancements have to be adaptive to variable lighting conditions in the image. Traditionally, color and contrast enhancements have been done using independent modules. Contrast adjustment is related to brightness and gamma settings, while color adjustment depends on lightness (perceptual dependency) and the color space used (chroma leak effect) [13, 12]. These independently interacting adjustments are not always tunable for optimum joint performance. Saturation is the key factor in increasing the colorfulness of an image. However, this feature of an image is tightly knit to its lightness. An increase in lightness often reduces the perceived saturation of an image, while a decrease in lightness often increases the perceived saturation. Hence, to achieve the best results in a video processing algorithm, a joint color, contrast and lightness enhancement is required to obtain visually appealing, high quality enhanced imagery. Proper overall processing of color along the video processing chain must deal with constraints such as chroma sub-sampling, compression artifacts, and color spaces used at the source, in the video algorithms, and in the display technology [2]. Since the final viewing experience is tied to the specific display modality, the enhancement algorithms may also need to drive specific parameters of the display (e.g. color gamut, and backlight level/timing control in LCD). In this paper we start in Section 2 with a discussion of the main characteristics of the input content in terms of standard formats and color space, and then in Section 3 review the components of the video chain that affect color and contrast. In Section 4 we address the effects of display-specific processing methods that are designed to match the color/contrast characteristics of the display. Then, in Section 5 we provide a discussion of critical issues and areas of research for future work.

II. CONSUMER VIDEO CONTENT

DTV standards include 18 formats including 6 HDTV formats. Vertical resolution ranges from 480 to 1080 lines and includes interlaced formats. Horizontal resolution ranges from 640 to 1020 pixels. Frame rates vary from 24 to 120Hz (the color space used in the ITU standards is YCbCr). In the age of internet-connected DTV, processing subSD content (e.g. QCIF) by the video pipe is also required. To make it even more challenging, 240Hz DTV systems with SuperHD resolution have been demonstrated and are expected to hit the market in the coming years. DTV is also compatible with consumer equipment which can output content in RGB format, which is usually converted to YCbCr for processing. Accuracy of color space conversion is guaranteed by standard formulae, but it does not solve the problem of illegal colors
which can be generated during processing. Method such as simple clipping to keep values within the legal range can be applied, but may result in visual artifacts. Mathematically and perceptually sound methods such as gamut mapping are preferable to deal with color processing and conversion to avoid artifacts related to inconsistent processing methods [6]. Digital broadcast content comes in compressed format, which uses chroma sub-sampling. The most common formats are 4:2:0 and 4:2:2 (4:4:4 includes all samples). Moreover, the chroma samples are not always spatially collocated with the luma samples. To meet bandwidth constraints, compression ratios of 100:1 or more are commonly used in HDTV. If we assume that the final picture will be viewed at the maximum resolution on a large display (1080p, 52”TV). The logical expectation on quality is higher for the input formats with higher resolutions and lowest compression. Although it must deal with all use cases, even the best isplay processing engine will exhibit peak performance or only a certain input quality and format range.

About-[1] Miet Engineering Colllege Trichy-07
(e-mail- seenube84@yahoo.co.in)

III. THE VIDEO PROCESSING CHAIN

The consumer video processing engine is typically made f a chain of modules that implement algorithms in three main categories. The categories are corrective processing, onditioning/formatting, and enhancement. Corrective rocessing takes care of reducing analog and digital including compression) noise and artifacts. Conditioning includes scaling, deinterlacing,
and scan rate conversion. Enhancement deals with color, contrast, sharpness, and resolution enhancement. The modules that deal specifically with color include chroma upconversion, i.e. conversion from 4:2:0 to 4:2:2 and 4:4:4 (see Figure 1).

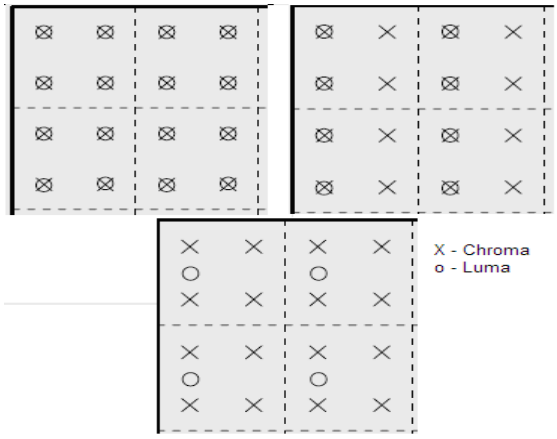

Figure 1. 4:4:4, 4:2:2 and 4:2:0 sampling patterns

If the input is in RGB, color space conversion to YCbCr is also used. Some modules such as skin tone enhancement may work on a different color space and thus require yet another color space conversion from and back to YCbCr. Advanced color and contrast enhancement modules such as the one proposed in [13], are placed towards the end of the video chain, and their performance depends on that of preceding modules starting from the chroma up conversion. Although it is a simple up-scaling applied tothe sub sampling patterns shown in Figure 1, proper chroma up conversion depends on whether the video is interlaced or progressive, and in the case of interlaced whether the pixels are in motion or not. Improper 4:2:0
upconversion of interlaced content (i.e. applying a simple chroma up-scaling filter to the frames) results in a visual artifact known as the chroma bug

Figure 2. Chroma bug example

Based on the theory of low information content in the color components (from the analog TV days), most processing was initially applied only to the luma component (while chroma, up-sampled to 4:2:2 was carried along); it was also used as a way to avoid the 3x increase in bandwidth required to process 3 full color components. As the quality race set off, color processing has become a more relevant subject. Noise reduction and compression artifact reduction in color components have become an active research area [1,3]. It has also become apparent that accurate removal of gamma correction is necessary for proper processing of the 3 components, e.g. R, G, and B. With the advent of high resolution formats, visibility and annoyance of color artifacts on large screen DTVS has called for more advanced algorithms not only for denoising and artifact reduction, but also for up-scaling. With the use of large scaling ratios, for example from subSD to HD, which can enlarge an image 3 to 5 times, other color artifacts related to scaling become apparent. Depending on the scaling method, artifacts such as blur, ringing, jaggies become apparent, and affect all components of the color space; plus scaling may amplify other errors stemming from improper color processing (e.g. edges may be mis aligned in the 3 components, causing color breakdown at sharp edges). The same is true for de-interlacing, where (depending on the approach) the main artifacts are flicker, jaggies and loss of resolution. Picture enhancement, particularly non-linear methods for sharpness enhancement and resolution enhancement (or up-scaling) have become compulsory features, making method such as Color Transient Improvement (CTI), statistical up conversion, and super-resolution well known topics in the consumer video industry [5,10,16]. The challenges of sharpness and resolution enhancement are easy to imagine, if we consider that the original input may be compressed, coded/decoded, and input in 4:2:0 SD format. Thus, we are witnessing the evolution of video processing from luma-only 2D processing to 2D+motion (motion adaptive and motion compensated), and to 3D processing of 3 components with increasing bit precision.

IV. DISPLAY-SPECIFIC PROCESSING

The transition from CRT to new display technologies including LCD, PDP, and DLP for the popular consumer segments has also brought about new display-specific or front-of-screen processing. LCD with its sample-and-hold and slow transition response characteristics (which cause artifacts not previously seen in CRT) has driven several innovations including 120Hz refresh rates, as well as backlight control to enhance global and local image contrast (and optimize power consumption) [8,9]—this work is also

related to the developments on HDR displays for consumer applications [15]. Motion compensated frame rate conversion from 24 to 120 fps has become a compulsory feature in today's LCD DTVs. Display gamut, support of deep color standard (HDMI 1.3, xvYCC[4]), require not only an output signal that is matched to the display input, but one that shows the visual advantage of features such as advanced lightness control (contrast), deep color (10/12/16 bits per color), and increased gamut (i.e., improved color rendition and colorfulness). Processing and quality evaluation that demonstrates the advantages of deeper color depends on display technology and proper content and viewing conditions. Starting with original content at 8bpc for example, is may the best way to show the advantages of a deep color display. As indicated before, color quality can be compromised from the early stages of processing. It is therefore critical to have the best possible signal (either from best possible source closely matched to the display characteristics, or after high quality video processing) to feed the display. Demonstrable enhancements afforded by display processing which match the display's resolution, gamut, response time, color depth, and contrast are the best way to showcase innovative technologies.

V. DISCUSSION

In spite of the advances in color processing achieved by the print and still imaging fields, consumer video processing has traditionally fallen behind. The advent of new display technologies and their technology-push effect has not only put increased pressure on the content providers and video capture equipment manufacturers to deliver improved visual quality, but on the video processing scientists and engineers to constantly deliver new methods that meet the challenges of matching state of the art display technology with processed content from a broad range of qualities and formats. We are thus facing the need for improved overall color.

Management in the framework of digital video processing. State of the art work on color and contrast enhancement and even on joint enhancement of lightness, color, and contrast can only result in limited gains in the large context of the consumer video experience. Previous attempts to design a video processing pipe have been aimed at increased color and tone reproduction, for instance by using RGB and CIELAB color space processing [7], do not solve the larger framework requirements of today's DTV systems. The range of visual quality distribution at the input of the video processing engine increases as we go from HD to SD, and to subSD input sources. In general, the capability of the video processing pipe is pushed to the limit by the smallest formats and the lowest quality (noisiest, most compressed) content. It is therefore imperative to define the region of performance in that space where video processing can afford the maximum improvement in visual quality, and design methods suited for that goal instead of using incremental improvements to the traditional architecture. We have discussed the main processing requirements related to source/format and display that must be met by the video processing engine. At the onset, if the color space used by the video pipe is not matched to the color space depth and gamut of the input (e.g. latest digital HD video cameras), we are already loosing information and quality that will not be easily recovered; especially if at the end we have a display compatible with latest color management standards. We indicated that although composed of many individual modules (e.g. denoising, scaling, color enhance, contrast enhance, sharpness enhance), to avoid complex interaction, the holistic approach to the video processing engine appears more promising than the multi-module cascade approach. Examples of this approach include joint processing for color/contrast enhancement [13], 3D processing instead of 2D+motion, and transformed space processing for multifunction processing [11,14]. Overall, we have pointed at present issues, as well as emerging ones stemming from the new trends in the field of consumer video. Color processing accuracy is only the first step. Future research is expected in the areas of multidimensional, multi-component processing, and objective color quality metrics that can be used in adaptive/intelligent processing. Further research on perception of color and color artifacts under variable motion conditions, perceptual adaptation (spatial and temporal), and the requirements of color processing for 3D video displays are also expected.

VI. REFERENCES

1) P. Bourdon, B. Augereau, C. Olivier and C. Chatellier, —MPEG-4 compression artifact removal in color video sequences using 3D nonlinear diffusion," in Proc. of ICASSP04, pp. III.729-III.732.
2) M. Fairchild, "A color scientist looks at video", Proc. of 3rd International Workshop on Video Processing and Quality Metrics for Consumer Electronics, Phoenix, Arizona, January 2007.
3) X. Han, Y. Chen and J. Lei, —Aspatio-chromatic ICA based noise reduction in color images," International Journal of Innovative Computing, Information and Control Volume 4, Number 3, March 2008, pp 661-669.
4) "HDMI-1.3 new capabilities", in http://www.hdmi.org/pdf/HDMI_Insert_FINAL_8-30-06.pdf.
5) H. Hu, P. Hoffman, and G. deHaan, —Image interpolation using classification-based neural networks", IEEE International Symposium on Consumer Electronics, 2004.
6) B. Kang, M. Cho, H. Choh and C. Kim, "Perceptual Gamut Mapping on the basis of Image Quality and Preference Factors", Proc. of SPIE-IS&T Electronic Imaging, SPIE Vol. 6058, 2005.
7) W. Kao, et al, —Designing image processing pipeline for color imaging systems," in Proceedings of ISCAS 2006, pp. 4679-4682.
8) C.-C. Lai and C.-C. Tsai, —Backlight Power Reduction and Image Contrast Enhancement Using Adaptive Dimming for Global Backlight Applications," in IEEE Transactions on

9) Consumer Electronics, Vol. 54, No. 2, MAY 2008, pp. 669-674.
W. Lee, K. Patel, M. Pedram, —White LED Backlight Control for Motion Blur Reduction and Power Minimization in Large LCD TVs,” to appear in Journal of the Society for Information Display, 2009.
10) P. Lin, and Y. Kim, —An adaptive color transient improvement algorithm,” in IEEE Transactions on Consumer Electronics, Vol. 49, No. 4, Nov. 2003, pp. 1236-1239.
11) S. Mallat and G. Peyre, —A review of bandlet methods for image representation,” Numerical Algorithms, Vol. 44, No. 3, March 2007.
12) C. Poynton, Digital Video and HDTV Algorithms and Interfaces, Morgan Kaufman Publishers, Elsevier, San Francisco, CA, 2007.
13) A, Sarkar, M.D. Fairchild, J.E. Caviedes and M. Subedar, "A Comparative Study of Color and Contrast Enhancement for Still Images and Consumer Video Applications," in Proceedings of the Sixteenth Color Imaging Conference, Portland, Oregon, Novembe

Greening Industries; a Strategic Approach to Reducing Industrial Emissions

O.S. Udeozor[1] A.N. Nzeako[2]

GJRE Classification (FOR)
GJRE:G 090799

***Abstract*-Adopting eco-friendly and sustainable practices in every industry is a strategic way of "Going Green" this will presents opportunities for investment, growth, savings and a healthy and sustainable future, therefore this paper gives a theoretical overview on how various industries could "Go Green" so as to make a shift towards a resource-efficient and low-carbon economy.**

Keywords-Green Growth, Low Carbon Economy, Co-generation, Waste-to-Energy, Carbon Sequestration, Green building.

I. Introduction

In developed and developing countries, the history of air pollution problem has typically been high levels of smoke and sulphur dioxide arising from the combustion of sulphur-containing fossil fuels such as coal for domestic and industrial purpose [1]. Industrial development and the use of fossil fuels have affected the world climate adversely. Africa is probably the fastest growing region in the world. Being the fastest growing region also probably means considerable increase in industrial emissions. Climate change is one of the biggest environmental challenges in world history. The shift to a low-carbon economy will change how industries operate, the products people use and their lifestyles. Business and consumers can benefit from significant savings and resource efficiency measures that will reduce greenhouse gas emissions and make climate safer for all and more conducive to growth.

All over the world, business communities are realising that to achieve global competitiveness, they have to embrace the green agenda and reduce their impact to the environment [2]. Green growth is an economic strategy that focuses on ecologically-sustainable economic progress to foster low carbon activities. A major part of green growth is a low carbon economy that refers to an economy with reduced or minimum emission of greenhouse gases and industrial emissions. This requires a shift from fossil fuels to renewable energy sources and more efficient production processes that will entail less energy per unit of output. Green industries are among the fastest-growing in the global economy. The top ten in the list are advanced biofuels, retrofitting of buildings, geothermal energy, green chemistry, green manufacturing, smart grid, solar energy, sustainable agriculture, sustainable green retailing and wind energy.

About-[1] Department of Electrical and Electronic Engineering, Ambrose Alli University, P.M.B, 14, Ekpoma, Nigeria.
(e-mail-ogcafe@yahoo.com)
About-[2] Department of Electronic Engineering University of Nigeria, Nsukka, Enugu State, Nigeria.
(e-mail-annzeako@hotmail.com)

Making the shift towards green growth presents opportunities for investment, growth, savings and healthy and sustainable future. Perspectives, mind sets and attitudes must be transformed for the country to make the shift to a Resource-efficient and low-carbon economy.

II. Method of Study

The theoretical basis of this study is to give an overview on ways in which the production industries can "go green" so as to reduce emissions to its barest minimum; examples will be cited in the text to show the methods industries can adopt in going green.

While it may be easy to observe and measure benefits like lower operating costs and increased market share, going green also provides intangible benefits that are equally important. Employee morale, health, and participation increases as eco-friendly improvements to factory working environments are made possible.

III. Effective Greening Practices for Industrial Processes and Factories

Making the industrial processes greener pays off tenfold in the future. Here are some of the most effective greening practices for industrial processes:

A. Make Use of Renewable Energy and Green Power

Green energy is quite literally the future of any industry. If power can be gotten from wind, solar, hydro, or biomass sources, the industries can be transformed into a more sustainable and eco-friendly operation. Many states offer tax breaks and incentives for businesses that choose this route, and such industries may even receive compensation for energy they generate and contribute back to the grid [3]. A reliable, consistent source of clean on-site energy is an excellent way to achieve true sustainability.

B. Energy-Saving Programs

A good starting point is to conduct an energy audit to see where improvements can be made. In Metro Manila, a hotel company implemented sustainable energy savings programs such as building management systems, and replacement of lightings and chillers thus allowing the company to save around 4,920,867kw-hrs of electricity or 2,952,520.20kgs. Equivalent reduction of carbon dioxide emission.

A brewery in Mandaue City has undertaken various energy conservation efforts such as reduction of light use and aircon, replacement of incandescent bulbs with energy-saving bulbs, rationalization of operations schedule to maximize usage of utilities and optimized the operation of its ammonia compressors, which contributes to 40% of the

plant's energy consumption. Total energy conservation efforts led to savings of 8% for power and water alone or over Php18 million in-generated savings.

C. Green Building

Also known as green construction or sustainable building, is the practice of creating structures and using processes that are environmentally responsible and resource-efficient throughout a building's life-cycle: from siting to design, construction, operation, maintenance, renovation, and deconstruction. This practice expands and complements the classical building design concerns of economy, utility, durability, and comfort [7]

Although new technologies are constantly being developed to complement current practices in creating greener structures, the common objective is that green buildings are designed to reduce the overall impact of the built environment on human health and the natural environment by:

- Efficiently using energy, water, and other resources
- Protecting occupant health and improving employee productivity
- Reducing waste, pollution and environmental degradation

A similar concept is natural building, which is usually on a smaller scale and tends to focus on the use of natural materials that are available locally.

A semi-conductor company in the Cordillera Autonomous Region has the first building in the Philippines to gain LEED (Leadership in Energy and Environmental Design) certification. The company's building was built with respect to the sun's path to minimize unwanted heat gain and to maximize natural day-lighting.

D. Optimizing Water Use

A water efficiency program is a smart way to conserve water and save money. For many factories and industries processes, water bills can escalate quickly due to high levels of consumption. A food manufacturing company with factories in batangas and Laguna, explored ways to optimize the used of water in its operations and eliminate unnecessary consumption. These efforts have cut down its water consumption by 16.76% since 1997 or an average of 65,500 cubic meters of water every year. Some of the measures that the company employed include the re-use of water for various parts of its operation. Water used for sealing, cooling and even treated wastewater is collected, pumped and re-circulated for irrigation of plants and grass as well as other uses instead of being discharged as waste. See figure 3.0 below.

Figure 1.0: A food manufacturing company with factories in Batangas and Laguna recover used water from their operations and reuse that water for other purposes resulting in huge savings [2].

E. Reduce, Reuse, and Recycle Whenever Possible

Another way to save more money is to cut down on the amount of waste produced by industrial processes. Less waste means less money spent on waste removal, lower cost on raw materials, and higher levels of efficiency overall. Industries should expect a spike in productivity as they streamline their processes and eliminate excess waste. Whenever possible, the use of inexpensive post-consumer recycled raw materials and industrial participation in recycling programs when the manufacturing process is complete should be encouraged. Another common area of improvement is product packaging; the industries if possible should rethink and redesign their current packaging to get rid of any excess or waste material.

Various examples of ways of reusing industrial waste are given as follows;

F. Waste-to-Energy

Majority of the sugar refineries in the Philippines (particularly those in Cagayan valley, Pampanga and Batangas) make use of ~~–b~~agasse," a by-product derived from sugarcane. One refinery in Leyte uses this by-product as fuel for its boilers to generate steam. The steam generated is then used to drive turbines of cane milling plant equipment and turbo-generators to produce electricity for the sugar processing plant. This helps lower energy costs of the company especially during the milling season. Also in leyte, a bio-ethanol plant utilises rice hull for running its boilers. With 100% rice hull fuel, fuel costs have dramatically shrank from whopping Php2.8 million monthly to only Php270, 000. See figure 1.0: below

Figure 2.0: A sugar milling company in Leyte utilizes bagasse to fuel its boilers to generate steam used in its cane milling plant thus lowering energy costs for its operations [2].

G. *Methane Recovery*

A controlled disposal facility in Metro Manila and a sanitary landfill in Rizal collect and convert methane to generate electricity. By capturing methane, which is a known greenhouse gas, environmental impacts are mitigated and the operational safety of the site is increased. See figure 2.0.

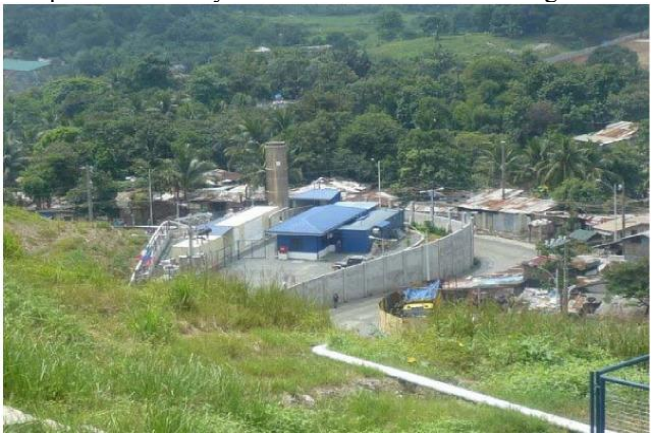

Figure 3.0: Payatas Controlled Disposal Facility in Quezon City Extracts methane gas from the old Payatas dumpsite and convert this to electricity [2].

Davao, a beer manufacturing plant recovers and utilizes methane to fire its boiler to produce steam. Annually, the brewery saves 180,000 litres of fuel or Php2.7 million using methane gas and has also earned carbon credits for this practice.

H. *Co-generation*

Majority of manufacturing plants of the three giant cement companies in the Philippines, reduce its environmental impact by using new forms of selected and pre-qualified waste material and by-products from other industries as either alternative fuel or alternative raw material. Co-processing of industrial and residual wastes to derive thermal energy in cement clinker production helps decrease the use of fossil fuel and carbon emissions.

A company in Cebu engaged in manufacturing various electronic peripherals likewise uses co-generation technology for its plant. Through this technology, heat that is otherwise discarded from conventional power generation is utilised to produce thermal energy. This energy is then used to provide cooling or heating for industrial facilities such as air-conditioning and machine cooling process in selected production divisions inside the plant. Recycling exhaust heat means more savings for the company which reported energy savings of 220,896kwh/month or Php1.3M monthly savings.

I. *Carbon Sequestration*

Carbon sequestration is capturing the carbon dioxide produced by burning fossil fuels and storing it safely away from the atmosphere.

How is CO_2 captured?

Methods already exist for key parts of the sequestration process. A chemical system for capturing carbon dioxide is already used at some facilities for commercial purposes, such as beverage carbonation and dry ice manufacture. The same approach could be adapted for coal-burning electric power plants, where smokestacks could be replaced with absorption towers. One tower would contain chemicals that isolate carbon dioxide from the other gases (nitrogen and water vapour) that escape into the air and absorb it. A second tower would separate the carbon dioxide from the absorbing chemicals, allowing them to be returned to the first tower for reuse [4]. The CO_2 in exhaust gas is separated and recovered from these gases at the emission source. Several methods of separation and recovery for CO_2 in exhaust gas are being researched and developed (see Table1.0), and some are already at a level permitting practical utilization. Polymer membrane separation is being researched and developed as a low-cost method. The membrane per se is costly, but recovery does not require a lot of energy. If it reaches the stage of practical utilization, this method is therefore expected to reduce separation and recovery costs [5].

Table 1.0: separation & recovery methods and their features

Separation & recovery methods		Features
Absorption method	Chemical absorption	The chemical reaction of a CO2 absorbent is applied to separate CO2. A large amount of energy (steam) is needed to extract the absorbed CO2. The method yields a CO2 recovery rate of 90 percent and a purity of 99.9 percent.
	Physical absorption	An absorbent is utilized to physically absorb the CO2, which is then recovered through pressure reduction (heating). The recovery rates and purity are on about the same level or slightly below those of chemical absorption (by the amine method).
Adsorption		CO2 is brought into contact with activated charcoal or some other adsorbent, and physicochemical adsorbed by its micropores. The CO2 recovery rate and purity are reportedly 90 and 99 percent, respectively.
Membrane separation	Polymer membrane	CO2 is separated by means of the difference between gas speeds of transmission through the polymer membrane.
	Liquid membrane	CO2 is separated by a membrane holding a carrier substance that selectively transmits CO2. At present, this method is at the stage of basic research.
	Inorganic membrane	Separation is effected by the surface diffusion flow arising in transmission through a porous material.
Oxygen combustion		Fossil fuels are combusted in oxygen to raise the CO2 concentration of the exhaust gas to nearly 100 percent. Testing has confirmed that this method can obtain exhaust gas with a CO2 concentration of 94 or 95 percent.
Sublimation		CO2 in gas is sublimated and recovered in the form of dry ice.
Cryogenic separation		A mixture that is a gas at normal temperature is cooled to a low temperature and separated into its constituent fractions by partial liquefaction for distillation or partial condensation.

How is CO_2 transported to its storage site?

Upon its separation and recovery from exhaust gas, the CO_2 is transported to the storage site. Table 2.0 shows the transportation methods and their characteristics.

Table 2.0: Transportation methods and characteristics

Method	Features
Pipeline	When the storage site is close to the emission source, pipelines can be used to transport the CO2 resulting from separation and recovery to the storage site in a supercritical state (in which the gas and liquid densities are the same and make it impossible to distinguish the two).
Tanker	When the storage site is far from the emission source (e.g., in another country), tankers can be used to transport the separated and recovered CO2 in liquefied form to the storage site.

How is CO_2 stored?

Upon transportation to the storage site, the CO_2 is forcibly injected into locations underground or at sea. These storage methods can be classified as shown in Table 3.0 in terms of the location and objective. With the Crude Oil Recovery and the Coal Bed Methane Recovery methods, the storage of CO_2 has Simultaneous by-products, (Oil and Methane Gas, respectively). Considering the utilization of these by-products, these methods could reduce the cost of carbon sequestration [6].

Table 3.0: Storage methods

Sequestration methods		Description	Storage capacity (worldwide)
Underground sequestration	Crude oil recovery	Injection of CO2 into oil fields on the occasion of tertiary recovery of crude oil, to induce recovery	73.3 - 238.8 billion t-CO2
	Coal seam methane recovery	Adsorption of CO2 in unexploitable deep- stratum coal seams, with simultaneous recovery of methane	146.7 billion t-CO2
	Depleted oil and gas wells	Use of the storage capacity of oil and gas fields that had held reserves of oil and natural gas; proven storage capacity	Oil wells: 366.7 billion t-CO2 Gas wells: 1,466.7 billion t-CO2
	Aquifers	Dissolution of CO2 in underground salt water subject to virtually no fluctuation	At least 3,666.7 billion t-CO2
Sea-bottom sequestration	Marine dissolution	Injection of CO2 into the sea to dissolve and diffuse it; termed 'gas dissolution' in the case of injection in a gas state and 'liquid dissolution' in that of injection in a liquid state	3,666.7 billion t-CO2
	Deep-sea injection	Formation of CO2 pools in sea-bottom depressions; expected isolation period of at least 2000 years	
Biological sequestration		Sequestration by flora (plants, sea weed, vegetable plankton, etc.) through photosynthesis	Flora on land: 4.4 billion t-CO2 per year

IV. Conclusion

The practice of —grow now, clean up later" followed in the past is no longer acceptable. Sustainable development means growing and solving economic problems in an environmentally-sustainable manner. It is protecting the environment in ways that will create economic growth and prosperity.

Governments and the private sector have a key role in ensuring that economic growth provides opportunities for the poor to engage in productive activities. The private sector is the primary driver of economic growth and employment creation.

There is a need to reduce negative environment impacts through the increased use of renewable energies and the adoption of clean and environmentally-sustainable practices.

To be able to shift to green growth, the government should provide the regulatory and promotion framework and the private sector to become the engine of growth. It is important to make green growth profitable for the private sector to invest on. But to be able to achieve this, there are certain things that need to be done and these are: formulate an effective climate change policy framework; develop cost-effective implementation strategies; mobilize resources and ensure their efficient allocation; create strong incentive system and eliminate market distortions; undertake public awareness; and undertake climate change researches.

Furthermore, to ensure environmental sustainability, it is crucial to improve the way natural resources are being used. Policies must be aimed at incorporating cleaner production in national development plans and formulating action plans to promote low-carbon and resource-efficient industries. Capacities must likewise be continuously developed to promote green innovations and provide the public more environment-friendly choices.

V. Reference

1) UK National Air Quality Achive: Causes of Air Pollution. Enviropedia.com Accessed on 14 Aug 09.

2) Greening Industries in the Philippines.
3) Going Green: Creating Sustainable Industrial Processes and Eco-Friendly Factories; solusource.
4) Herzog, H., and Golomb. 2004. Carbon Capture and Storage from Fossil Fuel Use. Encyclopedia of Energy, ed. C. J. Cleveland. Vol. 1 Elsevier Science.
5) Research of CO2 Separation and Recovery Technology," FY2001 Report, New Energy and Industrial Technology Development Organisation, 2002, Pp. 129-130.
6) Koichi. S., "Carbon Sequestration Technology – Current Status and Future Outlook," Environment Group, Second Research Department.
7) U.S. Environmental Protection Agency. (October 28, 2009). Green Building BasicInformation(USEP

Design Consideration of a Low Cost Battery-Operated Wheelchair

Dr. Osman Yildirim

GJRE Classification (FOR)
GJRE,F,A,100699

***Abstract*-In this paper, design considerations and implementation details of a simple, low-cost battery-operated wheelchair are presented. The control of the vehicle is performed by an 8-bit microcontroller. Two dc motors differentially driven by PWM signals provide a motion with easily controllable speed and direction. The user controls the vehicle using a joystick.**

Keywords-Battery-Operated,Wheelchair,Wheelchair Circuits, Microcontroller Control

I. Introduction

Pulse-width modulation (PWM) of a signal or power source involves the modulation of its duty cycle. PWM uses a square wave whose pulse width is modulated resulting in the variation of the average value of the waveform. PWM can be used to reduce the total amount of power delivered to a load without losses normally incurred when a power source is limited by resistive means. PWM is also often used to control the supply of electrical power to another device such as in speed control of electric motors, volume control of audio amplifiers and many other power electronics applications. PWM is applied in a variety of systems. The most common systems are measurement and communication systems, power control systems, energy conversion applications and power delivering systems. As it is known, a PWM-controlled brake can be done by controlling with an analog input signal. In other words, the more voltage or current that's applied to the brake, the more pressure the brake will exert. The output of a PWM controller could be connected to a switch between the supply and the brake.

As is well-known, wheelchairs are divided into battery-powered and manual types. Recently, there have been revolutionary advances in design of battery-operated wheelchairs. Some wheelchairs use voice control [1], [2], [3] and some of electric powered wheelchairs vary forward and backward speed [4], [5], and some wheelchairs use guiding systems (referencing path description) [6], [7] and some of them use assistive navigation system as control mechanisms [8], [9]. All design solutions are aimed to allow performance of daily life of user‘s activities and to enable user to function more independently. In manual types, the personal assistance to help wheelchair users is the basic mode of coping with limitations in activities of user. Battery-powered wheelchairs are useful in providing mobility especially for those who have upper limb impairment as well as lower limb impairment. This paper presents design considerations and implementation details of a battery-powered wheelchair prototype. The design considerations and implementation details of a simple, low-cost battery-operated wheelchair are presented. The control of the vehicle is performed by an 8-bit microcontroller. Two dc motors differentially driven by PWM signals provide a motion with easily controllable speed and direction. The user controls the vehicle using a joystick.

In this study, a PI controlled separately excited direct current (DC) motor speed has been controlled using PIC 16F877 controller. The PIC16F877 Microcontroller includes 8kb of internal flash Program Memory, together with a large RAM area and an internal EEPROM. An 8-channel 10-bit A/D convertor is also included within the microcontroller, making it ideal for real-time systems and monitoring applications. All port connectors are brought out to standard headers for easy connect and disconnect. In the PIC 16F877 programming as a PI controller, the voltage applied to the motor is adjusted by a semiconductor power switch using PWM technique. The new PIC16F877 Controller is the ideal solution for use as a standard controller in many applications.

II. Design Considerations and Implementation

A battery-operated wheelchair is mainly composed of a joystick, control unit, motor driver unit, motor, and batteries. The block diagram of a simple battery-operated wheelchair is depicted in Figure 1.

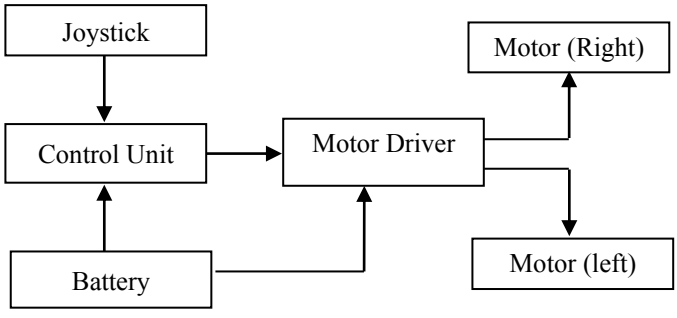

Figure 1 Block diagram of battery-operated wheelchair

A. Control Unit

The advances in semiconductor technology made it possible fast drivers which are able to process faster and relatively smaller than the previous versions using the controllers [10].

About-[1]Istanbul Kultur University, Vocational School of Technical Sciences, Bakirkoy, Istanbul, Turkey
www.iku.edu.tr (Fax:+902125613328, Phone:+902126606001
(e-mail-o.yildirim@iku.edu.tr)

There are several alternatives for implementing the control unit of a wheelchair ranging from programmable logic devices to embedded personal computers. Today low-cost microcontrollers are available which have rich sets of on-chip peripherals such as PWM modules, ADC modules and I/O ports with significant current drive capabilities. The presence of these on-chip peripherals reduces the number of integrated circuits and discrete devices in the control unit since many functions are already implemented on the microcontroller chip. The availability of well-established design methodologies and powerful design and test tools reduces the design complexity and engineering effort in a microcontroller-based design. High level programming languages such as C, Basic and Java can be used in development of the microcontroller code. The need for assembly language programming is decreasing as the compilers become more capable of generating efficient code. Today a programmer would typically use assembly language only for some time-critical applications. These considerations make the microcontroller based-implementation a good choice for building the control unit of a wheelchair.

In this application PIC16F877, an 8-bit microcontroller produced by the Microchip Corporation has been used in the implementation of the control unit [11]. In this study, the PIC series 16F877 controller of the microchip is used for the DA motor driver system. With its 20MHz clock, 25mA-rated output pins and its PWM generator, PIC16F877 provided the control facilities required for the system. The control program has been developed using the BASIC language. During the development stage, alterations of the program could be done thanks to the in-circuit serial programming capability of the PIC16F877 microcontroller.

The control unit interprets the user inputs and generates the control signals necessary to move the vehicle in the direction and speed desired by the user. The user controls the speed and direction of the travel using a joystick. The position of the joystick lever is converted to a DC signal by the electrical circuit inside the joystick and this signal is fed to the ADC module of the microcontroller. The maximum speed of the wheelchair can be set by the user through a potentiometer. When the vehicle is powered on the position of the joystick lever is checked by the control unit. If the lever is not in the idle position, motion of the vehicle is prevented. This serves to avoid any unintentional movement of the wheelchair at the start-up.

Based on the user input, proper controller signals are generated by the control unit and sent to the motor driver hardware. The speed control of the motors is achieved using Pulse Width Modulation (PWM). A 20 kHz PWM signal is generated by the PWM module on the microcontroller. By changing the duty cycle of the PWM signal the motor speed is adjusted.

A photograph of the control unit circuit board is shown in Figure 2.

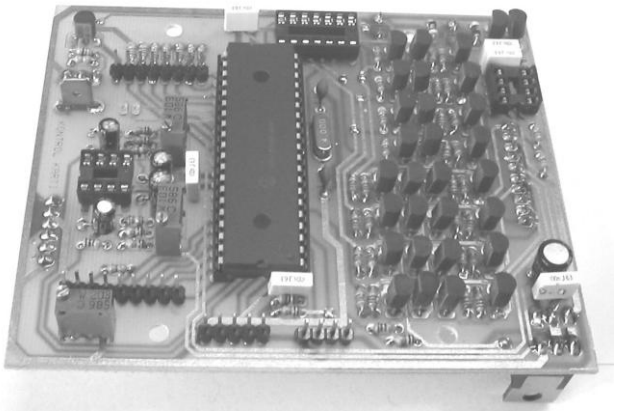

Figure 2 Control unit circuit

B. Batteries

The system is energized by two 12V sealed lead-sulfur batteries each having a charge capacity of 40A. The batteries are connected in series to obtain a 24V supply. Although lead-sulfur batteries have a poor capacity-to-weight ratio, they are preferable to devices based on alternative technologies such as Nickel-Cadmium batteries, due to their much lower cost. The condition of the batteries can be monitored by the user on a panel driven by the control unit. This is especially important to warn the user to utilize the scarce energy efficiently in the case of low batteries. The control unit prevents the start-up of the vehicle when the voltage goes below a certain limit in order to prevent damage to the batteries. During the charging operation all other functions are disabled by the control unit and the vehicle cannot move.

C. Motor Driver

Adjustable, fast motor drivers also played a significant role in the advancement of industrial automation [12]. The 5V square wave produced by PIC is applied to the servo motor. Up to the form of this wave servo motor rotates forward or backward. During the PIC programming process the direction of the impact and for how long it will be sent to the servo motor is the point. PWM produced at PIC and direction control signals are applied to the servo motor through the 4th and 5th pins of the D port. For the 3600 rotation of the motor 5500 pulses, for 10 rotation 15 pulses are required. This way the motor can turn in every angle desired. The speed of the high performance and easily controllable servo motors can be adjusted in wide limits. The outcome, PIC 16F877 controlled servo motor driving circuit, is simple, practical, sensitive, and flexible for various applications [13]. Motor Driver unit provides the interface between the control unit and the motor. An H-Bridge is used to allow the motor rotate in the forward and backward directions. An H-Bridge structure with electromechanical relays is illustrated in Figure 3.

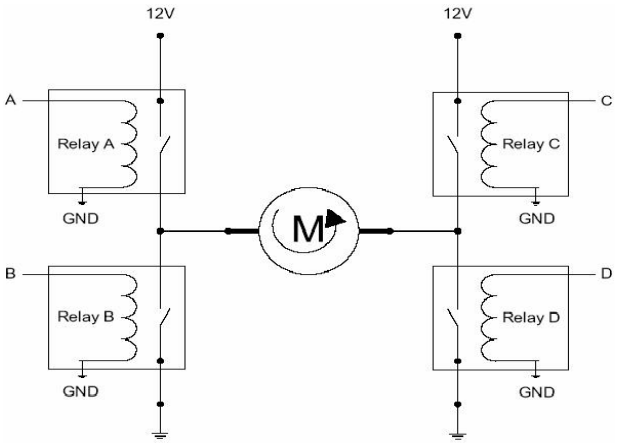

Figure 3 H-Bridge with electromechanical relays

In order to rotate the motor in the forward direction, relays A and D are turned on while relays B and C are turned off. Changing the relay states will make the motor rotate in the reverse direction. During direction changing operation, it is important not to turn on relay B (relay D) before relay A (relay C) turns off, since a heavy current would then flow between the supply and the ground, probably destroying the relays. This requires careful programming in case the relay states are controlled by a microcontroller.

In practice, transistors, rather than relays, are commonly used as control elements in H-bridges. In this application n channel MOSFET devices with 100A current ratings have been used. The direction-control signals generated by the microcontroller are compacted by the PWM signals using four AND gates. This makes it possible to control the speed of the motor as well as its direction of rotation using the same H bridge structure. The control signals pass through several transistor stages for current and voltage amplification before they reach the gates of the high-current MOSFETs. An electro-mechanical relay on the circuit board switches on and off the power of the circuit. The circuit diagram of the motor driver unit is shown in Figure 4.

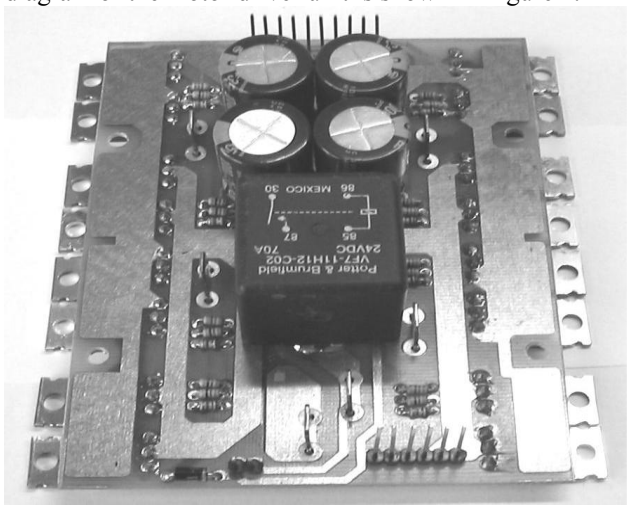

Figure 4 Motor driver unit circuit

D. Motor

The speed adjustment in DA motors was first realized by Ward Leonard in 1891 by means of voltage control. In this method the efficiency of the system was low due to the losses in the resistants. With the usage of thyristors as switching element in power electronics, adjustable voltage sources in speed adjustment of DA motors become more significant. As it is known, semi-conductors such as MOSFET, IGBT, and GTO are used as switching elements. As the switching frequencies of these elements are low in analog circuits, they are much affected by noise. However, with the usage of digital control elements they are less affected by the changing environmental conditions [14].

The wheelchair is powered by two permanent magnet dc motors each having a power rating of 250W and a voltage rating of 24V. A single-stage speed reducing gear is integrated with each motor. Adjustment of the motor speed by electronic means eliminated the need to use a multi-stage mechanical gear and provided an easier control. An electro-mechanical brake with electronic adjustment capability is also incorporated to the system. The motor-gear-brake combination appears as a single unit.

Motor controller is based on PWM system. If the current flowing to the motor has reached a previously determined level, control process is performed to interrupt and restart supply of PWM commands. By interrupting the supply of the PWM commands, the current flowing to the motor is returned from such a level to a normal level. After the motor current is returned to a normal level by the interruption of PWM command supply, PWM command supply is resumed, normal control by PWM command is again performed, and a non-controlling state in the controller is avoided.

Instead of a bipolar transistor, a Metal Oxide Semiconductor Field-Effect Transistor (MOSFET) is used as a switch to obtain high current levels. This transistor can be switched on and off very rapidly for the large currents required for big motors. The motors are driven differentially for direction control. If the user wants to turn right, the speed of the left-motor is increased with respect to the right-motor and vice versa.

III. Conclusion

A powerful, easily controllable battery-operated wheelchair was developed using state-of-the-art control and electronic drive technologies. Future improvements to the vehicle may include the addition of regenerative electronic breaking capabilities and use of lightweight batteries.

With minor modifications the motor driver and the control software can be used for speed and direction control of medium-power (200-400W) electrical vehicles that may replace small fuel-based vehicles such as scooters, golf carts etc.

IV. References

1) R.C.Simpson and P.L.Levine, ―Voice Control of a Powered Wheelchair,‖ IEEE Transactions On Neural Systems and Rehabilitation Engineering, Vol.10, No.2, June 2002, pp.122-125.

2) J.Clark and R.Roemer, —Voice Controlled Wheelchair," Arch. Physical Med. Rehab., Vol.58, No.2, 1977, pp.169-175.
3) G. Miller, T. Brown, and W. Randolph —Voice Controller for Wheelchairs," Med.Biol.Eng.Comput., Vol.23, 1985, pp.597-600.
4) K.E. Brown, R.M. Inigo, and B.W. Johnson, —An adaptable optimal controller for electric wheelchairs," J.Rehab.Res. and Develop., Vol.24, No.2, 1987, pp.87-98.
5) R.A.Cooper, Rehabilitation Engineering: Applied to Mobility and Manipulation, Bristol, U.K.:Institude of Physics Publishing, 1995.
6) E.T.Baumgartner and S.B. Skaar, —An autonomous vision-based mobile robot," IEEE Trans. Automatic Control, Vol.39, 1994, pp.493-502.
7) H.Wakaumi, K.Nakamura, and T.Matsumura, —Development of an automated wheelchair guided by a magnetic ferrite marker lane," J.Rehab.Res.Develop.,Vol.29, No.1, 1992, pp.27-34.
8) S.Levine, D.Bell, L.Jaros, R.Simpson, Y.Koren, and J.Borenstein, —The NavChair Assistive Wheelchair Navigation System," IEEE Trans.Rehab.Eng., Vol.7, 1999, pp.443-451.
9) D.P. Miller and M.G. Slack, —Design and testing of a low-cost robotic wheelchair prototype," Autonomous Robotics, Vol.2, 1995, pp.77-88.
10) P.C. Sen, Electric Motor Drives and Control- Past, Present, and Future, IEEE Transactions on Industrial Electronics, Vol. 37 (6), 1990, pp.562-575.
11) Microchip. 2001. PIC 16F87X Data Sheet, USA
12) M.Bodson, Trends in Electronics for Electric Motor Control, IEEE Control Systems Magazine, Vol.16 (5), 1996, pp.88-96.
13) K. Feher, Servo Motor Control Digital Communications, Prentice Hall.
14) A. E., Fitzgerald, C. Jr., Kingsley, and S. D. Umans, Electric Machinery, Mc Graw-Hill Book Co., Singapore, 1985, pp.247-299

.

Development of Computer Aided Process Planning (CAPP) for Rotational Parts

Md. Deloyer Jahan[1] Golam Kabir[2]

GJRE Classification (FOR)
GJRE:F,080106

***Abstract*-In the process of product design and manufacturing and its interface, the role of process planning becoming increasingly important as competitive pressure call for improvements in product performance and quality and for reduction in development time-scales. Feature extraction and classification is considered as the bridge between Computer-Aided Design (CAD) and Computer-Aided Process Planning (CAPP). This paper proposes a method that can extract and classify for rotational parts taking a 2D data file as input. In addition, feature interactions are also taken into consideration in this methodology. The proposed feature extraction and classification method consists of three basic procedures. First, polyline of desired profile for certain object is drawn in certain manner and saved in DXF format of AutoCAD. Second, feature is extracted from the 2D CAD DXF data file. Third, G-Code compatible for CNC machine is generated using several logics. Two sample application descriptions are presented for demonstration purposes. The system has been implemented in Visual Studio (Visual C++) on a PC-based system.**

Keywords-Computer-Aided Process Planning, Drawing Interchange Format, Feature Recognition

I. INTRODUCTION

Process planning translates design information into the process steps and instructions to efficiently and effectively manufacture products. As the design process is supported by many computer-aided tools, computer-aided process planning (CAPP) has evolved to simplify and improve process planning and achieve more effective use of manufacturing resources. Process planning encompasses the activities and functions to prepare a detailed set of plans and instructions to produce a part. The planning begins with engineering drawings, specifications, parts or material lists and a forecast of demand (Groover, 1987). CAPP systems ensure significant reduction of time needed for fabrication of manufacturing processes plan. Process planning approaches can be basically classified into two types such as traditional manual process planning and computer aided process planning (CAPP) (ElMaraghy, 1993).

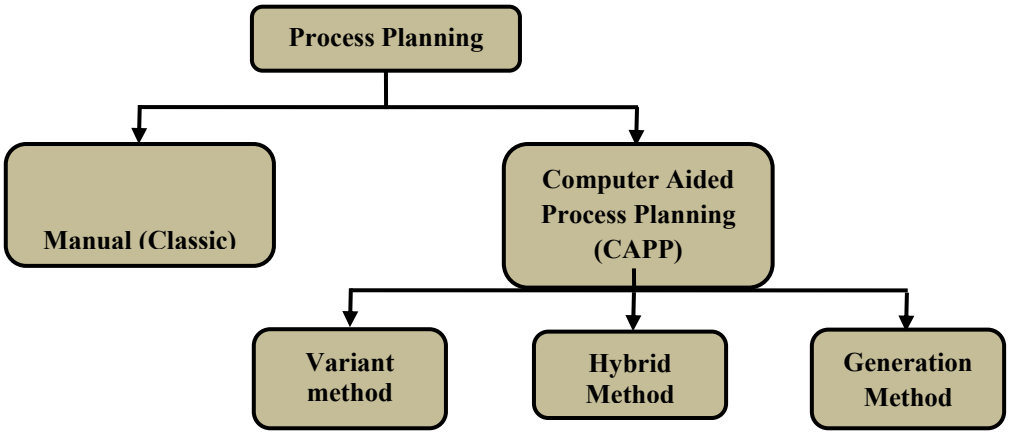

Figure 1: Process Planning

Manual process planning is based on a manufacturing engineer's experience and knowledge of production facilities, equipment, their capabilities, processes, and tooling. In some companies, process plans are manually classified and stored in workbooks (Lee, 1999). The manual approach is also considered a poor use of engineering skills because of the high clerical content in most of its functions (Zeid, 2002). Alting and Zhang (1989) reported that the idea of using the speed and consistency of the computer to assist in the determination of process plans was first presented by Niebel (1965).

Variant Approach: The variant approach, also known as the retrieval approach, can be regarded as an advanced manual approach in which the planner‘s memory retrieval process is aided by the computer. In other words, the planner‘s workbook is stored in the computer file (Lee, 1999). The first developed CAPP system, named CAPP (CAM-I Automated Process Planning), was a variant system (Link, 1976; Chang and Wysk, 1985). Houtzeel (1976) utilized the variant approach, where parts firstly are grouped into families considering their geometric or manufacturing similarities and a unique code is assigned for each family

About-[1]Department of Mechanical and Production Engineering, Ahsanullah University of Science and Technology, Bangladesh, (e-mail: mdjahan.mpe@aust.edu)
About-[2]Department of Industrial and Production Engineering, Bangladesh University of Engineering and Technology (BUET), Bangladesh,

based on GT coding systems like OPITZ, MICLASS, KK-3 and DCLASS (Cay and Chassapis, 1997). Generative Approach: The generative process planning approach is viewed as the true automated approach to process planning. Unlike the variant approach, the generative approach does not require assistance from the user to generate a process plan (Zeid, 2002). Wysk (1977) presented a generative system called APPAS which focused on detailed process selection (Cay and Chassapis, 1997). Kanai et al. (1988) described a process planning system based on generative approach which extracts machining features and decides cutter path and cutting conditions. Lee et al. (2001) proposed a framework for integrating artificial intelligence techniques and mechanistic models in the task of generating process plans for prismatic parts with interacting features.

Hybrid Approach: In the presence of difficulties with a purely generative system, some researchers have proposed a hybrid approach, also known as semi-generative approach, which is basically a combination of the variant and generative methods. The system may just modify this standard plan or may build a new one for a specific part by generative approach (Cay and Chassapis, 1997). Or the system can work in a reverse order – firstly generating a tentative process plan and then examining for errors and modifying if it does not fit to the real production environment. Emerson and Ham presented a semi-generative system titled ACAPS in 1982 (Alting and Zhang, 1989). Marefat and Britanik (1996) focused on the development of a process planner which combines the advantages of the variant and generative approaches to process planning. Alam et al. (2000) presented a methodology of a computer aided process planning system for an injection mould component, slider.

Feature Recognition: Li and Adiga (1987) emphasized that part feature recognition systems are the key factors influencing the degree of CAD and CAM integration in general and level of automation in achieving this integration in particular. Atkinson (1991) mentioned that regardless of the particular selections of commercial engineering, design and part programming systems, the manufacturing part features will ultimately be the technological link between part geometry and the manufacturing operation used to create that geometry. Gindy (1989) described that two approaches to using features in manufacturing applications have been used by researchers: feature recognition and feature based design. Feature recognition calls for a procedure that can (without human intervention) find the features in a part specified by its boundary information (Trika and Kashyap, 1994). Han et al. (2000) classified the most active current approaches as graph-based approach, volumetric decomposition approach and hint-based approach. Tyan and Devarjan (1998) presented algorithms which can identify 3D feature of a part from its 2D CAD views. Pande and Prabhu (1990) discussed an expert system for automatic extraction of machining features both the internal and external from 2D drawing. Here, the internal features are drawn using dashed line to separate them from external features. Aslan et al. (1999) described a feature extraction method from 2D drawing in which only external features can be recognized.

Object-Oriented Approach to Process Planning: IICT (Pressman, 2001) mentioned that throughout the 1990s, object-oriented software engineering became the paradigm of choice for many software product builders and a growing number of information systems and engineering professionals. In addition, object-oriented systems are easier to adapt and easier to scale (i.e., large systems can be created by assembling reusable subsystems) (Pressman, 2001).

The use of object-oriented approach is reported in the literature in different areas of application. Wong and Wong (1995) described the development of an object-oriented feature-based design system where the geometric information of a feature is stored in feature object while drawing the feature and this feature object can be used in assisting process planning. Naish (1996) developed a system module which models cutting process capabilities by using object-oriented technique and this module forms a part of a computer aided process planning system within an integrated concurrent engineering system. Marefat and Britanik (1996) focused on the development of a case-based process planner based on semi-generative process planning approach which used object to represent the knowledge of the system. Law, et al. (2001) proposed an object-oriented model of a CAPP system for the manufacturing of circuit boards which represents process constraints and planning knowledge as objects.

II. FEATURE BASED CAM SYSTEM

In spite of using advanced manufacturing and automation technology the link, between CAD and CAM systems, is still not as integrated as desired. The process planning stage, which consists of the explanation of design drawings, is seen as a hindrance in the flow of information between CAD and CAM. An intelligent interface between CAD and CAPP systems is imperative because the CAPP systems depend on correct data obtained from CAD systems to perform precise process planning (Zeid, 2002). Figure 2 shows flow diagram for automatic feature recognition. There have been many previous attempts to recognize form features for manufacturing purposes, which can be broadly categorized into three areas: Rule-based, Graph based and Neural Network-based systems.

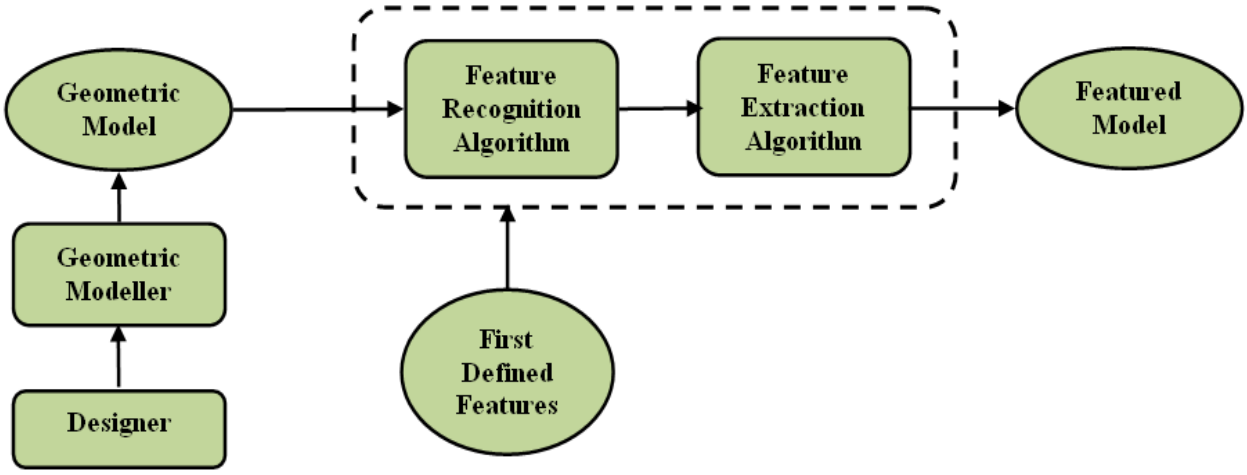

Figure 2: Flow Diagram for Automatic Feature Recognition

A. *Developed System*

CNC part programs are derived automatically using automatic feature recognition from 2D drawings in this system. The CAD model of the component including half of the 2D upper profile to be turned has to be designed in any CAD environment and be converted to DXF data structure to accomplish the feature recognition process of the system. Part programs have been derived appropriate to the Fanuc O-T control system. This system was prepared using Delphi version 7. In addition, the system is supported with material and cutting tool database prepared according to the Sandvik Cormorant catalogue. The system is composed of three important modules, file reading, feature recognition and tool path planning. The General structure of the system is shown in Figure 3.

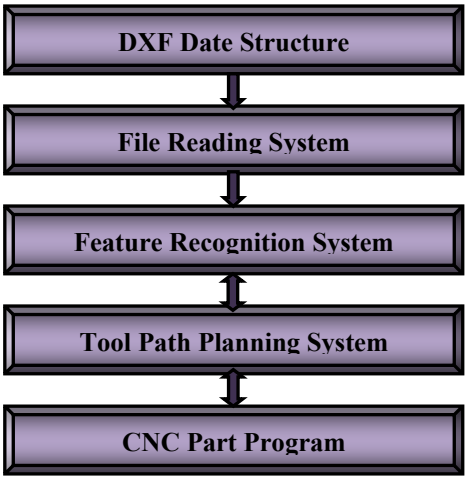

Figure 3: Structure of the System

File Reading System: After data input into the system using DXF format a set of processes is done automatically according to a specific hierarchy. Firstly, the features in the drawing are found and defined to the system. After these processes, all coordinates of the features are sequenced according to their start points and transferred to the origin. Finally the shape of the work piece is drawn with the program with its sub symmetry.

Feature Recognition System: Owing to the fact that the rotational parts are symmetrical along their axis, designing their processes can be done according to the symmetry axis so the feature recognition process is performed on the symmetry axis. Features including rotational parts could be classified as outside features and inside features according to machining attributes. Each feature in these figures could be used in recognition of turning operations such as long turning, grooving, drilling and boring.

Tool Path Planning System: In this stage operations are executed as external and internal processes (such as grooving and boring) by the developed system according to feature characteristics after whole recognitions. General turning operations to be done from the length or outside diameter of the part are made depending on the raw material sizes or the operator according to minimum and maximum measures taken from DXF data. Face and long turning operations are made according to differences between these minimum maximum and raw material sizes.

The method of profile recognition and necessary tool paths are shown in Figure 4. The figures under the geometry represent the number of feature sequence and the figures on top of the geometry represent the number of the feature.

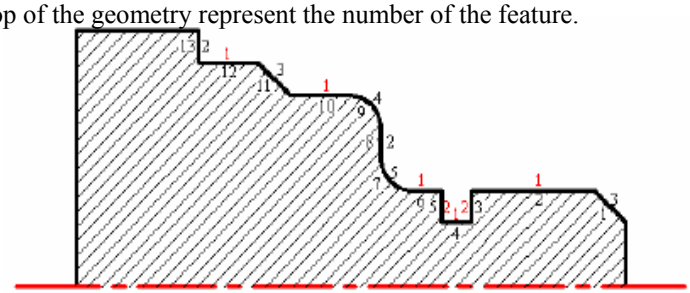

Figure 4: Method of Feature Recognition and Tool Path

The system separates the machining features such as grooving, threading and drilling after sequencing the features in respect of their start points. Tool paths are generated separately as to feature characteristics for each feature from the latest feature to the first feature appropriately with desired and equal depth.

B. Process Plans For Rotational Parts

Computer aided process planning is done in this study by generating G-CODE for CNC machine for rotational parts. Profile without fillet and profile with fillet are studied here. First of all it is needed to understand what G-code is.

G- Code, or preparatory code or function, are functions in the Numerical control programming language. The G-codes are the codes that position the tool and do the actual work. The programming language of Numerical Control (NC) is sometimes informally called G-code. But in actuality, G-codes are only a part of the NC-programming language that controls NC and CNC machine tools. Today, the main manufacturers of CNC control systems are GE Fanuc Automation (joint venture of General Electric and Fanuc), Siemens, Mitsubishi, and Heidenhain, but there still exist many smaller and/or older controller systems.

Some CNC machine manufacturers attempted to overcome compatibility difficulties by standardizing on a machine tool controller built by Fanuc. Unfortunately, Fanuc does not remain consistent with RS-274 or its own previous versions, and has been slow at adding new features, as well as exploiting increases in computing power. For example, they changed G70/G71 to G20/G21; they used parentheses for comments which caused difficulty when they introduced mathematical calculations so they use square parentheses for macro calculations; they now have nano technology recently in 32-bit mode but in the Fanuc 15MB control they introduced HPCC (high-precision contour control) which uses a 64-bit RISC processor and this now has a 500 block buffer for look-ahead for correct shape contouring and surfacing of small block programs and 5-axis continuous machining. This is also used for NURBS to be able to work closely with industrial designers and the systems that are used to design flowing surfaces. The NURBS has its origins from the ship building industry and is described by using a knot and a weight as for bending steamed wooden planks and beams.

G-codes are also called preparatory codes, and are any word in a CNC program that begins with the letter 'G'. Generally it is a code telling the machine tool what type of action to perform, such as:

1. Rapid move
2. Controlled feed move in a straight line or arc
3. Series of controlled feed moves that would result in a hole being bored, a workpiece cut (routed) to a specific dimension, or a decorative profile shape added to the edge of a workpiece.
4. Change a pallet
5. Set tool information such as offset.

Some G words alter the state of the machine so that it changes from cutting straight lines to cutting arcs. Other G words cause the interpretation of numbers as millimeters rather than inches.

G0 rapid positioning	G58 use preset work coordinate system 5
G1 linear interpolation	G59 use preset work coordinate system 6
G2 circular/helical interpolation (clockwise)	G59.1 use preset work coordinate system 7
G3 circular/helical interpolation (c-clockwise)	G59.2 use preset work coordinate system 8
G4 dwell	G59.3 use preset work coordinate system 9
G10 coordinate system origin setting	G80 cancel motion mode (includes canned)
G17 xy plane selection	G81 drilling canned cycle
G18 xz plane selection	G82 drilling with dwell canned cycle
G19 yz plane selection	G83 chip-breaking drilling canned cycle
G20 inch system selection	G84 right hand tapping canned cycle
G21 millimeter system selection	G85 boring, no dwell, feed out canned cycle
G40 cancel cutter diameter compensation	G86 boring, spindle stop, rapid out canned
G41 start cutter diameter compensation left	G87 back boring canned cycle
G42 start cutter diameter compensation right	G88 boring, spindle stop, manual out canned
G43 tool length offset (plus)	G89 boring, dwell, feed out canned cycle
G49 cancel tool length offset	G90 absolute distance mode
G53 motion in machine coordinate system	G91 incremental distance mode
G54 use preset work coordinate system 1	G92 offset coordinate systems
G55 use preset work coordinate system 2	G92.2 cancel offset coordinate systems
G56 use preset work coordinate system 3	G93 inverse time feed mode
G57 use preset work coordinate system 4	G94 feed per minute mode
	G98 initial level return in canned cycles

Figure 5: G- Code List

III. CASE STUDY

A. *Profile without Fillet*

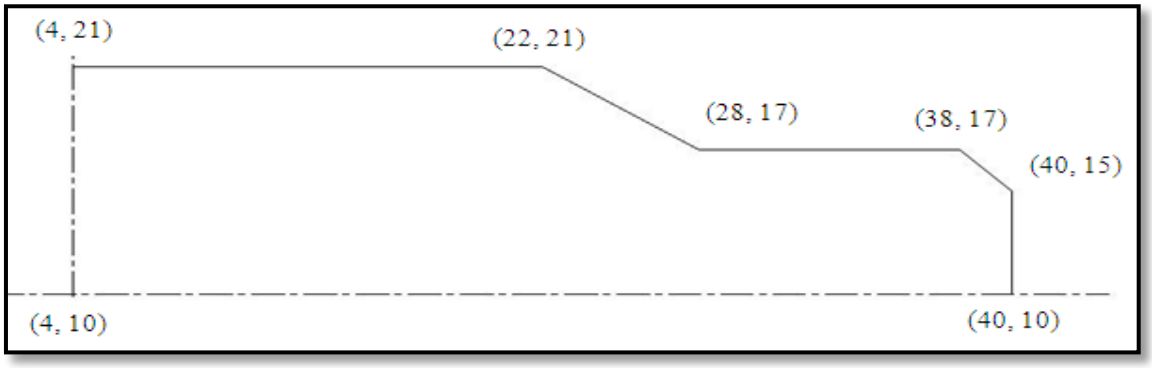

Figure: 6 Profile Without Fillet

For this profile first part zero is determined. Here part zero is at point (4, 10). Then for absolute positioning other points are determined from the vertex coordinate system. Points found from vertex coordinate system are (40, 10), (40, 15), (38, 17), (28, 17), (22, 21) and (4, 21). From those points least value of X coordinate and least value of Y coordinate is determined which is found to be (4, 10). So by subtracting the value of X and Y from all the coordinates' conversion from global to local system is made.

Steps to generate G-Code from DXF file format:

1. Drawing is saved in DXF format.
2. From large list of data ENTITIES is to be found
3. From ENTITIES several features are identified
4. Every line is start with AcDbLine and ends with a character 0
5. X_{start} is shown by 10 and Y_{start} is by 20
6. X_{end} is shown by 11 and Y_{end} is by 21
7. Lowest value of X and Y is determined and is set to origin of the coordinate by subtracting them from all the coordinates.
8. Generation of G-Code is executed from the highest value of x at which the value of Y is no equal to the value of coordinate origin value of Y. there is such one point, in this case this value is (40, 15)

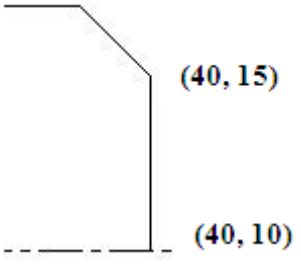

9. As cutting is starting from some far from the workpiece thus for rapid positioning cutting tool is positioned in the position at +2 in X axis and -2 in y axis from point(in this case (40, 15)).
10. For this case starting point is (42, 13).

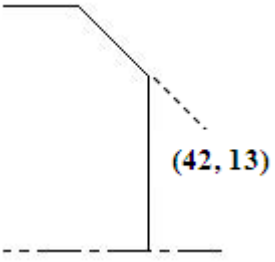

11. For G-Code representation X axis of the coordinate system is represented as Z and Y axis of coordinate system is as X. The Codes used is elaborated later in the chapter. So for initial rapid positioning G-code is G00. The formulae used to define is as following
    $(X-X_{origin}) = X_{start}$
    Represented as Z….
    $(Y-Y_{origin}) \times 2$ = diameter
    Represented as X…
    So after rapid positioning first line become
    G 00 Z 38 X 6
12. Then linear interpolation is made with respect to descending order of X axis coordinate in the DXF file 10, 11 commands. So next line in G-code become
    G 01 Z 34 X 14
    Similarly next interpolation is made by the formulae.

Figure 7: DXF Format for Profile without Fillet

B. Profile with Fillet

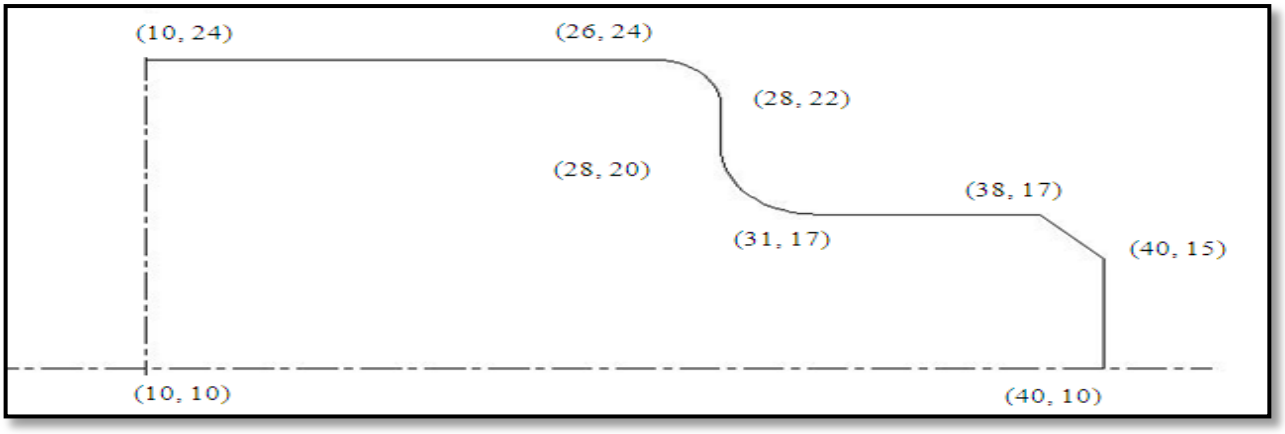

Figure 8: Profile with Fillet

For this profile first part zero is determined. Here part zero is at point (10, 10). Then for absolute positioning other points are determined from the vertex coordinate system. Points found from vertex coordinate system are (40, 10), (40, 15), (38, 17), (31, 17), (28, 20), (28, 22), (26, 24) and (10, 24). From those points least value of X coordinate and least value of Y coordinate is determined which is found to be (10, 10). So by subtracting the value of X and Y from all the coordinates' conversion from global to local system is made. Profile with fillet needs to consider extra features. For those features extra calculation and idea is generated.

Steps to generate G-Code from DXF file format:

1. Drawing is saved in DXF format.
2. From large list of data ENTITIES is to be found
3. From ENTITIES several features are identified
4. Every line is start with AcDbLine and ends with a character 0
5. X_{start} is shown by 10 and Y_{start} is by 20
6. X_{end} is shown by 11 and Y_{end} is by 21
7. Lowest value of X and Y is determined and is set to origin of the coordinate by subtracting them from all the coordinates.
8. Generation of G-Code is executed from the highest value of x at which the value of Y is no equal to the value of coordinate origin value of Y. there is such one point, in this case this value is (40, 15)

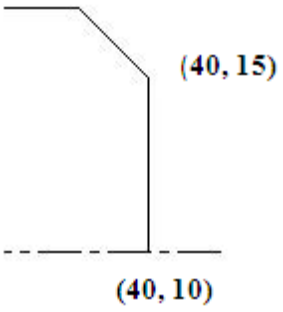

9. As cutting is starting from some far from the workpiece thus for rapid positioning cutting tool is

positioned in the position at +2 in X axis and -2 in y axis from the first point(in this case (40, 15)).

10. For this case starting point is (42, 13).

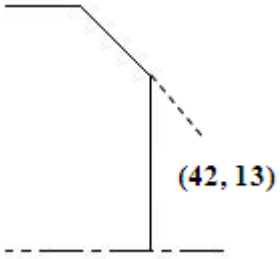

11. For G-Code representation X axis of the coordinate system is represented as Z and Y axis of coordinate system is as X. The Codes used is elaborated later in the chapter. So for initial rapid positioning G-code is G00. The formulae used to define is as following
    $(X\text{-}X_{origin}) = X_{start}$
    Represented as Z….
    $(Y\text{-}Y_{origin}) \times 2$ = diameteRepresented as X…
    So after rapid positioning first line become

So for corresponding G-code for clockwise circular interpolation is G02 and for counterclockwise circular interpolation is G03.

G 00 Z 32 X 6

12. Then linear interpolation is made with respect to descending order of X axis coordinate in the DXF file 10, 11 commands. So next line in G-code become G 01 Z 28 X 14
13. Another type of feature include in the profile is fillet. To represent fillet circular interpolation is necessary. When AcDbCircle is found in the DXF file it implies there is some circular shape.
14. For circular shape 10, 20 imply coordinate of center of the circle and 40 implies radius of the circle. One important measure is either the circle is clockwise or anticlockwise. 50, 51 imply the starting angle and ending angle. If 50 and 51 range from 0 to 179 degree then the circular shape is clockwise and if range of 50, 51 is 180 to 359 then circular shape is counterclockwise

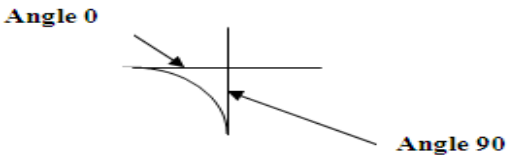

15. For this sample problem for first fillet which is clockwise and following G-code is obtained for the input of DXF file.
    G02 Z18 X20 R 3
16. For this sample problem for second fillet which is counterclockwise and following G-code is obtained for the input of DXF file.
    G03 Z16 X28 R 2
    After linear interpolation when there is some gap program understand it as fillet and by the descending order of X coordinate it arrange the G-code command.
    Similarly circular interpolation is done for all AcDb Circle command.

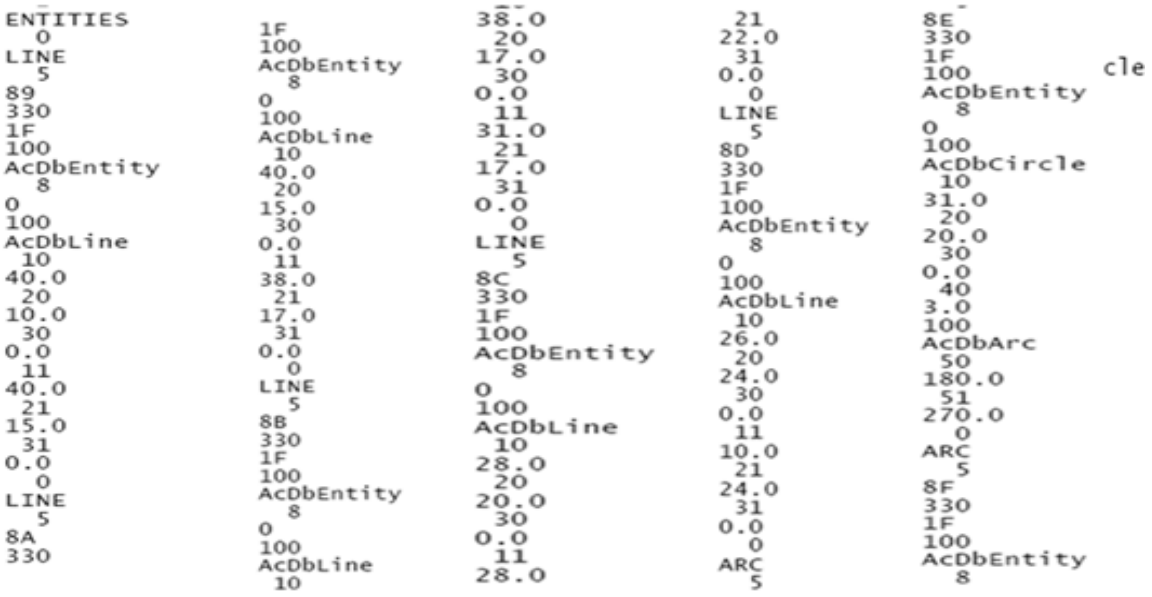

IV. CONCLUSION

Computer-Integrated Manufacturing has gained recognition as a most effective tool in increasing manufacturing competitiveness. The paper provides a rigorous basis for the understanding of process planning of rotational parts and the development of effective and efficient Computer-Aided Process Planning systems. This paper defined CAPP module for data transmissions which is based on information received from the computer aided design of the products and on the technological database with information on technological equipment, devices and cutting tools. Realizing the CAPP module for data transmissions has led to an increase of the flexibility and correctness of the technological planning, having favorable influences on the manufacturing costs.

IV. REFERENCES

1) Alting, L. and Zhang, H. C., (1989), "Computer aided process planning: the state-of-the-art survey", *International Journal of Production Research*, vol. 27(4), pp. 553 – 585.
2) Alam, M. R., Lee, K. S., Rahman, M. and Zhang, Y. F., (2000), "Automated process planning for the manufacture of sliders", *Computers in Industry*, vol. 43, pp. 249-262.
3) Aslan, E., Seker, U and Alpdemir, N., (1999), "Data extraction from CAD model for rotational parts to be machined at turning centres", *Journal of Engineering and Environmental Science*, vol. 23, pp. 339-347.
4) Atkinson, A., (1991), "Manufacturing parts features: CIM's technological common denominator", *Integrated Production Systems – Design, Planning, Control and Scheduling*, fourth edition, Institute of Industrial Engineers, Norcross, Georgia.
5) Cay, F. and Chassapis, C., (1997), "An IT view on perspectives of computer aided process planning research", *Computers in Industry*, vol. 34, pp. 307-337.
6) Chang, T. C. and Wysk, R. A, (1985), "Introduction to Automated Process Planning System", Prentice-Hall International Inc., pp 165-181.
7) ElMaraghy, H. A., (1993), "Evolution and future perspectives of CAPP", *Annals of CIRP*, vol. 42(2), pp. 1-13.
8) Groover, M. P., (1987), "Automation, production systems and computer integrated manufacturing", Prentice-Hall International Inc., pp 721.
9) Gindy, N. N. Z., (1989), "A hierarchical structure for form features", *International Journal of Production Research*, vol. 27, no. 12, pp. 2089-2103.
10) Han, J. H., Pratt, M. and Regli, W. C., (2000), "Manufacturing feature recognition from solid models: a status report", *IEEE Transactions on Robotics and Automation*, vol. 16, no. 6, December.
11) Houtzeel, A., (1976), "The MICLASS system", Proceedings of CAM-I's Executive Seminar – Coding, Classification and Group Technology for Automated Planning, p-76-ppp01, CAM-I, Arlington, TX, USA.
12) Kanai, S., Sugawara, M., Kishinami, T. and Saito, K., (1988), "The flexible process planning by combining the advanced CAPP, CAM and measuring system", 16th North American Manufacturing Research Conference Proceedings, University of Illinois, Urbana, Illinois, May 24-27.
13) Marefat, M. and Britanik, J, (1996), "Automated reuse of solutions in manufacturing process planning through a case-based approach", Proceedings of the 1996 ASME Design Engineering Technical Conference and Computers

in Engineering Conference, Irvine, California, August 18-22.

14) Naish, J. C., (1996) —Process capability modeling in an integrated concurrent engineering system – the feature-oriented capability module", *Journal of Materials Processing Technology*, vol. 61, pp. 124 – 129.
15) Niebel, B. W., (1965), —Mechanized process selection for planning new designs", *ASME*, paper no. 737
16) Pande, S. S. and Prabhu, B. S., (1990) —An expert system for automatic extraction of machining features and tooling selection for automats", *Computer Aided Engineering Journal*, pp. 99-103, August.
17) Pressman, R. S., (2001) —Software engineering – a practitioner's approach", McGraw Hill, 5th Edition.
18) Law, H. W., Tam, H. Y., Chan, A. H. S. and Hui, I. K., (2001), —Object-oriented knowledge-based computer-aided process planning system for bare circuit boards manufacturing", *Computers in Industry*, vol. 45, pp. 137 – 153.
19) Lee, K., (1999), —Principles of CAD/CAM/CAE Systems", Addison-Wesley, pp. 294-304.
20) Lee, K. S., Alam, M. R., Rahman, M. and Zhang, Y. F., (2001), —Automated process planning for the manufacture of lifters", *The International Journal of Advanced Manufacturing Technology*, vol. 17, pp. 727-734.
21) Li, R. K. and Adiga, S., (1987), —Part feature recognition system – a vital link in the integration of CAD and CAM", Proceedings of 9th International Conference on Production Research, Cincinnati, Ohio, USA, August 17-20.
22) Link, C. H., (1976), —CAPP – CAM-I automated process planning system", Proceedings of 13th Numerical Control Society Annual Meeting and Technical Conference, pp. 401-408, March.
23) Trika, S. N. and Kashyap, R. L., (1994), —Geometric reasoning for extraction of manufacturing features in iso-oriented polyhedrons", *IEEE Transactions on Pattern Analysis and Machine Intelligence*, vol. 16, no. 11, November.
24) Tyan, L. W. and Devarajan, V., (1998), —Automatic identification of non-intersecting machining features from 2D CAD input", *Computer Aided Design*, vol. 30, no. 5, pp. 357-366.
25) Wong, T. N. and Wong, K. W., (1995), —A feature-based design system for computer-aided process planning", *Journal of Materials Processing Technology*, vol. 52, pp. 122 – 132.
26) Wysk, R. A., (1977), —An automated process planning and selection program: APPAS", PhD dissertation, Purdue University, West Lafayette, IN, USA.
27) Zeid, Ibrahim, (2002), —CAD/CAM Theory and Practice", Tata-McGraw-Hill, sixth reprint,pp.9951

Influence of Matrix Stiffness, CNT Thickness, Poisson's Ratio, and Interphase on Effective Longitudinal Modulus of CNT Based Composites for Square RVE

GJRE Classification (FOR)
GJRE: D; 100702

Md. Mohiuddin[1] Mohammad Abu Hasan Khondoker[2] Golam Kabir[3] Md. Abdulla Al Masud[4]

***Abstract*-This paper presents a computational modeling approach for evaluating the mechanical behavior of CNT based nanocomposite. The CNT's interaction with matrix material was modeled using the continuum mechanics theory and finite element approach. The effective mechanical properties of CNT based nanocomposite were then evaluated by using the finite element method (FEM) models. Two different models were constructed. The first model was a CNT through the length of the square representative volume element (RVE). The second model considers a CNT inside the square representative volume element (RVE). Several numerical examples were carried out to investigate the influence of Young's modulus of matrix, CNT thickness, Poisson's ratio and interphase on the effective modulus of CNT based nanocomposite in longitudinal direction. The computed results were compared with those obtained from the simple rule of mixture for validity.**

Keywords-Carbon nanotube, Finite element method, Representative volume element

I. Introduction

Simulations of individual CNTs using atomistic or molecular dynamics (MD) models have provided abundant results for the understanding of mechanical and electrical behaviors of the CNTs (Kang and Hwang, 2001; Garg and Sinnott, 1998). However, these atomistic or MD simulations are currently limited to very small length and time scales and cannot deal with the larger length scales in nanocomposites, due to the limitations of current computing power (for example, a 1 × 1 × 1 μm3 cube could contain up to 1012 atoms). Nanocomposites for engineering applications expand from nano to micro, and eventually to macro length scales, which must be addressed by other simulation approaches or combinations of MD with other approaches. Continuum approaches based on continuum mechanics have also been applied successfully for simulating the mechanical responses of individual or isolated carbon nanotubes which are treated as beams, thin shells or solids in cylindrical shapes (Govindjee and Sackman, 1999). These studies suggest that the continuum mechanics approach can be applied safely to investigate the mechanical behaviors of the CNTs when the lengths of the CNTs are about 100 nm and above. For example, in the study of Wong et al., 1997, the authors successfully applied the simple beam theory to model CNTs and extracted Youngs modulus of the CNT from the force–deflection curve obtained from their experiment. Their results are consistent with other reported work. Although successful to some extent and efficient in computation for models at larger length scales, continuum mechanics at this threshold faces the risk of breakdowns more than ever before, compared with the micromechanics simulations. The preferred approach for simulations of CNT-based composites should be a multiscale one where the MD and continuum mechanics are integrated in a computing environment that is detailed enough to account for the physics at nanoscales while efficient enough to handle nanocomposites at larger length scales. Before a multiscale approach for simulations of nanocomposites is successfully developed, the continuum mechanics approach seems to be the only feasible approach now for conducting some preliminary studies of such materials.

Nomenclature:

ε_z = longitudinal extension resulting from the load in the composite
ε_z^t = longitudinal extension resulting from the load in the CNT
ε_z^t = longitudinal extension resulting from the load in the matrix
E^t = Young's modulus of the CNT
E^m = Young's modulus of the matrix
V^t = Volume fraction of the CNT = $(1-V^m)$
V^m = Volume fraction of the matrix = $(1- V^t)$
V = Volume of the total composite
A^t = Cross-sectional area of the CNT
A^m = Cross-sectional area of the matrix
A = Cross-sectional area of the total composite
F_z = Total force applied at longitudinal direction
F_t = Force shared by only CNT
F_m = Force shared by only matrix
σ_z = Total stress applied at longitudinal direction
σ_t = Stress experienced by only CNT
σ_m = Stress experienced by only matrix

About-[1]Department of Industrial and Production Engineering, Bangladesh University of Engineering and Technology, Bangladesh
About-[2]Department of Industrial and Production Engineering, Bangladesh University of Engineering and Technology, Bangladesh
About-[3]Department of Industrial and Production Engineering, Bangladesh University of Engineering and Technology, Bangladesh
About-[4]Department of Industrial and Production Engineering, Bangladesh University of Engineering and Technology, Bangladesh
(e-mail: aamasud@ipe.buet.ac.bd)

r_i = Inner radius of CNT
r_o = Outer radius of CNT
a = Side of the matrix of square RVE

In the study of Liu and Chen, 2002 the interactions of the CNT with the matrix, interfacial stresses and load-carrying capabilities of the CNTs are investigated based on 3-D elasticity models. It is proposed in that instead of beam or shell models, the 3-D elasticity models should be used for the CNTs, as well as the matrix, in order to ensure the accuracy and compatibility of the models for the CNTs and the matrix (Liu and Chen, 2002). One way to develop manageable 3-D continuum models for the study of CNT-based composites is to extend the concept of representative volume elements used for conventional fiber-reinforced composites at the microscale (Nasser and Hori, 1999). CNTs are in different sizes and forms when they are dispersed in a matrix to make a nanocomposite. They can be single-walled or multi-walled with length of a few nanometers or a few micrometers, and can be straight, twisted and curled, or in the form of ropes (Wagner, 2002; Qian et al., 2002). Their distribution and orientation in the matrix can be uniform and unidirectional (which may be the ultimate goal) or random. All these factors make the simulations of CNT-based composites extremely difficult. To start with, the concept of unit cells or representative volume elements, which have been applied successfully in the studies of conventional fiber-reinforced composites at the microscale (Nasser and Hori, 1999) can be extended to study the CNT-based composites at the nanoscale. In this RVE approach, a single (or multiple) nanotube(s) with surrounding matrix material can be modeled, with properly applied boundary and interface conditions to account for the effects of the surrounding materials. Numerical methods, such as the FEM, boundary element method (Liu and Chen, 2002) or meshfree method (Qian et al., 2002) can be applied to analyze the mechanical responses of these RVEs under different loading conditions. Interfaces between the CNTs and matrix are crucial regions to ensure the load carrying capacity and other functionalities of the nanocomposites. There are also more difficult regions for any simulation approaches. To start with, perfect bonding can be assumed between the CNTs and matrix in the continuum mechanics models of CNT-based composites. Research has demonstrated that the possibility of such a strong (C–C) bond exists for CNT-based composites (Thostenson et al., 2005). For a _less" perfect bond, a spring-like model can be used between the CNTs and matrix. A thin interphase model (e.g., a thin coating on the CNTs) can also be introduced to account for a third phase between the CNTs and matrix. The properties of this interphase region can be used to characterize the interface properties. Other interface models, such as friction models considering the slip/stick along a CNT/ matrix interface or a van der Waals type of models (Qian et al., 2002) (for multi-walled CNTs) can certainly be developed for modeling CNT-based composites, with improved understanding based on further nanoscale experiments and MD simulations. In this paper, only the perfect bonding between the CNT and the matrix in RVE models is considered. Three nanoscale representative volume elements based on the 3-D elasticity theory have been proposed in Liu and Chen, 2002 for the study of CNT-based composites. They are the cylindrical RVE, square RVE and hexagonal RVE. The cylindrical RVE can be applied to model the CNTs which have different diameters (Riddick and Hyer, 1998) or CNTs embedded in a regular carbon fiber. Under axi-symmetric as well as anti-symmetric loading, a 2-D axi-symmetric model can be applied for the cylindrical RVE, which can significantly reduce the computational work (Govindjee and Sackman, 1999). Similar to the study of conventional fiber-reinforced composites (Riddick and Hyer, 1998) the square RVE models can be applied when the CNTs are arranged evenly in a square array, while the hexagonal RVE models can be applied when CNTs are in a hexagonal array, in the transverse direction. These RVEs can be used to study the interactions of a CNT with the matrix, such as the load transfer mechanism and stress distributions along the interfaces (Govindjee and Sackman, 1999) or to evaluate the effective material properties of the CNT-based composites, which is the focus of this current paper.

To start with, the cylindrical RVE will be employed first in this paper to evaluate the effective Young's moduli and Poisson's ratios of the CNT based composites. The required mathematical results to be used to extract these material constants from the simulation results (by using either the FEM or other methods) will be established in section 2. In section three finite elements modeling technique for long continuous and short fiber is described. In results and discussion section, influence of matrix young modulus, CNT thickness, Poisson's ratio and interphase on the longitudinal elastic modulus of CNT based composites is studied.

II. Analysis

Depending on the problem definition, geometry, boundary conditions and material properties, three types of analysis can be performed on a structure. 2D analysis is mainly used to conserve the computational resources. It is less time consuming and is less accurate. 3D analysis is time consuming approach requiring high computational resources because of the 3-D elements used. It is relatively accurate than 2D analysis, and is used in situations where 2D degeneration is not possible. Symmetric analysis is performed taking advantage of the symmetric geometry. A quarter or half the model is created and analyzed by applying symmetric boundary conditions. This approach significantly reduces the cost, computer memory and the time required. In this study symmetric analysis is performed for the RVE models by modeling only the quarter model of the geometry and applying axi-symmetric boundary conditions.

Computational approaches consists of both molecular dynamics approach and numerical or continuum mechanics. Continuum mechanics in the past has been successfully used in characterizing CNT based composites. It is a very feasible, cost effective and an efficient approach at present to characterize large-scale CNT-based composites for mechanical properties using the finite element modeling and simulations. Preliminary results obtained in this research can

be compared with the available experimental and MD results from similar models reported in previous literature (Treacy et al., 1996). In all the studies performed in the literature (Thaw et al., C., 1987; Mortensen et al., 1988), CNTs are considered as homogeneous and isotropic materials and are represented by continuum beam, shell and 3-D solid elements. This approach is in general used to analyze for deformation, buckling, and dynamic responses of CNTs and overall response of the nanocomposite. Using this approach, emphasis is to be placed on overall responses of the CNT based composites and load carrying capabilities rather than the localized detailed phenomena, like interfacial stresses or bonding. MD approach, on the other hand, is preferred in studying the detailed interfacial characteristics.

Continuum mechanics approaches like the BEM other than the FEM are turning out to be ideal tools for RVE model, nanocomposites, and its validation has been demonstrated in previous literature (Gao et al., 1998; Buongiorno et al., 2000). This concept has been successfully applied in the past for characterizing conventional fiber-reinforced composites. The same has been extended to nanocomposites here. This kind of model works by modeling a single CNT or multiple CNTs in a surrounded matrix with appropriate boundary conditions and interface conditions (perfect bonding assumed in our case). Later on, after modeling the RVE model the FEM is applied to characterize for the overall mechanical response of the RVE (effective Young's modulus of the composite). Modeling considerations in characterizing CNT-based composites have been proposed and discussed in (Thaw et al., C., 1987). The first and foremost task is to employ 3-D elasticity models replacing beams and shell models for modeling CNT-based composites. This is basically to ensure accuracy and compatibility between CNTs and matrix in the composite. Hence 3-D solid elements for both CNTs and matrix have been used in the models demonstrated by Liu and Chen (2004) in characterizing CNT-based composites. The results reported are in complete agreement with the rule of mixtures results, although further development and validation of their models was required. The research work performed here successfully validates the FEM results with MD, constitutive modeling and rule of mixtures as well. The validation and agreement of the continuum mechanics results can play a significant role for numerical approaches like the FEM, which can be further used for characterizing large models. Emphasis is being placed on modeling large-scale composite models using pipe elements instead of beam and shell elements. The results shown in section 4 challenges that FEM can be an excellent estimate for evaluating elastic moduli of large-scale composites. Hence FEM, which is cost effective and efficient, in the future can be used for characterizing nanocomposites, significantly reducing computational time, memory and hard-disk space.

In this experiment it is assumed that both the CNTs and matrix in a RVE are continua of linearly elastic, isotropic and homogenous materials, with given Young's moduli and Poissons ratios. It is also assumed that the CNTs and matrix are perfectly bonded at the interface in the RVE to be studied. Other material models and interface conditions (Chen and Liu, 2002) can certainly be considered in more sophisticated investigations. The RVE can contain one CNT or multiple CNTs, determined by the main criterion that it should be large enough to be representative of the material and small enough to be modeled and analyzed efficiently using a solution method. Under the above assumptions, there will be four effective material constants to be determined for the CNT-based composite, namely, two Young's moduli E_x (= E_y) and E_z, and two Poisson's ratios ν_{xy} and ν_{zx} (= ν_{zy}). To derive the formulas for extracting the four material constants, a homogenized elasticity model corresponding to the RVE is considered. The geometry of the elasticity model is corresponding to a hollow cylindrical RVE with length L, inner radius r_i and outer radius R, so that analytical solutions can be obtained. This geometry can account for the cases when the CNT is relatively long and thus all the way through the length of the RVE. In the case that the CNT is relatively short and thus fully inside the RVE, a solid cylindrical RVE (r_i = 0) can be used for extracting the material constants, since the elasticity solutions are difficult to find in this case. The elasticity model has a single material with the four effective material constants (E_x, E_z, ν_{xy} and ν_{zx}) to be determined.

The geometry of the elasticity model is corresponding to a hollow cylindrical RVE with length L, inner radius r_i and outer radius R. This geometry can account for the cases when the CNT is relatively long and thus all the way through the length of the RVE. In the case that the CNT is relatively short and thus fully inside the RVE, a solid cylindrical RVE (r_i = 0) can be used for extracting the material constant, since the elasticity solution are difficult to find in this case.[12]

For axial loading, the stress and strain components at any point on the lateral surface are,

$\sigma_r = \sigma_\theta = 0$

$\varepsilon_z = \frac{\Delta L}{L}$ And $\varepsilon_\theta = \frac{\Delta R_a}{R}$

With ΔRa < 0, if $\Delta L > 0$. Where ΔRa is the radial displacement and r and θ indicate the radial and tangential components respectively. So,

$$\varepsilon_z = \frac{\sigma_z}{E} - \nu\frac{\sigma_z}{E} - \nu\frac{\sigma_\theta}{E}$$

Then, $E_z = \frac{\sigma_z}{\varepsilon_z} = \frac{\Delta L}{L}\sigma_{avg}$ (1)

Where the averaged stress is given by

$$\sigma_{avg} = \frac{1}{A}\iint_A \sigma_z\left(x, y, \frac{L}{2}\right) dx\, dy \quad (2)$$

Where, A is the area of the end surface and σ_{avg} can be found for the RVE using the FEM results (i.e.) from the ANSYS 10.0 outputs. Thus, to evaluate the effective Young's modulus of the CNT based nanocomposites; the RVEs are studied using the finite element method first. Then the deformations and stresses are computed for the axial loading case. After that, the FEM results are processed and

equations are used to extract the effective Young's modulus for the CNT based composites.

A. Rule of Mixtures Theory for Long CNT

Prediction of effective material properties of the compositebased on strength of materials theory is given by simpleanalytical expressions (rule of mixtures). This rule ofmixtures along with some extended results in the case of fiber-reinforced composites has been successfully applied in the past for carbon nanocomposites. The effective longitudinal Young's modulus of the CNT–reinforced composite using the rule of mixtures expression is used here to validate the numerical results obtained using the FEM. However this strength of materials theory is not accurate when evaluating the interfacial stress but is found to be efficient and accurate in predicting the effective material constants (Young's modulus, Poisson's ratio) in the axial and transverse direction of the RVE's, which are dependent on the overall responses of the RVE's.

The addition of long or continuous CNTs (with large aspect ratio i.e., the ratio of the characteristic length L to the characteristic diameter D of the CNT) to a polymer matrix mainly enhances its stiffness and strength. Taking advantage of the continuous structure only a segment can be modeled using RVE, which is shown in Figure 1.

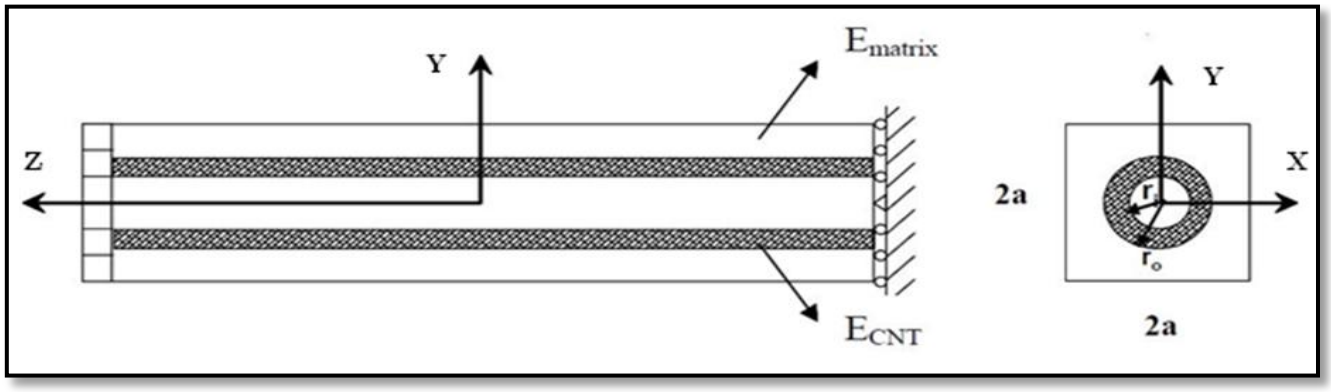

Figure 1: Continuous Fiber Reinforced Inside the Matrix

Therefore, a segment can be modeled using an RVE under some assumptions. They are-

1. CNT fibers are uniform, parallel and continuous
2. Perfect bonding between CNT and matrix therefore, load applied is shared by both CNT and matrix. So,

$$F_z = F_t + F_m$$

3. Longitudinal load produces equal strain in CNT and matrix: It is assumed that the longitudinal extensions resulting from the load are the same in the composite, CNT and the matrix. So,

$$\varepsilon_z = \varepsilon_z^t = \varepsilon_z^t$$

Stress can be calculated from force divided by area experiencing the stress. So,

$$\sigma_z A = \sigma_t A^t + \sigma_m A^m \quad (3)$$

Now, according to Hooke's law, Young's modulus is the ratio of stress by strain. So,

$$E_z \varepsilon_z A = E^t \varepsilon_z^t A_t + E^m \varepsilon_z^t A_m$$

Then, $E_z A = E^t A^t + E^m A^m$

And, $E_z = E^t \left(\frac{A^t}{A}\right) + E_m \left(\frac{A^m}{A}\right)$

Finally, $E_z = E^t V^t + E^m V^m = E^t V^t + E^m (1\text{-}V^t) \quad (4)$

For a square RVE the volume fraction of the CNT is defined by

$$V^t = \frac{\pi(r_o^2 - r_i^2)}{(4a^2 - \pi r_i^2)} \quad (5)$$

This is the same rule of mixtures, which is being applied for predicting the effective Young's modulus for the conventional fiber-reinforced composite in the fiber direction. It has been verified in the past for the agreement with the experimental results obtained from carefully controlled experiments for tensile loading. It agrees well (within 5%) while the predictions are not so good for the compressive loading case.

B. Rule Of Mixtures Theory For Short CNT

Short nanotube reinforced composites analyzed in the past, found not as strong as composites with continuous nanotubes and cannot be used for critical structural applications. It has been demonstrated from molecular dynamics (Qian et al., 2003) and continuum mechanics that the effective modulus of the composite using short CNTs is far less compared to the increase in modulus using long (continuous) CNTs. In this case, the RVE can be divided into two segments: one segment accounting for the two ends with total length L_e and Young's modulus E_m; and another segment accounting for the center part with length L_c and an effective Young's modulus E_C

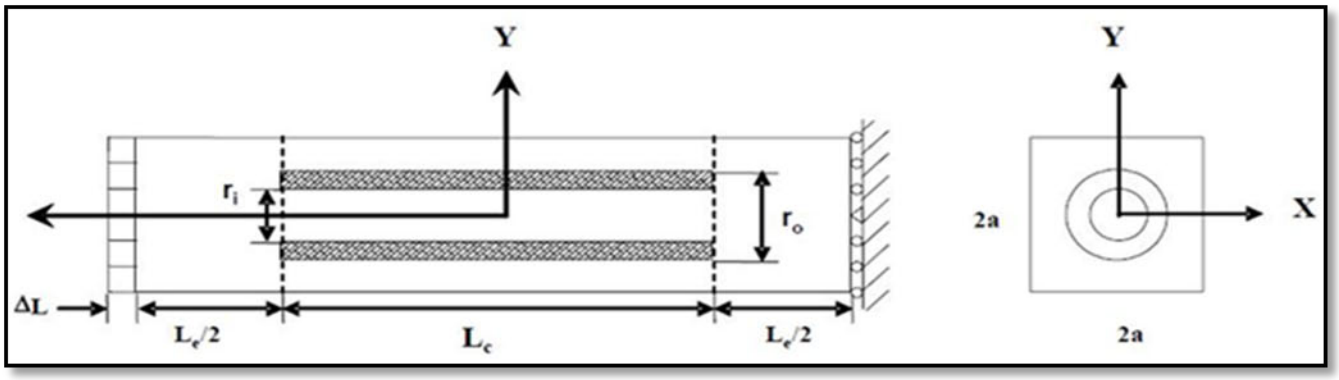

Figure 2: Short Fiber Reinforced Inside the Matrix

It is Notable that the two hemispherical end caps of the CNT have been ignored in this derivation. Since the center part is a special case of long CNT, its effective Young's modulus is found to be

$$E^c = E^t V^t + E^m (1 - V^t) \quad (6)$$

Again, by considering the compatibility of strains and equilibrium of stresses, one obtains the following expression for the effective Young's modulus in the axial direction.

$$E_z = \left[\frac{1}{E^m}\left(\frac{L_e}{L}\right) + \frac{1}{E^c}\left(\frac{L_c}{L}\right)\left(\frac{A}{A_c}\right)\right]^{-1} \quad (7)$$

Alternatively, in a more symmetric form:

$$\frac{1}{E_z} = \left[\frac{1}{E^m}\left(\frac{L_e}{L}\right) + \frac{1}{E^c}\left(\frac{L_c}{L}\right)\left(\frac{A}{A_c}\right)\right] \quad (8)$$

In which the areas $A = 4a^2$ and $A_c = (4a^2 - \pi r_i^2)$, above equation can be viewed as an extended rule of mixtures compared to that given in Equation (1), and can be employed to estimate the effective Young's modulus for the short CNT case when the CNT is inside the RVE. The equation of rule of mixture when using an additional interphase between CNT and matrix

$$E^c = K^1 E^t V^t + K^2 E^I V^I + E^m (1 - V^t - V^I) \quad (9)$$

where V^t and V^I are volume fractions of phases 1 and 2, representing carbon nanotubes and interphase respectively, E^t and E^I are properties of phases 1 and 2, representing carbon nanotubes and carbon fibers, respectively, E^m is property of the polymer matrix, K^1 is the CNT efficiency parameter, which will be assumed equal to 1, K^2 is the interphase efficiency parameter, which is equal to 1 for continuous aligned fibers in the direction of alignment.

III. Modeling

In this paper the cylindrical RVEs (Fig.1, 2) for a single-walled carbon nanotube in a matrix material are modeled using the finite element modeling software ANSYS 10.0. The deformations and stresses are computed for the axial loading cases (Fig. 1, 2). Two cases are studied, one on a RVE with a long CNT and the other on a RVE of the same size but with a short CNT.

A. Model Description for Long CNT

In long CNT, matrix was assumed as square with 20nm side length and the total length of matrix was 100nm and 100nm long CNT through the matrix was also assumed. Values of the dimensions and material constants are chosen for this thesis for illustration purposes only, which are within the wide ranges of those for CNTs reported in the literature (Chen and Liu, 2004; Qian et al., 2003; Wong et al., 1997; Lu, 1997 and Li and Saigal, 2007). Length of CNT and matrix was constant throughout the analysis. Model was symmetric so we took the benefit of symmetricity by taking quarter of model to simulate the results. The volumes comprising the NT and matrix immediately adjacent to it are meshed using 20 node bricks containing midside nodes. This allows element edges to be parabolic in shape, which accurately captures the CNT surface (Bradshaw1 et al., 2004). These higher order elements are also well suited to modeling the high strain gradients that exist close to the NT. The remaining volumes were meshed with 8 node bricks to reduce the number of degrees freedom while still providing sufficient detail to capture the slowly varying strain fields closer to the model exterior (Bradshaw1 et al., 2004).

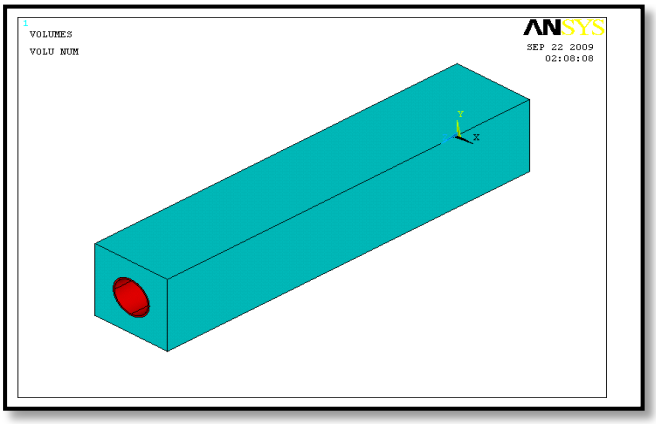

Figure 3: Full Model of Square RVE with Long CNT in Matrix

Proper boundary conditions were applied to the model to find the stress value of the square RVE with long CNT. One end of the matrix and CNT areas was constrained in the axial directions and frees to move in the lateral directions. One of the two free edges was constrained in vertical direction and the other in horizontal direction to allow for the expansion and contraction of the CNT in compression and tension respectively. Symmetric boundary conditions were applied on the quarter model to account for the full model. Displacement boundary conditions instead of pressure boundary conditions were applied on the model to exactly simulate the model as in experimental testing. Pressure boundary conditions on the CNT and matrix makes them elongate with different strain values, with matrix having more elongation than the CNT as CNT has very high stiffness compared to the matrix material. Hence, similar boundary conditions as applied in experimental testing, equal displacements on the matrix and CNT (1nm constant) in the longitudinal direction were applied for analysis, in evaluating the properties of a unidirectional composite (Fisher et al., 2002).

B. Model Description For Short CNT

Like long CNT, matrix of short CNT was assumed as square with 20nm side length and the total length of matrix was 100nm. Short CNT was 50nm in length with 5nm radius of each hemispherical cap. Length of CNT and matrix was constant throughout the analysis. Values of the dimensions and material constants are chosen for this thesis for illustration purposes only, which are within the wide ranges of those for CNTs reported in the literature (Chen and Liu, 2004; Qian et al., 2003; Wong et al., 1997; Lu, 1997 and Li and Saigal, 2007). Model was symmetric so we took the benefit of symmetricity by taking quarter of model to simulate the results[15]. 20 node bricks containing midside nodes used to mesh the CNT and 8 node bricks used to mesh the matrix (Fisher et al., 2002).

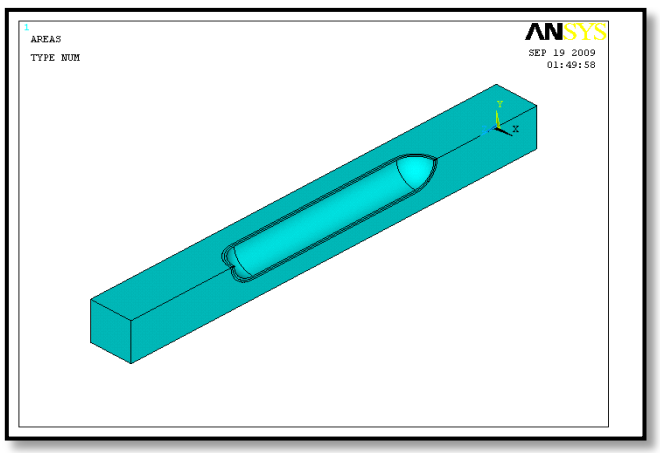

Figure 4: Square RVE, 3D Quarter Model of Short CNT Inside Matrix

Boundary conditions for short CNT-RVE was similar to long CNT model were applied to evaluate the effective longitudinal Young's modulus of the composite. CNT was aligned in axial (loading) direction and the area on one end is totally constrained in axial direction and a displacement of 1nm was applied on the other end. Displacement constraints are so applied that the system was allowed to contract and expand when in tension and compression respectively. Symmetric boundary conditions are applied accordingly to simulate the full model from the quarter model (Chen and Liu, 2004).

IV. Results and Discussion

A. Long Continuous CNT Reinforced RVE

In Long CNT RVE model CNT is through the matrix. In this section effect of matrix stiffness, poisson's ratio, CNT thickness and interphase will be discussed for long fiber. Finite element mesh quarter view of a long continuous CNT based model is shown below.

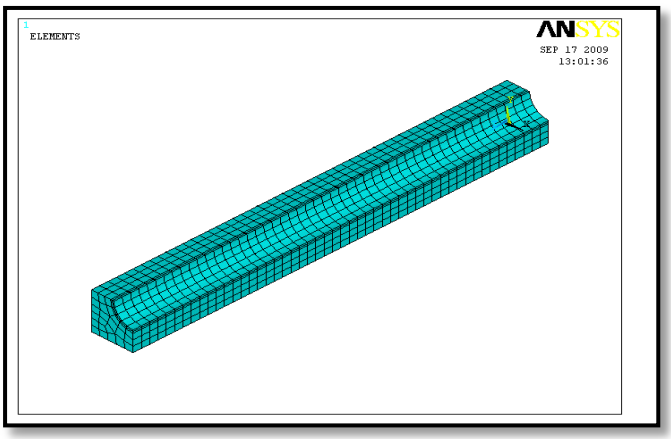

Figure 5: Finite Element Mesh Quarter of Model for the Long CNT Based Model with Et/Em = 1000/30.

B. Effect of Young's Modulus of Elasticity of Matrix on the Effective Longitudinal Modulus of the Nanocomposite (E_z)

Model parameters: For modeling purpose following parameters was used with 0.40nm CNT thickness and 10nm side length according to various previous literatures (Chen and Liu, 2004; Qian et al., 2003; Wong et al., 1997; Lu, 1997; Li and Saigal, 2007 and Bradshaw1 et al., 2004).

Phase	Poisson‘s ratio	Length (nm)	Young‘s modulus(GPa)
CNT	0.30	100	1000
Matrix	0.30	100	various

The Effective longitudinal modulus of the Composite is computed at different value of Young‘s modulus of matrix phase such as 5,10,15,20,25,30,40,50,60,70,80,90,100 using both finite element and rule of mixture. From figure, it was observed that variation of results for FEA and rule of mixture was negligible and effective longitudinal modulus of the Composite increase with the increase of Young‘s modulus of matrix as which was expected. Changing the value of Young‘s modulus of matrix from 5 to 100 causes almost 92.4404 GPa increase in effective longitudinal modulus of the nanocomposites. Figure 6 shows below the effective longitudinal modulus of the Composite with the increase of Young‘s modulus of matrix. Results obtained from rule of mixture theory are also shown in the Figure

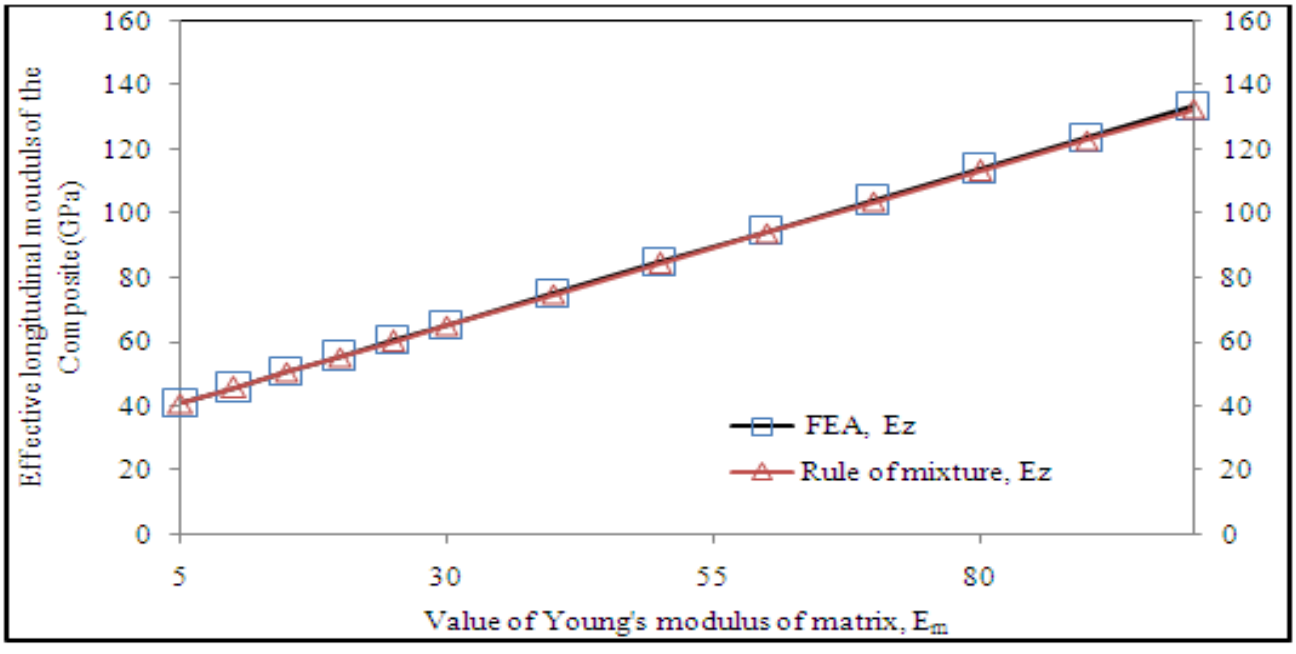

Figure 6: Comparison of Effective Modulus of the Composite in Longitudinal Direction Vs Varying Young‘s Modulus of the Matrix Reinforced with Long CNT Of Thickness 0.4nm with 3.617% Volume Fraction

C. Effect of Poisson’s Ratio on the Effective Longitudinal Modulus of the Nanocomposites

Model parameters: To find the effect of Poisson‘s Ratio on modulus of nanocomposites following parameters were used according to various previous literatures (Chen and Liu, 2004; Qian et al., 2003; Wong et al., 1997; Lu, 1997; Li and Saigal, 2007 and Bradshaw1 et al., 2004).

Phase	Poisson‘s ratio	Length (nm)	Young‘s modulus (GPa)
CNT	Various	100	1000
Matrix	Various	100	30

For all previous simulations the Poisson‘s ratios of the matrix and nanotube were assumed to be equal (Poisson‘s ratio of NT=Poisson‘s ratio of matrix=0.30) to simplify the analysis. For many practical nanotube-polymer systems, the difference in Poisson ratio is expected to be relatively small, with NT typically predicted in the range of 0.20–0.30 and possion‘ ratio of matrix for a typical structural polymer varies approximately 0.25–0.40 (Fisher et al., 2002). In this paper, Poisson‘s ratio of matrix and CNT varied from 0.2 to 0.4 to find the effect of various Poisson‘s ratio in effective

longitudinal modulus. Effect of Poisson's ratio on the effective longitudinal modulus of the nanocomposites is Shown in Figure7.

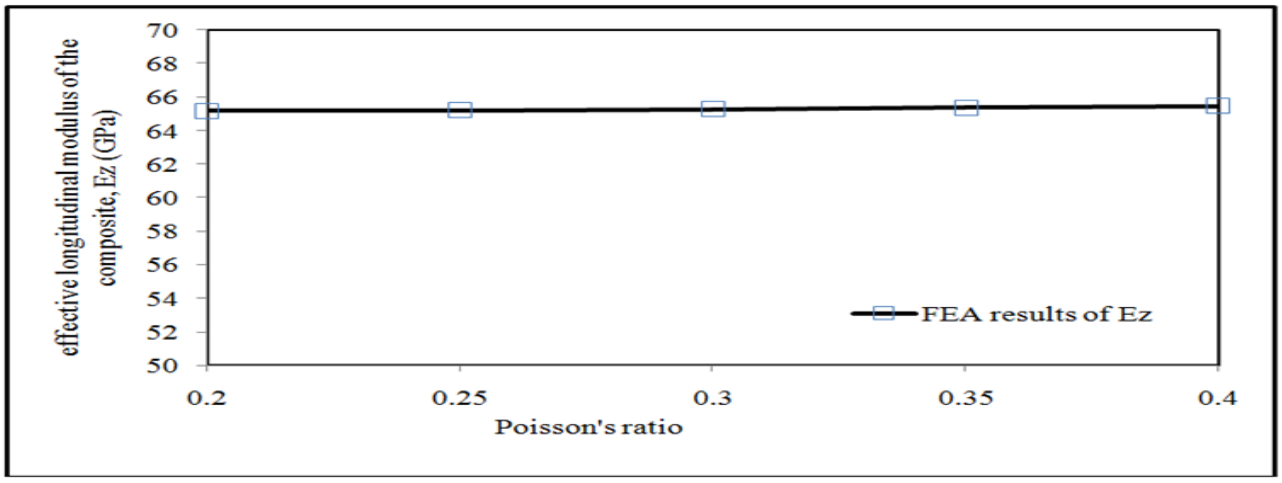

Figure 7: Comparison of Effective Modulus of the Composite in Longitudinal Direction Vs Various CNT and Matrix Poisson's Ratio with Long CNT of Thickness 0.4nm with 3.617% Volume

From the study it is found out that effective longitudinal modulus of the nanocomposites remains same with the increase of both Poisson's ratio of CNT and matrix. With the increase of Poisson's ratio from 0.2 to 0.4, effective longitudinal modulus of nanocomposites increased by 0.4704%. So we found that the effect of the Poisson's ratio of the CNT and matrix on the composite on the simulation is negligible.

D. Effect of CNT Thickness on the Effective Longitudinal Modulus of the Nanocomposites (E_z)

Model parameters

Phase	Poisson's ratio	Length (nm)	Young's modulus(GPa)
CNT	0.30	100	1000
Matrix	0.30	100	30

Composite effective modulus of the composite in longitudinal direction increases with the increase of CNT thickness. It can be explain that as thickness of CNT increase and as usual volume fraction, so total strength of the composite also increases. Because by rule of mixture theory composite's tensile modulus is directly proportional to CNT volume fraction. As CNT's modulus of elasticity is higher than matrix so increases of volume fraction of CNT increases the composite's strength. Figure 8 shows the effect of CNT thickness on the effective longitudinal modulus of the nanocomposites (E_z).

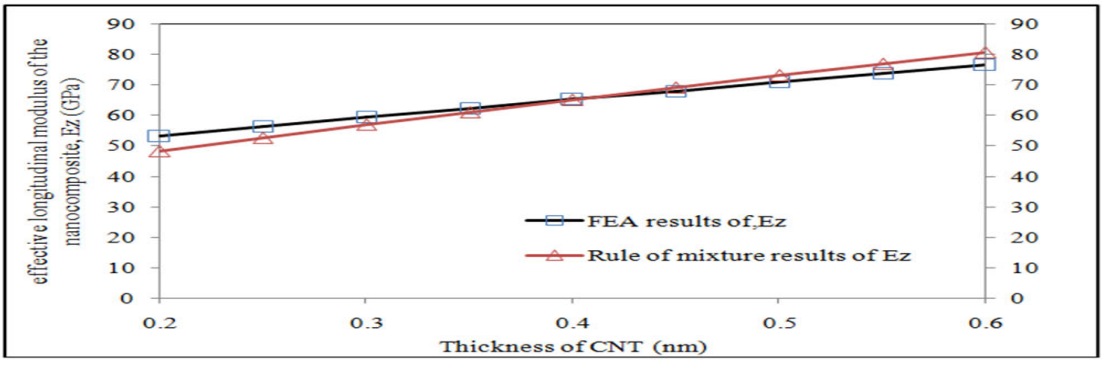

Figure 8: Comparison of Effective Modulus of the Composite in Longitudinal Direction Vs Varying CNT Thickness with Long CNT

CNT volume fraction also increases by increasing the thickness of CNT material without changing the length shown in Figure 9 Actually effective longitudinal modulus of the nanocomposites strongly depends on the volume fraction of CNT material. From the figure and data (thickness of CNT 0.20 with 30 Young's modulus of matrix) we observe that with the addition of only about 1.88% volume fraction of the CNTs in a matrix, the stiffness of the composite in the CNT axial direction can increase as much as 77.087% for the case of long CNT fibers.

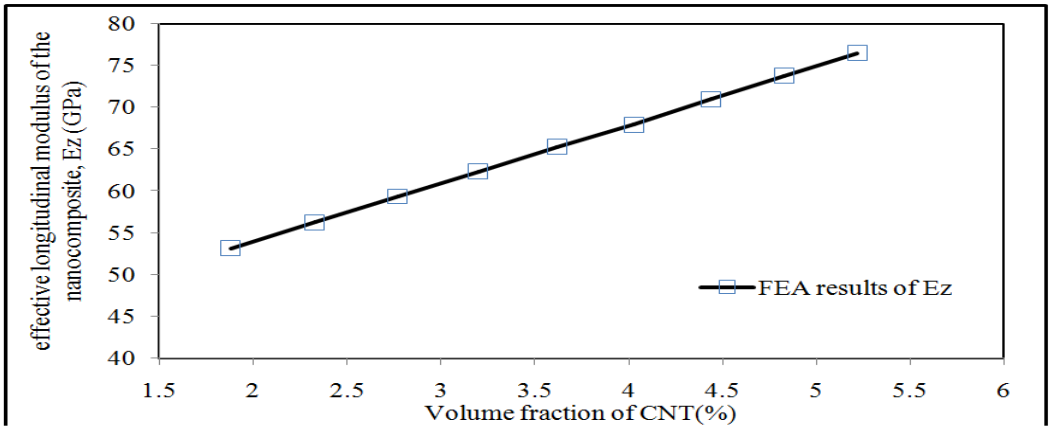

Figure 9: Comparison of Effective Modulus of the Composite in Longitudinal Direction Vs Varying CNT Volume Fraction with Long CNT.

E. Effect of Interphase on the Effective Longitudinal Modulus of the Nanocomposites

The presence of an interphase region between fibers and matrix in a composite system, can significantly affect the load transfer characteristics, even when the interphase is very thin. Three dimensional model of nanocomposite with interphase is shown in Figure 10.

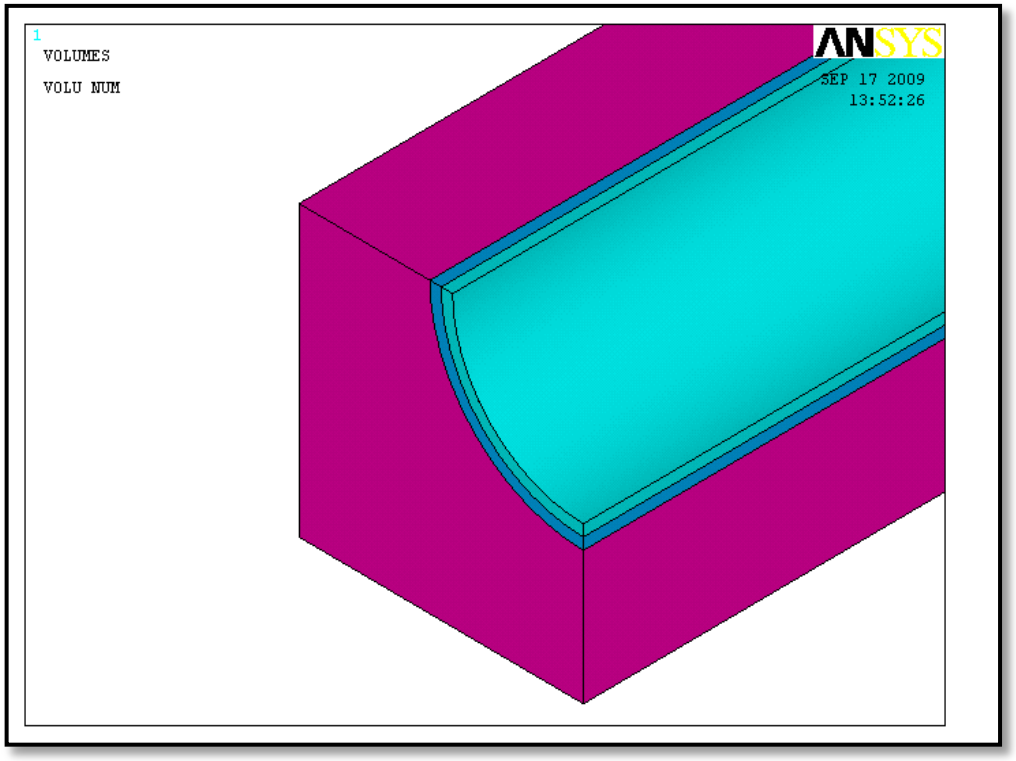

Figure 10: Three Dimensional Close View of Long CNT Nanocomposite with Interphase.

Model parameters

Phase	Poisson‘s ratio	Length (nm)	Young‘s modulus(GPa)
CNT	0.30	100	1000
Matrix	0.30	100	30
Interphase	0.30	100	Variable

For this model we use an interphase of 0.4nm thickness (CNT thickness=0.40nmconstant) and effective longitudinal modulus of the nanocomposite is investigated by changing the Young‘s modulus of interphase shown in Figure 11.

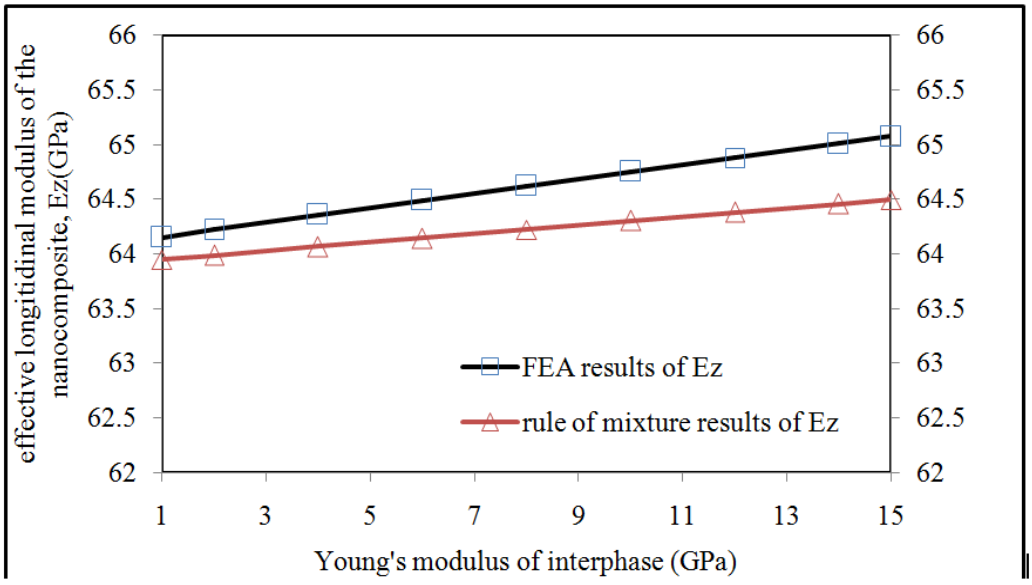

Figure 11: Comparison of Effective Modulus of the Composite in Longitudinal Direction (Both FEA and Rule of Mixture) Vs Varying Young‘s Modulus with Long CNT.

F. Short CNT Reinforced RVE

A short CNT unit cell model is the one in which a CNT short enough compared to long CNT with high D/L ratio and with end caps, is placed in a polymer matrix. It is completely inserted inside the matrix unlike the long CNT model, which is placed from one end to other end in the longitudinal direction in the matrix .From various previous section it is found that short CNTs do not possess good load carrying capabilities and also develop high stress concentrations at the ends of the CNT. First principle stress of short CNT reinforced composites is shown in Figure 12.

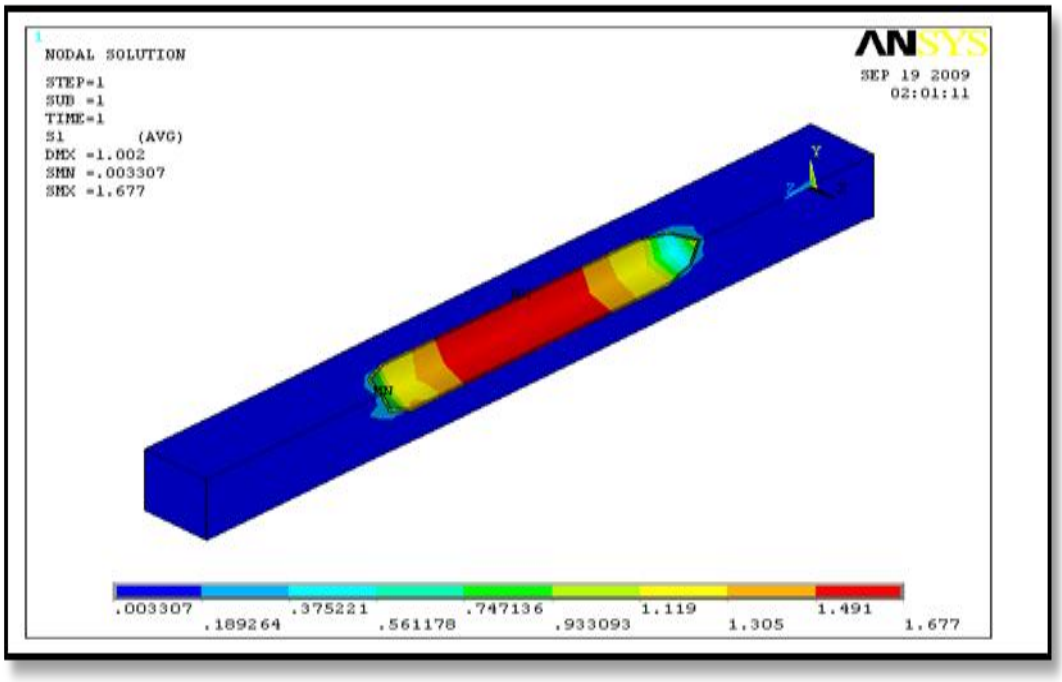

Figure 12: Contour Plot of First Principle Stress of Short CNT-RVE for Matrix Young's Modulus 30gpa and CNT Thickness 0.40nm, Length of CNT 50nm with Side Hemispherical Caps.

G. Effect of Matrix Young's Modulus of Elasticity on the Effective Longitudinal Modulus of the Nanocomposite (E_z) for Short CNT

In this case the model parameters were same as long CNT except the length of CNT is taken as 0.50nm and short CNT is situated at the center of matrix. From Figure 13 we observe that variation of results for FEA and rule of mixture is negligible and Effective longitudinal modulus of the Composite increase with the increase of Young's modulus of matrix which is expected. Changing the value of Young's modulus of matrix from 5 to 100 causes almost 96.5649 GPa increase in effective longitudinal modulus of the nanocomposites.

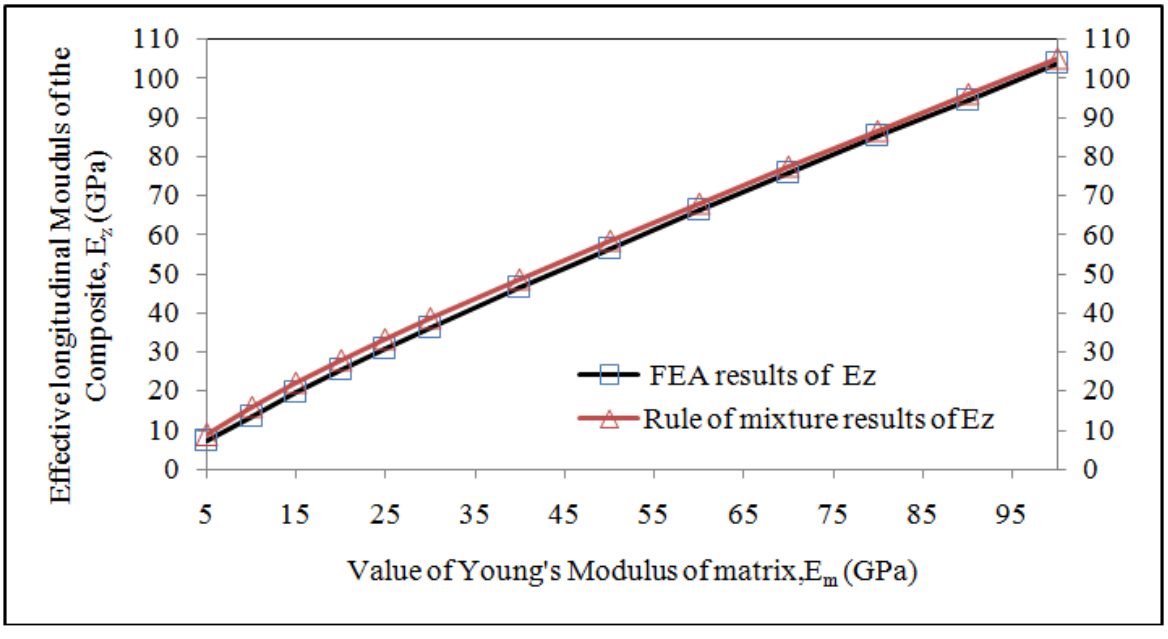

Figure 13: Comparison of Effective Modulus of the Composite in Longitudinal Direction Vs Varying Young's Modulus of the Matrix Reinforced with Short CNT of Thickness 0.4nm

H. Effect of Poisson's Ratio on the Effective Longitudinal Modulus of the Nanocomposite

Model parameters were same as long CNT. We found out that effective longitudinal modulus of the nanocomposite was remaining almost same with the increase of both Poisson's ratio of CNT and matrix. Results are calculate by increasing Poisson's ratio from .2 to 0.4 increase effective longitudinal modulus of the of nanocomposite value by 0.4422%, so we found that the effect of the Poisson ratio of the CNT and matrix on composite on the simulation was negligible which is shown in Figure 14.

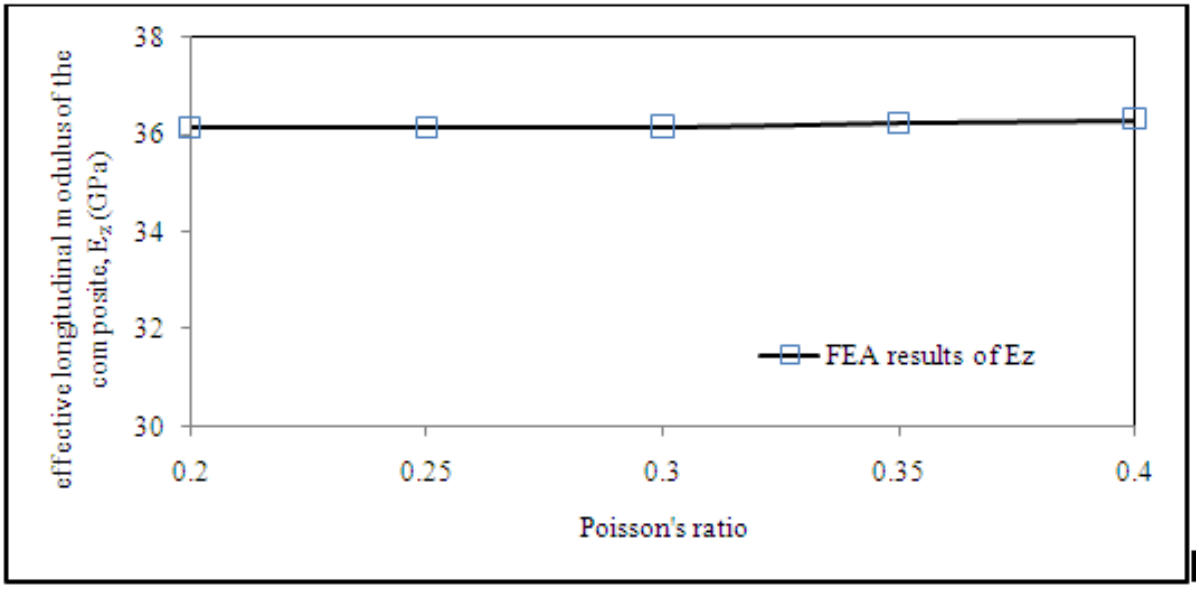

Figure 14: Effective Modulus of the Composite in Longitudinal Direction Vs Varying CNT and Matrix Poisson's Ratio with Short CNT of Thickness 0.4nm.

I. Effect of CNT Thickness on the Effective Longitudinal Modulus of the Nanocomposite

Here the modeling parameters are same as long CNT RVE. We found from Figure 15 that effective longitudinal modulus of the composite increase with the increase of thickness of CNT in short CNT case but results in FEA were not smooth as rule of mixture because in short CNT side caps produce stress concentration at two corners of short CNT. Rule of mixtures results were higher than FEA results because rule of mixture results ignore side caps of short CNT.

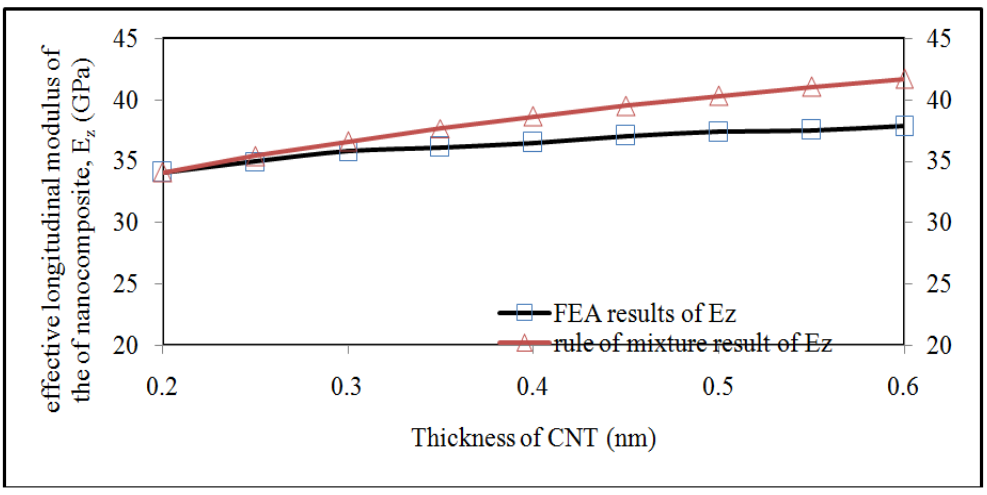

Figure 15: Effective Modulus of the Composite in Longitudinal Direction Vs Varying CNT Thickness with Short CNT.

Like long CNT, volume fraction of short CNT increases with the increases of the thickness of CNT without changing the length. Effective longitudinal modulus of the nanocomposite strongly depends on the volume fraction of CNT material. From the Figure 16 we observed that with the addition of only about 1.62% volume fraction of the CNTs in a matrix, the stiffness of the composite in the CNT axial direction can increase as much as 21.72% for the case of long CNT fibers. Variation of results between FEA and rule of mixture is large enough because rule of mixture calculation did not count the hemispherical caps of short CNT.

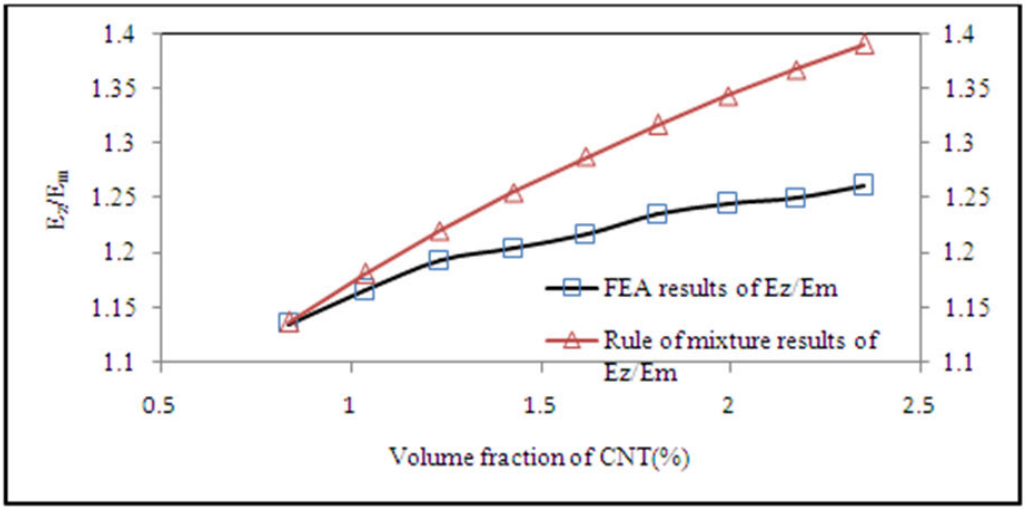

Figure 16: Comparison of Effective Modulus of the Composite in Longitudinal Direction Vs Various CNT Volume Fractions with Short CNT.

J. Effect of Interphase on the Effective Longitudinal Modulus of the Nanocomposite

In this case a layer of interphase is considered between CNT and matrix with thickness 0.40nm and Young's modulus of interphase is varied from 1 to 15 GPa. Here to find the value effective longitudinal modulus of composites, model parameters are kept same as long CNT except the length of short CNT and interphase. From Figure 17, we observe that value of E_z increase with the increase of E_i but the increase was not smoothed straight-line. Square RVE with short CNT and interphase between matrix and short CNT is still under investigation.

.

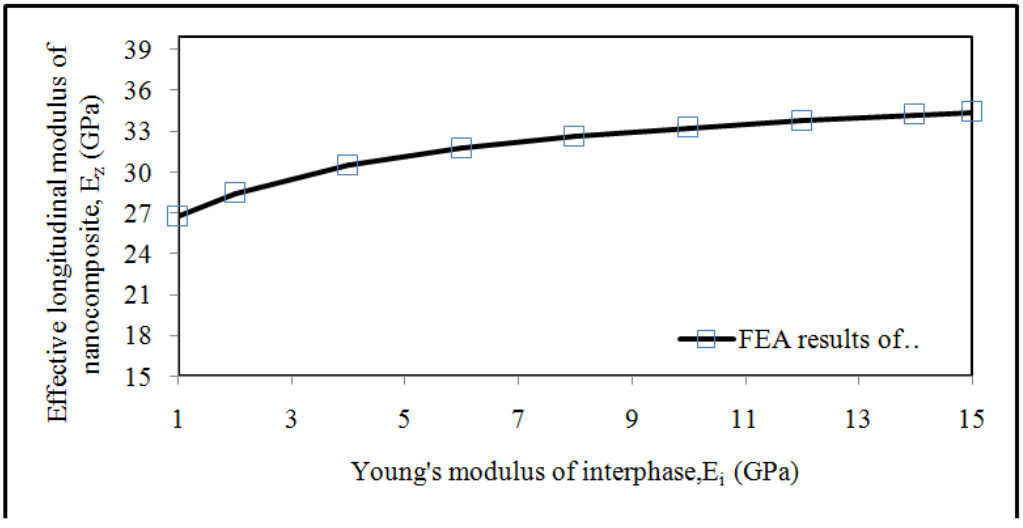

Figure 17: Effective Modulus of the Composite in Longitudinal Direction (Only FEA) Vs Varying Interphase Young's Modulus for Short CNT.

V. Conclusion

In this study, the effective Young's modulus of CNT-based nanocomposites has been evaluated, and as a preliminary step in this process, validation of continuum mechanics is done using 3-D square RVE models of the composite. Numerical examples using both long and short CNT-based composites have been studied and validated using the strength of materials approach. The results are in complete agreement revealing the fact that continuum mechanics can be an excellent approximate in estimating the overall response of the composite system. The FEM results evaluated assuming perfect bonding condition justifies the fact that,

1. With the increase of Young's modulus of matrix, the value of E_z/E_m decreases i.e. for higher Young's modulus of matrix, the increase in stiffness of composite is low, which is relatively higher for lower Young's modulus of matrix
2. Poisson's ratio of both CNT and matrix has almost negligible effect on the effective modulus of CNT based nanocomposite in longitudinal direction i.e. 100% increase in Poisson's ratio causes only 0.4704% and 0.4422% increase in the effective modulus of CNT based nanocomposite in longitudinal direction
3. With additions of only 0.40 nm of CNT thickness, effective modulus of CNT based composite in longitudinal direction increases 43.92% and 11.10% for long and short CNT respectively

And the FEM results evaluated assuming imperfect bonding condition justifies the fact that, Increase in Young's modulus of interphase causes increase in effective modulus of the CNT based nanocomposite in longitudinal direction for both long and short CNT but forthe short CNT the increasing rate was higher at lower valueof Young's modulus of interphase but that rate reduced atwith the increase of interphase Young's modulus.

VI References

1) Buongiorno, M., Nardelli, Fattebert, J.L., Orlikowski D., Roland C., Zhao Q. and Bernholc J., (2000), —Mechanical properties, defects and electronic behavior of carbon nanotubes," Carbon, Vol. 38, pp. 1703–1711.
2) Bradshaw1, R.D., Fisher, F.T. and Brinson, L.C., (2004), —Fibre waviness in nanotube-reinforced polymer composites—II: modeling via numerical approximation of the dilute strain concentration tensor," Department of Mechanical Engineering, Northwestern University, Evanston, IL 60208, USA
3) Chen, X. L. and Liu, Y. J., (2004), —Square representative volume elements for evaluation the effective material properties of carbon nanotube-based composites," Computational Material Science, Vol. 29.
4) Fisher, F.T., Bradshaw1, R.D.and Brinson, L.C., (2002), —Fibre waviness in nanotube-reinforced polymer composites—I: Modulus predictions using effective nanotube properties," Department of Mechanical Engineering, Northwestern University, 2145 Sheridan Road, Evanston, IL 60208, USA
5) Gao, G.H., Cagin, T. and Goddard, W.A., (1998), —Energetics, structure, mechanical and vibrational properties of single-walled carbon nanotubes," Nanotechnology, Vol. 9, pp. 184–191.
6) Garg, A., Han, J. and Sinnott, S. B., (1998), —Interactions of Carbon-Nanotubule Proximal Probe Tips with Diamond and Graphene," Phys. Rev. Lett., Vol. 81, pp. 2260–2263.
7) Govindjee S. & Sackman J.L., (1999), —On the use of continuum mechanics to estimate the properties of nanotubes," Solid State Communications," Vol. 110, pp. 227-230.
8) Kang, J.W. and Hwang, H.J., (2001), —Molecular-dynamics study of the interaction between energetic Al clusters and an Al surface," Phys. Rev. B 64, pp. 104-108.
9) Li, K. and Saigal, S., (2007), —Micromechanical modeling of stress transfer in carbon nanotube reinforced polymer composites," Materials Science and Engineering A, Vol. 457, pp. 44–57.
10) Liu, Y. J. and Chen, X. L., (2002), —Continuum models of carbon nanotube-based composites using the boundary element method." Electron J Bound Elem., Vol. 1(2), pp. 316–35.
11) Lu, J.P., (1997), —Elastic properties of single and multilayered nanotubes," Journal of Physics and Chemistry of Solids, Vol. 58, pp. 1649–1652.
12) Mortensen, A., Cornie, J.A. and Flemings, M.C., (1988), —Materials & Design," Vol. 10(2), pp. 68-76.
13) Nasser, S. N. and Hori, M., (1999), —Micromechanics: Overall Properties of Heterogeneous Solids," Elsevier Science Publishers, 2nd edition.
14) Qian, D., Li, W.K. and Ruoff, R.S., (2003), —Load transfer mechanism in nanoropes," Composite Science and Technology, Vol. 63, pp. 1561-1569.
15) Qian, D., Wagner, G. J., Liu, W. K., Yu, M. F. and Ruoff, R. S., (2002), —Mechanics of carbon nanotubes," Appl. Mech. Rev., Vol. 55, pp. 495-533.
16) Riddick, J. C. and Hyer, M. W., (1998), —The Response of Segmented-Stiffness Composite Cylinders to Axial Endshortening," Composite Structures, 40, pp. 103-114.
17) Thaw, C., Minet, R., Zemany, J. and Zweben, C., (1987), SAMPE J. 23(6), pp. 40-43.
18) Thostenson et al., (2005), —Composites Science and Technology," pp. 491–516.
19) Treacy, M.M.J., Ebbesen, T.W. and Gibson, J.M., (1996), —Exceptionally high Young's modulus

observed for individual carbon nanotubes", Nature 381, pp. 678–680.
20) Wagner, H. D., (2002), —Nanotube-polymer adhesion: a mechanics approach," Chem Phys Lett, Vol. 361, pp. 57–61.
21) Wong, E.W., Sheehan, P.E. and Lieber, C.M., (1997), —Nanobeam mechanics: Elasticity, strength, and toughness of nanorods and nanotubes," Science 277, pp. 1971–1975.

Study on Micro-Structure Rebuild Of Clay In Process Of Consolidation

Li Shun-qun[1], Ling-xia Gao[2], CHAI Shou-xi[3]

GJRE Classification (FOR)
GJRE: E, 090503

***Abstract*-Vacuum freeze drying method is applied to prepare samples for SEM from one-dimensional consolidation clay which respectively suffered 5 grade pressures from original remolded state. And then simple and synthetical micro-structure parameters of SEM photos obtained from horizontal, 45° inclined and vertical section are studied to uncover relation between macroscopical mechanics properties and micro-structure. Study on simple parameters indicated that grain area ratio and perimeter increase with consolidation pressure while other parameters have no constant tendency. The synthetical parameters are derived from the two data analysis methods, namely principal component analysis and pedigree cluster. It is clearly shown that the first principal component approximately linear increases with consolidation pressure. Samples can be exactly clustered into several families according to the grade of consolidation pressure and inner distance of a family nonlinearly increases with pressure. It is distinct that the synthetical parameters are superior to the simple parameters in construction soil mechanics relation because the former can reflect the whole micro-structure qualities, but the latter cannot.**

Keywords- clay; one-dimensional consolidation; micro-structure rebuild; principal component analysis

I. INTRODUCTION

It is clear that characteristics and state of any material are determined by its corresponding micro-structure. For these materials like rock and soil, their properties of micro-structure can reflect not only their stress history, physical nature and mechanics feature, but their current status （Hu et al. 2001）. At present, study on clay micro-structure and its relationship with macro-parameters becomes much hotter than ever and many methods or means have been introduced into the research field. As a result, some important conclusions were obtained by different researchers all over the world. For example, Tippkötter (2009) provided a method to detect soil water in macropores with X-ray tube computerized tomography utilized. And Kawaragi (2009) studied microstructure of saturated bentonites with X-ray CT technique employed.

In recent years, many researches worked hardly in order to bridge between micro-structure and macro-mechanics for different types of soil. Schäffer (2008, 2008) surveyed deformation and stability of macro-pore under uniaxial compression conditions. Chertkov (2008) thought that the intra-aggregate structure of a soil has important effect on its shrinkage characteristics. Agus (2005) studied the influence of shrinking and swelling on microstructures of a compacted bentonite-sand mixture.Bai (1997) peered the change of kaolin micro-structure in CD test. In confined condition, Cui (2002) studied micro-structure change of a swelling soil. With microstructure approach operated, Delage (2006) explored the ageing effects on a bentonite. After some experiments, Djéran-Maigre (1998) and Dudoignon (2001) bent themselves to constructed relationship between micro-structure and macroscopic properties respectively for clay and kaolinitic. Through investigation on micro-structure of Osaka Bay clay, Tanaka (1999) considered microfossils has impact on its mechanical behavior.

The Scan Electron microscope Method (SEM), together with various image processing techniques, can be utilized effectively to learn much about clay micro-structure. The SEM photos can show us much information about size, shape and distribution characters of pores and particles. Therefore, it is a good idea to bridge relationship between micro-structure and macromechanics for clay. In the process of information extraction, much more micro-parameters are picked up in order to acquire message as abundant as possible. Too much parameters, in one hand, can give us more information about characterizes of clay micro-structure, and in the other hand, result in message superposition and that make it difficult to apply micro-structure theory in soil mechanics. As a result, current study on relationship between micro-structure and macro-mechanics only can be conducted between certain single micro-structure parameter and certain macro-mechanics parameter. Therefore, it is necessary to bridge relationship between all-around micro-structure attributes and mechanics parameter.

Correlation analysis, principal component analysis and pedigree cluster analysis are the effective methods to study the extracted information, which can reduce dimension and evaluate characteristic from the original micro-structure parameters. The corresponding function of the methods is to build lower dimensional combined parameter from the higher dimensional parameters in which pertinence is prominent. Therefore, it is possible and reasonable to substitute simple parameters for complex parameters in the overall meanings while less information lost.

With the image manipulation software of Leica QWin utilized, the micro-structure parameters on different sections of samples, which were consolidated under five level pressures, are picked up firstly. And then, the lower dimensional synthetical parameters, including principal component index and interior (exterior) cluster distance, are

About-[1]. Department of Civil Engineering, Tianjin Institute of Urban Construction, Tianjin 300384
About[2].. Tianjin Key Laboratory of Soft Soil Characteristics and Engineering Environment, Tianjin 300384
About[3]- School of Architecture and Civil Engineering, Dalian nationalities University , Dalian 116600

constructed. After these, quantify and evaluation about different samples can be done with the synthetical parameters applied. It is concluded that the lower dimensional synthetical parameters can be used to substitute the original higher dimensional parameters with the reduplicate information filtrated. And the method can be used to describe the rebuild process of micro-structure simply and directly for clay consolidation.

II. Basic Properties of the Clay and its Consolidation Test

The studied clay was taken from a 35m depth bore drilled in the Key Project of Tianjin Railway Station. The main mechanics indexes of the clay constitute of the following: natural water content w=33%, void ratio e=0.735, natural gravity γ=19.8kN/m^3, internal friction angle φ=29.8^o, cohesion c=21.7kPa, compression index $\alpha_{1\text{-}2}$=0.351MPa^{-1}, liquid limit w_l=31.8% and plastic limit w_p=21.2%.

The remolded samples were employed in this paper because of the anisotropic distribution of particles in vertical and horizontal direction due to sedimentation process. The undisturbed clay was oven-dried under 115^o conditions. The dried clay was taken out of the oven after 24h and comminuted in a breaking machine in order to remove geometrical and physical anisotropy. Then a 0.25mm sieve was used to wipe off larger particles and organic substance.

The clay power was put on a plate for sprinkling until reach the natural water content, w=35%. It is unnecessary to stir or mix the clay in order to make the remolded samples isotropy before the later mechanics experiments. The wetted clay and the plate were enclosed together in a three-layered plastic bag. A week later, water and air contained in the clay would arrive the equilibrium condition due to capillary action and thermal force. The 25 remolded samples, which were made by pressing method, were classified into 5 identical groups. And consolidation process was list as table 1. The prepared samples were located in WGD-Ⅱ consolidation apparatuses and undergo a process of 12.4kPa precompression for three days. After these, the common consolidation procedure was applied on these samples.

Group	The first	The second	The third	The fourth	The fifth
The load process /kPa	12.5	12.5	12.5	12.5	12.5
	25	25	25	25	25
	50	50	50	50	50
	100	100	100	100	100
		200	200	200	200
			400	400	400
				800	800
					1600

III. Definition of Parameters for SEM Photos

After the consolidation experiments completed, some specimens were made from the consolidated samples which were used to obtain micro-structure of the remolded samples. The specimens must be in the condition of high degree vacuum when observed by a scan electron microscope. Even micro-content pore water in existence in specimens, the obtained photos would be distorted ascribing to directly boil away of pore water. Therefore, some measure must be applied to ensure the specimens completely dry. The popular measures include natural drying, critical point drying and vacuum freeze drying and so on. The last method can‘t bring any damage to the specimens because of no any affection of pore water surface tension on particles. The direct freeze drying and the dewatering freeze drying are the main two freeze drying methods which were both employed in this paper.

The progress of direct freeze drying, including lower and higher vacuum degree phases, was conducted in the apparatus of vacuum freeze drying which can provide a vacuum of 10^{-4}Pa. After drying for about 13h, the dried specimens were taken out of the apparatus and sealed in a small plastic bag quickly in order to keep them far away from outer vapor.

The redundant electric charge will cumulate on the surface of specimen in the process of scanning because the dry clay is a nonconductor. This phenomenon will make the photo of clay micro-structure fuzzy due to charge and discharge ceaselessly. Therefore, it is important to make a conducting coat on the dried specimen before observed. The popular methods include metal coating, vacuum coating and getter coating. In this paper, the first method was applied to make the specimen conductible.

Then the specimens are fixed in the box of the scan electron microscope and the process of dewatering freeze drying is begun in order to lustrate vapor intruded into the specimens when coating. When the required vacuum condition in scan electron microscope is achieved, observation and photo taking can be commenced.

The concept of soil micro-structure lies in two aspects, which are particle micro-structure and pore micro-structure. Even the proposed method in this paper is aimed at the particle micro-structure, it has the same meaning with the pore micro-structure. In this study, the Leica QWin software was employed to pick up two types of micro-structure parameters, namely field micro-structure and feature micro-structure. The former, including the six original parameters and the six induced parameters, can provide information for the whole study domain. The later only can tell us information for one unit body. This study focuses on the most important parameters, the six field particle micro-structure parameters.

In order to obtain reasonable data, same analysis fields were chosen for every photo taken by the scan electron microscope as shown in Fig.1. The study domain is a square of 500 μm×500 μm. Here, p_i is the particle numbered i with horizontal intercept of ε_i and vertical intercept of v_i.

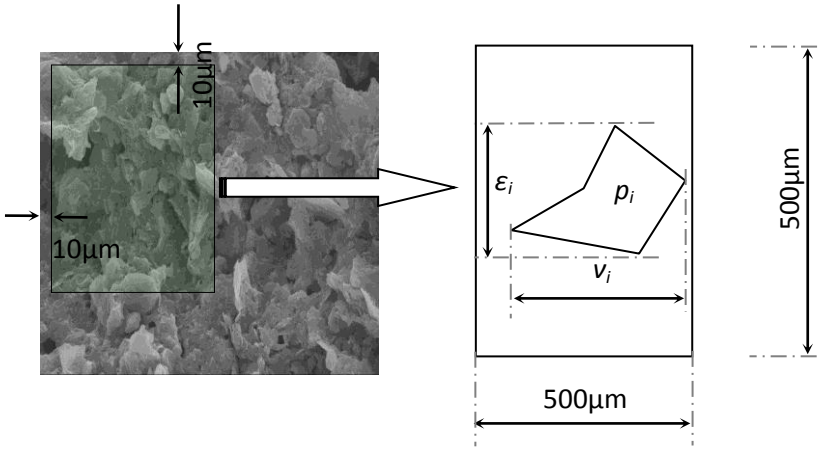

Fig. 1 Definition of particle micro-structure parameters

The obtained micro-structure parameters can be written as the followed matrix

$$x = \left(x_1,\ x_2,\ x_3,\ x_4,\ x_5,\ x_6\right)^{\mathrm{T}} \tag{1}$$

Here, x_1 and x_2 are respectively the sum of horizontal intercept of ε_i and the sum of vertical intercept of v_i, namely $x_1 = \sum \varepsilon_i$ and $x_2 = \sum v_i$. x_3 is the sum of the circumference of every particle in the domain, and x_5 is the arearatio of the total particle to field area. x_6 is a grey threshold determined by the Leica QWin software when the maximal variance of grey distribution achieved. It is clear that the primary properties of the particle micro-structure in the analysis field, including size, shape, gradation, anisotropy and so on, can be characterized by the stated parameters in formula (1).

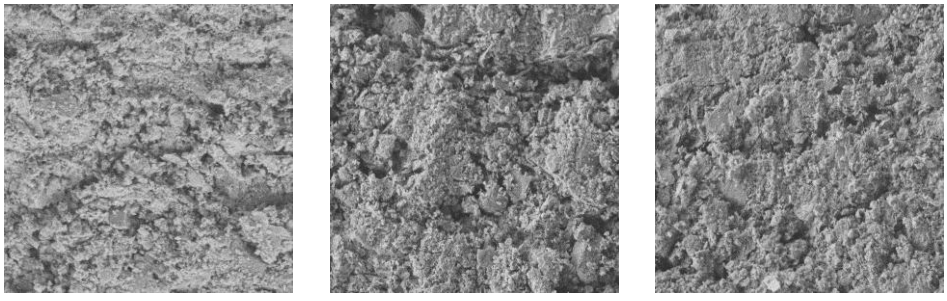

Section *A* Section *B* Section *C*

(a) 1600kPa

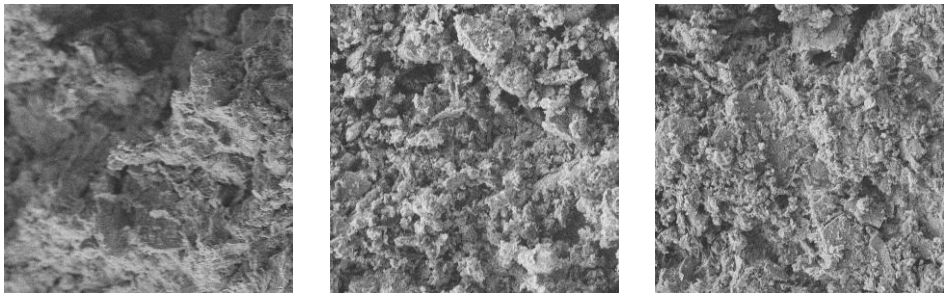

Section *A* Section *B* Section *C*

(b) 800kPa

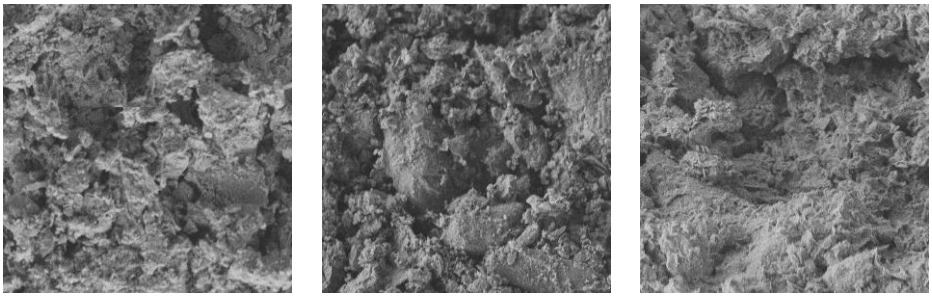

Section *A* Section *B* Section *C*

(c) 400kPa

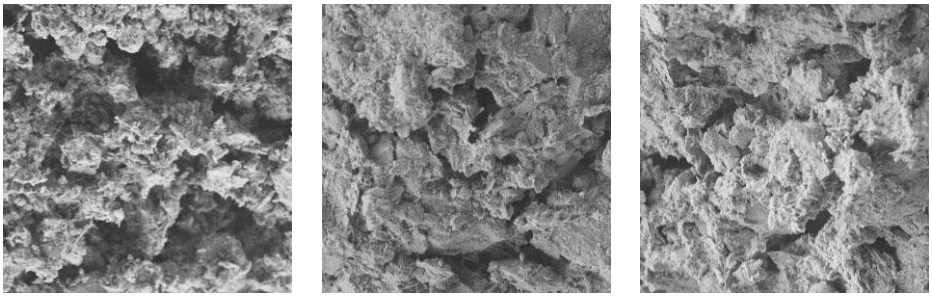

Section *A* Section *B* Section *C*

(d) 200kPa

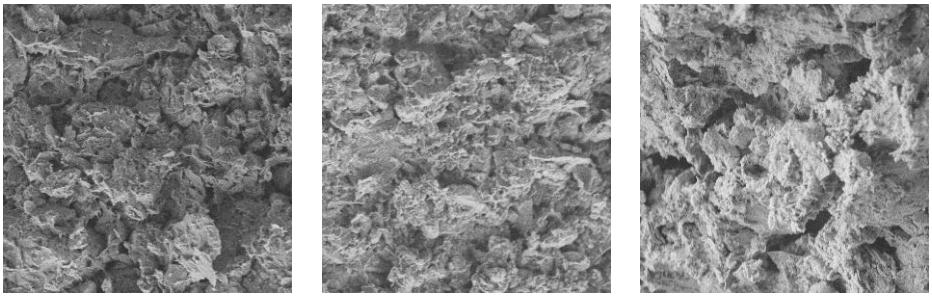

Section *A* Section *B* Section *C*

(e) 100kPa

Fig.2 SEM photos on the three planes from consolidated samples under the different pressure

The Fig.2 shows some SEM photos which were taken from different section of the samples. These sections are named as section *A*, section *B* and section *C* which are corresponding to vertical, 45° inclined and horizontal direction. It can be seen that the total particle area in the analysis field increases with consolidation pressure for section *A*. Furthermore, same situation is for section *B* and section *C*.

In general, the particles micro-structure parameters in formula (1) picked-up directly from SEM photos can be called simple parameters because they only reflect one side of the photo. For example, x_3 can only give us information about circumference of particles, but not the shape. In fact, different parameter may give us some similar information about one character which is called overlapped information. For a certain type of soil, x_3 will rise with the increasing of x_5. The synthetical parameters are induced from the simple ones which can show us the overall meaning of the micro-structure. In addition, the synthetical parameter can remove the overlapped information displayed by the different simple parameter.

Owing to the points stated above, the construction of synthetical parameter and corresponding application in soil mechanics, especially for consolidation problem, will be studied carefully in the following part.

IV. Principal Component Analysis for Micro-Structure

The method of principal component analysis aims at constructing a possible lower dimensional matrix from a higher dimensional matrix while the most information of the later is reserved. For example, the linear correlation relationship exists for a two-dimensional matrix, $x=(x_1,\ x_2)$. An observed sample for the matrix is shown in Fig.3.

.

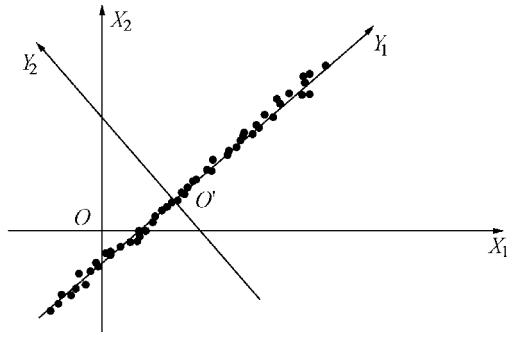

Fig. 3 Principal component analysis for two-dimensional vectors

It is easy that a linear combination can be constructed for the data of $(x_1,\ x_2)$ shown in Fig.2.

$$\left.\begin{aligned} y_1 &= x_1\cos\theta + x_2\sin\theta + \beta_1, \\ y_2 &= -x_1\sin\theta + x_2\cos\theta + \beta_2 \end{aligned}\right\} \quad (2)$$

Some methods can be utilized to determine θ and β in the condition of variance of y_1, Var(y_1), achieving maximum. Hereby, the new vector of y_1 can basically display the distribution characters of $(x_1,\ x_2)$. Therefore, some two-dimensional matrix can be approximately transferred into one-dimensional matrix. If the overall information needed, y_2, which can exhibit the vertical distribution characters, can be built. Here, y_1 and y_2 are respectively called the first and the second principal component of the two-dimensional matrix. Similarly, principal components for ploy-dimensional vector can also be constructed. The data for micro-structure of clay in this paper is a six-dimensional vector. The physical meaning of every vector is very different from others. Therefore, the first step is to obtain the standardization parameters of every vector. That is

$$x_i^* = \frac{x_i - \mu_i}{\sigma_i} \quad (i=1,2,\cdots,6) \qquad (3)$$

Here, μ_i and σ_i is average value and variance of variable x_i. Therefore, formula (1) can be transformed into formula (4).

$$x^* = \left(x_1^*,\ x_2^*,\ x_3^*,\ x_4^*,\ x_5^*,\ x_6^*\right)^{\mathrm{T}} \qquad (4)$$

From formula (4), a linear combination can be obtained like this:

$$y_1^* = a_{11}x_1^* + a_{12}x_2^* + a_{13}x_3^* + a_{14}x_4^* + a_{15}x_5^* + a_{16}x_6^* \qquad (5)$$

From the regulation of coordinate conversion, formula (6) is necessary.

$$a_1^{\mathrm{T}}a_1 = 1 \qquad (6)$$

Where, a_1 is the vector of (a_{11}, a_{12}, a_{13}, a_{14}, a_{15}, a_{16}). In formula (5), there are six undetermined coefficients need to be defined. When letting differential coefficient of y_1^* about x_1^* equals to zero in the condition of formula (6), a_{11} can be defined. Similarly, other coefficients in formula (5) can also be determined one by one. In addition, the maximum of $\mathrm{Var}\left(y_1^*\right)$ and y_1^* can be easily gained subsequently. It is generally speaking that y_1^* is the formula for the first principal component of formula (1). The second principal component can be constructed if the first one is not enough to illustrate necessary information of the original data. Namely

$$y_2^* = a_{21}x_1^* + a_{22}x_2^* + a_{23}x_3^* + a_{24}x_4^* + a_{25}x_5^* + a_{26}x_6^* \qquad (7)$$

In the process of determination of a_2= (a_{21}, a_{22}, a_{23}, a_{24}, a_{25}, a_{26})$^{\mathrm{T}}$, $\boldsymbol{y}_1^*$ and $\boldsymbol{y}_2^*$ should be considered uncorrelated independent random variable. That is

$$\mathrm{Cov}\left(y_2^*,\ y_1^*\right) = \mathrm{Cov}\left(a_2^{\mathrm{T}}x^*,\ a_1^{\mathrm{T}}x^*\right) = a_2^{\mathrm{T}}\sum a_1 = 0 \qquad (8)$$

Here, $\sum$ is the covariance matrix of vector x^*. Same to formula (6), formula (9) is the restricted condition in a_2 determination. Thereby,

$$a_2^{\mathrm{T}}a_2 = 1 \qquad (9)$$

Here, a_2 is the vector of (a_{21}, a_{22}, a_{23}, a_{24}, a_{25}, a_{26}). In the conditions of formula (8) and (9), a_2 can be determined as the differential coefficient of y_2^* about x_2^* equal zero. Consequently, the second principal component of formula (1) can be found. It is easy to achieve the third, the fourth,

the fifth and the sixth principal component in the same way. Therefore, the following three formulae can be derived.

$$y^* = a^{\mathrm{T}} x^* \tag{10}$$

$$y^* = \left(y_1^*,\ y_2^*,\ y_3^*,\ y_4^*,\ y_5^*,\ y_6^*\right)^{\mathrm{T}} \tag{11}$$

$$a = \left(a_1,\ a_2,\ a_3,\ a_4,\ a_5,\ a_6\right) \tag{12}$$

In fact, the process of principal component determination can be used to define process of the characteristic roots of $\sum$, λ_i and the corresponding orthogonal unit characteristic vectors. The covariance matrix of y^* can be written as

$$\mathrm{Cov}\left(\boldsymbol{y}^*\right) = a^{\mathrm{T}} \sum a = \mathrm{Diag}\left(\lambda_1, \lambda_2, \lambda_3, \lambda_4, \lambda_5, \lambda_6\right) \tag{13}$$

The total variance of every principal component is

$$\sum_{i=1}^{6} \mathrm{Var}\left(\boldsymbol{y}_i^*\right) = \sum_{i=1}^{6} \lambda_i \tag{14}$$

It can be said that the total variance of the standardized variables, $\sum_{i=1}^{6} \mathrm{Var}\left(x_i^*\right)$, can be broken down as the sum of the six data which respectively are variances of the uncorrelated variables. In order to explore importance of the first principal component, the following variable can be defined.

$$\eta_1 = \frac{\lambda_1}{\sum_{i=1}^{6} \lambda_i} \tag{15}$$

The variable of η_1, called the contributing ratio of the first principal component, implies the rate of information carried by the principal component to that carried by the original matrix, formula (1). Similarly, the contributing ratio of the No. k principal component can be defined as η_k. Therefore, the cumulated contributing ratio of the former m principal components should be written as

$$\xi_m = \sum_{i=1}^{m} \eta_i \tag{16}$$

V. Pedigree Cluster Analysis for Micro-Structure

In this section, $l_{ij} = d(a_i, a_j)$ is defined as the distance between the element a_i and a_j. Namely

$$l_{ij} = \sqrt{\sum_{k=1}^{6} \left(\boldsymbol{a}_{ki} - \boldsymbol{a}_{kj}\right)^2} \tag{17}$$

If G_p and G_q are two different clusters constituted of n_p and n_q elements respectively, the centroids of G_p, $\bar{\boldsymbol{a}}_p$, and the centroids of G_q, $\bar{\boldsymbol{a}}_q$, can be written as

$$\bar{\boldsymbol{a}}_p = \frac{1}{n_p} \sum_{i=1}^{n_p} \boldsymbol{a}_i^{(p)} \tag{18a}$$

$$\bar{\boldsymbol{a}}_q = \frac{1}{n_q} \sum_{i=1}^{n_q} \boldsymbol{a}_i^{(q)} \tag{18b}$$

Here, $\boldsymbol{a}_1^{(p)}$, $\boldsymbol{a}_2^{(p)}$,…, $\boldsymbol{a}_{n_p}^{(p)}$ and $\boldsymbol{a}_1^{(q)}$, $\boldsymbol{a}_2^{(q)}$,…, $\boldsymbol{a}_{n_q}^{(q)}$ are the elements of the cluster G_p and cluster G_q.

4.1 Definition of distance between clusters

The most popular types of distance, used to evaluate characteristic of relationship between clusters, are the longest distance, the shortest distance, the average distance and the centroid distance.

(1) The longest distance defined as the longest distance between any two elements which respectively belongs to the two different clusters.

$$D_{pq} = \max_{i \in G_p, j \in G_q} d\left(\boldsymbol{a}_i, \boldsymbol{a}_j\right) \tag{19}$$

(2) The shortest distance defined as the shorted distance between any two elements which respectively belongs to the two different clusters.

$$D_{pq} = \min_{i \in G_p, j \in G_q} d\left(\boldsymbol{a}_i, \boldsymbol{a}_j\right) \tag{20}$$

(3) The average distance defined as the average distance between any two elements which respectively belongs to the two different clusters.

$$D_{pq} = \frac{1}{n_p n_q} \sum_{i \in G_p} \sum_{j \in G_q} d\left(\boldsymbol{a}_i, \boldsymbol{a}_j\right) \tag{21}$$

And (4) the centroid distance defined as the distance between the two clusters‘ centroids.

$$D_{pq} = d\left(\bar{\boldsymbol{a}}_p, \bar{\boldsymbol{a}}_q\right) \tag{22}$$

4.2 Deduction of distance between clusters

If the distance of cluster G_k to cluster G_p and cluster G_q is D_{pk} and D_{qk} respectively, cluster G_r is composed of G_p and G_q, the distance between cluster G_r and cluster G_k can be described as following.

(1) The longest distance

$$D_{rk} = \max\left\{D_{pk}, D_{qk}\right\} \tag{23}$$

(2) The shortest distance

$$D_{rk} = \min\left\{D_{pk}, D_{qk}\right\} \tag{24}$$

(3) The average distance

$$D_{rk} = \frac{n_p}{n_r} D_{pk} + \frac{n_q}{n_r} D_{qk} \tag{25}$$

And (4) the centroid distance

$$D_{rk} = \sqrt{\frac{n_p}{n_r} D_{pk}^2 + \frac{n_q}{n_r} D_{qk}^2 - \frac{n_p n_q}{n_r^2} D_{pq}^2} \tag{26}$$

4.3 The analysis process

The analysis process of pedigree cluster can be divided into several parts.

(1) Every SEM photos taken from the three different sections is solely set as a cluster at the beginning of analysis. 5 photos were taken in the horizontal section for every consolidated pressure. And that is to say there are 25 clusters (elements) at the beginning. The distance matrix $D_{(0)}$, which is a 25×25 phalanx, can be calculated from

formula (27) when the distances between any two clusters computed.

$$D_{(0)} = \begin{bmatrix} 0 & l_{1,2} & l_{1,3} & \cdots & l_{1,25} \\ l_{2,1} & 0 & l_{2,3} & \cdots & l_{2,25} \\ l_{3,1} & l_{3,2} & 0 & \cdots & l_{3,25} \\ \vdots & \vdots & \vdots & & \vdots \\ l_{25,1} & l_{25,2} & l_{25,3} & \cdots & 0 \end{bmatrix} \quad (27)$$

(2) The minimum in matrix $D_{(0)}$, minl_{pq}, is selected and the corresponding cluster of G_p and G_q are combined into a new cluster G_r. The rows and the columns depended on G_p and G_q are eliminated from the matrix. At the same time, a new row and a new column, depended on the cluster G_r, are added into the matrix. Therefore, a new 24×24 matrix, $D_{(1)}$, is obtained.

(3) The process stated above is repeated, another new 23×23 matrix $D_{(2)}$, displayed the distance of clusters, can also be obtained. The process is repeated again and again until all clusters merged into one. Then the analysis process terminate.

And (4), based on the order number and analysis process, the scheme of pedigree cluster can be drawn.

VI. Comparison of Synthetical Parameters

The principal component indexes

The correlation coefficients between parameters of particles and pore aggregates for section *A* are list in table 2. It is clear that different parameter is correlative in some extent, especially a_2, a_3 and a_4.

Table 2 Correlation Coefficient Of Micro-Structure Parameters For Grain Aggregate And Pore Aggregate For Section *A*

Parameters		a_1	a_2	a_3	a_4	a_5	a_6
Particles	a_1	1	0.12	0.16	0.04	-0.61	0.78
	a_2		1	0.98	0.99	0.54	-0.27
	a_3			1	0.99	0.49	-0.23
	a_4				1	0.60	-0.33
	a_5			Symmetry		1	-0.64
	a_6						1
Pore	a_1	1	-0.06	-0.09	-0.17	-0.71	-0.06
	a_2		1	0.98	0.99	0.60	-0.13
	a_3			1	0.99	0.61	-0.13
	a_4				1	0.69	-0.13
	a_5			Symmetry		1	0.03
	a_6						1

Both for grain aggregate and for pore aggregate, correlations between a_2 and a_3, a_2 and a_4, a_3 and a_4 are all remarkable. That is to say some information displayed by the three parameters is reduplicate. Therefore, the reasonable method is to find some synthetical parameters, which are incorrelate to each other, to illustrate feature of SEM photos.

Table 3 Comparison Of Grain Principal Component To Pore's For The Five Group Samples

	Item	Ratio	Cumulated contributing ratio
For particles	The first principal component	0.596	0.596
	The second principal component	0.336	0.932
	The third principal component	0.051	0.983
For pores	The first principal component	0.593	0.593
	The second principal component	0.229	0.822
	The third principal component	0.156	0.977

It can be seen from the table 3 that the cumulated contributing ratio of the first and the second principal component for the particles and for the pores are 0.932 and 0.822 respectively. Therefore, it can be concluded that when the first two principal components are selected to illustrate properties of the SEM photo, the particle micro-structure is superior to the pore micro-structure.

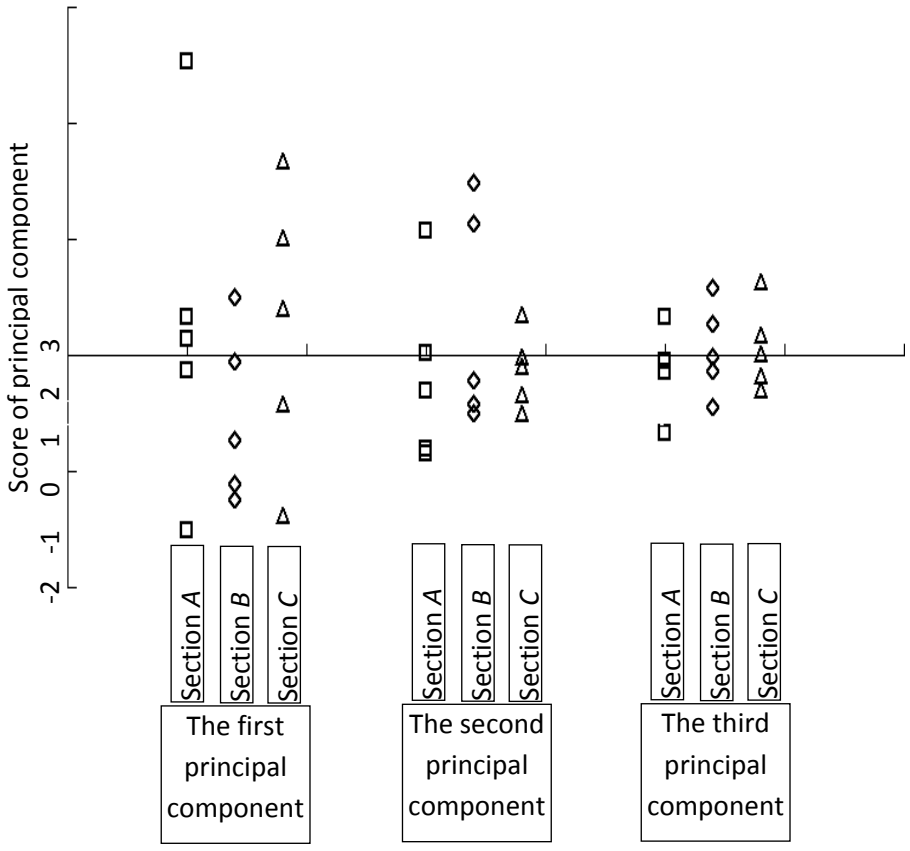

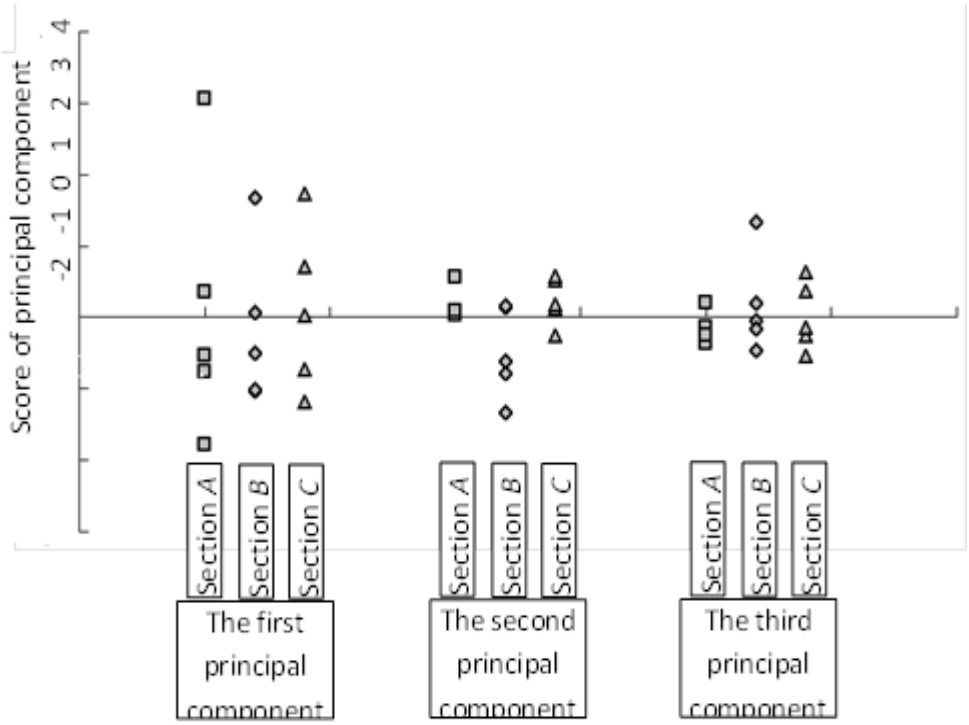

(b) Pore aggregate

Fig.4 Scores of the three principal components of the 5 groups

In the conditions of different consolidated pressure, scores of principal component for different sections are illustrated in Fig.4 carefully. The study on the SEM photos on section *A* is more meaning, interesting and instructive than that on other sections due to close and clear correlation between micro-structure of the three sections. Accordingly, the latter study is focused on the SEM photos from the section *A*.

For the SEM photos taken on the section *A*, the relationship of first three principal components with the consolidation pressure is shown in Fig.5. It is clear that the first principal component increases with the enlargement of the pressure, while the tendencies of the other two principal components are not very evident.

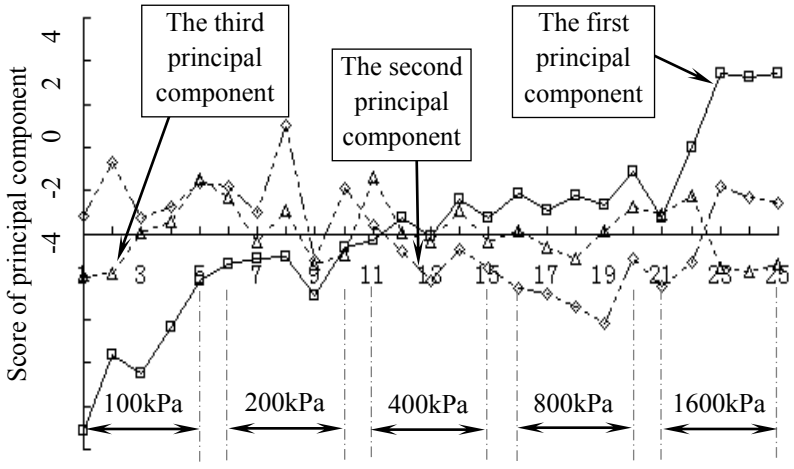

Fig.5 Scores of the three principal components of the 5 groups

The average of the first three principal components in the different consolidated are plot in Fig.6. At the same time, contributing ratio of the three principal components can be computed as 0.682、0.220 and 0.076 respectively. That is to say, the cumulated contributing ratio is 0.682, 0.902 and 0.979 correspondingly. It can be concluded that the first two

(or the first three) principal components could display about 90.2% (or 97.9%) information displayed by the 6 original micro-structure parameters. Then, the original 6 dimensional parameters can be dimensionality reduced into 2 (or 3) accordingly.

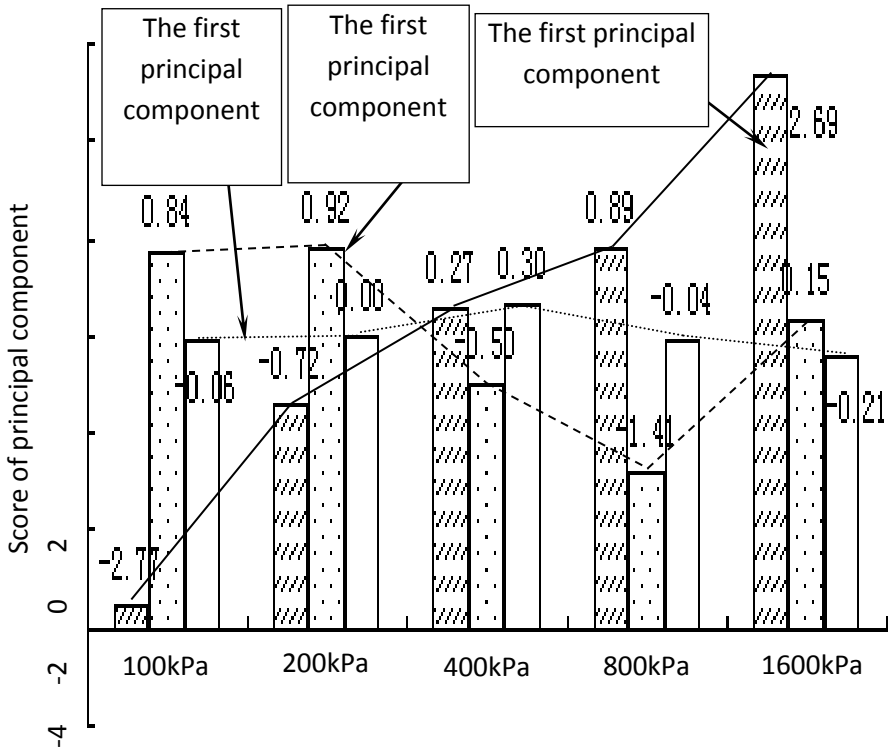

Fig.6 Means of the three principal components of the 5 groups

It is obvious from Fig.6 that the score of the first principal component climbs up from -2.77 to 2.69 with the increase of consolidated pressure from 100kPa to 1600kPa. Amplitude of variation for the first, the second and the third principal component is smaller and smaller. Other more, the second and the third principal component are all not monotone variables, while the first one is. Therefore, it is reasonable and necessary to introduce the first (or the first and the second) principal component into shear strength expressions and constitutive equations in order to reflect the micro-structure of the soil.

The linear fitting equation for the first principal component can be written as

$$m_1 = 0.003p - 1.795 \quad (28)$$

The corresponding correlation coefficient for linear fitting is R^2=0.83. The logarithmic fitting equation can be written as

$$m_1 = 1.81\ln p - 10.76 \quad (29)$$

The corresponding correlation coefficient is R^2=0.97. Here, m_1 is the first principal component and p is consolidated pressure.

Distance in cluster method

When average distance is used as the criterion in cluster method, the SEM photos on section *A* can be sorted as shown in Fig.7. It is distinct that all specimens are divided into 5 clusters depended on the five level different consolidated pressures. That is cluster *A*, *B*, *C*, *D* and *E* are corresponding to 1600Kpa, 800Kpa, 400Kpa, 200Kpa and 100Kpa, respectively. Thereby, taxonomic character of the micro-structure of soil in different consolidated pressure is remarkable. Subsequently, the cluster *A* and the cluster *B* are merged into a bigger cluster. The cluster *C* and the cluster *D* are merged into another bigger cluster, and then further combined with cluster *E* into a cluster. Therefore, it can be concluded that the specimens consolidated under the higher pressure conditions (>800kPa) are very different from those consolidated under lower pressure conditions.

\

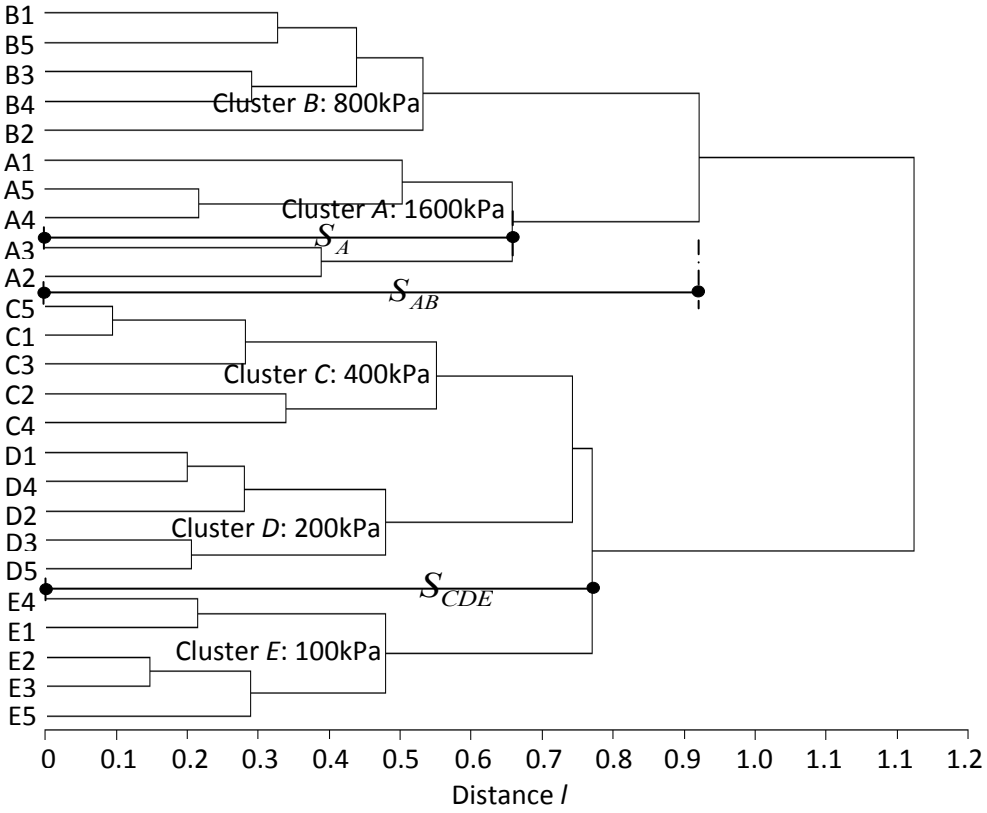

Fig.7 Result of the pedigree cluster of average distance method for different consolidation pressure

The concept of inner distance is defined as the distance between the small latest clusters in the new cluster. For example, the cluster *AB* is composed of the cluster *A* and the cluster *B*. Therefore, the inner distance of the cluster *AB* is the distance between the cluster *A* and *B*. Accordingly, the inner distance of the five cluster can be written as S_A, S_B, S_C, S_D and S_E. It is evident that S_A is the biggest one and S_D, S_E is the smallest one. The phenomenon may imply that the micro-structure properties of the soil consolidated under the higher pressure are more dispersive than that consolidated under the lower pressure.

VII. Conclusion

In this paper, two methods to evaluate characters of soil micro-structure are proposed and constructed and were successfully utilized to quantity the difference of the specimens obtained in consolidated condition. The first method is the principal component analysis and the second one is the cluster analysis. The studied specimens were cut from samples which had been consolidated in different five grades pressure. The study shows that the first principal component approximately linear increases with consolidation pressure. Consolidated specimens can be easily clustered into five families according to different consolidation pressure. Therefore, it is likely that synthetical parameters are superior to simple parameters in building constitutive equations in soil mechanics because the former can display the overall meaning of the micro-structure characteristic.

VIII. Acknowledgements

The work presented in this paper is part of the Study on *Determination of Shear Strength Indexes for Remolded Unsaturated Soil with Synthetic Micro-structure Parameters Taken into Consideration* (No. 200902276) research works funded by the China postdoctor science foundation and *A Method to Determine Shear Strength Indexes of frozen clay with micro-structure theory employed* (No. SKLFSE200906) funded by the State Key Laboratory of Frozen Soil Engineering in China. The authors would like to acknowledge Prof. Gang Zheng of the Tianjin University in China and Prof. Stefano Aversa of University of Naples Parthenope in Italy for the helpful suggestions and instruction.

IX. Reference

1) Hu R. L., Yeung M. R., Lee C. F., *et al*, 2001. Mechanical behavior and microstructural variation of loess under dynamic compaction. *Engineering Geology*, 59(3–4): 203-217.
2) Tippkötter, Rolf; Eickhorst, Thilo; Taubner, Heidi; et al, (2009). Detection of soil water in macropores of undisturbed soil using microfocus X-ray tube computerized tomography (μCT). *Soil and Tillage Research*, 105(1): 12-20.
3) Microstructure of saturated bentonites characterized by X-ray CT observations. Kawaragi, Chie; Yoneda, Tetsuro; Sato, Tsutomu; et al. *Engineering Geology*, 106(1-2): 51-57.

4) SHI Bin, JIANG Hong-tao, 2001. Research on the analysis techniques for clayey soil microstructure. *Chinese Journal of Rock Mechanics and Engineering*, 20(6): 864-870.
5) Schäffer, B.; Mueller, T.L.; Stauber, M.; et al. (2008). Soil and macro-pores under uniaxial compression. II. Morphometric analysis of macro-pore stability in undisturbed and repacked soil. *Geoderma*, 146(1-2): 175-182.
6) Schäffer, B.; Stauber, M.; Mueller, T.L.; et al 2008. Soil and macro-pores under uniaxial compression. I. Mechanical stability of repacked soil and deformation of different types of macro-pores. *Geoderma*, 146(1-2): 183-191.
7) Chertkov, V.Y. 2008. The physical effects of an intra-aggregate structure on soil shrinkage. *Geoderma*, 146(1-2): 147-156.
8) Agus, S. S. and Schanz, T., 2005. Effect of shrinking and swelling on microstructures and fabric of a compacted bentonite-sand mixture, *Proc. Int. Conf. on Problematic Soils, Cyprus,* 2, 543-550.
9) Bai, X. and Smart, P., 1997. Change in microstructure of kaolin in consolidation and undrained shear, *Géotechnique*, 47(5): 1009-1017.
10) Cui, Y. J., Loiseau, C., Delage, P., 2002. Microstructure change of a confined swelling soil due to suction controlled hydration, *Proc. 3rd Int. Conf. on Unsaturated Soils,* UNSAT' 2002, Recife, Brazil, Balkema, 2, 593-598.
11) Delage, P., Marcial, D., Cui, Y. J., et al. 2006. Ageing effects in a compacted bentonite: a microstructure approach. *Géotechnique*, 56 (5): 291-304.
12) Djéran-Maigre, I., Tessier, D., Grunberger, D., et al. 1998. Evolution of microstructures and of macroscopic properties of some clays during experimental compaction. *Marine and Petroleum Geology,* 15(2): 109-128.
13) Dudoignon, P., Pantet, A., Carrara, L. and Velde, B., 2001. Macro-micro measurement of particle arrangement in sheared kaolinitic matrices, *Géotechnique*, 51 (6): 493-499.
14) Tanaka, H. and Locat, J., 1999. A microstructural investigation of Osaka Bay clay: the impact of microfossils on its mechanical behavior, *Can. Geotech. J.,* 36(3):493-508.

Reactive Acoustic Filters as a Replacement for Absorbing Material

GJRE Classification (FOR)
GJRE C : 091299

O. I. Ilkorur[1], K. Yuksek[*2]

***Abstract*-The usefulness of reactive acoustic low pass filters inside transmission line enclosures, instead of absorbing materials, was examined by means of linearity and efficiency. Wave equation was solved numerically in an unbounded domain, and the numerical solution was used to simulate the behaviour of acoustic filters inside transmission line enclosures. The filters inside the transmission line were placed based on the Thiele and Small parameters of the test unit used. A relation between the numerical results and SPL values was found and this relation was used to decide whether a filter is suitable for audio purposes.**

I. INTRODUCTION

After the model of transmission line enclosures was introduced in 1965 by Bailey and Radford, the need for controlling the resonance peaks inside the line has gained significant importance. Studies on removing the resonances inside the transmission line loudspeaker enclosures are mainly concentrated on using fibrous stuffing or absorptive linings [1], [2], [3]. In order to achieve the highest possible efficiency with minimal pass band ripple some suggestions have been made. For instance, Augspurger (2000) tested different types of fibrous materials and found these fibrous absorbers had different absorbing characteristics [5]. For simulation purposes, the model of Locanthi's horn equation, with some empirical parameters, which have been received from the real life measurements, were used [4], [5]. Locanthi's analogy includes the mobility model of the loudspeaker, followed by an LC ladder in which series inductors represent air compliance and shunt capacitors represent mass. In the model, each LC section is equivalent to a cylindrical element of specified diameter and length. The accuracy of the model depends on the length of the elements used. The performance of Locanthi's horn equation has been shown to be depended on the material, which can be used inside the line, by adding shunt resistances to model the damping losses. On the other hand, Augspurger (2000) introduced the idea of changing the cross-sectional area of the line abruptly to reduce the cancellation in the troublesome fourth-harmonic region, but no details were given in this work. Resonance problems in pipes with varying cross-sections, such as exhaust systems and HVAC (Heating Ventilating and Air Conditioning) installations, have been investigated in different studies. But, in all those cases, the fluid is not stationary, unlike the condition in loudspeaker enclosures. The cases examined had similar boundary conditions [6], [7], [8], [9]. Although, structure and modelled the low-pass Butterworth filter as 18dB/octave, using electro-acoustic analogy [10], the borders of the sections of the cavity were not drawn clearly. The same cavity was also examined by Leach Jr. (2003) with electro-acoustic analogy, but, the borders of the cavity were still not defined in detail [11]. Morse also worked on the same problem and generated a solution using conformal transformations under steady-state flow conditions [12]. Munjal (1987) examined sudden area changes by using transfer matrix method [13]. He emphasized the importance of how the resonances inside the transmission line affect the output amplitudes. He also gave information about how resonators, which are placed as a branch on the lines, can affect the transmission loss as they resonate. The transfer matrix method, however, can not be used with sudden area changes, where the discontinuity has negligible thickness. In present work, further studies were carried out to investigate the effect of sudden area chances in the line. In this work, to reach the goal of achieving the highest possible efficiency with minimal pass band ripple, instead of fibrous absorbers or absorptive linings, a third-order low-pass filter was used. Two sudden changes, forming a cavity in the middle, were placed inside the line. The position of the filter was chosen according to the length of the transmission line. A solution was found by solving the wave equation numerically in a time domain with absorbing boundary layers. A test cylinder, which has a length of 1meter and a diameter of 0.16meter, was used for measurements. A suitable loudspeaker was used as the source. Depending on the radial resonances caused by the boundary of the test cylinder, the simulations were limited with 1000Hz. A low-pass filter, which reduces all the resonance peaks between the nominal quarter-wave pipe resonance frequency and 1000Hz, was searched and the filter, satisfying that condition was tested. The positive and negative aspects of the filter were investigated.

II. MATHEMATICAL MODEL

The mathematical model is based on the wave equation in two dimensions using Cartesian co-ordinate system [14].

The diffusion equation, subjected to u(x,y,t) = 0 on the boundaries x=0,1 and y=0,1 is given by;

$$\frac{\partial u}{\partial t} = D\left(\frac{\partial^2 u}{\partial x^2} + \frac{\partial^2 u}{\partial y^2}\right) \qquad (1)$$

About[1]. Yildiz Technical University, 34349, Istanbul, Turkey
*About[2].*Istanbul Kultur University,34156 Istanbul, Turkey*

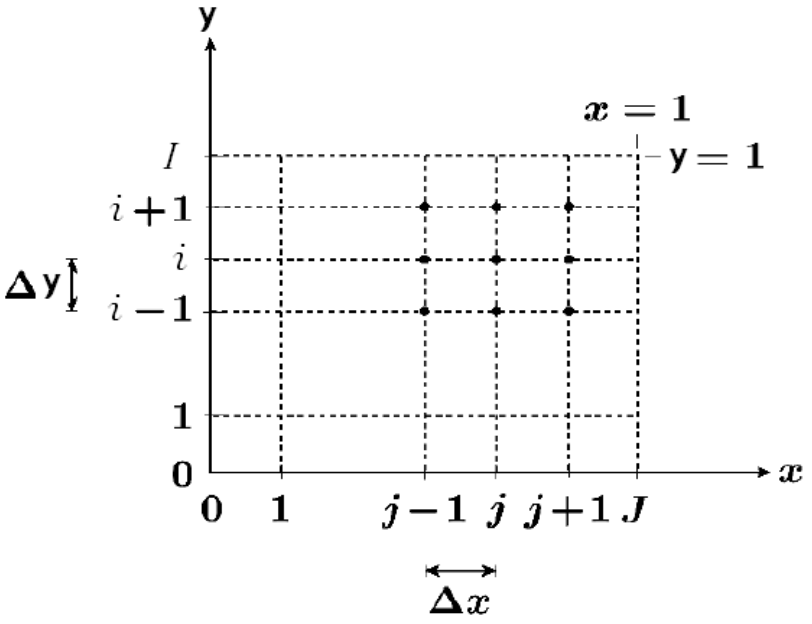

Fig. 1. Numerical Solution Variables

For the boundary conditions given as; $u(x,y,t=0) = u_0(x,y)$,the solution for $t > 0$ was found. Using a square mesh size, $\Delta x = \Delta y = 1/m$, and D=1, the Laplacian operator can be used for approximation for the internal points i=1, m-1 and j=1, m-1. On the boundaries (i=0,j), (i=m,j), (i,j=0) and (i,j=m), have $u_{ij}=0$. The diffusion equation is simplified to

$$\frac{\partial u_{i,j}}{\partial t} \approx \left(u_{i+1,j} + u_{i-1,j} + u_{i,j+1} + u_{i,j-1} - 4u_{i,j}\right)/\Delta x^2 \qquad (2)$$

If the derivative of equation 2 is taken, it becomes:

$$U'_{i,j}(t) = \left(U_{i+1,j} + U_{i-1,j} + U_{i,j+1} + U_{i,j-1} - 4U_{i,j}\right)/\Delta x^2 \qquad (3)$$

where the U_{ij} represents our approximation of U at the mesh point x_{ij}. Using the Euler method in which $Y_{n+1} = Y_n + \Delta t \cdot f(Y_n, t_n)$ equation 3 is given by;

$$U_{i,j}^{(n+1)} = U_{i,j}^{(n)} + \mu\left(U_{i+1,j}^{(n)} + U_{i-1,j}^{(n)} + U_{i,j+1}^{(n)} + U_{i,j-1}^{(n)} - 4U_{i+1,j}^{(n)}\right) \qquad (4)$$

where the Courant number is $\mu = \Delta t/\Delta x^2$ and where the stability depends on both time and μ [15].

The absorbing boundaries can be added to the solution as a damping function. An imaginary single degree damping function can be defined as;

$$A(x) = c_{slope} \cdot (x - (x_{\max} + x_{border})) + c_{offset} \qquad (5)$$

where equation A is the damping term, which is depended on the position at which the coordinate it is calculated

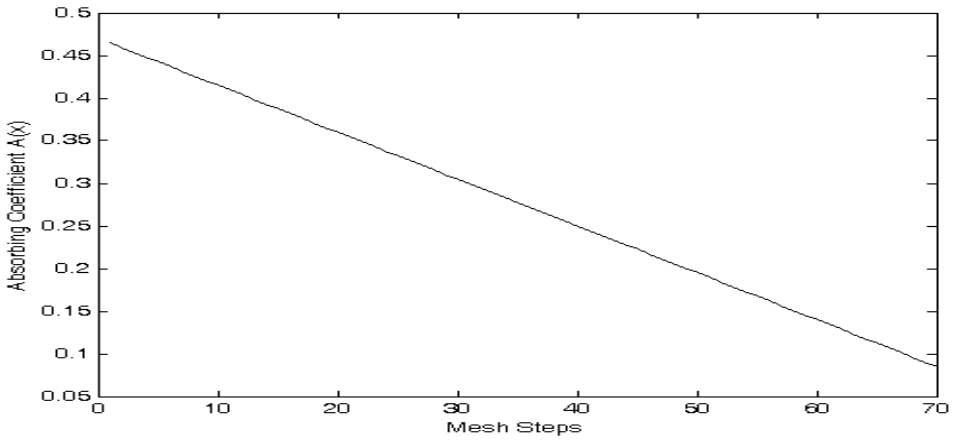

Fig. 2. Absorbing Coefficient with Respect to Mesh Steps

c_{slope} and c_{offset} are the two parameters defining the character of the absorbing function. x_{max} and x_{border} are the two parameters keeping the values of the maximum dimension of the total solution area of the simulation and the width of the absorbing border, respectively. As the wave enters the border, the absorption coefficient reduces from its' maximum to its' minimum to reduce the amplitude of undesired reflected waves. c_{slope} and c_{offset} values were calculated by a simple optimization process. An impulse signal was generated inside the solution area and the amplitude of the reflected wave was measured. The software was set to select the constants which give the minimum amplitude for the reflected wave.

Equation 5 was integrated on the borders of the solution area. The width of the border, surrounding the solution area, was defined as the half of the wavelength of the lowest frequency used in the simulations [16]. This ensures that the wave has to travel a full of its' wavelength before it leaves the absorbing boundary. The simulation conducted under steady state conditions between the nominal quarter-wave pipe resonance frequency and 1000Hz was found to be stable.

III. TEST ENCLOSURE

The test enclosure is made of a rigid cylinder and a speaker unit, mounted on the one side of the cylinder. The other end of the cylinder is open. The enclosure tuning was checked and the impedance of the speaker, mounted on the empty pipe, was measured. (Figure 3)

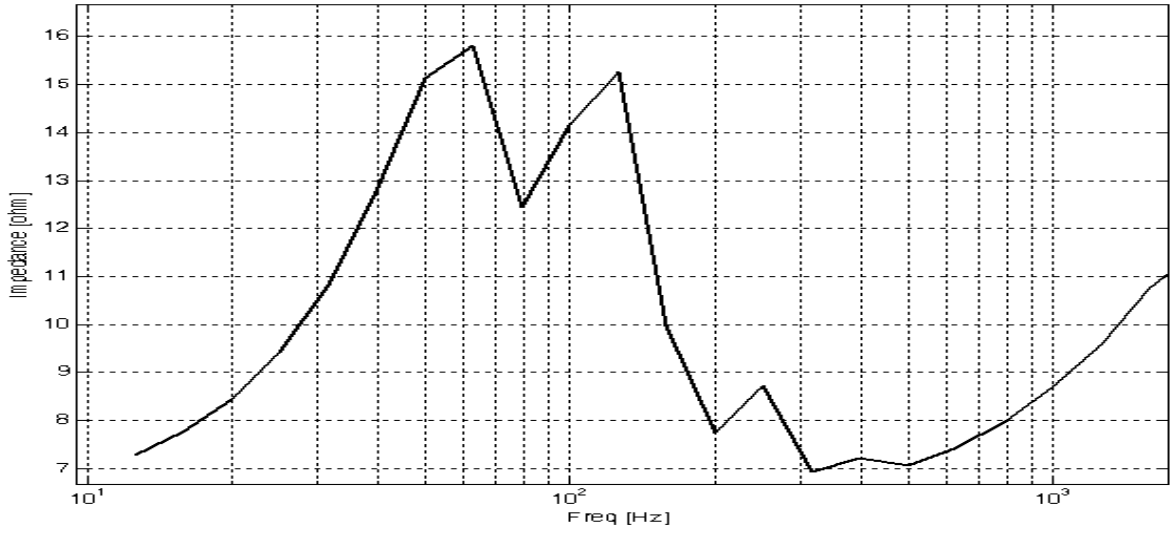

Fig. 3. Impedance Graph of the Speaker at the End of Empty Pipe

The Thiele/Small parameters of the speaker unit are measured and found to be F_s = 77 Hz, R_e = 5.7 Ohm, Q_e = 0.54, Q_m = 1.73, Q_t = 0.4, V_{as} = 5.47lt and S_d is measured to be 87 cm^2 according to Clio Standard Measurement System [17].

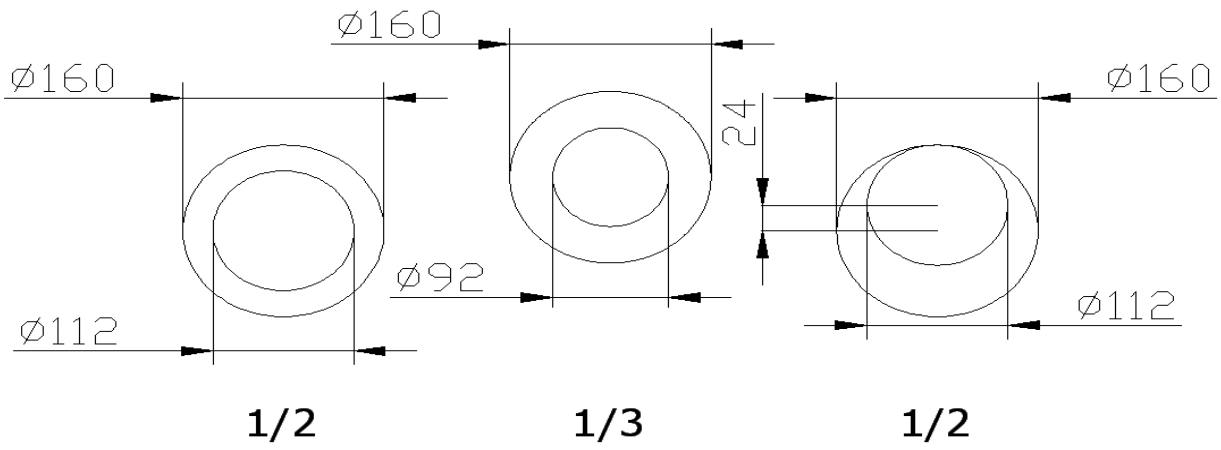

Fig. 4. Filter Parts

Thin aluminium disks with a thickness of 4mm were drilled. Two of the pairs were prepared to have holes at their centres. Two types of holes having an area equal to half of the cross sectional area of the transmission line (S_{TL}) and one third of the S_{TL} were drilled on those disks. A third pair was prepared where the holes were off the axis. Holes having an area equal to the half of the S_{TL} were drilled. A schematic representation of the system, showing all the possible filter placements used in the study, is given in Figure 5.

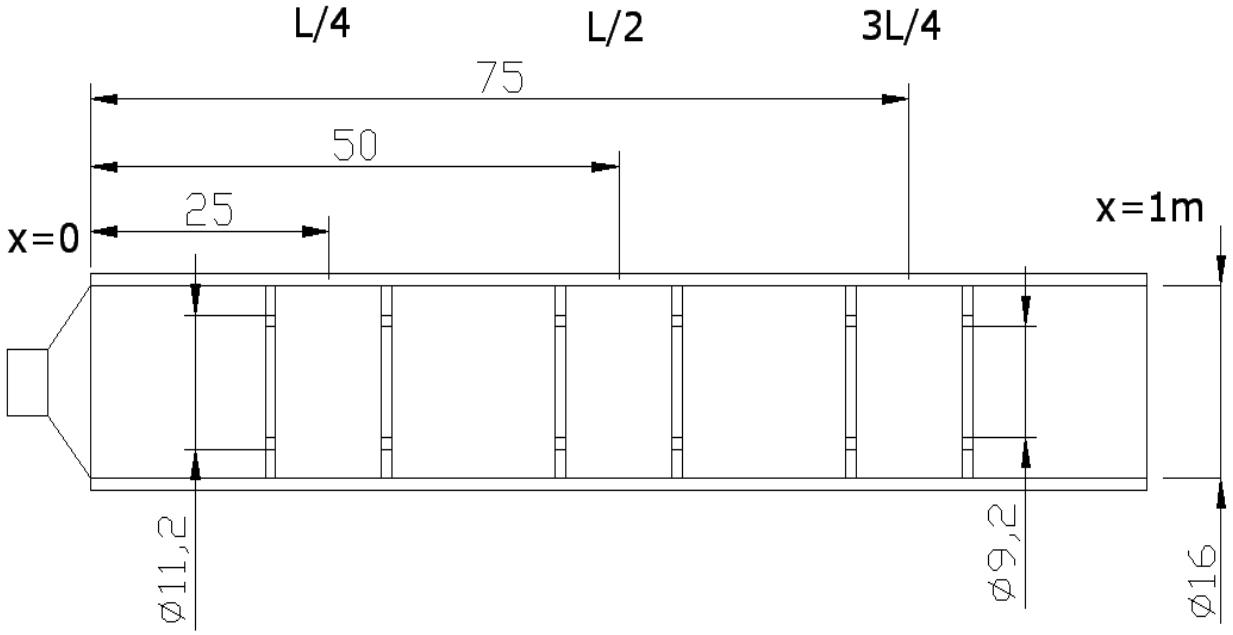

Fig. 5. Placement of Filter Parts

Depending on the length of the transmission line, the pairs were placed inside the test enclosure. The length of the transmission line was divided into three equal parts. The filters were placed inside the transmission line, in such a way that, the mid points between the two filter parts coincided with these three specified points. Only one pair was left in the transmission line during measurement.

IV. Simulation Results and Measurements

For the model used in numerical solution, a two-dimensional slice of the test enclosure, dividing it into two equal parts from the symmetry axis, was used. The rigid boundaries of the test enclosure were assigned as purely reflective boundaries in the two-dimensional simulation area. The source was defined as an ideal piston, which was not affected by the reflected waves coming from the obstacles inside the line. A simulation programme was generated to obtain a sine sweep between the nominal quarter-wave pipe resonance frequency and 1000Hz. The transfer function was also generated to identify the resonances inside the test enclosure.During a sine sweep for a particular filter, the RMS pressure of input and RMS pressure of output amplitudes were recorded under steady-state conditions for each frequency. Those values were used to generate a normalized transmission ratio graph. Transmission ratio (TR) is given by;

$$TR = \frac{Output\ Signal(RMS)}{Input\ Signal(RMS)}$$

In transmission ratio graphs (Figures 6, 8, 10 and 13), higher values indicate lower radiation amplitude and lower values show higher radiation amplitude from the line opening. These graphs are used to detect if any resonances in the selected frequency band occur. The location of the filter parts was decided according to the length of the calculated transmission line. The filters were placed at three different locations with the same cavity volume in between. The volume between the filter parts was determined according to the desired cross-over point. The volume between the filter parts was found to be the only effective parameter on the cross-over frequency. The location of the filter parts inside the transmission line and the cross-sectional area of the holes on the filter parts were found to have no effect on the cross-over frequency. In order to control the resonances over third harmonic, the volume between the filter pars is found to be $0.002m^3$. This value was achieved by running a range of volume values, which are capable of generating cross-over frequencies below and above the third harmonic, to the simulation software. The software generated results for the values within the given range and the volume which resulted in a cross-over point at 500Hz was selected.

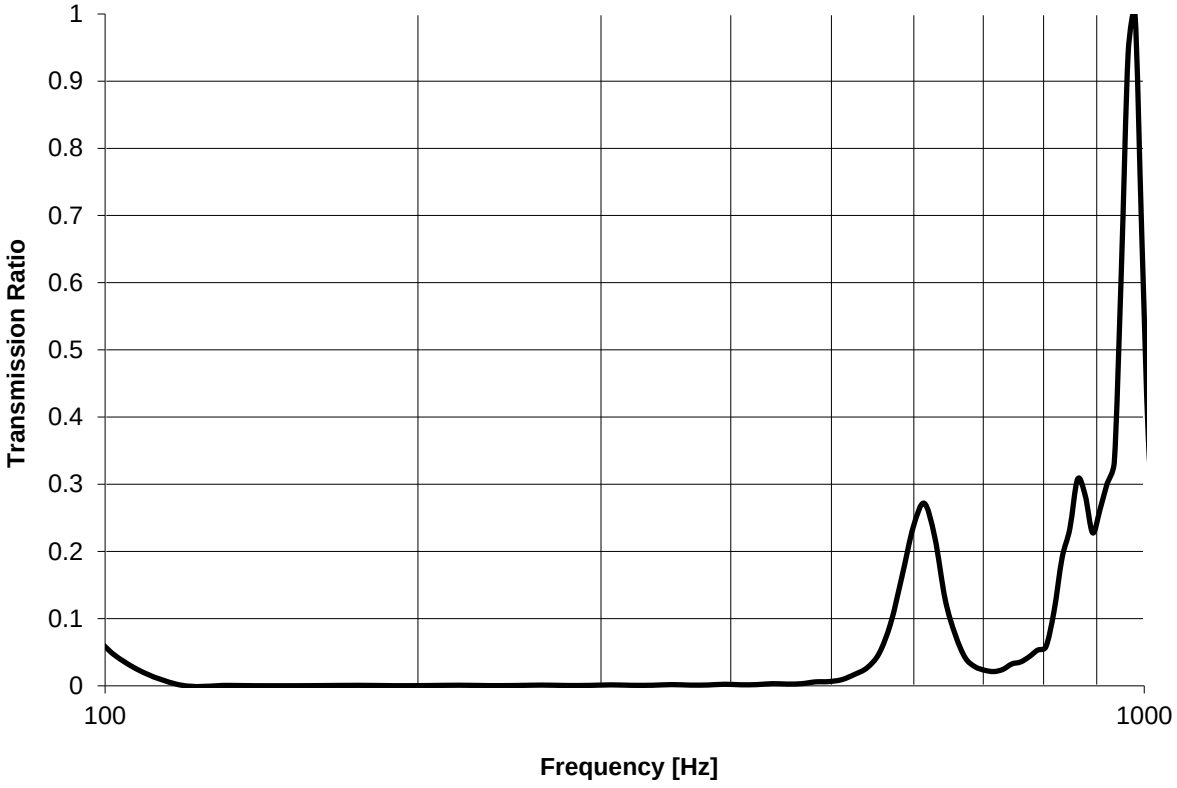

Fig. 6. Response for 20cm - 30cm Placement

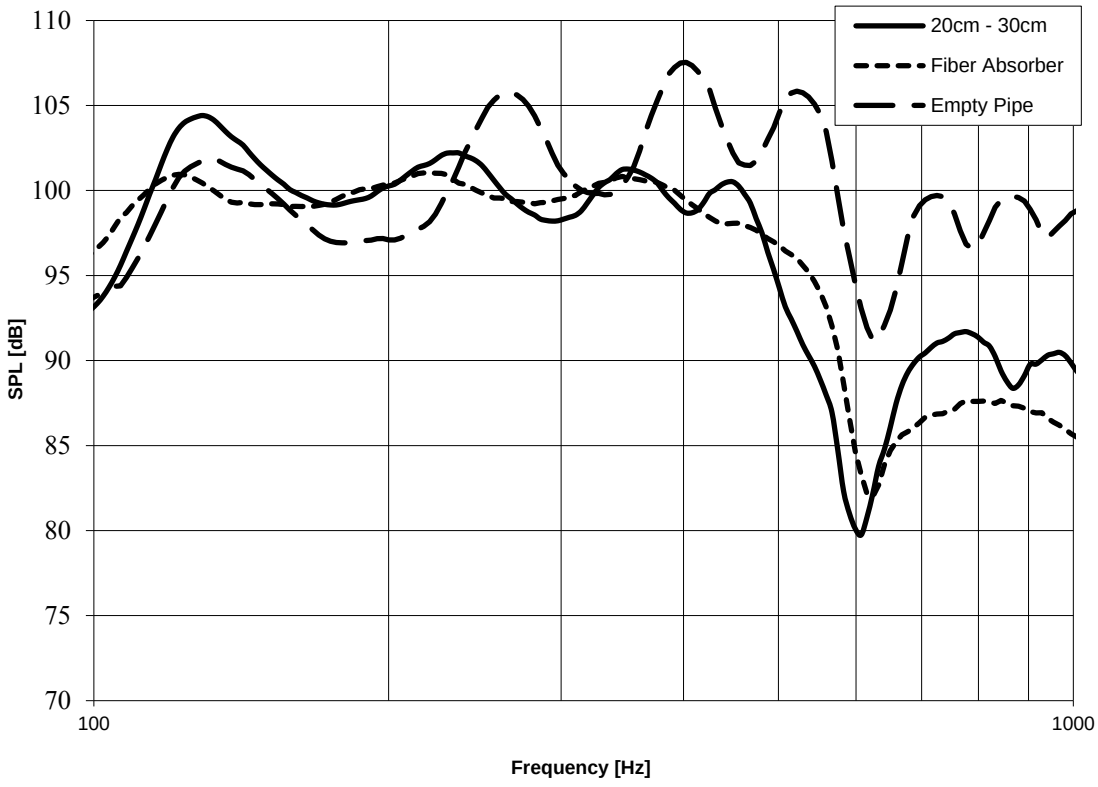

Fig. 7. Frequency Response for 20cm-30cm Placement

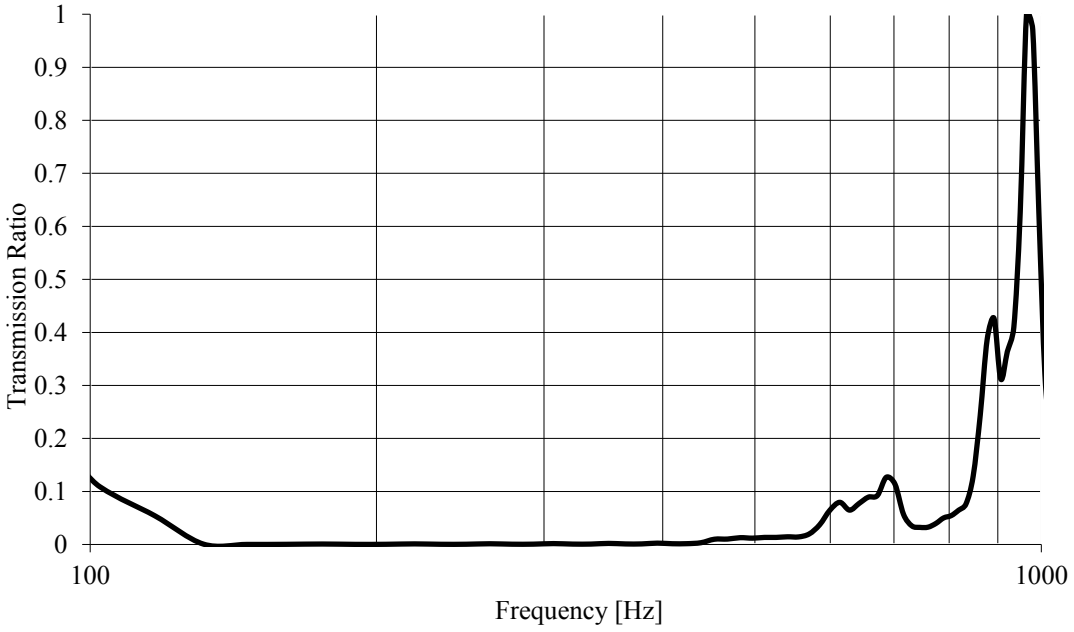

Fig. 8. Response for 45cm - 55cm Placement

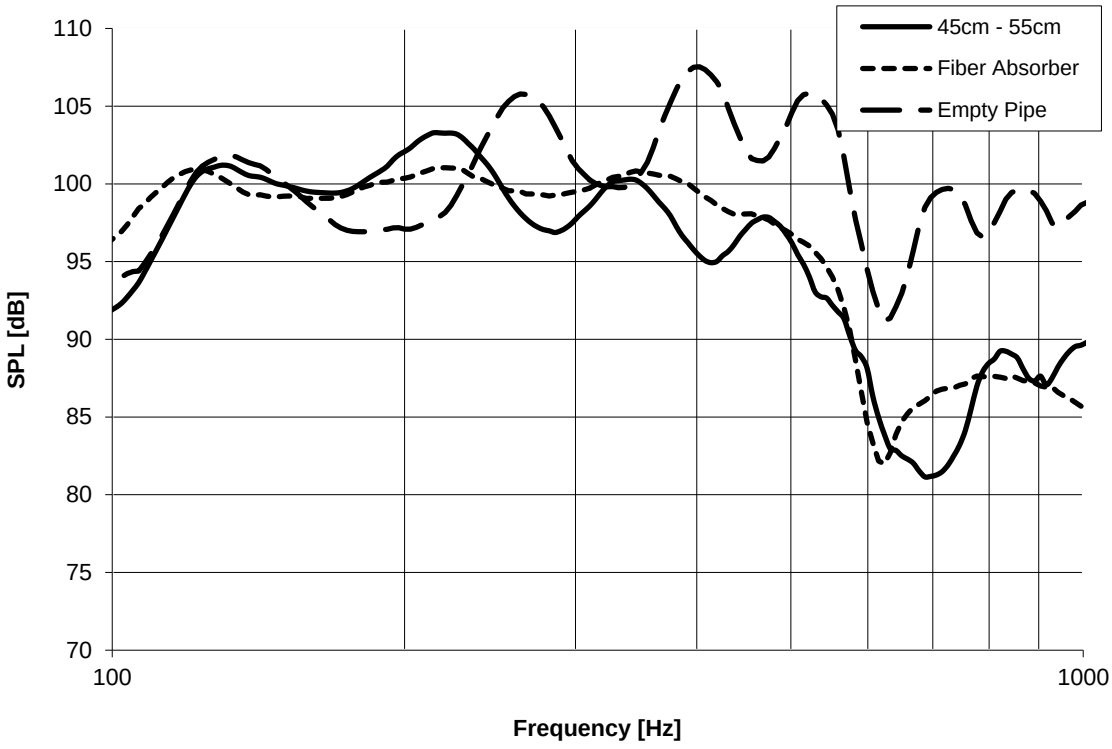

Fig. 9. Frequency Response for 45cm-55cm Placemen

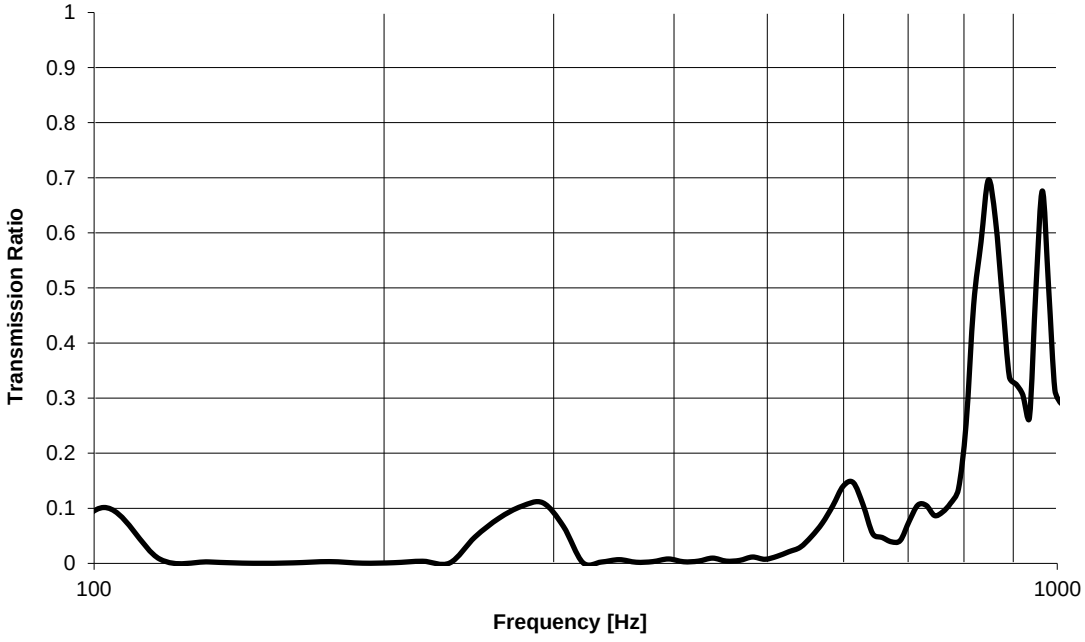

Fig. 10. Response for 70cm-80cm Placement

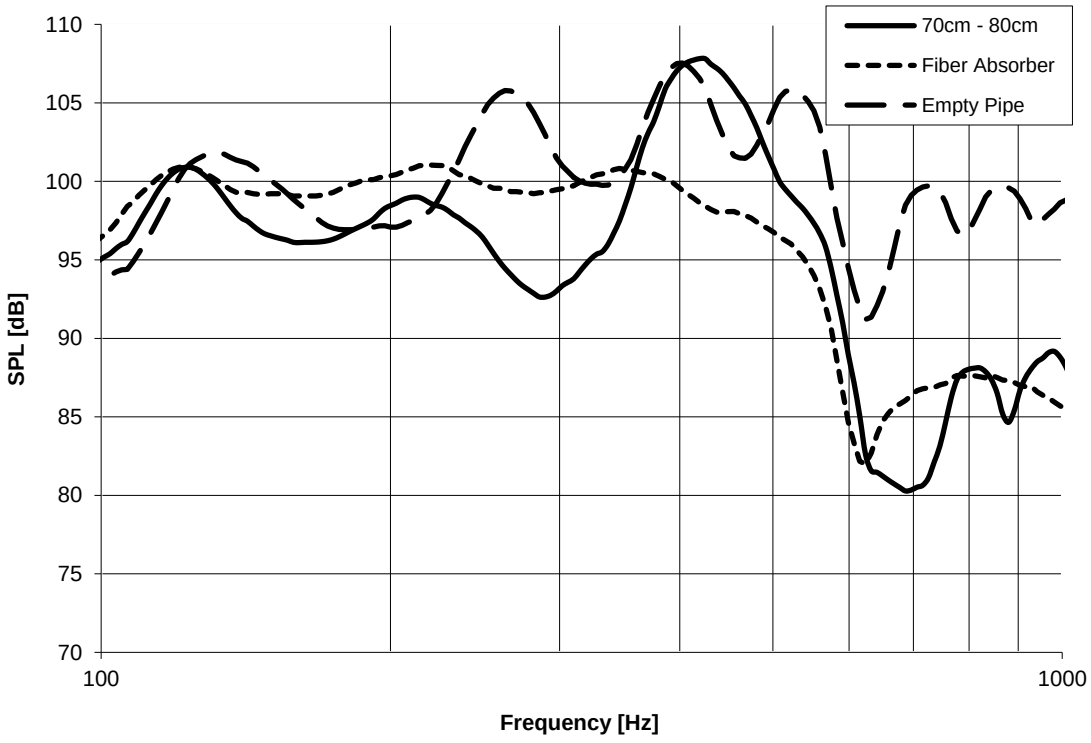

Fig. 11. Frequency Response for 70cm-80cm Placement

In order to have a flat response in the 100 – 1000Hz frequency band, asymmetrical placement of the discs at 45cm and 55cm, was studied also.

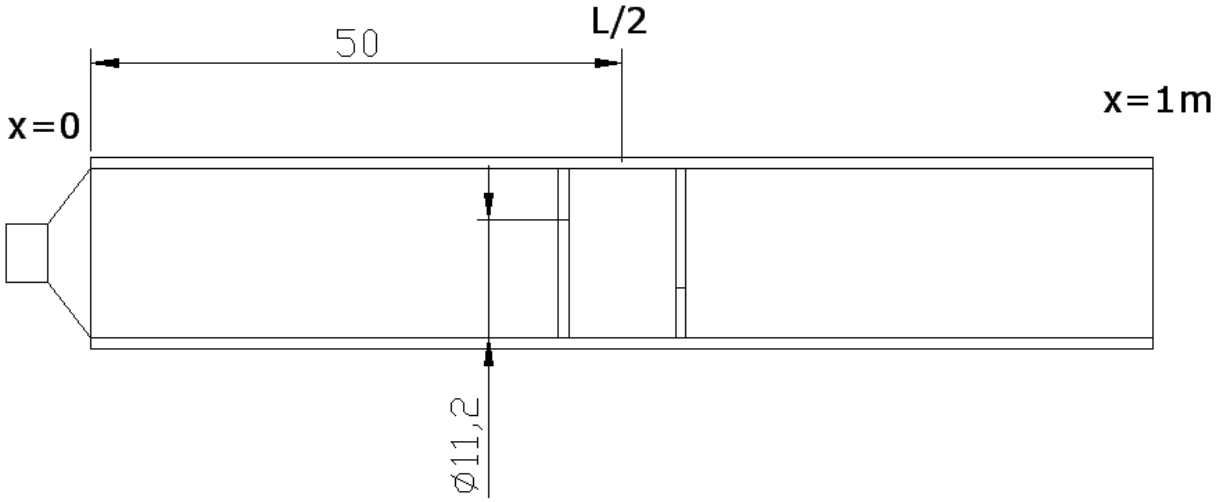

Fig. 12. 45cm - 55cm Asymmetrical Placement

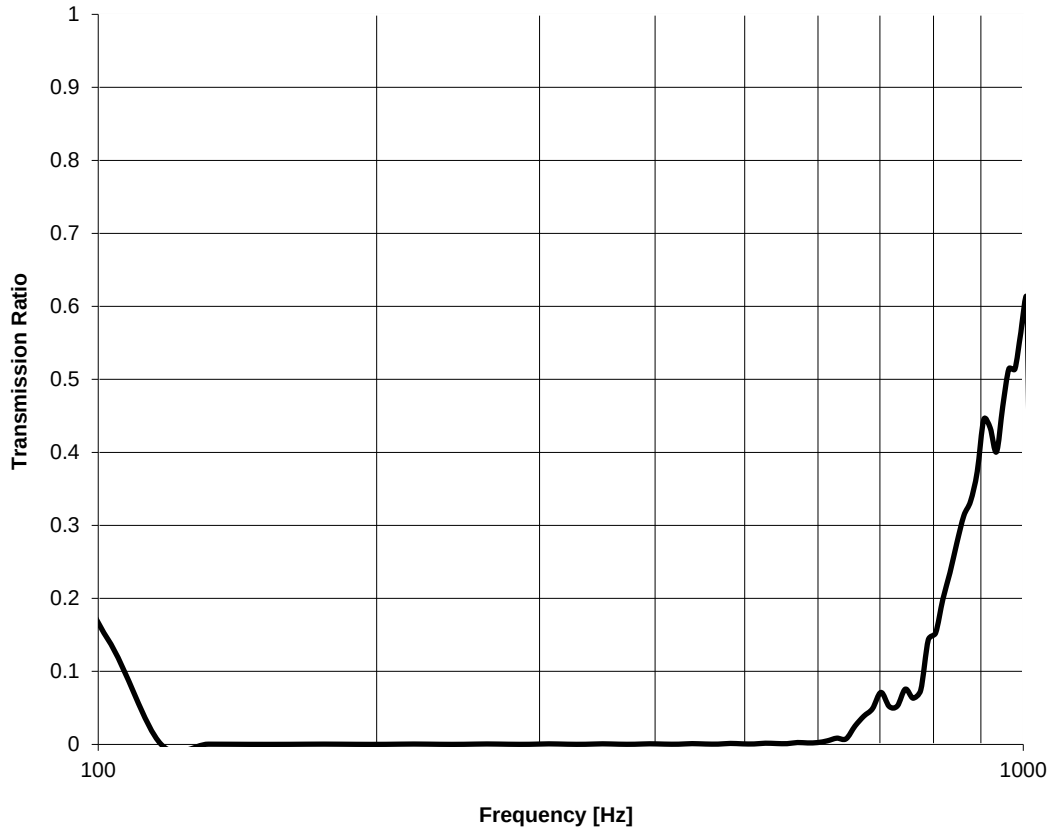

Fig. 13. Response for 45cm - 55cm Asymmetrical Placement

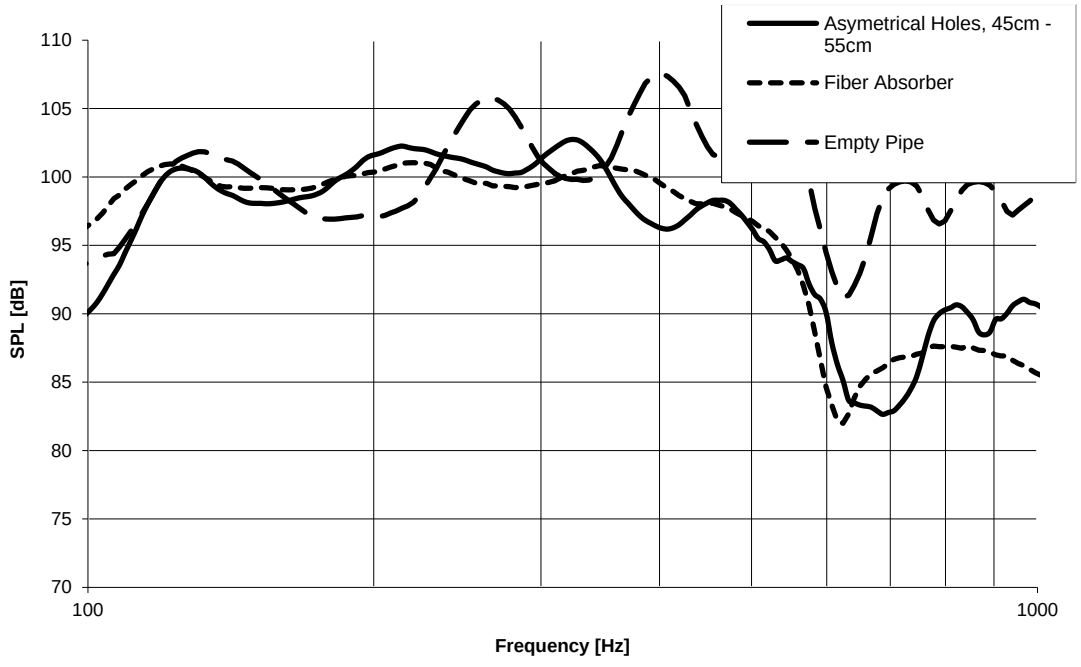

Fig. 14. Frequency Response for 45cm - 55cm Asymmetrical Placemen

The filter parts had openings which were equal to the half of the cross sectional area of the transmission line. The openings had an offset of one radius from the centre and were placed with 180° angle (Figure 12). As it can be seen from Figure 12, no resonances in the selected frequency band were found. Based on the results obtained from the simulations, comparative measurements between the absorber filled, acoustical filter placed and empty transmission line, were performed. The comparison of SPL values for the asymmetrical filter, the filter with the 1/3 S_{TL} and the absorber are shown in Figures 7, 9, 11 and 14. Responses in the desired frequency range were similar in Figures 9 and 14. Therefore, results suggested that asymmetrically placed filters and filters having openings equal to the 1/2 S_{TL} and 45cm – 55cm placement can be used for audio purposes.The frequency responses of other filters, which have smaller openings were also measured (Figure 15). The frequency responses were measured based on the absorber response which taken as the reference. Because the frequency responses of these filters were not in the range of ± 3 dB or the SPL values are not as high as absorber response, they were found not to be appropriate for audiopurposes.

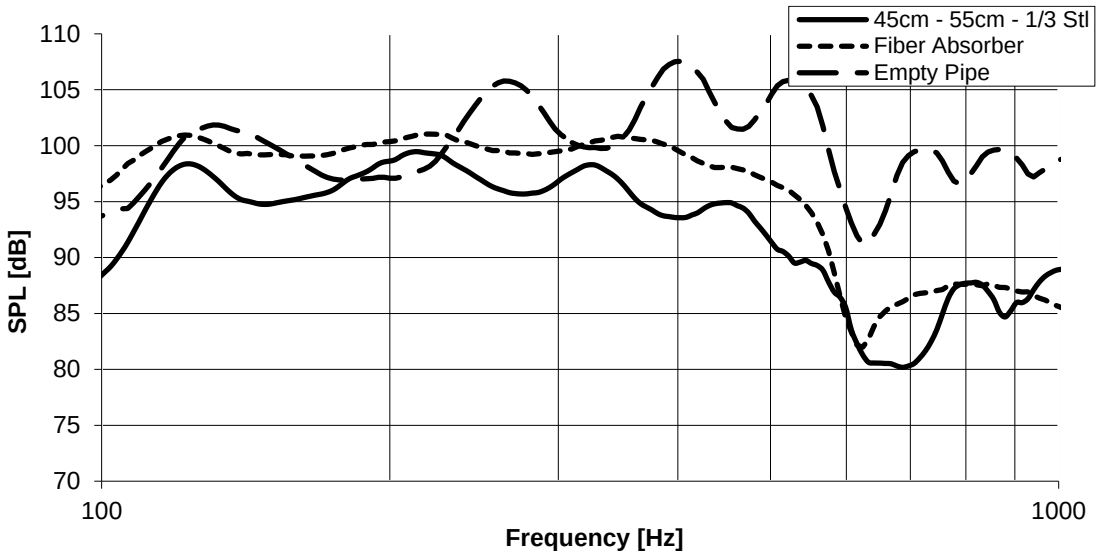

Fig. 15. Frequency Response for 45cm - 55cm with 1/3 S_{TL}

V. Results and Conclusions

A study to investigate the effectiveness of using reactive acoustical filters inside the transmission line enclosures instead of absorbers was carried out. In order to filter the frequencies over third harmonic, the volume, between the filter parts, was determined. The filter parts were placed inside the transmission line depending on the length of the line. Wave equation was solved numerically to investigate the behaviour of the acoustic low-pass filters inside the transmission line. The numeric solution was used to determine the resonances in the frequency band where planar standing waves could occur. Several simulations were carried out to find a flat response. Results of the simulations showed that two filters satisfied the condition of flatness. Comparisons within the desired frequency limits were made to compare the performance of the filters. No plane wave resonance within the desired frequency range (Figures 9 and 14) was observed. The filters, with some resonances exhibited undesirable frequency characteristics (Figures 7 and 11). The simulations showed that when there were less resonance peaks in the desired frequency range, the frequency response of that filter moved closer to the character of a damped transmission line.

The filter with an opening equal to the ½ S_{TL} and placed asymmetrically, and the filter with an opening of 1/2 S_{TL} and placed in the middle of the transmission line had similar frequency responses. The frequency responses of both filters were very close to that of the absorber response, but, the slopes were sharper than the slope of the absorber below the 100 Hz.

Results suggested that acoustical low pass filters, built by making sudden area changes can be used as a replacement for absorbers in the transmission lines.

VI. References

[1] B. Onley, "A Method of Eliminating Cavity Resonance, Extending Low Frequency Response and Increasing Acoustic Damping in Cabinet Type Loudspeakers", J. Acoust. Soc. Am., vol 8 (Oct. 1936)

[2] A. R. Bailey, "Non-Resonant Loudspeaker Enclosure", Wireless World (Oct. 1965)

[3] L. J. S. Bradbury, "The Use of Fibrous Materials in Loudspeaker Enclosures", J. Audio Eng. Soc., vol. 24, pp 162-170, (April 1976)

[4] B. N. Locanthi, "Application of Electric Circuit Analogies to Loudspeaker Design Problems", IRE National Convention, vol. PGA-6, (March 1952)

[5] G. L. Augspurger, "Loudspeakers on Damped Pipes", J. Audio Eng. Soc. Vol 48, pp 424-436, (May 2000)

[6] B. L. Simith, G. W. Swift, "Power dissipation and time-averaged pressure in oscillating flow through a sudden area change", J. Acoust. Soc. Am. vol 113, (May 2003)

[7] A. M. G. Gentemann, A. Fischer, S. Evesque, W. Polifke, "Acoustic Transfer Matrix Reconstruction and Analysis for Ducts with Sudden Change of Area", 9th AIAA/CEAS Aeroacoustics Conference and Exhibit 12-14 (May 2003)

[8] I. D. J. Dupere, A. P. Dowling, "Absorption of Sound near Abrupt Area Expansions", AIAA Journal, vol. 38, No. 2, (Feb. 2000)

[9] K. J. Baumeister, W. Eversman, R. J. Astley, J. W. White, "Acoustics in Variable Area Duct: Finite Element and Finite Difference Comparisons to Experiment", AIAA Journal, vol 21, no 2, (Feb 1983)

[10] L. L. Beranek, Acoustics (McGraw-Hill, New York, 1996), p. 136

[11] W. M. Leach Jr., Introduction to Electroacoustics and Audio Amplifier Design Kendall/Hunt Publishing Co., p.42 (2003)

[12] P. M. Morse, K. U. Ingard, Theoretical Acoustics, Princeton University Press, Princeton, New Jersey, p. 490 (1968)

[13] M. L. Munjal, Acoustics of Ducts and Mufflers with Application to Exhaust and Ventilation Systems (John Willey & Sons, Canada, 1987), p. 68

[14] D. D. McCracken, W. S. Dorn, Numerical Methods and Fortran Programming (John Wiley & Sons, New York, 1964), p. 337

[15] L. Lapidus, G. F. Pinder, Numerical Solution of Partial Differential Equations in Science and Engineering, (John Wiley & Sons, New York, 1982), p. 486

[16] G. C. Cohen, Higher-Order Numerical Methods for Transient Wave Equations (Springer, 2006), p.

[17] Clio Electro-Acoustic Measurement System Manual, Audiomatica, Italy, 2005

Absolute Positioning Instruments for Odometry System Integrated with Gyroscope by Using IKF

Surachai Panich[1] Nitin Afzulpurkar[2]

GJRE Classification (FOR)
GJRE:F , 671401 099902

***Abstract*- In this paper, absolute positioning instrument using trilateration ultrasonic sensor is mainly proposed to estimate absolute position errors combined with estimated position and orientation from differential odometry integrated with gyroscope to calculate absolute position of mobile robot. In the method, the indirect Kalman filter is mainly used to estimate absolute position errors and the estimated errors are fed back to odometry system, and also estimates some parameter errors to correct encoder and gyroscope error. The simulation and experiment results show the estimated position and orientation of odometry system integrated with gyroscope, systematic errors of encoder and gyroscope and absolute position from trilateration ultrasonic sensor compared with odometry system integrated with gyroscope.**

Keywords- absolute positioning, indirect Kalman filter, odometry system, trilateration ultrasonic sensor.

I. INTRODUCTION

Typically, mobile robots behavior such as navigation, map building, the estimation of own position is very important. There are a lot of researches regarding the mobile robot in navigation such as (Maeyama, 1996; Borenstein, 1996; Hakyoung, 2001; Bostani, A., et al., 2008; Byoung-Suk Choi, 2009; Takeshi Sasaki, 2010). In navigation system can be categorized in relative and absolute positioning systems. The relative positioning system estimates a current position by using the information about previous positions and velocities. Basically, the method of estimation for a wheel type mobile robot's position uses the wheel encoder called odometry system. This is based on the wheel sensor readings of a differential-drive robot. In odometry (wheel sensors only) and dead reckoning (also heading sensors) the position update is based on sensors information. The movement of the robot sensed with wheel encoders or heading sensors or both, is integrated to compute position. Thus the position has to be updated from time to time by other localization mechanisms. Because the sensor measurement errors are integrated, the position error accumulates over time. However, these cumulative errors can be reduced by additional sensors. In outdoor environment, the estimated position by encoder has the unpredictable error caused by traveling over an unexpected small obstacle or a bump under the wheels. In this case, the accuracy of the estimated robot‘s position is suddenly getting worse.

About-[1] School of Engineering and Technology, Asian Institute of Technology, P.O. Box 4, Klong Luang, Pathumthani 12120, Thailand, (surachai.panich@ait.ac.th)
About-[2] School of Engineering and Technology, Asian Institute of Technology, P.O. Box 4, Klong Luang, Pathumthani 12120, Thailand, (nitin@ait.ac.th)

The position error is detailed in differential equation either inertia measurement unit (IMU) or support sensors nowadays with some solutions in textbook (Britting, 1971). The analysis of navigation process from Kelly (Kelly, 2001) is under special consideration about systematic error and theory on navigation. Also the compensation of position‘s error with redundant sensors is discussed (Larsen, 1998; Chung, 2001), however always limits on some redundant support systems. Despite these limitations, most researchers agree that encoder is an important part of a robot navigation system and that navigation tasks will be simplified if encoder accuracy can be improved. For example, the map-based positioning system is the method in absolute positioning system by using environment as landmark (Luis M. Valentin-Coronado, et al., 2009; Sotirios Ch. Diamantas and Richard M. Crowder, 2009). A mobile robot builds a local map by using onboard sensors and compares the local map with a global map. If the features from local map and the global map match, an absolute position of the mobile robot is computed. Researches on the map-based positioning have been mainly focused on creating an accurate local map and estimating the positions by a map matching techniques. Cameras are the most complex sensors recently utilized due to high computational and memory requirements, as well as high cost in robotics. On researches in robotic field are using either local or global vision. In global vision, the camera is used as external instrument to monitor area, which covers both of the robot and environment. The global vision is easy to realize and widely used such as in factory environments or in robotic filed, i.e. the popular competition of robot soccer. The absolute positioning system estimates a current position measuring the position from predefined positions. The position errors of the absolute positioning system are bounded, because the information on previous positions is not required. However the absolute positioning system cannot provide absolute position information along path because of absolute positioning instrument‘s cost and operation in large area. Therefore, a hybrid navigation system plays an important role in combination of the relative or absolute positioning system by selection one from each category. Optimal localization should take into account the information provided by all of these sensors. A powerful technique for achieving this sensor fusion, called the Kalman filter (Kang Li, et al., 2009). It is a mathematical mechanism for producing an optimal estimate of the system state based on the knowledge of the system and the measuring device, the description of the system noise and measurement errors and the uncertainty in the dynamics models. Thus the Kalman filter fuses sensor information and system knowledge in an optimal solution. Optimality

depends on the criteria chosen to evaluate the performance. Within the Kalman filter theory the system is assumed to be linear with Gaussian noise. This paper proposes two main points. The first point is the integration of absolute positioning instruments in navigation process, which can support mainly differential odometry system. For the second point the navigation parameter with complementary support system based on indirect Kalman filter (IKF) and with model of redundant error sources can compensate each other. The indirect Kalman filter can estimates the errors in the navigation and attitude information using the difference between inertial navigation system (INS) and external source data (Maybeck, 1979). The error model is separated between systematic and non-systematic. The different measurement of error level is performed by complement of redundant support system. For all relevant navigation parameters is with concept of relative and absolute support system in form of external redundant source. In scope of hybrid approach the differential odometry and support system for our purpose are combined that the navigation problem in real-time can be solved. By the experimental test sensor information are from real physical sensors. Section 2 describes the generally differential drive for mobile robot including encoder model. Section 3 explains the widely relative support of gyroscope. The trilateration ultrasonic sensor is explained in section 4. The hybrid navigation system is described in section 5. Simulations and experiments are presented in section 6 and finally concludes the paper.

II. DIFFERENTIAL DRIVE FOR MOBILE ROBOT AS MAIN SYSTEM

Generally, in navigation of mobile robot localization plays an important role. The robot's position is defined as $\mathbf{P}_k = [\mathbf{X}_k, \mathbf{Y}_k, \boldsymbol{\theta}_k]^T$ and the next position $\mathbf{P}_{k+1}$ is calculated from current position plus the position's increment both translation $\Delta\mathbf{S}_k = [\Delta\mathbf{S}_{x,k} \quad \Delta\mathbf{S}_{y,k}]^T$ and rotation increment $\Delta\boldsymbol{\theta}_k$ with reference to geometry as

$$\mathbf{P}_{k+1} = \mathbf{P}_k + \begin{bmatrix} \Delta\mathbf{S}_{x,k} \\ \Delta\mathbf{S}_{y,k} \\ \Delta\boldsymbol{\theta}_k \end{bmatrix} \qquad (1)$$

With the increment $\Delta\mathbf{S}_k$ and $\Delta\boldsymbol{\theta}_k$ are used as couple function to construct mobile robot. In the differential drive system may consider that mobile robot move in curve path. Generally, the kinematics of differential drive consists of two wheels with wheel base $\mathbf{B}_k$. In Fig.1 mobile robots are widely integrated with encoders at the left and right wheels, which generate the increment translation $\Delta\mathbf{S}_{L,k}$ and $\Delta\mathbf{S}_{R,k}$.

A. Position error analysis

By the real robot path the parameter $\mathbf{B}_k$, $\Delta\mathbf{S}_{L,k}$ and $\Delta\mathbf{S}_{R,k}$ behavior are not linear, because they are affected with error. These errors cannot be solved by exact equation, however their state-space model can be considered as linear. With these errors can be separated in so called systematic and nonsystematic errors (Borenstein, 1997; Komoriya, 1994; Bostani, A., et al., 2008).

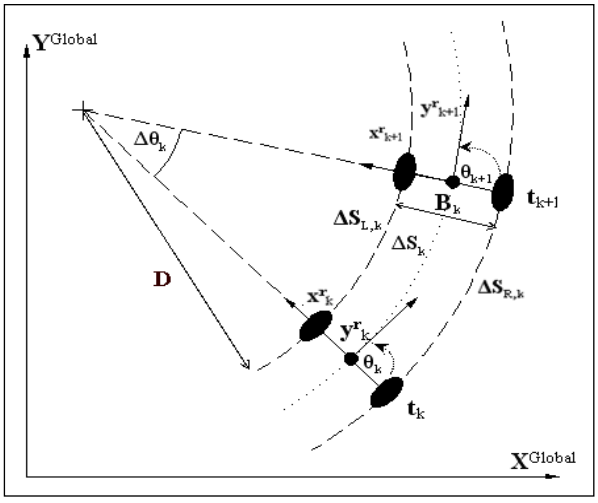

Fig.1. Kinematics relation between $\Delta\mathbf{S}_k$, $\Delta\boldsymbol{\theta}_k$, B_k, $\Delta\mathbf{S}_{L,k}$ and $\Delta\mathbf{S}_{R,k}$.

B. Wheel-base (distance between drive wheels) error

The wheel base is distance between both drive wheels. The distance B cannot be exactly measured because it can change during running (Bostani, A., et al., 2008). Uncertainty in the effective wheelbase is caused by the fact that rubber tires, which do not contact the floor in one point, but rather in a contact area. This resulting uncertainty about the effective wheelbase can be changed always during the robot run. This generates wheel-base error $\Delta\mathbf{B}_k$ and affects in equation (3) especially during fast turn. Therefore the rotation increment is affect by errors and the robot's orientation error is unbounded too.

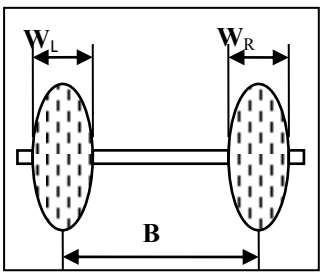

Fig.2.Wheel base of a mobile robot.

C. Theoretical wheel encoder model

The basic concept of odometry is the transformation from wheel revolution to linear translation on the floor (Naveen Kumar Boggarpu and Richard C. Kavanagh, 2010; Takeshi Sasaki, 2010). This transformation is affected with errors by wheel slippage, unequal wheel diameter, inaccurate wheel

base distance, unknown factor and others. The real increment translation of wheel encoder is prone to systematic and some non-systematic errors. The theoretical translation and rotation increment at the center of the robot is calculated by

$$\Delta \mathbf{S}_k^t = \frac{\Delta \mathbf{S}_{R,k}^t + \Delta \mathbf{S}_{L,k}^t}{2}, \quad (2)$$

$$\Delta \boldsymbol{\theta}_k^t = \frac{\Delta \mathbf{S}_{R,k}^t - \Delta \mathbf{S}_{L,k}^t}{\mathbf{B}_k}. \quad (3)$$

Position extrapolation with theoretical encoder model is written as

$$\mathbf{P}_{k+1}^t = \mathbf{P}_k^t + \Delta \mathbf{P}_k^t, \quad (4)$$

and is detailed below

$$\mathbf{X}_{k+1}^t = \mathbf{X}_k^t + \Delta \mathbf{S}_k^t \cos \boldsymbol{\theta}_k^t, \quad (5)$$

$$\mathbf{Y}_{k+1}^t = \mathbf{Y}_k^t + \Delta \mathbf{S}_k^t \sin \boldsymbol{\theta}_k^t, \quad (6)$$

$$\boldsymbol{\theta}_{k+1}^t = \boldsymbol{\theta}_k^t + \Delta \boldsymbol{\theta}_k^t. \quad (7)$$

D. *Practical encoder model*

Incremental wheel encoders are based on the assumption that wheel revolutions can be translated into linear displacement relative to the floor. Wheel encoder error will occur, when if one wheel is to slip on, the associated encoder will not correctly correspond to a linear displacement of the wheel. All error sources are into one of two categories, which are systematic and non-systematic errors. Systematic errors are particularly considered, because they accumulate constantly, which can be reduced by careful mechanical design and by calibration. Non-systematic errors are not directly caused by the kinematic properties of the vehicle, example, wheel-slippage or irregularities of the floor. With smooth floor, systematic errors cause much more to wheel encoders errors than non-systematic errors. On rough surfaces non-systematic errors are the dominant source of wheel encoder errors. In practice encoders are prone to various systematic and non-systematic errors in the detection of $\Delta \mathbf{S}_{R,k}$ land $\Delta \mathbf{S}_{L,k}$. The output of ideal wheel encoder is corrupted by systematic error from hardware imperfections as time and temperature varying scale factor errors (Yang H., et al., 2000; Chung H., et al., 2001). From practical system inputs

$$\Delta \mathbf{S}_{R,k}^p = (1 + \boldsymbol{\Omega}_{R,k}) g \Delta \mathbf{S}_{R,k}^t = \Delta \mathbf{S}_{R,k}^t + \boldsymbol{\Omega}_{R,k} g \Delta \mathbf{S}_{R,k}^t, \quad (8)$$

$$\Delta \mathbf{S}_{L,k}^p = (1 + \boldsymbol{\Omega}_{L,k}) g \Delta \mathbf{S}_{L,k}^t = \Delta \mathbf{S}_{L,k}^t + \boldsymbol{\Omega}_{L,k} g \Delta \mathbf{S}_{L,k}^t, \quad (9)$$

and from equations (2), (3), (8) and (9) can be transformed in to a translation increment as

$$\Delta \mathbf{S}_k^p = \frac{\Delta \mathbf{S}_{R,k}^p + \Delta \mathbf{S}_{L,k}^p}{2} = \frac{(\Delta \mathbf{S}_{R,k}^t + \boldsymbol{\Omega}_{R,k} g \Delta \mathbf{S}_{R,k}^t) + (\Delta \mathbf{S}_{L,k}^t + \boldsymbol{\Omega}_{L,k} g \Delta \mathbf{S}_{L,k}^t)}{2} \quad (10)$$

and rotation increment

$$\Delta \boldsymbol{\theta}_k^p = \frac{\Delta \mathbf{S}_{R,k}^p - \Delta \mathbf{S}_{L,k}^p}{\mathbf{B}_k + \Delta \mathbf{B}_k} = \frac{(\Delta \mathbf{S}_{R,k}^t + \boldsymbol{\Omega}_{R,k} g \Delta \mathbf{S}_{R,k}^t) - (\Delta \mathbf{S}_{L,k}^t + \boldsymbol{\Omega}_{L,k} g \Delta \mathbf{S}_{L,k}^t)}{\mathbf{B}_k + \Delta \mathbf{B}_k}. \quad (11)$$

Q

Position with practical encoder model can be estimated as

$$\mathbf{X}_{k+1}^p = \mathbf{X}_k^p + \frac{(\Delta \mathbf{S}_{R,k}^t + \boldsymbol{\Omega}_{R,k} g \Delta \mathbf{S}_{R,k}^t) \cos \boldsymbol{\theta}_k^p}{2} + \frac{(\Delta \mathbf{S}_{L,k}^t + \boldsymbol{\Omega}_{L,k} g \Delta \mathbf{S}_{L,k}^t) \cos \boldsymbol{\theta}_k^p}{2} \quad (12)$$

$$\mathbf{Y}_{k+1}^p = \mathbf{Y}_k^p + \frac{(\Delta \mathbf{S}_{R,k}^t + \boldsymbol{\Omega}_{R,k} g \Delta \mathbf{S}_{R,k}^t) \sin \boldsymbol{\theta}_k^p}{2} + \frac{(\Delta \mathbf{S}_{L,k}^t + \boldsymbol{\Omega}_{L,k} g \Delta \mathbf{S}_{L,k}^t) \sin \boldsymbol{\theta}_k^p}{2}, \quad (13)$$

$$\boldsymbol{\theta}_{k+1}^p = \boldsymbol{\theta}_k^p + \frac{(\Delta \mathbf{S}_{R,k}^t + \boldsymbol{\Omega}_{R,k} g \Delta \mathbf{S}_{R,k}^t)}{\mathbf{B}_k + \Delta \mathbf{B}_k} - \frac{(\Delta \mathbf{S}_{L,k}^t + \boldsymbol{\Omega}_{L,k} g \Delta \mathbf{S}_{L,k}^t)}{\mathbf{B}_k + \Delta \mathbf{B}_k}. \quad (14)$$

Firstly, the error state $\delta \mathbf{X}$ can be calculated by subtraction of the theoretical position values from practical position values yields the error propagation equations

$$\delta \mathbf{X}_{k+1} = \delta \mathbf{X}_k + \frac{\boldsymbol{\Omega}_{R,k} g \Delta \mathbf{S}_{R,k}^t \cos \boldsymbol{\theta}_k^t}{2} + \frac{\boldsymbol{\Omega}_{L,k} g \Delta \mathbf{S}_{L,k}^t \cos \boldsymbol{\theta}_k^t}{2} - \frac{(\Delta \mathbf{S}_{R,k}^t + \Delta \mathbf{S}_{L,k}^t) \sin \boldsymbol{\theta}_k^t g \delta \boldsymbol{\theta}_k}{2} \quad (15)$$

$$\delta \mathbf{Y}_{k+1} = \delta \mathbf{Y}_k + \frac{\boldsymbol{\Omega}_{R,k} g \Delta \mathbf{S}_{R,k}^t \sin \boldsymbol{\theta}_k^t}{2} + \frac{\boldsymbol{\Omega}_{L,k} g \Delta \mathbf{S}_{L,k}^t \sin \boldsymbol{\theta}_k^t}{2} + \frac{(\Delta \mathbf{S}_{R,k}^t + \Delta \mathbf{S}_{L,k}^t) \cos \boldsymbol{\theta}_k^t g \delta \boldsymbol{\theta}_k}{2} \quad (16)$$

$$\delta \boldsymbol{\theta}_{k+1} = \delta \boldsymbol{\theta}_k + \frac{\boldsymbol{\Omega}_{R,k} g \Delta \mathbf{S}_{R,k}^t}{\mathbf{B}_k} - \frac{\boldsymbol{\Omega}_{L,k} g \Delta \mathbf{S}_{L,k}^t}{\mathbf{B}_k} + \frac{(\Delta \mathbf{S}_{L,k}^t - \Delta \mathbf{S}_{R,k}^t) g \Delta \mathbf{B}}{\mathbf{B}_k^2}, \quad (17)$$

with the assumption that $\delta \boldsymbol{\theta}_k$ is small then $\cos \delta \boldsymbol{\theta}_k \approx 1$, $\sin \delta \boldsymbol{\theta}_k \approx \delta \boldsymbol{\theta}_k$, $\delta \boldsymbol{\theta}_k g \boldsymbol{\Omega}_{R,k} \approx 0$, $\delta \boldsymbol{\theta}_k g \boldsymbol{\Omega}_{L,k} \approx 0$ and $\mathbf{B}_k ? \Delta \mathbf{B}_k$.

$$\begin{bmatrix} \delta X_{k+1} \\ \delta Y_{k+1} \\ \delta \theta_{k+1} \\ \Omega^{O}_{R,\,k+1} \\ \Omega^{O}_{L,\,k+1} \\ \Delta B_{k+1} \end{bmatrix} = \begin{bmatrix} 1 & 0 & -\frac{\Delta S^{p}_{R,\,k} + \Delta S^{p}_{L,\,k}}{2} \sin\theta^{p}_{k} & \frac{\Delta S^{t}_{R,\,k} \cos\theta^{p}_{k}}{2} & \frac{\Delta S^{t}_{R,\,k} \cos\theta^{p}_{k}}{2} & 0 \\ 0 & 1 & \frac{\Delta S^{p}_{R,\,k} + \Delta S^{p}_{L,\,k}}{2} \cos\theta^{p}_{k} & \frac{\Delta S^{t}_{R,\,k} \sin\theta^{p}_{k}}{2} & \frac{\Delta S^{t}_{L,\,k} \sin\theta^{p}_{k}}{2} & 0 \\ 0 & 0 & 1 & \frac{\Delta S^{t}_{R,\,k}}{B_{k}} & -\frac{\Delta S^{t}_{L,\,k}}{B_{k}} & -\frac{\Delta S^{p}_{R,\,k} + \Delta S^{p}_{L,\,k}}{B^{2}_{k}} \\ 0 & 0 & 0 & 1 & 0 & 0 \\ 0 & 0 & 0 & 0 & 1 & 0 \\ 0 & 0 & 0 & 0 & 0 & 1 \end{bmatrix} \begin{bmatrix} \delta X_{k} \\ \delta Y_{k} \\ \delta \theta_{k} \\ \Omega^{O}_{R,\,k} \\ \Omega^{O}_{L,\,k} \\ \Delta B_{k} \end{bmatrix} \quad . (18)$$

Also the encoder scale factor of both wheels and wheel-base distance are regarded as random constants varying slightly in practice, so $\Omega_{R/L,\,k+1} = \Omega_{R/L,\,k}$, $\Delta B_{k+1} = \Delta B_{k}$.

E. State space of navigation system

A first-order linearization of equations (15)-(17) can be evaluated by Jacobians method and the result of navigation system matrix is detailed as equation (18). The state ariable, using X_k as the robot's position including some parameters of systematic errors is formulated as

$$x^{O}_{k} = \begin{bmatrix} X_{k} & Y_{k} & \theta_{k} & \Omega^{O}_{R,\,k} & \Omega^{O}_{L,\,k} & \Delta B_{k} \end{bmatrix}^{T} . (19)$$

The position and heading is computed by the differential encoder. As the wheel diameter error (encoder scale factor error) and the wheel base error are the dominant systematic errors of the encoder, we are mainly concerned to reduce those errors using the gyroscope.

III. DIFFERENTIAL ODOMETRY INTEGRATED WITH GYROSCOPE

The creation of relative support for differential odometry is the compensation both translation and rotation increment. The relative support can compensate error from odometry system for translation and rotation increment. With compensation by relative support system can reduce errors generated by noise. This paper presents also relative support system of rotation increment $\Delta\theta^{G}_{k}$ with gyroscope sensor. This work selects the commercial gyroscope CRS-03 (Silicon Sensing, 2000) working in measurement area ± 200°/s and $\Delta\theta^{G} = 3.2° \pm 0.01°$ shown in Fig.3.

A. Gyroscope model

Many researchers on robotic field work on about gyroscope sensor (Komoriya & Oyama, 1993; Karthick Srinivasan and Jason Gu, 2007). The theoretical gyroscope produces rotation increment in time interval k defined as $\Delta\theta^{G,\,t}_{k}$. For position extrapolation with theoretical gyroscope is written as

$$\theta^{G,\,t}_{k+1} = \theta^{G,\,t}_{k} + \Delta\theta^{G,\,t}_{k} . \qquad (20)$$

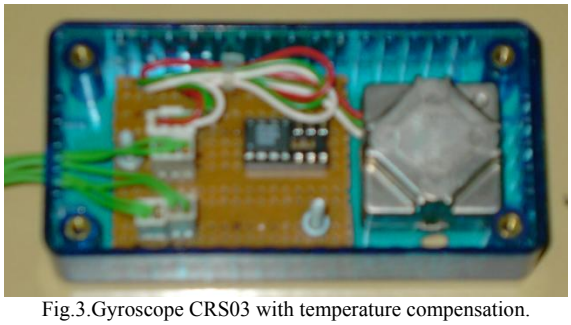

Fig.3.Gyroscope CRS03 with temperature compensation.

The practical gyroscope output

$$\Delta\theta^{G,\,P}_{k} = \Delta\theta^{G,\,t}_{k} + \Omega^{G}_{k}\, g\Delta\theta^{G,\,t}_{k} \qquad (21)$$

is corrupted by the scale factor error Ω^{G}_{k} and bias Ψ^{G}_{k}. The dominant gyroscope random errors are the random bias and the scale factor error. Generally, the gyroscope output signal is not zero even though there is no input and the effect of the earth rotation is neglected. The bias error of gyroscope is the signal output from the gyroscope when it is not any rotation. It is one of errors from gyroscope output reading. The bias error tends to vary with temperature and over time. The scale factor relates the output of the gyroscope to the corresponding gyroscope rotation angle about its input axis. By error of the scale factor in gyroscope it means the deviation between the actual scale factor and the nominal scale factor. The output beat frequency changes with the changing of the scale factor when the input rate is the same, which affects precision of gyro directly. For position extrapolation with practical gyroscope can be formulated as

$$\theta^{G,\,p}_{k+1} = \theta^{G,\,P}_{k} + \Delta\theta^{G,\,P}_{k} = \theta^{G,\,P}_{k} + \Delta\theta^{G,\,t}_{k} + \Omega^{G}_{k}\, g\Delta\theta^{G,\,t}_{k} + \Psi^{G}_{k} . \qquad (22)$$

The scale factor error Ω^{G}_{k} and bias error Ψ^{G}_{k} can be regarded as random constants varying slightly in practical as $\Omega^{G}_{k+1} = \Omega^{G}_{k}$, $\Psi^{G}_{k+1} = \Psi^{G}_{k}$. The error state vector is calculated by subtraction of the theoretical orientation value from practical orientation value yields the error orientation propagation

$$\delta\theta^{G}_{k+1} = \delta\theta^{G}_{k} + \Omega^{G}_{k}\, g\Delta\theta^{G,\,t}_{k} + \Psi^{G}_{k} . \qquad (23)$$

$$\begin{bmatrix} \delta X_{k+1} \\ \delta Y_{k+1} \\ \delta\theta_{k+1} \\ \Omega^{O}_{R,k+1} \\ \Omega^{O}_{L,k+1} \\ \Delta B_{k+1} \\ \delta\theta^{G}_{k+1} \\ \Omega^{G}_{k+1} \\ \Psi^{G}_{k+1} \end{bmatrix} = \begin{bmatrix} 1 & 0 & -\frac{\Delta S^{p}_{R,k} + \Delta S^{p}_{L,k}}{2}\sin\theta^{p}_{k} & \frac{\Delta S^{t}_{R,k}\cos\theta^{p}_{k}}{2} & \frac{\Delta S^{t}_{R,k}\cos\theta^{p}_{k}}{2} & 0 & 0 & 0 & 0 \\ 0 & 1 & \frac{\Delta S^{p}_{R,k} + \Delta S^{p}_{L,k}}{2}\cos\theta^{p}_{k} & \frac{\Delta S^{t}_{R,k}\sin\theta^{p}_{k}}{2} & \frac{\Delta S^{t}_{L,k}\sin\theta^{p}_{k}}{2} & 0 & 0 & 0 & 0 \\ 0 & 0 & 1 & \frac{\Delta S^{t}_{R,k}}{B_k} & -\frac{\Delta S^{t}_{L,k}}{B_k} & -\frac{\Delta S^{p}_{R,k} + \Delta S^{p}_{L,k}}{B_k^2} & 0 & 0 & 0 \\ 0 & 0 & 0 & 1 & 0 & 0 & 0 & 0 & 0 \\ 0 & 0 & 0 & 0 & 1 & 0 & 0 & 0 & 0 \\ 0 & 0 & 0 & 0 & 0 & 1 & 0 & 0 & 0 \\ 0 & 0 & 0 & 0 & 0 & 0 & 1 & \Delta\theta^{G,t}_{k} & 1 \\ 0 & 0 & 0 & 0 & 0 & 0 & 0 & 1 & 0 \\ 0 & 0 & 0 & 0 & 0 & 0 & 0 & 0 & 1 \end{bmatrix} \begin{bmatrix} \delta X_{k} \\ \delta Y_{k} \\ \delta\theta_{k} \\ \Omega^{O}_{R,k} \\ \Omega^{O}_{L,k} \\ \Delta B_{k} \\ \delta\theta^{G}_{k} \\ \Omega^{G}_{k} \\ \Psi^{G}_{k} \end{bmatrix}$$

$$+ \mathbf{w}_k . \tag{27}$$

$$\begin{aligned} \delta Z^{OG}_{k} &= \delta\Delta\theta^{O}_{k} - \delta\Delta\theta^{G}_{k} \\ &= \left\{ \begin{bmatrix} \frac{\Omega_{R,k}\, g\Delta S^{t}_{R,k}}{B_k} & -\frac{\Omega_{L,k}\, g\Delta S^{t}_{L,k}}{B_k} & \frac{(\Delta S^{t}_{L,k} - \Delta S^{t}_{R,k})\, g\Delta B_k}{B_k^2} \end{bmatrix} - \begin{bmatrix} \Omega^{G}_{k}\, g\Delta\theta^{G,t}_{k} & \Psi^{G}_{k} \end{bmatrix} \right\} + \mathbf{v}_k \end{aligned} \tag{28}$$

$$\delta Z^{OG}_{k} = \begin{bmatrix} 0 & 0 & 0 & \frac{\Delta S^{t}_{R,k}}{B_k} & -\frac{\Delta S^{t}_{L,k}}{B_k} & \frac{\Delta S^{t}_{L,k} - \Delta S^{t}_{R,k}}{B_k^2} & 0 & -\Delta\theta^{G,t}_{k} & -1 \end{bmatrix} \begin{bmatrix} \delta X_{k} \\ \delta Y_{k} \\ \delta\theta_{k} \\ \Omega^{O}_{R,k} \\ \Omega^{O}_{L,k} \\ \Delta B_{k} \\ \delta\theta^{G}_{k} \\ \Omega^{G}_{k} \\ \Psi^{G}_{k} \end{bmatrix} + \mathbf{v}_k . \tag{29}$$

B. *State-space model of gyroscope*

From a first-order linearization equation of gyroscope, the resulting time-variant perturbation model can be obtained by

$$\begin{bmatrix} \delta\theta^{G}_{k+1} \\ \Omega^{G}_{k+1} \\ \Psi^{G}_{k+1} \end{bmatrix} = \begin{bmatrix} 1 & \Delta\theta^{G,t}_{k} & 1 \\ 0 & 1 & 0 \\ 0 & 0 & 1 \end{bmatrix} \begin{bmatrix} \delta\theta^{G}_{k} \\ \Omega^{G}_{k} \\ \Psi^{G}_{k} \end{bmatrix} + \mathbf{w}_k , \tag{24}$$

and

$$\delta X^{G}_{k+1} = A^{G}_{k} \delta X^{G}_{k} + \mathbf{w}_k . \tag{25}$$

The state variable, using $\mathbf{x}^{G}_{k}$ including parameters of systematic error is obtained as $\mathbf{x}^{G}_{k} = \begin{bmatrix} \theta^{G}_{k} & \Omega^{G}_{k} & \Psi^{G}_{k} \end{bmatrix}^{T}$.

C. *Combination of state-space localization model between odometry and gyroscope*

The combination of state space model can be written as

$$\delta X^{OG}_{k+1} = A^{OG}_{k} \delta X^{OG}_{k} + \mathbf{w}_k \tag{26}$$

and detailed as equation (27).

D. *Combination of odometry system and gyroscope by using different measurement model*

The different measurement (Komoriya, 1994; Park, 1998) of rotation increment from the encoders and gyroscope is written as is calculated by equation (28) and detailed as equation(30). General form of different model between odometry system and gyroscope can be written as

$$\delta Z^{OG}_{k} = H^{OG}_{k} \delta X^{OG}_{k} + \mathbf{v}_k \tag{30}$$

, where v_k is the measurement noise.

In this section, gyroscope is proposed to combine with odometry system for error compensation. The indirect Kalman filter which feeds back the error estimates to the main navigation algorithm mutually compensates the differential encoder errors and the gyroscope errors.

IV. ABSOLUTE POSITION SUPPORT WITH TRILATERATION ULTRASONIC POSITIONING SYSTEM (TUPS)

The design of navigation algorithm needs knowledge about ground truth. In order to quality of the estimated position $\hat{\mathbf{P}}_i \approx \mathbf{P}^{Real}_i$ can be analyzed, $\mathbf{P}^{Real}_i$ must be known.

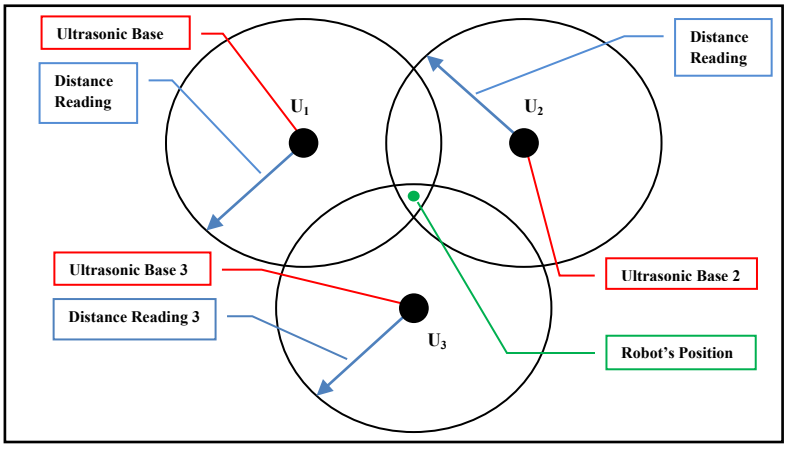

Fig.4 Principle geometry of robot's work space.

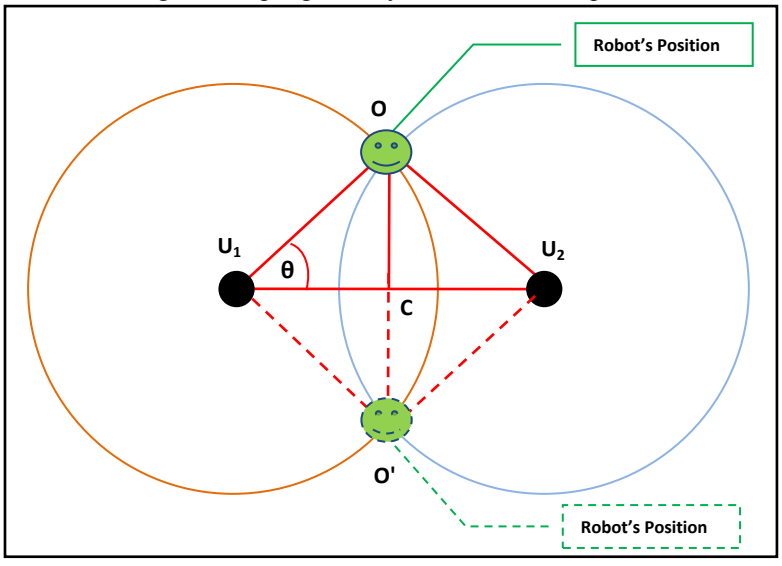

Fig.5 Intersection points from ultrasonic bases.

In practice on mobile robot field racks tool to measure $\mathbf{P}_i^{Real}$ and need more reference points to use $\mathbf{P}_i^{Reference}$ as$\mathbf{P}_i^{Real}$. The robot is stopped and its position is measured with measurement tape, but this method has disadvantages. The position error from position measurement with measurement tape can be not avoided. Because the robot must be stopped to mark a reference points, this damages the continuous dynamic of trajectory. This is the motivation to make a tool, which can support the absolute reference position ($\mathbf{P}_i^{Reference}$) for the mobile robot. The trilateration ultrasonic positioning system (**TUPS**) is designed for robot's positioning. It uses the principle of distance measurement that needs at least two landmarks with Cartesian's reference position. The principle geometry of robot's work space based on ultrasonic range is shown in Fig.4. The **TUPS** can calculate the object's position by using the relation of distance measurement from ultrasonic bases. With two ultrasonic distances from $\mathbf{U_1O}$ and $\mathbf{U_2O}$ and triangular relationship of $\triangle\ \mathbf{U_1U_2O}$ from Pythagorean Theorem, the robot's position can be calculated and detailed later. From Fig.5 two ultrasonic send two intersection points, which are possible to be right (**O**) and false (**O'**) solution, so the third ultrasonic play an important role to specify the right solution. In work space limited in half area only two ultrasonic are required to determine the right solution. The first ultrasonic base is located at point $\mathbf{U_1}$ ($\mathbf{X_{u1}}$, $\mathbf{Y_{u1}}$) and another ultrasonic base is placed at point $\mathbf{U_2}$ ($\mathbf{X_{u2}}$, $\mathbf{Y_{u2}}$). Before the object's position can be calculated, it must be considered whether the intersection of two ultrasonic will occur or not. If the distance between point $\mathbf{U_1}$ and point $\mathbf{U_2}$ is more than the summation of distance reading from ultrasonic base 1 and 2, the intersection of two ultrasonic does not occur. Next, the robot's position (**O**) can be calculated from Pythagoras as below. From ultrasonic base 1, the relation is given as

$$(\mathbf{U_1C})^2 + (\mathbf{CO})^2 = (\mathbf{U_1O})^2, \qquad (31)$$

and from ultrasonic base 2 is

$$(\mathbf{U_2C})^2 + (\mathbf{CO})^2 = (\mathbf{U_2O})^2. \qquad (32)$$

From the subtraction of equation (1) and (2) the result is obtain as

$$(U_1C)^2-(U_2C)^2=(U_1O)^2-(U_2O)^2 \quad (33)$$

, then

$$[(U_1C)+(U_2C)][(U_1C)-(U_2C)]=(U_1O)^2-(U_2O)^2 \quad (34)$$

With $U_2C=U_1U_2-U_1C$ and $U_1U_2=U_1C+U_2C$, this gives the following expression as

$$[U_1C-(U_1U_2-U_1C)]*U_1U_2=(U_1O)^2-(U_2O)^2, \quad (35)$$

and

$$2*U_1C*U_1U_2-(U_1U_2)^2=(U_1O)^2-(U_2O)^2, \quad (36)$$

then

$$U_1C=\frac{(U_1O)^2-(U_2O)^2+(U_1U_2)^2}{2*U_1U_2} \quad (37)$$

The angle (θ) is calculated as

$$cos\theta=\frac{U_1C}{U_1O}, \quad (38)$$

and

$$\theta=cos^{-1}\left(\frac{U_1C}{U_1O}\right). \quad (39)$$

Finally, the robot's position is

$$X_{Robot}^{ref.}=X_{U_1}+(U_1O)cos\theta, \quad (40)$$

$$Y_{Robot}^{ref.}=Y_{U_1}+(U_1O)sin\theta. \quad (41)$$

In this section the **TUPS** as shown in figure 6 is in IKF-algorithm integrated. The absolute position of mobile robot is calculated from the **TUPS** and then fed to IKF algorithm. From equation (40) and (41) the absolute position (X^{Ref}, Y^{Ref}) of the robot can be generated from the **TUPS**. This absolute position from the **TUPS** will be compared with the absolute position from odometry integrated with gyroscope by using difference measurement of absolute position. The navigation method about absolute positioning system needs the environment map to localize the object's position.

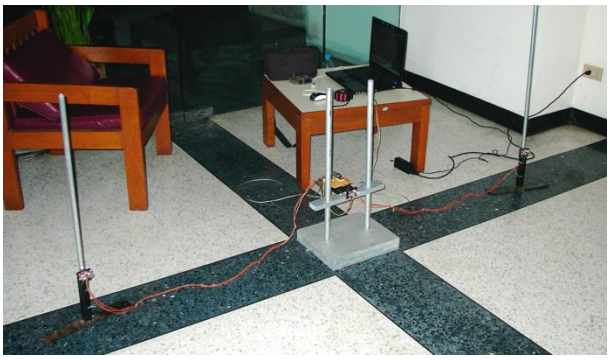

Fig.6.The **TUPS** Hardware.

In case of the **TUPS**, the navigation system of mobile robot does not need environment information, because the robot's absolute position is directly measured as

$$P_k^{Ref}=\begin{bmatrix}X_k^{Ref}\\Y_k^{Ref}\end{bmatrix}=P_k^{TUPS}=\begin{bmatrix}X_k^{TUPS}\\Y_k^{TUPS}\end{bmatrix}. \quad (42)$$

The TUPS can generate absolute position (P_k^{TUPS}) at center of mobile robot and the estimated position from odometry integrated with gyroscope can be calculated as

$$\hat{P}_k^{OG}=\begin{bmatrix}\hat{X}_k^{OG}\\\hat{Y}_k^{OG}\end{bmatrix}. \quad (43)$$

By subtraction equation (43) from equation (42), a different measurement equation for position error is obtained by

$$\delta P_k^{OG,\,TUPS}=\hat{P}_k^{OG}-P_k^{TUPS}=\begin{bmatrix}\hat{X}_k^{OG}\\\hat{Y}_k^{OG}\end{bmatrix}-\begin{bmatrix}X_k^{TUPS}\\Y_k^{TUPS}\end{bmatrix}. \quad (44)$$

V. HYBRID NAVIGATION SYSTEM FROM ABSOLUTE POSITIONING SYSTEM

This paper presents the systems of main differential odometry integrated with gyroscope in mobile robot.

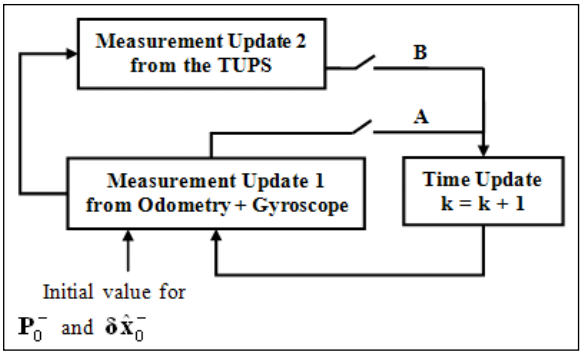

Fig.7.IKF loop the combination of support system and odometry system in measurement step.

Gyroscope generates rotation increment used to compensate rotation increment from differential odometry. The **TUPS** as the absolute positioning system is used as reference position for mobile robot. To construct the combination of the support system with odometry system of mobile robot is different measurement in the same physical variable, i.e. rotation or translation increment or absolute orientation or position between odometry and external support system. Then the estimate of error state $\delta\mathbf{X}$ from IKF (indirect Kalman filter) is calculated to correct the navigation state. The support systems are integrated in "Measurement Update" step of IKF algorithm in Fig.7. If the connector **A** is only closed by software, the IKF loop to combine main odometry system and gyroscope is started. The IKF loop of odometry system integrated with gyroscope, which is combined with the **TUPS**, will start by only closed connector **B**.

A. *The combination of odometry integrated with gyroscope and the TUPS*

A state equation from basic odometry integrated with gyroscope is obtained by equation (27). The measurement equation $\mathbf{Z}_k = \mathbf{H}\mathbf{X}_k + \mathbf{V}_k$ between odometry integrated with gyroscope system and the **TUPS** can be written as

$$\mathbf{Z}_k = \hat{\mathbf{P}}_k^{OG} - \mathbf{P}_k^{TUPS} = \begin{bmatrix} \hat{\mathbf{X}}_k^{OG} \\ \hat{\mathbf{Y}}_k^{OG} \end{bmatrix} - \begin{bmatrix} \mathbf{X}_k^{TUPS} \\ \mathbf{Y}_k^{TUPS} \end{bmatrix} + \mathbf{v}_k . \quad (45)$$

Then the measurement matrix of equation (45) is

$$\mathbf{Z}_k^{OG,\,TUPS} = \begin{bmatrix} 1 & 0 & 0 & 0 & 0 & 0 & 0 & 0 & 0 \\ 0 & 1 & 0 & 0 & 0 & 0 & 0 & 0 & 0 \end{bmatrix} \begin{bmatrix} \delta\mathbf{X}_k \\ \delta\mathbf{Y}_k \\ \delta\boldsymbol{\theta}_k \\ \boldsymbol{\Omega}_{R,\,k}^{O} \\ \boldsymbol{\Omega}_{L,\,k}^{O} \\ \Delta\mathbf{B}_k \\ \delta\boldsymbol{\theta}_k^{G} \\ \boldsymbol{\Omega}_k^{G} \\ \boldsymbol{\Psi}_k^{G} \end{bmatrix} + \mathbf{v}_k$$

$$= \mathbf{H}_k^{OG,TUPS}\delta\mathbf{X}_k^{OG} + \mathbf{v}_k \quad (46)$$

, where $\mathbf{v}_k$ is the measurement noise.

B. *Overall structure of navigation system*

The main odometry integrated with gyroscope system and absolute positioning instruments (Byoung - Suk Choi, 2009; Luis M. Valentin-Coronado, et al., 2009) is shown in Fig.8. To estimate the absolute orientation error, the different orientation between compass and odometry system integrated with gyroscope is used as a measurement value in IKF loop. In IKF loop error parameters of main system are also estimated and fed back to correct encoder error and gyroscope error.

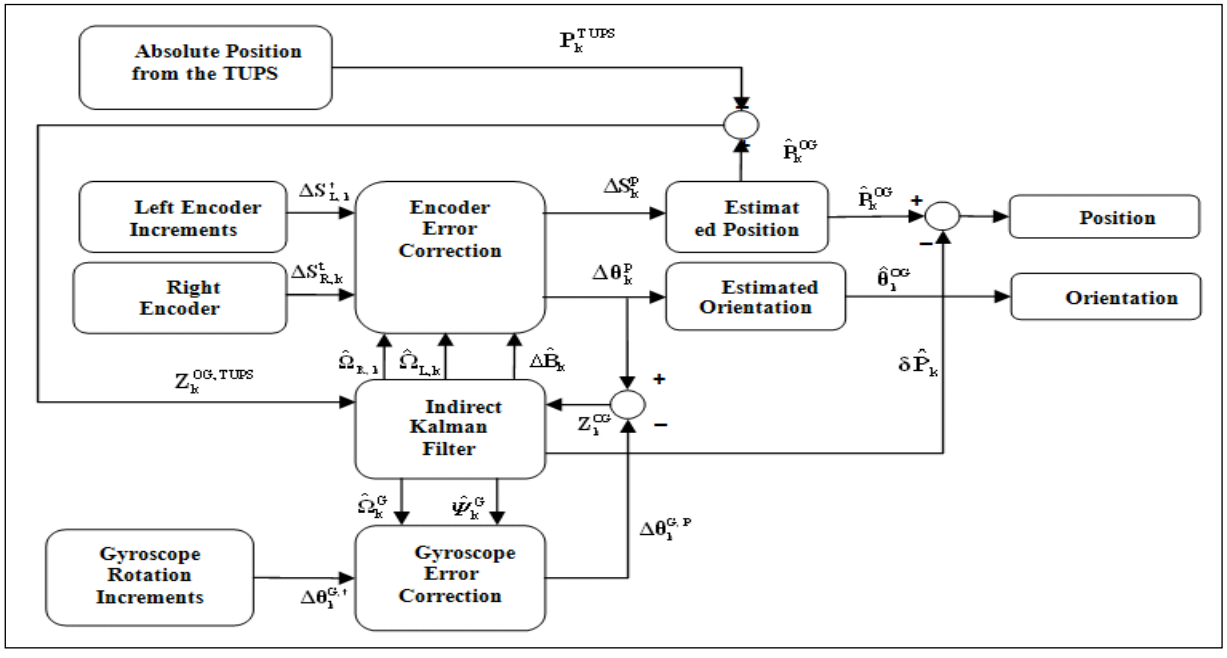

Fig.8.Overall combinations of support system and odometry system.

VI. SIMULATION AND EXPERIMENTAL RESULTS

The navigation error state from odometry $\delta \mathbf{X}^{O}$ occurring during long trajectory and high dynamic environment is reduced by linear state vector and estimated by IKF algorithm. To keep the position estimation of mobile robot with pinpoint accuracy is based on the reciprocal error compensation between odometry error and gyroscope error.

A. Result of combination with gyroscope support

The mobile robot (Pioneer-II from active media company) driven by differential odometry system integrated with gyroscope and compass shown in Fig.7 is used for experiment in square shape 2.5x2.0 m. In experiment the robot starts at the position coordinate (x = 0, y = 0, θ = 0°) and runs from start point in right direction and returns at the start point again with speed 0.2 m/s.

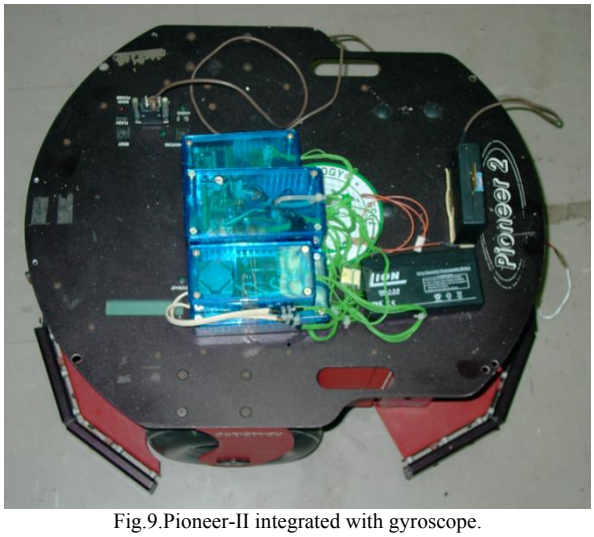

Fig.9.Pioneer-II integrated with gyroscope.

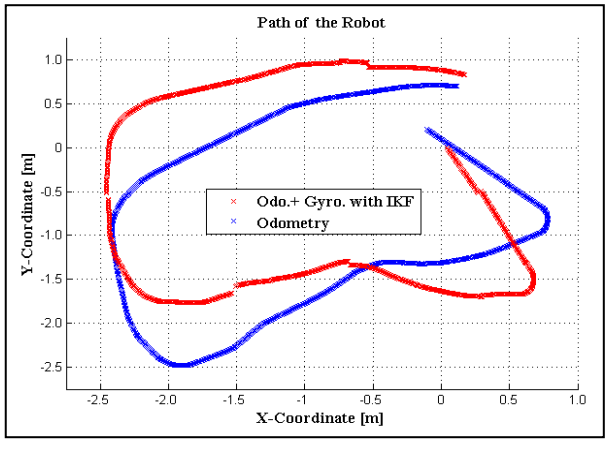

Fig.10 Position generated by encoders is shown in blue line and the red line shows the position estimation of the robot by using different measurement of rotation increment between encoders and gyroscope with IKF algorithm.

From experiment the robot's final position from odometry system are $\hat{\mathbf{P}}^{O}$ ($\hat{\mathbf{x}}^{O} = 18.4$ cm , $\hat{\mathbf{y}}^{O} = 71.1$ cm) and from odometry system integrated with gyroscope $\hat{\mathbf{P}}^{OG}$ ($\hat{\mathbf{x}}^{OG} = 20.7$ cm , $\hat{\mathbf{y}}^{OG} = 85.4$ cm) as shown in Fig.10. Also systematic errors of odometry system are shown in Fig.11 and gyroscope in Fig.12 and detail in Table 1.

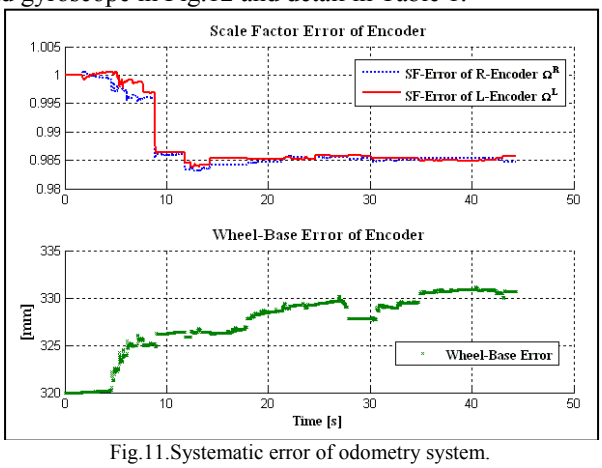

Fig.11.Systematic error of odometry system.

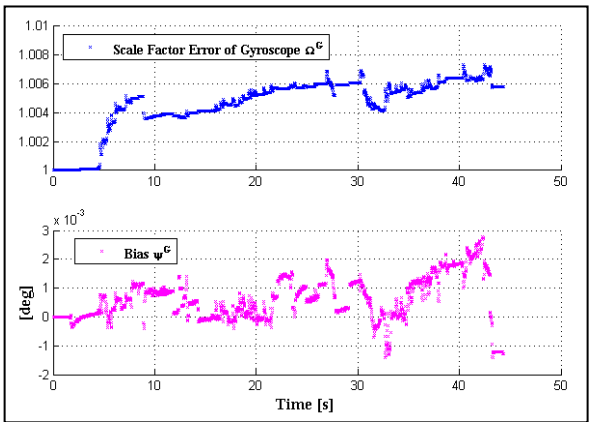

Fig.12.Systematic error of gyroscope.

For the navigation algorithm the reference position plays an important role. To reduce position error of odometry, the reference position must be known to find the difference position between odometry system and reference position in time.

B. Result of combination with the TUPS support

In this section, details the powerful IKF algorithm with the TUPS support. The TUPS concept is more details in previous section. In Fig.13 shows the graphic of robot's trajectory in square shape from the TUPS compared with the reference point. The different measurement of position $\hat{\mathbf{P}}^{OG,IKF}$ and $\mathbf{P}^{TUPS}$ as shown in Fig.14 will be send to the second measurement update as shown in Fig.7 to reduce absolute position error. In Fig.15 shows trajectory of the robot running from the calculated position $\mathbf{P}^{O}$ from odometry equation, $\mathbf{P}^{TUPS}$ generated by the TUPS and estimated position $\hat{\mathbf{P}}$ with gyroscope and the TUPS support by using IKF algorithm. For the navigation algorithm the reference position plays an important role. To reduce position error of odometry, the reference position must be known to find the difference position between odometry

system and reference position in time. Generally the reference positions are constructed by manual measurement, which is difficult and not possible to measure the reference position in time. But the TUPS can generate the reference or absolute position compared with position from odometry system in the same time. In Table 2 shows the results of final coordinate of robot trajectory compared with actual reference coordinate.

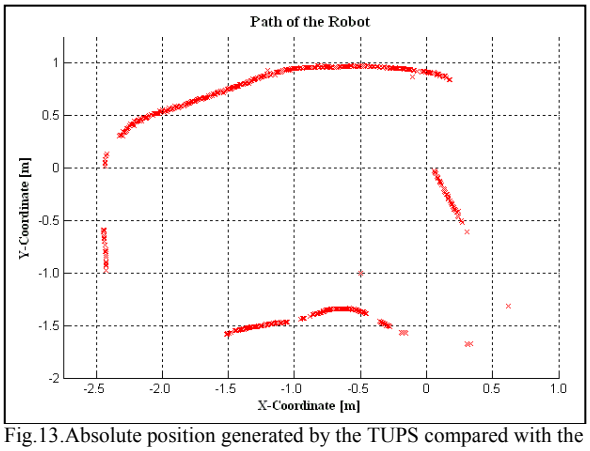

Fig.13.Absolute position generated by the TUPS compared with the reference position.

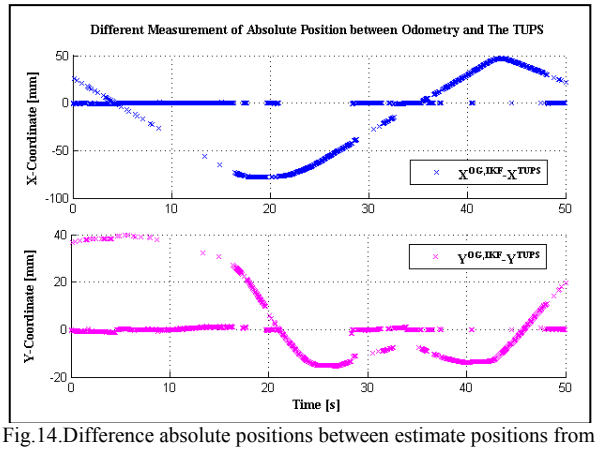

Fig.14.Difference absolute positions between estimate positions from odometry integrated with gyroscope and from the TUPS.

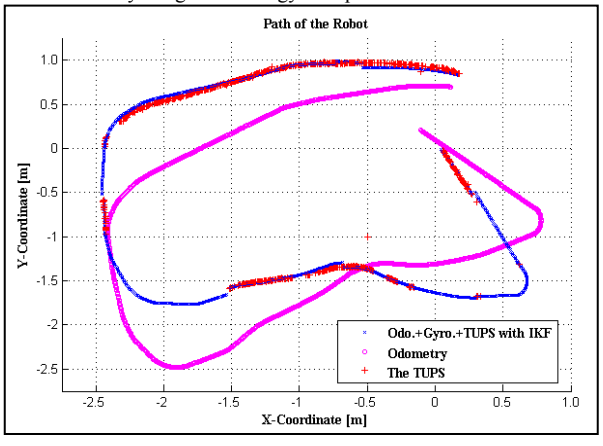

Fig.15.Implement of the TUPS positioning system in IKF algorithm for estimate of robot position in global coordinate.

VII. CONCLUSION

This paper proposed the hybrid absolute positioning system using trilateration ultrasonic positioning system for odometry system integrated with gyroscope for mobile robot in an indoor environment. To reduce the absolute position error, the TUPS is combined with odometry system integrated with gyroscope. The indirect feedback Kalman filter (IKF) is used as the combination of odometry system, gyroscope and the absolute orientation to estimate and compensate errors. The IKF can estimate the error of estimated absolute position by using the information from the TUPS. Then mobile robot's position and orientation are obtained from addition of the estimated position and orientation error with the estimated position and orientation from main system. Also the IKF estimated the scale factor error of encoders, the distance error between wheels and scale factor and bias errors of gyroscope to correct errors from encoders and gyroscope. The simulation results show that the IKF can give precisely estimated position and orientation by using absolute positioning system. Further research aims to support the translation increment for odometry system with an accelerometer. The complementary measurement between translation increment from encoder and accelerometer can be passed to the filter.

REFERENCES

1. **Shoichi Maeyama, Nobuyuki Ishikawa and Shin'ichi Yuta. 1996.** Rule based filtering and fusion of odometry and gyroscope for a fail safe dead reckoning system of a mobile robot, IEEE International Conference on Multi sensor Fusion and Integration for Intelligence Systems, pp.541-548.
2. **Y. Watanabe and S. Yuta. 1990.** Position Estimation of Mobile Robots with Internal and External Sensors Using Uncertainty Evolution Technique, Proceedings of IEEE International Conference on Robotics and Automation Vol.3, pp.2011-2016.
3. **Shoichi Maeyama, Akihisa Ohya and Shin'ichi Yuta. 1995**. Non-stop outdoor navigation of a mobile robot - Retroactive positioning data fusion with a time consuming sensor system, IEEE/RSJ International Conference on Intelligent Robot and Systems, vol.1, pp.130-135.
4. **S. Maeyama, A. Ohya and S. Yuta. 1994**. Positioning by tree detection sensor and dead- reckoning for outdoor navigation of a mobile robot, IEEE International Conference on Multi sensor Fusion and Integration Systems, pp. 653-660.
5. **J. Borenstein and L. Feng. Gyrodometry. 1996**. A new method for combining data from gyroscope and odometry in Mobile Robots, IEEE International

Conference on Robotics and Automation, Vol.1,pp.423-428.

6. **J. Borenstein, H.R.Everett, L.Feng, and D. Wehe**. **1997**. Mobile Robot Positioning-Sensor and Techniques, Journal of Robotic System, Vol. 14, No.4, pp.231-249.
7. **Hakyoung Chung, Lauro Ojeda and Johann Borenstein**. **2001**. Sensor Fusion for Mobile Robot Dead-Reckoning with A Precision-Calibrated Fiber Optic Gyroscope, IEEE, Seoul, Korea, May 21-26, pp.3588-3593.
8. **Borenstein J. and Feng L**. **1997**. Measurement and correction of Systematic Odometry Errors in Mobile Robots, IEEE Trans. On Robotic and Automation, Vol.12, No.6, pp.869-880, 1640-1648.
9. **K. Komoriya and E. Oyama**. **1994**. Position Estimation of a Mobile Robot Using Optical Fiber Gyroscope (OFG, Proc. IROS'94, pages 143-149,
10. **Britting, K.R**. **1971**. Inertial Navigation Systems Analysis, Wiley Interscience, Newyork, USA.
11. **Kelly, A. 2001**. A General Solution for Linearized Systematic Error Propagation in Vehicle Odometry, in Proceedings of the 2001 JEEE/RSJ International Conference on Intelligent Robots and Systems, Band 4, 5. 1938-1945.
12. **Larsen, T. D., Bak, M., Aurlersen, N, A. & Ravn, O**. **1998**. Location Estimation for an Autonomously Guided Vehicle Using an Augmented Kalman Filter to Auto calibrate the odometry in Proceedings of the 1st international Conference on Multisource - Multisensor Information Fusion, Band 1, S. 21-27.
13. **Chnug. H, O.jeda, L. & Borenstein, J**. **2001**. Accurate Mobile Robot Dead-Reckoning with a Precision-calibrated Fiber-optic Gyroscope, IEEE Transactions on Robotics and Automation 17. S. 80-84.
14. **Mayback, P.S. 1979**. Stochastic Models, Estimation and Control, Band 141 in Mathematics in Science and Engineering, Academic Press, New York, USA.
15. **Barshan, B., and Durrant-Whyte, H. F. 1995**. Inertial Navigation Systems for Mobile Robots. IEEE Transaction on Robotics and Automation, vol.11, June, pp. 328-342.
16. **Park, K., Chung, H., and Lee, J. 199l.** Dead Reckoning Navigation for Autonomous Mobile Robots. Proc .of Intelligent Autonomous Vehicle, Madrid, Spain, March 25-28, pp. 775-781.
17. **Kakuba and Arenas. 1987.** Position Verification of a Mobile Robot Using Standard Pattern" IEEE Journal of Robotics and Automation, vol. RA-3, NO.6, December, pp.505-516.
18. **Sony Corporation, 2004**. Color Digital Camera DFW-SX910 Technical Manual.
19. **Ojeda, L. and Borenstein, J. 2000.** Experimental Results with the KVH C-100 Fluxgate Compass in Mobile Robots. Proceedings of the IASTED International Conference Robotics and Applications 2000 August 14-16, Honolulu, Hawaii, USA, pp.1-7.
20. **Brown, R. 1997.** Introduction to random signals and applied Kalman filtering with Matlab exercises and solutions third edition, ISBN: 978-0-471-12839-7, Wiley, New York.
21. **Xie, M. 2003.** Fundamentals of robotics linking perception to action, ISBN: 981-238-313-1, World Scientific Publishing Co. Pte. Ltd., Singapore.
22. **Panich, S. 2008.** A Mobile Robot with a Inter– Integrated Circuit System. IEEE 10th International Conference on Control, Automation, Robotics & Vision, December 17-20, Hanoi, Vietnam, pp. 2010-2014.
23. **Naveen Kumar Boggarpu and Richard C. Kavanagh. 2010.** New Learning Algorithm f or High-Quality Velocity Measurement and Control When Using Low-Cost Optical Encoders, IEEE Transactions on Instrumentation and Measurement, vol. 59, no. 3, March, pp. 565-574.
24. **Ali Bostani, Ahmad Vakili and Tayb.A.Denidni. 2008.** A Novel Method to Measure and Correct the Odometry Errors in Mobile Robots, 21th Canadian Conference on Electrical and Computer Engineering (CCECE), May 5-7, Ontario, Canada, pp.897-900.
25. **Byoung-Suk Choi. 2009.** Mobile Robot Localization in Indoor Environment using RFID and Sonar Fusion System, IEEE/RSJ International Conference on Intelligent Robots and Systems October 11-15, St. Louis, USA, pp. 2039-2044.
26. **Srinivasan, K. and Gu, J. 2007.** Multiple Sensor Fusion in Mobile Robot Localization, 20th Canadian Conference on Electrical and Computer Engineering (CCECE), April 22-26, Vancouver British Columbia, Canada, pp.1207-1210.
27. **Diansheng Chen, Feng Bai and Lin Wu**. **2008.** Kinematics Control of Wheeled Robot Based on

Angular Rate Sensors, IEEE Conference on Robotics, Automation and Mechatronics, September 21-24, Chengdu, China, pp. 598-602.

28. **Takeshi Sasaki. 2010**. Human-Observation-Based Extraction of Path Patterns for Mobile Robot Navigation, IEEE Transactions on Industrial Electronics, vol. 57, no. 4, pp.1401 - 1410.
29. **Luis M. Valentin-Coronado, Victor Ayala-Ramirez and Raul E. Sanchez-Yanez**, 2009. Error Modeling of Mapping Approaches Using Mobile Robots, University of Guanajuato IEEE Students Chapter (IEEExPO),
30. **Sotirios Ch. Diamantas and Richard M. Crowder**. **2009**. Localization and Mapping Using a Laser Range Finder: A Goal-Seeking Approach. Fifth International Conference on Autonomic and Autonomous Systems, April 20- 25, Valencia, Spain, pp.270-276.
31. **Kang Li, Han-Shue Tan, and J. Karl Hedrick. 2009**. Map-Aided GPS/INS Localization Using a Low-Order Constrained Unscented Kalman Filter. Joint 48th IEEE Conference on Decision and Control and 28th Chinese Control Conference Shanghai, P.R. China, December 16-18, pp.4607-4612.

Incessant Incidents of Building Collapse in Nigeria: A Challenge to Stakeholders

Kingsley .O. Dimuna

GJRE Classification (FOR)
GJRE: E 090504

***Abstract*-The paper examines the increasing incidences of building collapse in Nigeria. The paper attributes the rising incidents of building collapse to the use of substandard building materials and incompetent professionals in construction activities; the refusal of the wider society to recongnise professionalism and pay for the services and the attitude of the building contractors and other stakeholders as the major problem. The paper asserts that promoting or achieving an enduring safety culture in building involves designing, constructing and using buildings, in such a manner as to make the building safe for occupation and for carrying out all desired activities. Strategies for ameliorating the trend are suggested. The paper posits that stakeholders in the building development have great roles to play to reduce and avert this trend.**

Keywords: Incessant, Building Collapse and Nigeria.

I. INTRODUCTION

The frequency of collapse of building structures in Nigeria in the past few years had become very alarming and worrisome. Many lives and properties have been lost in the collapse of buildings mostly in Port Harcourt, Abuja and Lagos. Many property owners have developed high blood pressure and some have been sent to an early grave. A visit to the collapsed scenes were as revealing as they were pathetic and one could not but wonder why such contraption could have been allowed to stand or to what extend people can go to cut corners at the expenses of respect for safety and respect for lives. Unfortunately, there are still a number of buildings of similar circumstances dotting the skyline of many cities in Nigeria.That building collapse incidence are still regularly occurring despite increasing diffusion of engineering knowledge over the years calls for some reexamination of developments in building production and control process. As observed by Adeniya in (2002) why must a preventable incidence continue to traumatize us all the time? These incidents have brought to question the effectiveness of building contractors in the country.The menace also casts a slur on the competence of the nation's building community of architects, structural engineers and builders – who are the professionals responsible for designing and monitoring construction works at building sites.These professionals are being attacked from all angles because of the recurring incidents of building collapse. But the building professionals should not bear the blame alone. This is because, firstly, it has been proved that owners of building under construction derail from their approved plans relying more on imagination and fantasy. Secondly, the approving authorities are also known to fail to monitor compliance with approved plans. Thirdly, some building owners shun professionals in order to cut costs. Fourthly, the high cost of building materials has led greedy contractors with eyes on profits, to patronize substandard materials. These short-cut measures have contributed immensely to the occurrence of failed buildings in the country.The paper will critically examine the reasons for building failures or collapse and types of failures. It will also examine the roles of stakeholders in building and construction industry and articulate strategies that would help to arrest these ugly occurrences.

About- Department of ArchitectureFaculty of Environmental Studies Ambrose Alli University,P.M.B. 14, Ekpoma – Nigeria.
E-Mail – kodimuna@yahoo.com

II. THEOCRETICAL FRAMEWORK

One fundamental principle of building design is that a building should be designed and constructed to meet its owner's requirements and also satisfy public health, welfare and safety requirement. No part of such building should pose a hazard to its occupants (Fredrick etal 1989). Simply put, the purpose of structural design is the provision of a structure satisfying the client's and user's requirements. It must be economical, safe, serviceable and aesthetically adequate. Fundamentally, the design process consists of findings and detailing the most economical structure consistent with the safety and serviceability requirements. This should be the basic design concepts of any architect and structural engineer.Mosley et al (1985), posited that the design of an engineering structure must ensure that (1) under the worst loading the structure is safe. (2) During normal working conditions the deformation of the members does not detract from the appearance, durability or performance of the structure. Despite the difficulty in assessing the precise loading and variations in the strength of the concrete steel theses requirements have to be met. Three basic methods using factors of safety to achieve safe, workable structures have been developed for engineering designs; Mosley et al (1985) identified them as:The permissible stress method in which ultimate strengths of materials are divided by a factor of safety to provide design stresses which are usually within the elastic range.The load factor method in which the working loads are multiplied by a factor of safety.The limit state method which multiplies the working loads, by partial factors of safety and also divides the materials ultimate strength by further partial factors.The engineering code of practice (CP.110) is based on limit state principle. When a structure is rendered "unfit for use", it is

said to have attained a limit state. The code listed the limit states as:

(a) Ultimate Limit State – Collapse

This requires that the structure must be able to withstand, with an adequate factor of safety against collapse, the loads for which it is designed. The possibility of building or overturning must also be taken into account, as must the possibility of accidental damage as caused, for example by an internal explosion.

(b) Serviceability Limits State – Deflection, Cracking And Vibration.

Deflection – the appearance or efficiency of any part of the structure must not be adversely affected by deflections.
Cracking – local damage due to cracking and spalling must not affect the appearance, efficiency or durability of the structure.Other limit states that may be reached include:
Durability – this must be considered in terms of the proposed life of the structure and its conditions of exposure.
Excessive Vibration – This may cause discomfort or alarm as well as damage.Fatigue – must be considered if cyclic loading is likely.Fire Resistance – this must be considered in terms of resistance to collapse, flame penetration and heat transfer.ViiSpecial Circumstance – any special requirement of the structure which is not covered by any of the more common limit state, such as earthquake resistance must be taking into account.

(c)Other Limit State – Fatigue, Durability, Fire Resistance Etc.

A structure will become unfit for use if parts or all of it collapses, but will also become unfit if it deflects too much, if large cracks forms or if the vibration is so great that discomforts and fear is caused to the occupants, or the operation of machinery is interfered with. This state is technically referred as failure; when structure ceases to be fit for human habitation and occurs when the limit state is reached. This state is reached when deflection exceeds L 250, where L is the span of the element and cracks width exceeds 0.3mm, Obiechina (2005).The structural design should therefore, ensure that the structure will not, during its life span, become unfit for use i.e. reaches a limit state. Each limit sate must, therefore, be considered in design and suitable margin of safety used; Mosley etal (1985), Obiechina (2005), Sinha (2002)
Most buildings are composed of foundations, columns, beams, slabs, roof, load bearing partition walls and complex mixture of constructional units and materials. All these put together provide and almost impossible indeterminate structures. Cracking in buildings are indicators of onset of failure. These failures or defects will now be examined in the various structural elements.

1 Foundations

Whatever the type of structure, the qualities of the subsoil must be investigated and the design and construction made to absorb stresses from the super-structure. Causes of foundation failure include: faulty or no soil investigation, wrong choice and or design of suitable foundation; use of structure for purpose other than or total settlement of substructure accompanied by excessive cracking of ground floor slab, sinking of column footings, that is, punching shear failure as shown in figure 1.

2 Columns

Columns are usually struts and therefore very strong element of the structure. They hardly fail. Causes of column failure are attributed to: most due to the use of structure for purpose other than originally intended for instance office blocks being used for storage e.g. books, machinery and heavy point loads for instance bank safes, etc., use of small or highly spaced column stirrups as shown in figure 2; Excessive slender columns leading to buckling; use of poor quality materials. The danger signals are column crushing and spalling and splitting of concrete.

3 Beams

Beams are most susceptible to all kinds of stress than other structural elements. Such stresses include that due to bending, shear and torsion. Other failure includes deflection, bond and anchorage. Causes of collapse may be due to faulty design, use of structure for purposes other than designed, poor construction methods leading to displacement of stirrups during vibration as shown in figure 3. The symptoms depend on the type of failure as shown in figure 4, viz bending, shear, torsion, deflection.
Bending: vertical cracks mostly near middle of beam length.
Shear: inclined cracks (45^0) mostly at the ends of the beam.
Shear failure very sudden.Torsion: combination of horizontal and inclined cracks.

4 Slabs

Causes of failure in slab are as result of: Excessive loading especially with partition walls; Reinforcement placed in the wrong position especially due to inadequate chaining up; omission of top reinforcement at beam positions and slab ends see figure 5‘; excessive spans, that is span or effective depth ratio; lack of adequate cover to reinforcements., and poor quality of materials and inadequate mixes. The common symptoms include; slab vibrates when in use; crackings especially at positions where top reinforcements are needed; rusting of bottom reinforcements and concrete spalling.

5 Cantilevers

Cantilevers are structural elements that fail most in buildings and in fact should be avoided if it is possible. However, Architects seem to like them and so the structural engineers are stuck with designing them. The causes of cantilever failure can be attributed to: Displacement or displacement of the top reinforcements during construction – see figure 6.; Insufficient bond or anchorage lengths especially in discontinuous and slabs see figure 7.; In roof gutters, column reinforcement not anchored into the roof beam as shown in figure 8.; excessive length or effective

depth ratios. Cantilever failures often occur suddenly and without warning as all three stresses – bending, shear and torsion occur simultaneously and at the same point as shown in figure 9. However, most often cracks form at positions of maximum stress, visible defection coupled with cracking of the walls above the cantilever.

III. CAUSES OF BUILDING FAILURES OR COLLAPSE

Collapse according to the Dictionary of Architecture and Construction refers to mechanical failure. Collapse is a state of complete failure, when the structure has literally given way and most members have caved-in, crumbled or buckled; the building can no longer stand as originally built. It can be seen therefore, that collapse is very extreme state of failure.
The causes of building collapse can be categorized as:Thatcaused by the influence of man;That due to natural forces (force majeur).For the purpose of this paper attention is given to that caused by the influence of man either due to his negligence or incompetence.In a communiqué issued at the end of a two-day seminar on structural failure and building collapse in August 1996; professionals in the building industry summarized the major causes of building collapse to include the following: The attitude of the public, professional bodies and governments.The absence of soil test before constructionStructural designs and details are sometimes defectiveLack of proper planningAbsence of co-ordination between professional bodies and town planning authoritiesLack of adherence to specifications by contractors.Use of unqualified and unskilled personnelPoor or bad construction practicesUse of substandard building materials Inadequate enforcement of existing laws.
However, for the purpose of this paper, attention would be focused on the under listed:

(i) Deficient Structural Drawing

Building collapse when structural drawings are based on false assumptions of soil strength, they can also collapse as a result of faulty structural details. Oyewande (1992) identified design defaults s accounting for 50 percent of collapse of engineering facilities in Nigeria.

(ii) Absence Of Proper Supervision

Even where a structural design is not deficient, absence of proper supervision on the site by qualified personnel can led to building failure.

(iii) Alteration Of Approved Drawings

During construction, many contractors either on the directive of the client or in a bid to cut corners and maximize profit, alter approved building plans without corresponding amendment to structural drawings to the detriment of the structure.

(iv) Building Without Approved Building Drawings

Building without approved drawings and in some cases no drawings at all, can result in the collapse of the building more so when the drawings were not vetted by qualified professionals or relevant authorities before the buildings are erected. Without drawings, all constructions are based on guess work.

(v) Approval of Technically Deficient Drawings

Town Planning Authorities at times approved technically deficient drawings. This may be as a result of ignorance on the part of Town Planning Personnel who vet and approved these drawings or as a result of outright corruption on their part. Money may at times changed hands resulting in the approval of such drawings.

(vi) Illegal Alteration To Existing Buildings

Client at time, on their own, alter existing structures (buildings) beyond and above the original design without any drawings, and relevant Town Planning approval. In some instances existing bungalows have been converted to either a storey building or two to three-storey structures without any drawings and supervision by qualified personnel. The result can be anybody‘s guess.

(vii) Absence Of Town Planning Inspection Or Monitoring Of Sites

In some cases, Town Planning Authority staff seldom visit sties to inspect or monitor progress of approved work on sites, the result of which is documented in their forms. Unfortunately in many cases, this inspection is non-existent. What this means is that buildings are put up without the Authority knowing anything about details of the construction. Unfortunately, these details are only known when such buildings collapse and their element get exposed for all to see. By that time lives probably may have been lost.

(viii) Clients Penchant To Cut Corners

A study of collapsed buildings shows that most of them are residential buildings and owned by individuals. What this meant is that one person takes all the decisions concerning the construction; due process is not followed. Nigerian client (mostly individuals) have a penchant for cutting corners by not employing qualified personnel to produce the contract documents and supervise the building while under construction, as they want to spend minimum (not optimum) amount of money on the construction (Madu, 2005). Even where qualified professionals are employed for design and supervision, most clients insist on having the final say on what goes on in the site to detriment of proper execution of the contract. Unfortunately, if there is any mishap on site, the client blames the consultants and the contractor. It is therefore obvious that client‘s penchant to cut corners is one of the problems in the building production process.

(ix) Use Of Substandard Materials

Substandard material especially reinforcement rods, steel sections and cement can contribute immensely to failure of buildings. Other substandard materials can also contribute to failure of buildings. Hall (1984) posited that use of low quality materials is one of the major causes of structural

failure. Aniekwu and Orie (2006), in their study, also identified low quality materials as the most important cause of failure of engineering facilities in Nigeria.

(x) Inefficient Workmanship (Labour)

Inefficient and fraudulent labour input can also contribute to failure of buildings. When a contractor cannot read drawings or where he refuses to listen to the instruction of the consultants anything can happen. Oyewande (1992) posited that faults on construction sites accounts for (40%) of collapse of structures.

(xii) Use Of Acidic And Salty Water

Use of acidic and salty water, as sourced from oceans and seas in cities like Lagos and Port Harcourt can affect the strength of concrete when used to effect the mix of cement, and sand and rods.

(xiii) The Activities Of Quacks

A cursory look at the building industry in Nigeria today reveals a preponderance of individuals who are ill equipped to carry out functions associated with construction. The industry has had more than its fair share of the activities of quacks that have nothing at stake whenever problems arise. The unsuspecting public is also at a loss differentiating the real professionals form the quacks until the real harm has been done.Today, it is not strange to find staff of Town Planning offices who are mainly Town Planners and Site Inspectors, even some Land Surveyors and Builders taken architectural commissions, and masquerading as architects and deceiving the unsuspecting public. Masons have overnight transformed to engineers and builders. This is a major problem of the building industry.

(xiv) Clients' Over Reliance On Contractors For Decision Making On Site

Most clients rely more on contractors than consultants on site. This is because most contractors are either their friends, relations of the clients, or are recommended by friends or relations. The result of this relationship is that client rely more on the contractors for decision making than on the consultants.What the clients fails to realize however, is that profit is the prime motive of most contractors and not because the contractor is saving them some cost. They end up reducing the thickness of floor slabs and foundation and even foundation depth; sizes of reinforcement rods, head room (height) of structures, all in attempt to maximize profits to the detriment of the construction, and because most clients cannot read drawings, they are _taken for a ride' by most contractors. It is only when buildings fall that these fact come to the surface. Even for big projects owned by corporate bodies and governments etc, the contractors seem to have special relationship with agents of the client, some desperate contractors use blackmail and intimidation to scare away and discourage consultants from projects sites.

Usually, a combination of factors are implicated in the collapse of building as listed above; but the timing of the recent happenings in Lagos and Port-Harcourt indicates that the nature of soil is very central and the main culprit in the collapse, as these are happening especially now in the rainy season. More attention should therefore be given to geotechnical investigation for high rise structures in areas with soil that are very suspect and the water table high. Onitsha town is an instance of where such high rise buildings are the norm, but so far no building collapse has been reported. The reason is that the soil bearing capacity is very high in most areas of the town.

IV. CONSEQUENCES OF BUILDING COLLAPSE

The incidents of building collapse witnessed in the country in the recent years has resulted in the loss of many lives and the destruction of properties worth several millions of naira; as reflected in the table 1, 2 and 3 below. Many families have been traumatized and many developers have lost their life investments. From table 1, it can be inferred that between 1975 to 1995, about 26 incidents; which claimed about 226 lives were recorded in Nigeria. Table 2 reveals that between 1982 – 1996, Lagos State alone recorded about 14 incidents and about 64 dead. While in a period of two years (2004 – 2006) as reflected in table 3 about 10 incidents were reported which claimed the lives of about 243 people. In all the cases, many people were injured and some permanently disabled.

A List Of Available Records Of Collapsed Buildings
Withing The Last Two Decades In Nigeria

DATES OF INCIDENT	STATES	TYPES OF BUILDINGS	NO OF LIVES LOST/INJURED	REMOTE CAUSES
Dec, 1976	Ondo	1 Storey	8 Died	Sub-standard building material/structure
May, 1977	Oyo	2 Storey	10 Died	
June, 1977	Kaduna	School building	16 died (several injured)	Poor workmanship by contractors
Oct, 1977	Borno	4 Storey	10 died	Poor performance by contractor
March, 1978	Rivers	4 Storey	16 died	Lack of concrete services to hold foundation
June, 1982	Ondo	2 Storey	7 died	Heavy down pour/structural defects
Sept, 1983	Lagos	2 Storey	8 died	Structural defective
Dec, 1983	Lagos	4 Blocks of flats	6 died	Heavy down
July, 1985	Lagos	3 Storey	9 died	Heavy down pour/structural defects
May, 1987	Lagos	2 Storey	4 died	Structural defect/poor
Sept, 1987	Lagos	3 Storey	8 died	Structural defect/poor building materials.
Nov, 1988	Lagos	School Building	1 died (Others injured)	Substandard building materials Defective structural design
June, 1990	Rivers	School Building	50 died (several injured)	Sub-standard building materials
July, 1991	Kano	1 Storey	3 died	Heavy down pour/structural defects
July, 1991	Sokoto	1 Storey	4 died	Poor workmanship/ structural defect
August, 1991	Lagos	2 Storey	10 died	Structural defects
March, 1992	Lagos	3 Storey	10 died	Defective structural design
June, 1992	Lagos	Hotel building	2 died (several injured)	Dilapidated structures
Oct, 1993	Kano	1 Storey	5 died	Structural defects
March, 1994	Oyo	2 Storey	4 died (11 injured)	Sub-standard building materials. Structural defects/poor workmanship
June, 1994	Lagos	3 Storey	17 injured	Structural defects/ sub-standard materials
Aug, 1994	Kwara	1 Storey	2 died (6 injured)	Structural defects/poor building materials
Aug, 1994	Oyo	2 Storey	10 died (74 injured)	Structural defects
June, 1994	Lagos	4 Storey	4 died (several injured)	Structural defect/sub- standard materials
Aug, 1994	Ondo	1 Storey	1 died (several injured)	
Jan, 1995	Lagos	6 Storey	1 died	

Source: Boye Ajai – 1995 Factors Responsible for Collapsed Building P.19. Tell Magazine No.3.January 16th 1995 Culled from S.O. Izomoh (1997) the Provision of Housing and Management in Nigeria P.20.

Table 2:
Available Statistics Of Collapsed Building In Lagos Since 1982-1996

S/N	MONTH	YEAR	TY PES OF BUILDING	LIVES SAVED	LIVES LOST	POSSIBLE CAUSES
1	March	1982	Three Storey	No record	10	Weak foundation
2	June	1982	Two Storey	—	7	”
3	Sept	1983	Two Storey	—	8	—
4	May	1985	-	—	9	Faulty Foundation & bad workmanship
5	June	1985	Two Storey	—	5	Weak Foundation
6	July	1985	Three Storey	—	9	—
7	Nov	1986	-	—	1	Faulty Foundation & bad workmanship
8	May	1987	Two Storey	Many people escaped	4	Faulty Foundation & bad workmanship
9	Sept		-	Many people escaped before arrival of fire service	7	Structural Defect
10	Nov	1988	School Building	-	-	
11	Feb	1989	-	It is believed that many people escaped	-	Faulty Foundation & bad workmanship
12	May		Uncompleted Hospital Building	-	-	-
13	June	1994	Uncompleted 4 Storey Building	It is believed that many people escaped	1	Removal of form work before curing of concrete decking
14	May	1996	Uncompleted Church Building	Many people escaped	3	Bad workmanship

Source: Federal Fire Service, Lagos and Lagos State Fire Service – Ikeja

Table 3
Recent Building Collapses 2004-2006

DATE OF INCIDENT	STATES	TYPES OF BUILDINGS	NO OF LIVES LOST/INJURED	REMOTE CAUSES
Oct. 2004	Umuahia	3 Storey Building	4 dead, many injured	Unknown
May 2005	IIudun, Ogun State	4 Storey Building	10 dead, many injured	Unknown
June 2005	Aba	4 Storey Building	25 dead, many injured	Unknown
June 2005	Lagos	3 Storey	20 dead, many injured	Unknown
July 2005	Port-Harcourt	4 Storey	25 dead, many injured	Defective Foundation
July 2005	Lagos	3 Storey	30 dead, many injured	Defective Foundation
July 2005	Port-Harcourt	5 Storey Office Building	30 dead, many injured	Deviation from Approved Play / Addition of Floors
August 2005	Adamawa	Collapse of Bridge	45 dead, many injured	Defective Foundation
August 2006	Oworonshoki, Lagos	2 Storey Building	4 dead, many injured	Defective Foundation
August 2006	Lagos	4 Storey Building	50 dead, many injured	Deviation from Approved Plan.

Source: Author‘s Complication from National Dailies 2004-2006.

V. ROLE OF STAKEHOLDERS

It is necessary to identify the stakeholder in the process of building plan production and approval eventual execution; for better understanding of the building process. They are namely: the clients, the building professionals – architects, engineers, quantity surveyors, the approving body and then the contractor.

A. The Client

The client refers to the individual or a corporate body e.g. Banks, Institutions, Governments (Federal, State, and Local), churches, etc., that wants to develop building.It is the responsibility of the client to secure the services of qualified professionals – the architects, structural,

mechanical and electrical engineers. But most clients especially the individual clients have the erroneous impression that the service of these consultants is high and therefore prefer to patronize quacks. The results of their actions often have led to regrettable consequences in what is commonly referred to as —Penny Wise, Pound Foolish". The client must ensure that he provides building materials of good qualities and quantities as specified by the consultants for him to have a durable structure. He should respect the opinions of the professional consultants, who have their names and integrity to protect.

VI. THE BUILDING PROFESSIONALS

a) *The Architects*

Architects are persons who are trained in the art and science of building design and construction. The architect is also referred to as persons who designs buildings and supervises their erection; someone who plans something (New English Dictionary and Thesaurus, 2000). The architect according to Longman Dictionary of Contemporary English (2003) is someone whose job is to design buildings and the architect of something as the person who originally thought of an important and successful idea.It is this last definition that clearly places the architect as the number one (Prime) consultant in the building industry; just as the Civil and Electrical Engineer are the prime consultants for roads and bridges and power electrification projects respectively. He is the master builder; it has always been so, because the Greek Word _architeckon', from which the term architect was translated from, refers to him as a chief builder.The architect co-ordinates the activities of the other members of the building team (consultants) e.g. the Engineers, Quantity Surveyors, etc. The architect initiates and finalises the design of the building by which he ensures that the form and functions of the building are in order. He also ensures that the building meets with its owners' requirement and should satisfy public safety and should not constitute any hazard to its users. He must ensure that all consultants to a contract follow due process in project design and implementation and they must be qualified to participate in the project. As the master builder and the ultimate authority on site, he must be a man of professional integrity and, should not allow himself to be _settled' either by the contractor or supplier to detriment of the works on site. He must inspect and approve materials used on site, and ensure they are not substandard. The architect has a great stake in buildings designed by him; because he has a name to protect and would not want to be associated with any building Failure.

b) *The Engineer*

Engineering is the widest field in consulting as there are many fields of Engineering e.g. Civil or Structural Engineering, Mechanical, Electrical etc. for the purpose of buildings the above listed are the main engineering consultants involved. But in the issue of structural stability, the structural engineer is the most prominent and relevant. He must ensure that necessary tests (e.g. soil or geotechnical, cube test etc) are carried out for strength of materials on site. He must ensure that structural drawings for the project are designed to the specifics of the site, e.g. nature of soil, location of the building and type of structure, soil test must be carried out as necessary. The structural engineer is responsible for the stability or otherwise of the building. He, so to say is responsible for the skeleton of the building. The architect relies so much in his expert advice in taken decisions.The structural engineer's duty includes also supervising the structural aspect of the construction work. Besides being mentioned in the Article of Agreement, he is not given any power under the contract, hence any instruction given by him to the contractor should be passed through the architect. And this also applies to mechanical and electrical engineers if appointed Akapbio, (1978).The structural Engineer is required to submit a letter of undertaken to supervise any building more than two floors, designed by them to the Town Planning Authorities in most states before approval is issued for development. But unfortunately, most of them are ignored after the developer has gotten approval for his building plan. Most clients do not appreciate that there is a big difference between doing a paper work and physically being on site monitoring or supervising the construction process.

c) *The Building Contractor*

The building contractor is the individual or the company which undertakes to execute the building project for the client. In Nigeria, building construction contract is a big business and has become an all comers affair. Politicians, even medical practitioners, lawyers and others without any training in any of the building or built environment disciplines are now building contractors. Their only qualification in this field is political or social connections. Unfortunately, most of these contractors do not bother to employ a trained builder who is a specialist in the field of building construction, neither an architect nor structural engineers in their firms. This is also part of the problem, because some major projects are left in the hands of those who have no competence to engage in the tasks they are undertaking. Some problems that are associated with Nigeria building contractors include: penchant to cutting corners, use of substandard materials, poor workmanship, _big eye' for profit maximization. Because majority of the contractors are not professionals in the real sense of it; they are not bound by any professional ethics or code of conduct. In normal situation, it is the architect in collaboration with other professionals in the building team that ought to prepare tender documents, call for tender on behalf of the client, analyzes the tender and make recommendations to the clients as to the most suitable contractor to execute the work. The consultants take some factors into consideration in recommending contractors to the client for the award of the project. These are: availability of expertise, experience, manpower, equipments, and records of past jobs successfully executed by the company, etc.Most times, however, clients especially the individual clients do not bother to follow due process in the award of their projects. They prefer awarding the projects to those they know without necessarily considering their competence to execute

the project. Engagement of competent contactor and supervisory team with relevant knowledge and due diligence will ensure that the project is executed to specification and expected quality.

d) Town Planning Authority (Tpa)

The completed drawings are now submitted to the approving body, which is the Town Planning Authority (TPA) in local or municipal government office. The department is supposed to have qualified personnel with integrity to expertly and diligently vet and approve the drawings. Most times, these departments do not have the personnel with the requisite expertise and even when they have them, most lack integrity.The Development control Units (DCU) in most states play a limited role as they lack the number of staff with expertise o supervise the many developments in progress concurrently across their areas of jurisdiction. Their main function is to ensure that the clients engage the services of qualified professional to oversee their works.

Some developers are forced into illegal developments because of the bottleneck created by the approving bodies. Many obstacles are put in the way of intending developer as it can take a developer over one year to obtain approval for complete working drawings submitted. Issues usually mentioned are proper survey, good title, consent, certificate of occupancy; tax clearance certificates, development levies, processing fees etc. are cumbersome, financially tasking and unwieldy.Recently developments in the building industry have given rise to the development of high-rise buildings. This is to maximize the value and utilisation of land, which has become very scarce and expensive. Most developers do not appreciate the dangers associated with such high-rise buildings and therefore engage services of those who do not have the expertise on such projects. Another new development that has contributed to the malaise is the addition of new floors to existing buildings because of the pressure of demand in choice locations.

VII. STRATEGIES TO OVERCOME BUILDING COLLAPSE

It is obvious from the discussions above that the problem of building collapse can be addressed first form the client or prime consultant relationship. The caliber of prime consultant engaged by the clients goes a long way to determine the quality of finished work. The prime consultant should ensure that the right things are done by all other professionals involved in the project. The prime consultant knows his limitations and allows all other professionals to discharge their responsibilities to the best of their abilities.

Second part has to do with the approving bodies. Such organizations shall be staffed with people with expertise and integrity. If the expertises to approve certain designs are not within the organisation they shall seek for assistance from the relevant professional body or consulting firms, albeit at a fee. A situation, where the following approval authorities constitute of only Tow Planning to the exclusion of architects and structural engineers is not healthy.As a matter of urgency government should put in place approving procedures that are not cumbersome a one-stop shop that will reduce the time required for the approval of building plans. A time frame shall be set and given wide publicity. This will re-assure intending developers that the process is not open-ended.The third is in the areas of execution and supervision of the approved drawings. The quality of the executing contractor is very critical and crucial. The integrity and competence of the contractor holds the key to a successful competition of the project. The contractor must posses the following attributes: Play by the books, posses expertise to do things the right way and notice defective designs have a name to protect.Contractors shall meet some criteria to qualify to execute certain categories of projects, of which buildings that are three floors and above fall into. There shall be on the staff of the contractor a registered building officer, civil or building engineer, who must take responsibility for the integrity of the structure.Supervision is also very important because it ensures that he contractor follows the drawings, keep to specifications and ensures that the quality of materials used are of required standard. It is concerned with total quality management. Good examples include ensuring that the reinforcements are of right sizes, strengths and concrete grade specified are used at all times, adequate curing of concrete, enough time allowed for concrete to gain strength before proceeding to the next stage of work etc.Also, in the area of supervision, government can through the TPA play a commanding role to ensure that collapse don not occur. In the case of buildings of three floors and above, the TPA shall demand that registered engineers be engaged by the developers to supervise the project like is done in Lagos State.This shall be take a step further, the engineer shall be made to visit the head office of the TPA where he shall undergo an interview and properly documented including taken his photograph, by a professional colleague of the rank of a director, before ratification of his engagement. Once engaged, the RE will sign of completion. In case he ceases to supervise, he shall inform the director in writing to forestall impersonation and forgery.The TPA through the DCU shall be proactive, more robust and decisive in the performance of their functions. They shall be empowered to stop illegal developments and those that do not conform to all laid down conditionalities, either by persuasion or force, if need be, with assistance of law enforcement agents. They shall also be empowered to demolish offending structures before they constitute danger to the society.The Federal Government through the Standard Organisation of Nigeria (SON) must ensure that the construction materials in the market meet required standard. Like the cases of steel reinforcement, high yield steel must be seen to have the strength stipulated, so also is materials like cement.A monitoring team should be set up under the leadership of the commissioner of housing comprising all the professionals in the industry to visit construction sites and carry out on the spot check of the activities of the contractors and the supervising engineers. This is with the view of having first hand information of how they operate and discharge their functions. The report of the team shall be used in advising the local planning authority on what necessary actions to take against the contractors and supervisors (consultants).Zoning methods can be used to limit the number of floors to be developed in areas where

the soil bearing capacity is very low. Even the type of foundation to be used in such areas can also be specified. There must be the resolve to ensure that the law is not violated or breached.The general public including civil society organizations must report any development (new building and restructuring of old ones) in their neighbourhood to the TPA and follow it up to ensure proper approvals were obtained before the commencement of such developments. The NGOs shall go a step further by the contractors by regularly monitoring these developments.

Penalties and sanctions shall be put in place for all parties involved in the actualization of the building project to the extent of their involvement, violations and contraventions. A developer of a collapsed building shall be made to forfeit the plot to the government and in addition face criminal charges for poor quality works and be sanctioned by his professional bodies, so also are other professionals, they shall all be sanctioned by their professional bodies and charged to court where criminal negligence is established.Developers shall be informed of these penalties and sanctions at the time they obtain the building plan approval. It shall be stated clearly in the approval letter.Regulatory professional bodies and their corresponding societies or association shall regularly run workshops or seminars for their members to update their knowledge and highlight the dangers and penalties associated with collapsed or failed buildings. They shall monitor activities of their members and penalise them when necessary.Developers and professional shall be educated on the need to enter into proper contracts before the commencement of any project. Now, most developers feel reluctant to enter into properly executed contract rather they prefer the informal approach. They need for proper contract cannot be over-emphasized as the document defines the duties and obligations of the parties concerned.Some completed buildings initially may appear suitable for human habitation, but with the passage of time, mostly in weak soils, the buildings begin to settle, materials begin to suffer fatigue and corrosion begin to reduce to strength of materials used. All these combine to affect the continued satisfactory performance of the building.Government as a matter of policy shall periodically inspect existing building which may be over five or ten years to ascertain whether the buildings are behaving in the manner expected of them. Those with excessive cracks, deflections and settlements shall be subjected to more close examinations to ascertain their continued suitability for human habilitation.The reason for this recommendation is not farfetched. Now, there are existing buildings that have in engineering terms failed, though they are still standing but have developed cracks, deflections and settlements of unacceptable proportion and are tilting. They pose great threats to lives and properties and are disasters waiting to happen.It is pertinent therefore to state that building collapse cannot completely be eliminated as some aspects of soil investigation and even structural analyses and design are not fully understood and predictable since they are both science and art.

Secondly, some factors incorporated in the design are based on probabilities and therefore some degrees of uncertainty are inherent. Thirdly, the soil that carries all the structures varies widely in all directions.Finally, the performance of most materials over time especially fatigue, elasticity, dynamic and cyclical loading etc are not fully understood and predictable. If all things are done accordingly, the chances of collapse occurring are very minimal and rather the few cases of collapses will afford the opportunity to study and understand the phenomenon better.The recent approval of a national building code for the building industry is seen by all professionals in the construction industry as a welcome development that will help sanitize the industry.

VIII. Recommendation and Conclusion

The recommendations shall be presented under subheadings that are considered as the main stakeholders in the industry. The following roles are expected in this regard.

1. *Government:*

At the Federal Government level. Standard Organisation of Nigeria should vigorously pursue all those involve in the production or importation of sub-standard goods especially building materials. It should rid the society of sub-standard construction materials.Ministry of Housing and Urban Development should, when expedient, use the zoning approach to limit the number of floors to be developed in areas where the soil is very suspect. It shall even go further to stipulate the type of foundation to be used.State Government through the appropriate ministry, should as a matter of urgency streamline the process of granting building plan approvals. It should provide a one-stop with a view to reducing the time required for such approvals.A monitoring team should be set up under the commissioner or Works and Housing to make regular visits to different construction sites with the view of assessing how well the contractors and supervisors (consultant engineers) play their roles.Penalties and sanctions should be developed and enacted by the state governments and houses of assemblies. The consequences of developing a failed structure shall be well publicized.State ministries in charge of building plan approvals should also ensure that the engineers supervising developments take responsibility for the structural integrity and are properly documented including taken main photographs. The engineer should be interviewed by a professional colleague in the relevant ministry of the rank of a director or it equivalent. This will forestall any impersonation, forgery and denials in the future. Governments should put in place a policy for checking existing building periodically, may be every 5 or ten years, to ascertain their continued suitabity for human habilitation. Hence, the local planning authority shall concern itself with only approval buildings of two floors and only oversee higher buildings in collaboration with the zonal town planning office or the head office.

2. *Developers:*

Clients or developers will need to be circumspect fin the choice of prime consultant to ensure they engage competent prime consultants with integrity.

Clients or developers should rely on professional advice to engage contractors to execute their projects. This will not only ensure that the right contractor gets the job, but that it gets it done correctly and on time.Developers should also endeavour to sign proper contracts with both prime consultant and the contractor, defining responsibilities and obligations. Acrimonies in the scope of works that are associated with informal contracts will in this way become a thing of the past.

3. *Professionals:*

Professionals must be men of knowledge and integrity. In cases of jobs they are not trained for or lack competence to execute, they must always secure the best services for their clients if requested to, otherwise they should not undertake such works.Pecuniary benefits should not be the driving force in their relationship with their clients, but they should be motivated towards providing the best professional service at reasonable price and in a timely manner. Besides, they should always strive to enter into formal contracts with their clients as this will define the scope of services/works expected of them (responsibilities), the time frame and the consideration.

4. *Regulatory Bodies:*

Professional bodies like the regulatory organs and their corresponding societies or associations will be expected to conduct mandatory regular workshops or seminars for their members to keep them abreast of current developments in their chosen profession.Members will be expected to attain some basic points by attending such seminars and failure to meet up with the stipulated minimum, should result in striking off their names from the register of registered members.These bodies should set-up units to monitor the activities of their members, make random visits to project sites where those found wanting in the discharge of their duties should be sanctioned.

5. *Civil Society And Non-Governmental Organisation:*

Civil society, especially the NGOs‘ are to act as watch-dogs to report any new developments and even the restructuring of old buildings to the relevant authorities.Specialized NGOs in matters relating to safety of the environment shall be encouraged. They will be expected to monitor these developments and report their findings to the relevant authorities.If these recommendations are religiously implemented, it is expected that the menace of building collapse will become a thin of the past and only occur in situation of *force majore.*

IX. References

1) Adeniya (200): How Public-Private Partnership can Tackle Building Collapse.The Guardian, Monday, August 26, 2002. P.45.Aniekwu, N. and Orie, O.U. (2005): The Determination of Severity Indices of Vairables that Cause Collapse of Engineering Facilities in Nigeria. A Case Study of Benin City. The Journal of Engineering Science and Application (JESA) Vol.4, No. 2. Pp. 63 -70.
2) Akpabio (1978): Building Contract Administration – a Handbook for architects, Administrators and Building Professionals. Modern Business Press Ltd. Uyo- Nigeria. P.34.Boye Ajai (1995): Factors Responsible for Collapsed Building. Tell Magazine No.3, January 16, 1995. P. 19. Mentioned in Izomoh, S.O. (1997). The Provision of Housing and Management in Nigeria. P.20.Communiqué Issued by Building Professionals (1996). Entitled Brainstorm onStructural Failures and Building Collapse in Nigeria. This Day Newspaper, August 28, 1996. P.25Dimuna K.O. (2006): Compilation of Collapsed Buildings in Nigeria 2004 – 2006 from National Dailies.Dictionary of Architecture and Construction. Cyril M. Harris (Ed). McGraw-HillBook Company, New York. 1975. P.193.English Dictionary and Thesaurus (2000) 5th Edition Geddes and Crosset, Fuiland. P.42.Federal Fire Service, Lagos and Lagos Sate Fire Service, Ikeja. Mentioned in Chukwemeka. C.E. (1996) Collapse of Building – A Case Study of Collapsed Building at Oshodi, Lagos. State. An unpublished Research Essay Submitted to the Department of Architecture, Edo State University, Ekpoma. 1996.Frederick, M. and Ambrose, J. (1989): Building Engineering and System Design. Van Nostraud Reinhold, New York. Vol 2. P.4.Hall, G.T. (1984): Revision Notes on Building Maintenance and Adaptation. Butterworth‘s and Co., England.Longman Dictionary of Contemporary English (2003): Third Edition, Person Education, London. P.56.Madu, L.E.C. (2005): Averting the Increasing Incidents of Collapsed Buildings. The Vanguard, Tuesday, November 29, 2005. P.36Mosley W.H and Bungay J.H (1985); Reinforced Conctete Desijgn. London, Macmillian Ltd. Pp15-17Obiechina, N. (2005): How Stakeholders can Conquer the Monster of BuildingCollapse. The Guardian, Monday, August 22, 2005. Pp.37-43.
3) Onibudo, D. (2006): And Another Building Collapse. The Vanguard, Thursday,July 27, 2006. P.39.Oyewande, B. (1992): A Research for Quality in the Construction Industry. Builders. Magazine, June/July. Lagos.Singha S.N. (2002):, Reinforced Concrete Design New Delhi, India, Tata McGraw Hill Publishing Company pp44-47The Punch, Thursday, July 20, 2006. P.11.The Guardian, ―Works Minister Indicts Structural Engineers Over Building Collapse”. October 11, 2004. P.33The Punch, Monday, August 7, 2006. Pp. 37-42. Udegbe, M.I. and Amadi, C.O. (2005): Structural Failures in Buildings. BabInternational Publishers of Nigeria, Benin City. P.14.

Zinc Incorporated Hydroxyapatite as Catalysts for Oxidative Desulphurization Process

M.Riad* and S Mikhail

GJRE Classification (FOR)
GJRE: C, 090402

Abstract- **Ca-hydroxyapatite was freshly prepared by precipitation method and used as a support material for preparing zinc catalysts. The catalysts were prepared by two different techniques: incipient impregnation and ionic exchange. The freshly preparedzinc catalysts were characterized via; X-ray diffraction pattern, Fourier transformer infra red spectroscopy, differential scanning calorimetery and thermo-gravimetric analyses. X-ray diffraction results established the replacement of Ca^{2+} by Zn^{2+} for the catalyst prepared by ionic exchange method and formation of Zn oxide species after impregnation. The evaluation of the catalytic activity of Zn-haydroxyapatite catalysts were investigated towards oxidative desulphurization reaction of gas oil. The results presented that desulphurization wt% was achieved to 68.5 wt% by reaction under mild conditions on using ionic exchanged zinc catalyst.**

Keywords: Hydroxyapatite, Impregnation, Ionic exchange, Zinc, Catalysts, Oxidative desulphurization.

I. INTRODUCTION

Hydroxyapatite ($Ca_{10}(PO_4)_6(OH)_2$ is widely used as bio-ceramic materials and as adsorbents for separation of bio-molecules. These materials have also been used as adsorbents for heavy metals [1], supports [2-5] and as catalysts in oxidation and dehydrogenation reactions. The catalytic performance of these materials depend on the lattice substitution of Ca sites in hydroxyapatite structure by varied cations as Na, Mg, Sr and Mn, which result in changes in various structural properties as crystallinity and morphology. The preparation of hydroxyapatite with controlled morphology, stoichiometery, crystallinity and size has the main role in production of an active catalytic material. Various synthesis methods have been used for hydroxyapatite preparation such as, soild state reaction [6], chemical precipitation [7], formation of hydroxyapatite crystals on glass or brushite growth of hydroxyapatite crystal using sol gel synthesis and surfactant tamplating method.Hanna and Hamid [8] studied the preparation of Ca-hydroxyapatite via electro-deposition method of highly pure brushite ($CaHPO_4.2H_2O$) on titanium alloy substrate and the transformation of brushite to hydroxyapatite as a coating for orthopaedic implants. Filho et al, [9] investigate the preparation of Fe-hydroxyapatite by high energy dry milling of calcium nitrate and ammonium phosphate with different amounts of iron oxide (0.5, 1 , 2.5 and 5wt%) and calcined at 900°C. Cd-hydroxyapatite were synthesized by high temperature mixing method using solution of $Cd(NO_3)_2.4H_2O$ and $(NH_4)_2HPO_4$ at different pH values: 10 14 and found the pH values have a great influence on the crystallinity and morphology of hydroxyapatite [10].

Akuma et al, [11] study the preparation of Ag-loaded hydroxyapatite by incipient impregnation technique using different silver loading of $AgNO_3$ (0.5, 1, 1.5 and 2 wt%). Fe- [12] and V- substitute hydroxyapatite [13] were prepared by co-precipitation technique. Zn -substituted hydroxyapatite prepared by ionic exchange technique was an efficient catalyst for the synthesis of 3-substituted indoles [14].The aim of this work is to prepare Ca-hydroxyapatite by precipitation technique to be used as a support material. The effect of incorporation of Zn^{2+} ions either by impregnation and or ionic exchange techniques with different zinc loading on the crystallinity, crystallite size, formed phases and thermal stability of all prepared materials were investigated. The catalytic activity of the prepared Zn-hydroxyapatite catalysts towards oxidative desulphurization of gas oil was also studied

II. EXPEIMENTAL

1. *Preparation Of The Support Materials*

Hydroxyapatite (Hap) was prepared by co-precipitation technique according to Narasaraju et al, [15] and Tkalcec et al, [16] methods. A 0.3 M $(NH_4)_2HPO_4$ solution was drop wisely added to 0.5 M $Ca(NO_3)_2$ solution and the pH was adjusted to 11 by adding ammonia solution until a white suspension was obtained. The suspension was further stirred for 24 hours, then filtered and washed with distilled water. The resultant cake dried at 100°C and then calcined at 400°C in presence of flow of purified air.

2. *Preparation Of Zn-Hydroxyapatite Catalysts*

a) *Wet Impregnation Technique*

10 and 20wt % Zn/hydroxyapatite catalysts (based on the weight of support) were prepared by wet impregnation technique using zinc nitrate as a salt solution. The prepared catalysts ($ZnHap_{Imp1}$ and $ZnHap_{Imp2}$) dried at 120°C and then calcined at 350°C for 3 hours.

b) *Ionic Exchange Technique*

A 0.1 and 0.2 M solutions of $Zn(NO_3)_2.H_2O$ were kept in contact with 10gm of the prepared hydroxyapatite material for 48 h under agitation at room temperature to prepare $ZnHap_{Ion1}$ and $ZnHap_{Ion2}$ catalysts. The resultant cake was filtered, dried at 100°C for 24 h and then calcined at 350°C for 3h.

3. *Characterization*

X –ray Diffraction Pattern (XRD) was carried out on XD-D1- x-ray diffraction Schimadzu, CuKα radiation was the light source

About-Egyptian Petroleum Research InstituteNasr City, Hai Al-Zehour PO Box 11727, Cairo, Egypt

with applied voltage of 40K and current of 40 mA. Two theta angles ranged from 4 to 80° with speed of 2° per minute, the formed phases of the prepared and calcined materials were detected. The crystallite size was calculated from X-ray line broadening using Sherrer's equation $D= k\lambda /\beta_{1/2}\cos\theta$, where D is crystallite size estimated using the reflection (002), k is a shape factor equal 0.9, λ is X-ray wave length (CuK_α =1.5405), θ is the diffraction angle related to reflection 002 (θ = 25.86), and $\beta_{1/2}$ calculated using the formula $\beta_{1/2}= (B^2-b^2)^{1/2}$, where B being the diffraction peak width at half height and b is the natural width of the instrument [17].The crystallinity degree (Xc) corresponding to the fraction of crystalline phase present in examined volume was evaluated according to Landi et al., [18]. $Xc \approx 1- (V_{112-300}/I_{300})I_{300}$ is the intensity of (300) reflection of apatite and $V_{112-300}$ is the intensity of the hollow between (112) and (300) reflection.The values of lattice parameter were determined from characteristics diffraction pattern using the Retiveld full profile method and Koalarie computer software [19,20]. In addition, the volume of unit cell is calculated using lattice parameter of hydroxyl-apatite a/c by the formula : $V=2.589a^2c$ Fourier Transformer Infra Red (FT-IR) spectra were run on Perkin Elmer FT-IR apparatus working in the range of 4000-400 cm^{-1} to identify the hydroxyl and functional groups contained the prepared and calcined materials.Differential Scanning Calorimetry Analysis (DSC) was carried out using the Differential Thermal Analyzer, Perken Elmer apparatus, to study the phases formed upon thermal treatment and the enthalpy of prepared catalysts.The Ca/P ratio and the metal loading was determined by X-ray flourcence (XRF) using Rigaku Seqential Spectrometer (RIx3100) equipment with Rh source

4. Catalytic Reaction

The catalytic oxidative desulphurization reaction of gas oil (supplied from Cairo Refining Petroleum Company) was carried out in a triple-necked round bottomed flask at reaction temperature 60°C in the presence of the different prepared zinc catalysts and using hydrogen peroxide as oxidizing reagent. For each, 50 ml of gas oil and 50ml of hydrogen peroxide (30%water, Prolabo) was added to 1 gm freshly prepared catalyst. The reaction mixture was stirred for 1 hour and settled to attain phase separation. Then, the separated gas oil was adsorbed on activated bentonitec-clay material at 50°C. The sulphur concentration was measured by X-ray flourcence apparatus (Horiba SFLA-1800).

III. Results and Discussions

The chemical composition of support and the prepared catalysts was obtained by XRF and the results are tabulated in Table 1). The measured Ca/P atomic ratio is 1.67 which is coincident with that for the stoichiometric hydroxyapatite material.

1. Catalysts Characterization

a) X-Ray Diffraction Pattern

Fig.1 shows X-ray diffraction patterns for hydroxyapatite and the prepared zinc catalysts. The diffraction lines appeared at 2θ = 25.8, 29.1, 31.9, 33.1, 32.2, 34.1, 40.1, 46.9, 49.1° (Fig.1a) attributed to the presence of crystalline hydroxyapatite phase $Ca_5(PO_4)_3(OH)$ {ASTM 76-0694}.The diffracto-gram for calcined hydroxy-apatite (Fig.1b) ascribed a well crystalline structure as established from the increase in the crystallinity degree from 35 to 45% (Table2) and the appearance of sharp diffraction lines with high intensities, in comparing to as-prepared one. The diffraction pattern for $ZnHap_{Imp1}$ catalyst (Fig.1c) reflects a decrease in line's intensities which ensure an incorporation of Zn cation in the hydroxyapatite lattice structure. Further increase of Zn loading the intensity of the hydroxyapatite lines are also decreased. Upon calcination of $ZnHap_{Imp1}$ the diffraction lines became sharp and the crystallinity degree increases from 45% then to 55 and 63% with the increase in Zn content up to 20 wt% (Fig. 1e & Table 2), in agreement with Suchanek et al, [21] and Feng et al, [22] investigations. In addition, new diffraction lines appeared at 2θ =32.0, 37.2, 49.5° emphasized the presence of ZnO species (Fig. 1f). For $ZnHap_{Ion1}$ catalyst no visible changes are observed in the diffraction lines (Fig.1g). Meanwhile, XRD pattern for $ZnHap_{Ion2}$ catalyst reveals a shift in the hydroxyapatite diffraction lines to higher angles which indicated that Ca^{2+} cations were substituted by Zn ones in the hydroxyapatite structure (Fig. 1h). At the same time, the diffraction lines are broadened owing to the low crystallinity of Zn replaced hydroxyapatite compared to the support material, in accordance with Wakamura et al, [23] proposal that divalent ions difficult to obtain high crystallinity and greatly inhibit hydroxyapatite crystallization.On the other hand, parascholzite phase $CaZn_2(PO_4)_2.2H_2O$ appeared at 2θ = 10, 12.5, 20° (ASTM 76-0725) upon calcination of. $ZnHap_{Ion2}$ catalyst, in agreement with the results of Mujaji et al, [24] who reported that the formation of Zn substituted hydroxyapatite by precipitation technique and the formation of parascholzite phase started to form at Zn fraction up to 18 wt% and estimated a limit of 15 mole % for Zn substitution in Hap lattice.

b) Crystallite Size

The average crystallite size for the prepared materials was determined using Sherrer's equation at 2θ = 25.86° (002) plane. The results in Table 2 reveal an increase in crystallite size from 16.0 to 21.6 nm for the calcined hydroxyapatite one due to the removal of the hydroxyl groups upon heating, which allow the aggregation of the particles, in accordance with the sharpness of diffraction lines and the increase in the crystallinity degree. For $ZnHap_{Imp1,2}$ catalysts, the crystallite size shows an increase that may be resulted from the aggregation of ZnO species within apatite lattice. On contrary, the crystallite size for $ZnHap_{Ion}$ decreases with the increase of the replaced Zn cations up to 20%.

c) Lattice Parameter

Diffracto-gram analysis allowed the identifications of the hexagonal phase with lattice parameter of hydroxyapatite which augmented gradually from 0.9425 to 0.9462 nm (for a=b) and from 0.6906 to 0.648 nm (for c) with the increase of zinc loading (impregnation method) from 10 to 20 wt% respectively, in agreement with Parhi et al investigations [25]. Where the expansion of lattice parameter was consistent with the incorporation of Zn^{2+} into Ca^{2+}-hydroxyapatite lattice. For $ZnHap_{Ion}$ catalysts, both a and c decrease with the increase in the Zn substituted catalysts. Whereas, a=b shows a further decease upon heating and c shows the reverse (Table 2). As well known that the divalent cations like Zn causes a lattice strain upon heating, and consequently the lattice structure of Ca-hydroxyapatite was disordered, in accordance with the results of unit cell volume which contracts and relaxes as the lattice parameter either decrease and or increase (Table 2).

d) Thermal Behavior

Fig. 2 represented differential scanning calorimetery (DSC) and thermogravimetric (TG) profiles for the prepared hydroxyapatite and Zn-hydroxyapatite catalysts and the calculated enthalpy and weight loss% included in Table 3.DSC profile for hydroxyapatite reveals the appearance of an endothermic peak in the range of 30-120^{o}C attributed to the desorption of water adsorbed on the crystallite surface of hydroxyapatite and a second endothermic peak appeared at 860-930 ^{o}C which related to decomposition of hydroxyapatite structure. From literature, hydroxyapatite is stable at higher temperature and decompose to the β-tricalcium phosphate at temperature higher than 1350 ^{o}C above this temperature β- irreversibly transform to α- form [8]. Tkalcec et al, [16] established that hydroxyapatite prepared by precipitation start to decompose at 800^{o}C when heated and transforms to tri-calcium phosphate.For $ZnHap_{Imp1}$ catalyst the DSC profile shows the same behavior as hydroxyapatite material. Further increase in Zn loading to 20w%, a new endothermic peak appeared at 250 -300^{o}C which imply the formation of ZnO species. On the other hand, the heat of enthalpy for the endothermic peak appeared at 860-930^{o}C (Table 3) increased with increasing the zinc loading [26] which means the more restrained hydroxyapatite structure.DSC profile for $ZnHap_{Ion1}$ catalyst is also similar to that for the support with an observed increase in heat of enthalpy related to the incorporation of Zn species in the support lattice (Table 3). For $ZnHap_{Ion2}$ catalyst DSC profile reveals the appearance of two endothermic peaks in addition to the surface adsorbed peak at 30-160^{o}C. The peak appeared at 480-620^{o}C related to the removal of lattice water, in accordance with Le Geros et al, [27] who reported that Ca deficient hydroxyapatite incorporate water which substitute for OH sites and called lattice water that vaporized gradually at 140-600^{o}C. The endothermic peak that appeared at 650-820^{o}C is ascribed to the transformation of hydroxyapatite to tri-calcium phosphate which means Zn might promote this transformation process. Moreover, an exothermic peak appeared at 220-320^{o}C which imply the dehydroxylation of hydroxyapatite structure and the formation of paraschlozite phase.

Thermo-gravimetric line for the prepared hydroxyapatite (Fig. 2) exhibits two steps for weight loss, the first at 30-120^{o}C due to the desorption of water adsorbed on the surface of apatite particles and the second at 860-930^{o}C due to the transformation of hydroxyapatite to tri-calcium phosphate. It is noticed that, the weight losses increase with increasing Zn content.

e) Ft-Ir Spectroscopy

Fig. 3 shows FT-IR spectra for Hap and zinc catalysts recorded at wave number ranged from 4000 to 400 cm^{-1}.FT-IR spectrum for hydroxyapatite in Fig. 3a reveals the appearance of phosphate (PO_4^{-3}) bands which attested by the P-O asymmetric and symmetric stretching mode appeared at 965, 1030, 1095 cm^{-1} and the O-P-O bending modes at 605, 565, 475 cm^{-1}. Adsorbed molecular water band appeared at 1630 cm^{-1} and also a shoulder at 875cm^{-1} assigned to $(HPO_4)^{-2}$ which formed upon the reaction of some surface PO_4^{-3} with water. Two bands appeared at 630 & 3580 cm^{-1} assigned to vibrational and stretching modes of OH groups respectively. After heat treatment, Fig.3b reveals that the broad band appeared at ~3400 cm^{-1} became smaller which related to the decrease in the amount of lattice and adsorbed water. Tanaka et al, [28] found that the number of surface P-OH decreased by 60% on heating to 600^{o}C resulting in the formation of P-O-P group as 2P-OH = P-O-P +H_2O. Loading of Zn on hydroxyapatite leads to increase in the band intensity appeared at 1630 cm^{-1}. With the increase in Zn loading the spectrum in Fig. 3c,d clarified the intensities of stretching bands (associated with phosphate bands) at 965, 1030, 1095 cm^{-1} reduced and the resolution of such bands became obscure and the OH bending band at 630 cm^{-1} was broadened owing to the decrease in the crystallinity of the prepared material, in agreement with XRD results. For calcined Zn catalysts the profile in Fig. 3 shows a decrease in the intensity of the band at 3580 cm^{-1} assigned to stretching vibration of structural OH group located on hydroxyapatite tunnels. The decrease in peaks intensity may be ascribed to the dehydroxylation that accompanied the calcination step and the formation of other species. In addition, band appeared at 2150 cm^{-1} assigned to the formation of ZnO species (for $ZnHap_{Imp2}$ catalyst, Fig. 3h), whereas, band appeared at 2200 cm^{-1} assigned to the formation of paraschlozite phase (for calcined $ZnHap_{Ion2}$ catalyst, Fig. 3j).

2. Catalytic Evaluation

The activity of support and the prepared catalysts was evaluated towards oxidative desulphurization reaction of light gas oil containing 1281.8 ppmw sulphur. As previously investigated [29], sulphur compounds containing light gas oil consist mostly of benzothiophene and dibenzothiophene derivatives. Experimentally, gas oil was mixed with hydrogen peroxide as oxidizing reagent (1:1 vol ratio) at 60^{o}C with vigorous stirring for one hour. The formed sulphons was removed via adsorption on activated

bentonitec clay materials. The results are included in Table 4. From data, it is clear that, the sulphur content decreased from 1281.8 (Feed) to 930.5 ppm on using the prepared hydoxyapatite material i.e. desulphurization wt% reached to ~27wt%. The results in Table 4 revealed that the prepared catalysts exhibits remarkably high activities in the removal of sulphur compounds by mild oxidation with hydrogen peroxide compared with support material. The sulphur content decreases to 490.7 ppmw on using $ZnHap_{Imp1}$ catalyst. Whereas, on increasing zinc loading from 10 to 20 wt%, the removal of sulphur does not affected.On the other hand, the content of sulphur deceases from 1281.2 (Feed) to 512.9 ppmw using $ZnHap_{Ion1}$ catalyst, further increase in the replaced Zn cations, the removal shows a sharp increase (Table 4).As shown in Table 4 $ZnHap_{Ion2}$ has the highest activity in sulphur removal reaches to 877.6 ppmw (desulphurization 68.5 wt%) after 60 min of reaction. These results are in agreement with that studied by Ishihara et al, [30] who reported that the removal of sulphur in light gas oil from 39 to 5 ppmw (~88%) by an oxidation –adsorption continuous flow process. Also, it decreased from 320 to 10 ppmw in diesel fuel fraction on using Mo/Al_2O_3 catalysts [31]. Moreover, Venugopal et al, [32] and Venugopal et al, [33] studied the oxidative desulphurization reaction of light petroleum fractions on titanium containing molecular sieve and gold supported on hydroxyapatite, where the sulphur removal reached to 56% and 80% respectively under the same experimental conditions. These established that the preparation of hydroxyapatite material to be used as support to prepare Zn catalysts for oxidative desulphurization reaction. of gas oil. Thus, the sulphur removal data emphasizes that $ZnHap_{Ion2}$ is the most active catalyst towards oxidative desulphurization process where the sulphur removal reaches 68.5wt%.

3. Mechanism Of Reaction

According to Basolo et al, [34] active species of Zn oxide can be formed by the nucleophilic attack of hydrogen peroxide on Zn atoms, electrons are withdrawn from the peroxyl moiety, thereby increasing the electrophilic characters of the peroxidic oxygen. The oxidation of sulphur atom in the organo-sulphur compound must proceed by nuclophilic attack of an active hydroperoxy to form sulphoxide and a regenerated zinc species. Subsequently, the sulphoxide undergoes further oxidation by hydroperoxy to form sulphone, it is possible to rationalize the presence of electronegative phosphate species as they help withdraw electrons density from Zn species and thereby conferring a higher electrophilic character to the Zn, in agreement with the mechanism proposed by Ramirez et al, [31] . Hydrogen peroxide migrates to Zn sites with an OH to form an intergradations of hydroperoxide species responsible for oxidation of sulphur compound, sulphur substrates possibly going through two steps pathways are oxidized into sulphoxide or sulphone. Concurrently, the formed paraschllozite phase in calcined Zn (20wt%) exchanged apatite catalyst offers the required species for oxidative desulphurization mechanism of light gas oil.

IV. Conclusion

- The hydroxyapatite material was prepared by precipitation method, 10 & 20wt% zinc-hydroxyapatite catalysts were prepared via either impregnation and or ionic exchange techniques.
- The different preparation techniques used were suitable to incorporate zinc phase and the catalyst presented significant differences in relation to the formed phase
- For zinc catalyst loaded hydroxyapatite, Zn was incorporated as ZnO species (after calcinations) as confirmed from X-ray diffraction analysis.
- For zinc replaced hydroxyapatite Zn was incorporated into apatite lattice.
- Zinc replaced catalyst has high activity towards the oxidative dehydrogenation reaction of gas oil under mild conditions.

V. References

1) M. Miyake, K. Watanabe, Y. Nagayama, H. Nagasawa, T. Suzuki, J. Chem. Soc. Faraday Trans. 86 (1990) 2303.
2) AVenugopal, M.S. Scurell, Appl. Catal. 245 (2003) 137.
3) Z. Opre, J.D. Grunwaldt, M. Maciejewski, D. Ferri, T. Mallat, A. Baiker, J. Catal. 230 (2005) 406.
4) N.S. Resende, M. Nele, V. M. Salim, Thermochim Acta 451 (2006) 16.
5) G. Lopez, R. Pomes, C.O. Vedova, R. Vina, J. Raman Spectrosc. 32 (2001) 255.
6) S. Sugiyama, T. Shona, D. Makino, T. Moriga, H. Hayashi, J. Catal. 214 (2003) 8.
7) K. Elkabouss, M. Kacimi, M. Ziyad, S. Ammar , F. Bozon-Verduraz, J. Catal. 226 (2004) 16.
8) F. Hanna, Z. Hamid, Pigment and resine technology, 5 (2003)19
9) F.P.Filho, R.E.F.Q. Nogueira, M.P.F. Graca, M.A. Valentie, A.S.B. Sombra, C.C.Silva, Physica B, 403 (2008)3826-3829.
10) K.Zhu, K. Yangiswa, A. Onda, K. Kajiyoshi, J. Qiu, Materials Chemistry and Physics, 113 (2009) 239.
11) P.Akumar, M.P. Reddy, L.K. Ju, H. H. Phil, Catal Lett., 49 (2008)31.
12) W. Pon-on, S. Meejoo, I-M. Tang, Materials Research Bulletin , 43 (2008) 2137.
13) S.Sing, S.B. Jonnalagaddo, Catal. Lett., 49 (2008) 45.
14) R. Tahir, K. Banest, A. Solhy, S. Sebti, J. Mol. Catal. 246(2006)39.
15)] T.S.B. Narasaraju, D.E. Phebe, J. Mater. Sci., 31 (1996) 1.
16) E. Tkalcec, M. Sauer, R. Nonninger, H. Schmidt, J. Mater . Sci. 361 (2001) 5233.
17) T. J. Burgues, R.R. Clemente, Cryst. Res. Technol. 36 (2001) 1075.
18) E. Landi, A. Tampier, G. Celotti, S. Spria, J. Eur. Ceram. Soc. 20(2002)2377.

19) H. Rietveld, J. App. Cryst. 2 (1969)65
20) R.W. Cheary, A. A. Coechlo, J. App. Cryst. 25(1992) 109
21) W.L.Suchanek, K. Byrappa, P. Shuk, R.E. Riman, V.F. Janas, K.S. Ten-Huisien, Biomaterials, 25(2004) 2647
22) Z.D. Feng , Y.M. Liao, M. ye, J.Mater. Sci. Mater. Med. 16(2005) 417.
23) M. Wakamura, K. Kandori, T. Ishikawa, Colliod and Surf. A. 164 (2000) 297
24) F. Mujaji, Y. Kono, Y. Suyama, Materials Research Bulletin. 40 (2005)209.
25) P. Parhi, A. Ramanan, A.R. Ray, J. Mater. Sci, 41(2006)1455.
26) T.M. Sridhar, U.K. Mudali, M. Subbaiyan Corr. Sci. , 45 (2003) 2337.
27) G. Z. Le Geros, C. B.Bleiwas, M. Retino, R. Rohanizadeh, I.P. Le Geros, Am. J. Dent. 12 (1999) 65.
28) H.Tanaka, M. Chikazawa, K. Kandori, T. Ishikawa, Phys. Chem. Chem. Phys. 2 (2000) 2647.
29) J. L. Garcia-Gutierrez, G. A. Fuentes, M. E. Hamandez-Teran, F. Murrieta, J. Navarrete, F. Jimenez-Cruz, Appl. Catal. A. 305 (2006) 15.
30) A. Ishihara, D. Wang, F. Dameignil, H. Amano, E. W. Quiam, T. Kabe, Appl. Catal. A 275 (2005) 279.
31) L.F. Ramirez, E. Torres, R. Gomez, V. Gonzalez, F. Murrieta, Catal. Today, 98 (2004) 289.
32) V. Hulea, F. Fajula, J. Bousquet, J. Catal. 198 (2001) 179.
33) A. Venugopal, M. S. Scurrecll, Appl. Catal. A 245 ((2003) 137.
34) F. Basolo, R. G. Pearson, Mechanism of Inorganic Reaction , Second ed., Wiley, NewYork,1962.

Table (1): Chemical Composition of the Prepared Hydroxy-apatite and Zinc Catalysts

Catalysts	Calcium wt%	Phosphorus wt%	Ca/P ratio
Hap	35.67	16.54	1.67
$ZnHap_{Imp1}$	35.88	16.53	1.70
$ZnHap_{Imp2}$	35.78	16.54	1.69
$ZnHap_{Ion1}$	34.56	16.51	1.57
$ZnHap_{Ion2}$	34.49	16.51	1.56

Table (2): Lattice Parameters, Crystallite Size and Degree of Crystallinity for Hydroxy-apatite and Zinc Catalysts

Catalysts	a=b (nm)	c (nm)	Volume of unit cell (nm^3)	Crystallite Size (nm)	Degree of Crystallinity(%)
Hap	0.9425	0.6881	0.5311	16.0	35
Calcined Hap	0.9441	0.6906	0.5330	21.6	45
$ZnHap_{Im1}$	0.9450	0.6873	0.5292	28.7	39
Calcined $ZnHap_{Im1}$	0.9442	0.6858	0.5290	30.4	55
$ZnHap_{Im2}$	0.9453	0.6860	0.5277	35.5	33
Calcined $ZnHap_{Im2}$	0.9438	0.6843	0.5271	44.8	63
$ZnHap_{Ion1}$	0.9420	0.6876	0.5308	20.9	28
Calcined $ZnHap_{Ion1}$	0.9416	0.6882	0.5306	19.3	21
$ZnHap_{Ion2}$	0.9418	0.6873	0.5305	14.5	22
	0.9415	0.6870	0.5302	10.2	18

Table (3): Thermal Behavior Data for Hydroxy-apatite and Zinc Catalysts

Catalysts	Peaks Location (^{o}C)	Enthalpy(Cal/gm.sec.)	Weight Loss%
Hap	30-120 (endo) 860-930 (endo)	17.71 14.3	4.34 10.47
$ZnHap_{Im1}$	35-125 (endo) 850-930 (endo)	27.3 18.6	10.45 12.82
Zn Hap_{Im2}	30-100 (endo) 250-300 (endo) 860-920 (endo)	37.99 19.65 23.52	16.53 17.71 19.66
Zn Hap_{Ion1}	25-100 (endo) 850-930 (endo)	8.65 27.8	7.59 21.6
Zn Hap_{Ion2}	30-160 (endo) 220-320 (exo) 480-620 (endo) 650-820 (endo)	17.74 16.35 24.85 39.57	11.24 5.97 12.16 29.45

Table (4): Oxidative Desulphurization Results of Light Gas Oil on the Prepared Zinc Catalysts

Catalyst	Feed	Hap	ZnHapIm1	ZnHapIm2	ZnHapIon1	ZnHapIon2
Sulphur Content ppm	1281.2	930.5	490.7	612.8	512.9	403.6
Sulphur removal ppm	0	350.3	790.5	668.4	768.3	877.6
Desulphurization,wt%	0	27.3	63.4	52.2	60.0	68.5

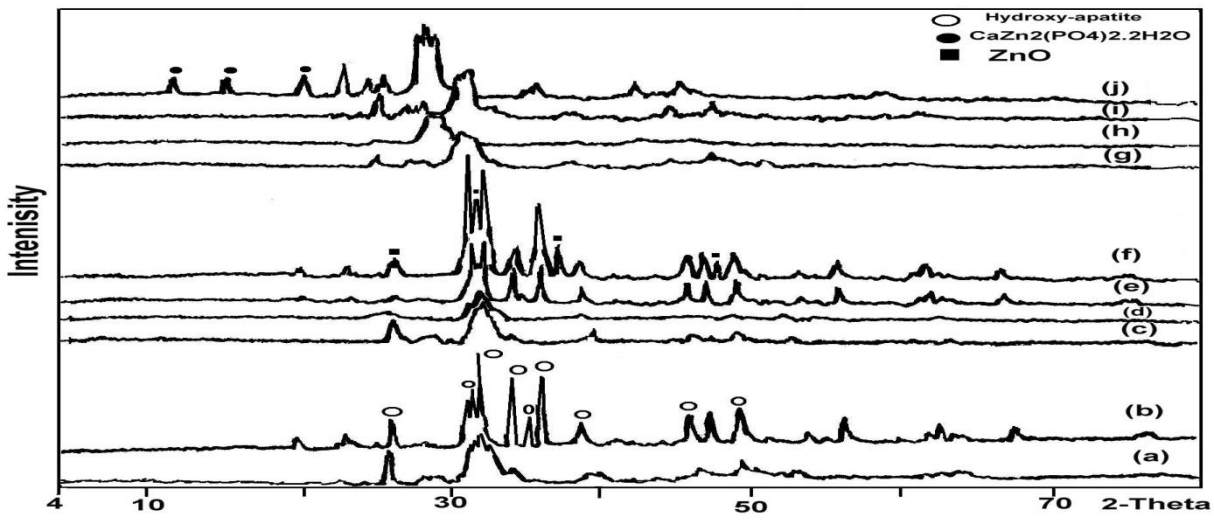

Fig. (1): XRD Spectrum for: (a) Hap (b) Calcined Hap (c) Prepared $ZnHap_{Im1}$ (d)Prepared Zn Hap_{Im2} (e) Calcined $ZnHap_{Im1}$ (f)Calcined $ZnHap_{Im2}$ (g) Prepared $ZnHap_{Ion1}$ (h) Prepared Zn Hap_{Ion2} (i) Calcined Zn Hap_{Ion1} (j) Calcined Zn Hap_{Ion2}

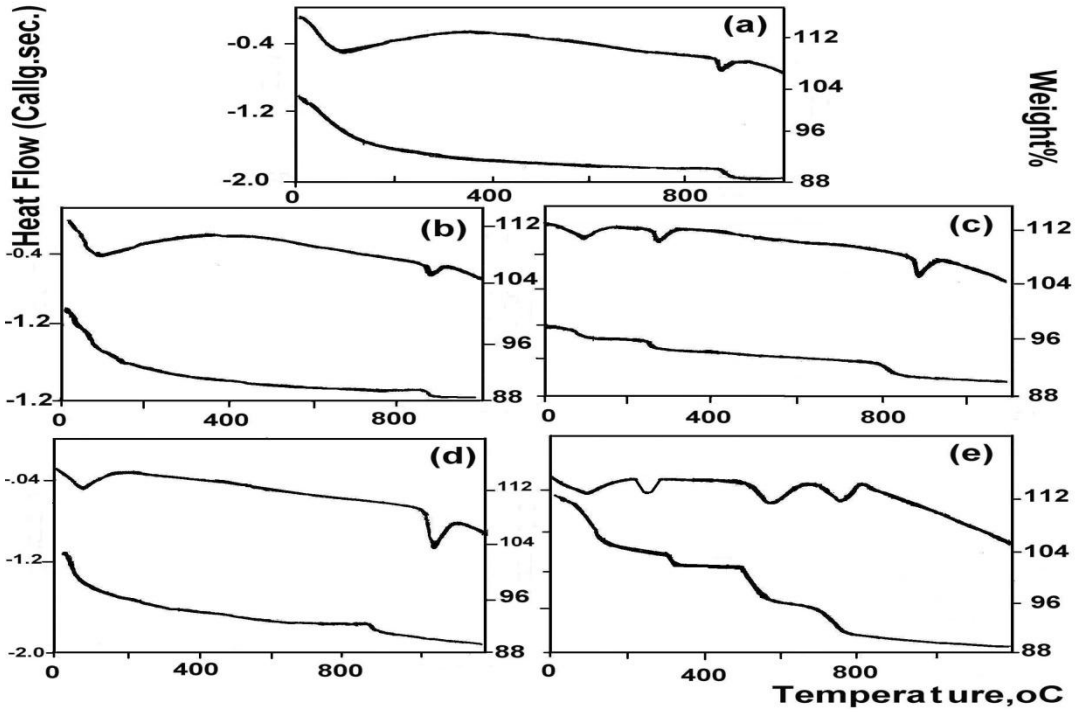

Fig. (**2**): Differential Scanning Calorimetery Profile for:
(a) Hap (b) Prepared $ZnHap_{Im1}$ (c) Prepared Zn Hap_{Im2}
(d) Prepared $ZnHap_{Ion1}$ (e) Prepared Zn Hap_{Ion2}

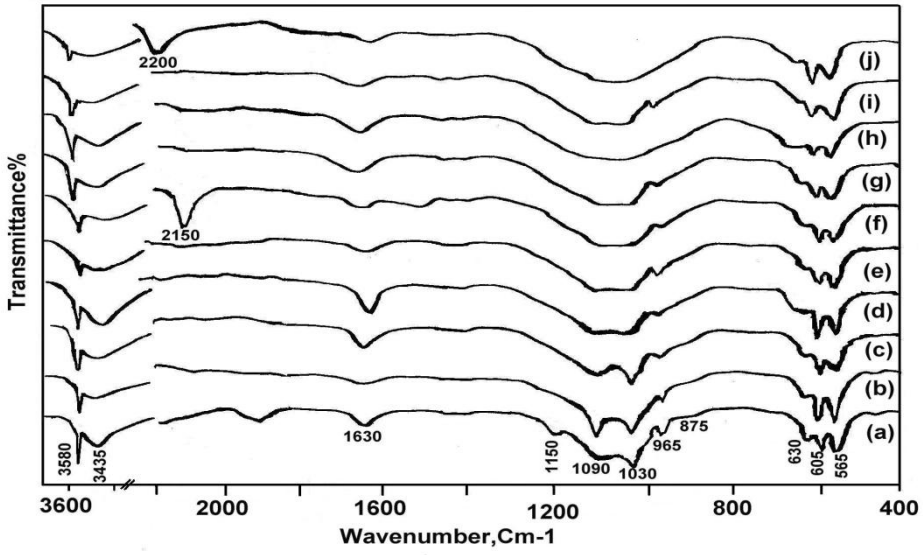

Fig. (3): FT-IR Spectrum for: (a) Hap (b) Calcined Hap (c) Prepared $ZnHap_{Im1}$ (d) Calcined $ZnHap_{Im1}$ (e) Prepared Zn Hap_{Im2} (f)Calcined $ZnHap_{Im2}$ (g) Prepared $ZnHap_{Ion1}$ (h) Calcined Zn Hap_{Ion1} (i) Prepared Zn Hap_{Ion2} (j) Calcined Zn Hap_{Ion2}

Experimental and numerical studies on the behavior of cylindrical and conical shells with varying thickness along the length subjected to axial compression

GJRE Classification (FOR)
GJRE: A, 091308

C Thinvongpituk[a]*, V Chomkwah[b]

Abstract-The behavior of aluminum cylindrical and conical shells of thickness variation along their lengths subjected to quasi-static axial compression was examined. The study was conducted using experimental and FE simulation approaches. The cylinders had mean radius of 25 mm, while the cones had smaller and larger radii of 15 mm and 35 mm respectively. Their thicknesses were increased linearly from top end to bottom end with the thickness ratio (TR) of 0.0, 0.1 and 0.2. The mean thicknesses of specimens were 1.0 mm, 1.5 mm and 2.0 mm. The numerical simulations on those experiments were also conducted using the finite element code, ABAQUS. The results from experiment and FEA simulation were compared and good agreement was achieved. It was found that the energy absorption capacity of cylinder with thickness varying along the length is increasing as the value of TR increases. In contrast, the cone with thickness varying along the length seems to lose its energy absorption capacity as the value of TR increases. In addition, their deformation histories and load-displacement curves were presented and discussed.

Keywords: Cylindrical shells; Conical shells; Energy absorption; Axial compression

I. Introduction

In the view of impact-prevention engineering, various shell structures are usually selected since they offer high energy absorption capacity compared to their own weight. Among several kinds of shell structures, cylindrical and conical shells have gained high interest since they are considered as the most effective energy absorber elements. Many attempts have been made to understand the collapse mechanism of those structures, and link to their energy absorption characteristics.In case of cylindrical shells, Pugsley and Macaulay [1] was one of the pioneer who studied the progressive collapse of cylindrical shells. The three and four-lobe modes were analyzed and assumed that no residual elastic strain energy was stored in the tube. The expression for the mean compressive load was derived. In the same year Alexander [2] also performed an analysis for the deformation of cylinders but focused on concertina mode. His model has been developed by many researchers such as Abramowicz and Jones [3, 4], Wierzbicki et al [5] and later by Singace et al [6, 7]. Experimental study on the collapse mode of cylindrical shells under axial compression was made by Singace and El-Sobky [8]. Effect of end-constraints on the collapse behavior was discussed. The progressive folding of cylindrical tube was investigated by Karagiozova et al [9, 10] using simulation technique. Their studies focused on the influence of inertia effect and impact velocity. They suggested that cylinder can absorb more energy by increasing the impact velocity and reducing the impact mass. Recently, Gupta and Venkatesh [11] performed a study on the crush characteristic of cylindrical shells by experiment and numerical simulation. The influence of diameter to thickness ratio (*D/t*) on the mode of collapse and energy absorption capacity was discussed as well as the static and dynamic responses. Focusing on conical shells, experimental and analytical studies on its' crush behaviors have also been developed for few decades. Some examples of these pioneers are Seid [12], Singer [13], Weingarten et al [14] and Esslinger and Geier [15]. Their studies focused on the stability of conical shell using different approaches. The energy absorption capacity and collapse mechanics of conical shells were investigated comprehensively by Mamalis et al [16, 17, 18, and 19]. Some analytical models for estimating the energy absorbed by the structure were proposed. Xue et al [20] used a plastic hinge line technique to calculate energy dissipating in a flat-topped cone during collapse process. The result provided an upper bound for the load displacement curve of the specimen. El-Sobky et al [21] also investigate the energy absorption capacity and collapse mode of cones, but focused on the effect of end condition. Modes of collapse were categorized in groups and were found to depend on geometric ratio parameters, i.e. radius-to-thickness ratio and length-to-thickness ratio. Recently Gupta et al [22, 23] conducted experiment and FE simulation on the crush characteristic of conical shells. Effect of geometrical parameters on the mode of collapse, load-deformation curve and energy absorption capacity were discussed. The comparison between the experimental and simulation result was made and good agreement was achieved. Although the behavior of cylindrical and conical shells subjected to axial compression has been studied extensively for several decades, the influence of thickness variation on the crush characteristic has not gained sufficiently attention. It is usually assumed that the thickness of shell is uniform and

About[1]-Mechanical Engineering, Ubon Ratchathani University,Warinchamrab, Ubon Ratchathani, Thailand, 34190 (email: chawalit@rocketmail.com)
About[2]- Mechanical Engineering, King Mongkut's University of Technology North Bangkok, Bang Sue, Bangkok

constant over the whole surface in order to simplify the problem. In fact, the thickness of shell is rarely constant. In addition, it may be necessary to use variable thickness shell for some applications such as joining two unequal thickness tubes. In this concern, there are some reports revealed the influence of the variable thickness on the buckling behavior of shells. Koiter et al [24] studied the stability of variable thickness cylinder and found that the buckling resistance capacity of cylinder is reduced as the thickness variable parameter increases. The effect of thickness variation and initial imperfection on the buckling behavior of composite cylinder was studied by Li et al [25, 26]. It was concluded that the load carrying capacity of composite cylinder is sensitive to thickness variation and especially sensitive to initial geometry imperfection. Recently, Aghajari et al [27] studied the buckling and post-buckling of cylindrical shells with varying thickness under external pressure. The study was conducted by experiment and finite element model. The result from experiment agreed well with the simulation. It also found that thickness variation has direct influence on the location of final waves in general buckling stage.

The present study was aimed to investigate the crush characteristic of cylindrical and conical shells with thickness variation along the length, subjected to axial compression. The study was conducted by experiment and finite element simulation. Their collapse progression, load-displacement curves and energy absorption capacities were presented.

II. Experimental Setup and Finite Element Modeling

The specimens were made from aluminum, fabricated by using EDM-wire cutting process in order to achieve precise thickness variation. Figure 1 illustrates the diagram of linearly variable thickness cylinder and cone used in the present study. The mean radius (R) of cylindrical shell was 25 mm while the top and bottom radii of conical shell were 15 mm and 35 mm respectively. The height of cone and cylinder were 90 mm. The mean thickness of shell was varied from 1.0, 1.5 and 2.0 mm.

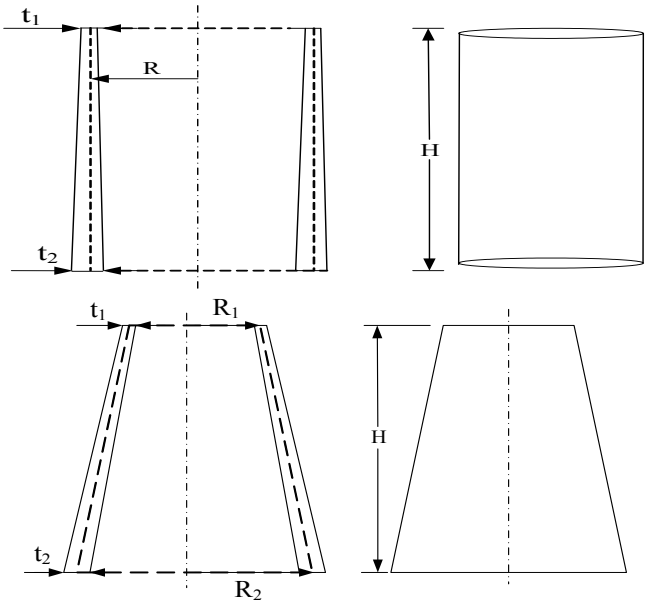

The local thickness of shell wall was increased linearly from minimum thickness (t_1) at the top end to maximum thickness (t_2) at the bottom end. The degree of thickness increasing gradient is called thickness ratio (TR) and is defined by equation (1).

$$TR = \frac{(t_2 - t_1)}{(t_2 + t_1)} \qquad (1)$$

The value of thickness ratio (TR) was varied from $TR = 0.0$ (constant thickness), $TR = 0.1$ and $TR = 0.2$. The geometric parameters of the cylindrical and conical shells are tabulated in Tables 1.

1 Dimensions of cylindrical and conical shells with thickness varying along the length

Minimum thickness (t_1, mm)	Maximum thickness (t_2, mm)	Mean thickness (mm)	Thickness ratio (ε)	Height (H, mm)
1.0	1.0	1.0	0.00	90
1.5	1.5	1.5	0.00	90
2.0	2.0	2.0	0.00	90
0.9	1.1	1.0	0.1	90
1.3	1.7	1.5	0.1	90
1.8	2.2	2.0	0.1	90
0.8	1.2	1.0	0.2	90
1.2	1.8	1.5	0.2	90
1.6	2.4	2.0	0.2	90

The specimens were quasi-statically crushed in axial direction using the universal testing machine.The crush speed was 5 mm/min and the specimens were tested under simply supported end condition. The progressive collapse of specimens was observed. Their load and displacement were recorded and plotted.

The general-purpose finite element program called ABAQUS was used to perform the simulation in this study. The three dimensional cylindrical and conical shells were modeled using S4R shell elements. The mechanical properties of specimens were determined by standard tensile test. The stress-strain behavior and other properties of the tested specimens were assigned in the FE model. The models were simulated to be crushed between two platens under the same condition as the experiment.

III. RESULT AND DISCUSSION

a) *Progressive collapse observation*

It is well known that the failure modes of structures provide useful information to understand their crush characteristics. Therefore, the deformation histories of cylindrical and conical shells were observed and the results are presented and discussed in this section. Figures 2-3 show the experimental and numerical results of the progressive folding of cylindrical shells under axial compression. It should be noted that the cylinder is generally failed in concertina mode or in multi-lobes mode, depending on their *D/t* and *L/D* ratios. In the present study, the geometric parameters of all specimens were in the rage to fail in concertina mode, followed Andrews's suggestion [28]. Therefore, all of them were collapsed in axisymmetric concertina mode, as expected. An example of progressive collapse of a cylinder with constant thickness ($TR = 0$) is shown in Figure 2.

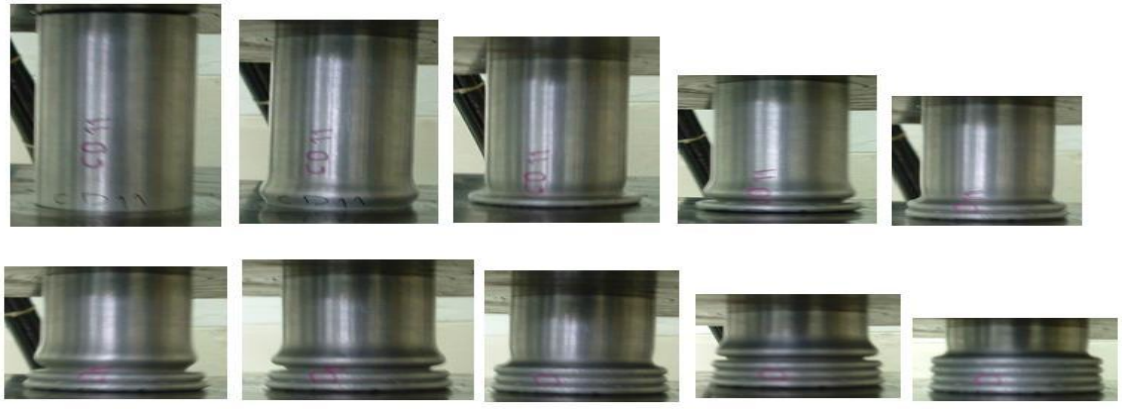

Fig.2.Typical deformation history of cylindrical shells under axial compression

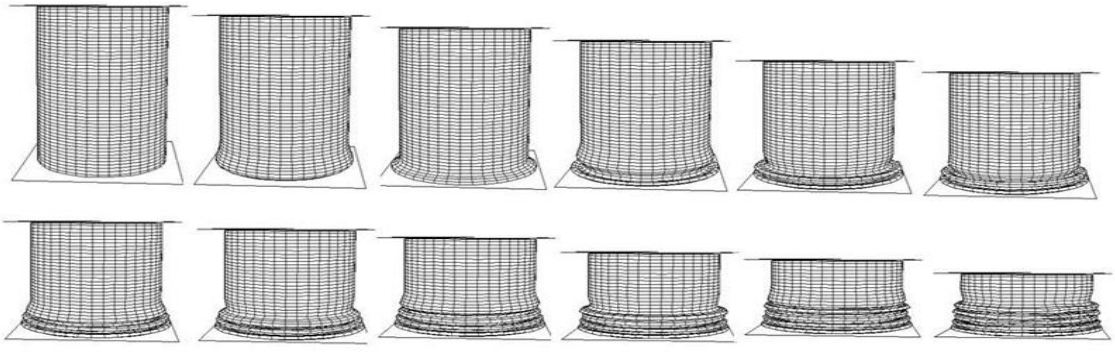

Fig. 3. The FE model of deformation history of cylindrical shells under axial compression.

Fig. 4. Typical deformed specimens (a) cylindrical shell with varying thickness along the length (b) conical shells with varying thickness along the length.

It is observed that the cylindrical shell starts to collapse by forming a first expanded axisymmetric ring near bottom end. As the first ring is completed, the cylinder continues to form other rings throughout the collapse process and finally ends up in a regular concertina mode. In cases of the cylindrical shells with thickness variation along the length ($TR \neq 0$), the collapse starts from the top end, where the wall is thinner, and progresses to bottom end. The collapse process is happened in similar manner as the progressive collapse of constant thickness cylinder, but the later rings are bigger than the former rings as can be observed from Figure 4 (a). This is because the wall thickness that is increasing as the collapse progresses downward along the length. The FE simulation of collapse history of the corresponding cylinder is shown in Figure 3. It is obviously seen that the collapse histories observed from experiment and from FE simulation are very similar. Good agreement between experiment and FE simulation was found for all tested cylindrical shells.

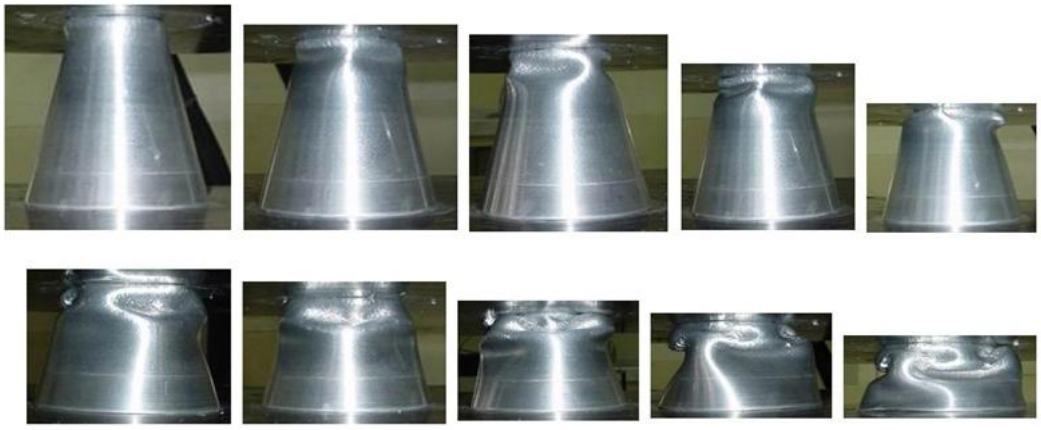

Fig. 5. Typical deformation history of conical shells under axial compression.

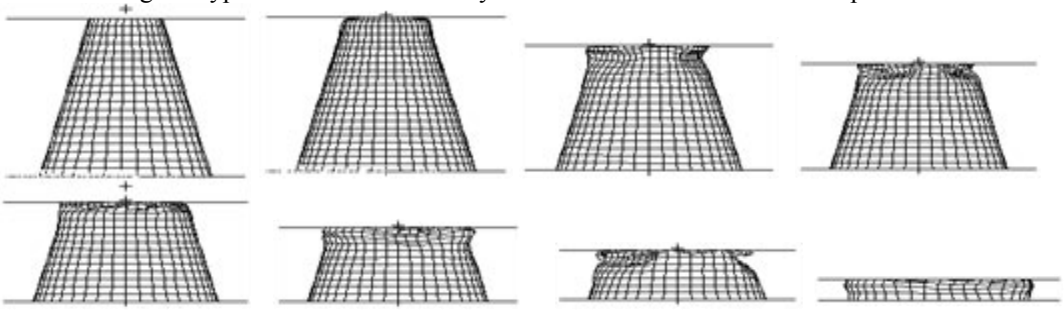

Fig. 6. The FE model of deformation history of conical shells under axial compression.

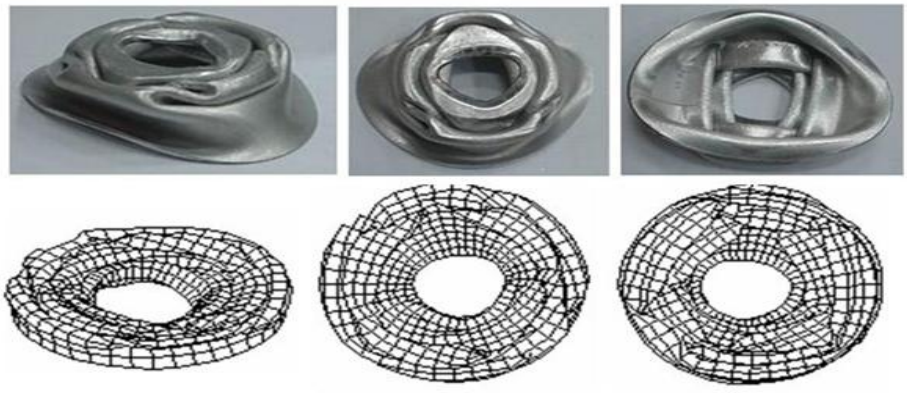

Fig. 7. The comparison of final collapse of conical shells achieved from experiment and FE model

An example of the folding process of constant thickness conical shell($TR = 0$) is presented in Figure 5. It is observed that the cone starts to collapse from the narrower end by bending the top edge inwards, forming an expanded ring near the top. As the collapse progresses downward, the

cross section of cone is increasing and the ring transfers to be a series of 3-lobes mode which piles on the following layers. The FE simulation also provides the same progressive collapse for conical shells, as shown in Figure 6. Figure 7 shows the comparison of terminal mode of collapse for cone achieved from experiment and FE simulation. Good agreement between them can be observed. In case of the conical shells with thickness variation along the length ($TR \neq 0$), the collapse is also processed in similar manner as the progressive collapse of constant thickness cone. An example of the final collapse of conical shells with thickness varying along the length is shown in Figure 4 (b) and it is found similar to the collapse mode of constant thickness cone but with the larger size of lobe

b) Load-displacement curves observations

As the conical and cylindrical shells were being crushed, the response force and corresponding displacement were recorded and then plotted. The typical experimental load-displacement curves of cylindrical and conical shells with thickness varying along their length are presented in Figure 8 and 9, respectively

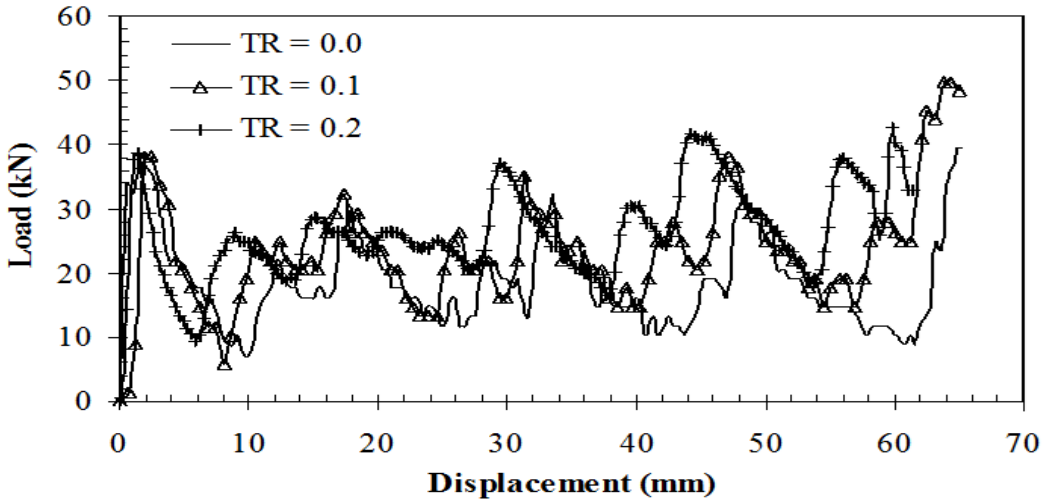

Fig. 8. The comparison of load-displacement curves of cylindrical shells having thickness variation with different values of tr

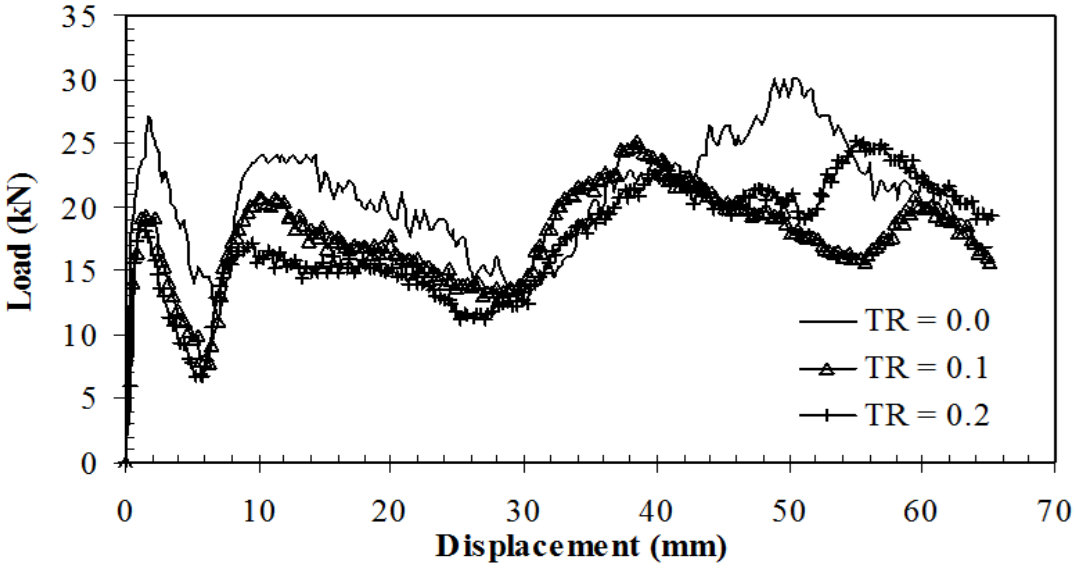

Fig. 9. The comparison of load-displacement curves of conical shells having thickness variation with different values of TR.

.

As can be seen from Figure 8 that the load-displacement curves of the cylindrical shells fluctuate in wavy shapes. Each wave in the curve is corresponding to each axisymmetric ring that formed in the collapse process. For cylindrical shells, they usually produce the first peak which is highest in the whole curve. The first peak corresponds to the onset of the first ring when the shell starts buckling. After the first peak, the load-displacement curve of constant thickness cylinder ($TR = 0$) fluctuates up and dawn in almost the same values. In contrast, the cylinders with varying thickness along the length ($TR = 0.1$ and $TR = 0.2$), they produce the load-displacement curves which are fluctuating higher as the collapse progresses. This implies that the cylindrical shells with thickness varying along the length may be able to absorb more energy as their failures progress. In addition, it is also observed that the load-displacement curve of the cylindrical shell with $TR = 0.2$ tends to lie above the curves of cylindrical shell with $TR = 0.1$ and above that of the cylindrical shell with $TR = 0.0$ (constant thickness), respectively. This may suggests that the cylindrical shells with thickness varying along the length may offer higher energy absorption capacity compared to constant thickness cylinders.In case of conical shells, see Figure 9, their load-displacement curves are also fluctuating in wavy shape but with less numbers of wave compared to the cylindrical shells. The first peak of the constant thickness conical shell ($TR = 0$) is highest compared to those of the conical shells of thickness variation with $TR = 0.1$ and $TR = 0.2$ respectively. This indicates that as the value of *TR* increases the first peak in the load-displacement curve of conical shells tends to be decreased. In addition, the load-displacement curve of the conical shell with $TR = 0.2$ tends to lie below the curves of conical shell with $TR = 0.1$ and that of the conical shell with $TR = 0.0$ (constant thickness), respectively. This is in contrast with the cylindrical shells, and implies that the conical shells with thickness varying along the length lose their energy absorption capacities as the value of *TR* increases

c) Energy absorption characteristic

The energy absorptions (E_a) of the cylindrical and conical shells were approximated by the area under their load-displacement curves. Therefore, the different patterns of the load-displacement curves yield different energy absorption values. In this study the energy absorption of each specimen was calculated and summarized in Table 2, compared to the results from FE simulations.

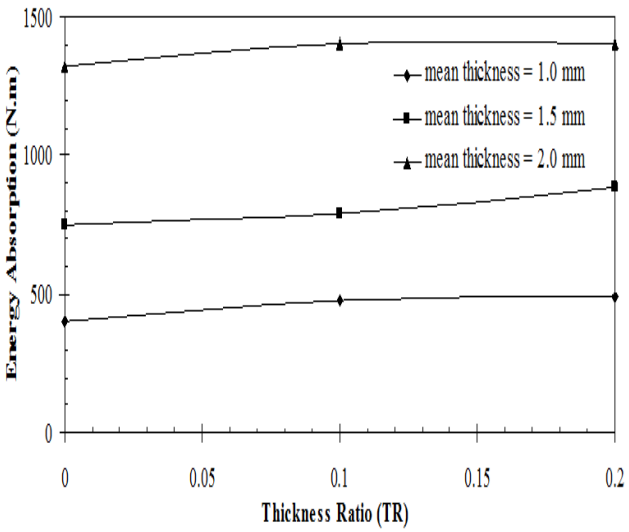

(a) Cylindrical shells with varying thickness along the length

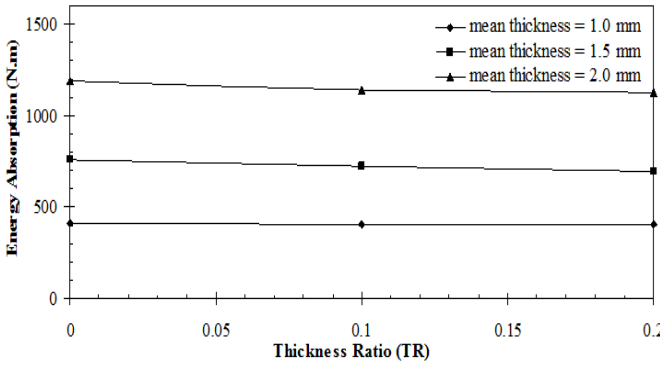

b) Conical shells with varying thickness along the length

as can be seen from the comparison in Table 2 that, in general, the FE simulation provides the prediction for energy absorption of each specimen with acceptable degree of error. In order to observe the tendency of the energy absorption capacities of the cylindrical and conical shells with thickness variation along the length, their experimental energy absorptions are plotted as shown in Figures 10 (a) and (b), respectively.

Table 2 Energy absorption values of cylindrical and conical shells with thickness varying along the length achieved from experiment compared to FE model.

Mean thickness	Thickness rati	Cylindrical shells			Conical shells		
(mm)	(*TR*)	FE Model	Experiment	Error (%)	FE Model	Experiment	Error (%)
1.00	0.00	405.24	401.23	0.99	377.40	412.34	-9.26
1.50	0.00	707.19	750.12	-6.07	775.19	760.56	1.89
2.00	0.00	1,226.10	1,321.55	-7.78	1,216.60	1,186.13	2.50
1.00	0.10	416.34	476.78	-14.52	368.19	401.24	-8.98
1.50	0.10	781.95	789.02	-0.90	774.90	720.34	7.04
2.00	0.10	1,353.65	1,401.23	-3.51	1,176.19	1,137.35	3.30
1.00	0.20	444.86	489.01	-9.92	358.79	401.20	-11.82
1.50	0.20	807.06	884.51	-9.60	752.82	695.98	7.55
2.00	0.20	1,385.22	1,404.31	-1.38	1,117.45	1,125.12	-0.69

Table 3Energy absorption increments of cylindrical and conical shells with thickness varying along the length.

Mean thickness (mm)	Thickness ratio parameter (*TR*)	Energy absorption increment (%)	
		Cylindrical shells	Conical shells
1.0	0.1	18.83	-2.69
1.0	0.2	21.88	-2.70
1.5	0.1	5.19	-5.29
1.5	0.2	17.92	-8.49
2.0	0.1	6.03	-4.11
2.0	0.2	6.26	-5.14

In case of cylindrical shells with varying thickness along the length (see Figure 10 (a)), their energy absorption capacities tend to increase as the value of *TR* is increasing. The increment of energy absorption of cylindrical shell with varying thickness along the length ($TR = 0.1$ and $TR = 0.2$ compared to the constant thickness cylindrical shell($TR = 0.0$) is shown in Table 3. It is observed that the cylindrical shells of 1 mm mean thickness can absorb more energy by 18.83% and 21.88% when their thicknesses are varied along the length with the value of *TR*=0.1 and *TR*=0.2, respectively. For the cylindrical shells with mean thickness of 1.5 mm, their energy absorptions are increased by 5.19% and 17.92% when the thicknesses are varied with *TR*=0.1 and

TR=0.2, respectively. For thicker cylindrical shells, mean thickness = 2 mm, the increments of energy absorptions due to thickness variation are smaller, which are about 6.03% and 6.26% with *TR*=0.1 and *TR*=0.2, respectively.The relationship between the energy absorption capacities and the thickness ratio parameters (*TR*) of conical shells with varying thickness along the length is shown in Figure 10 (b). In contrast with the cylinder, it is observed that the energy absorption capacity of cone is decreased as the value of *TR* is increasing. The data in Table 3 indicates that the conical shells of 1 mm mean thickness with varying thickness of *TR* = 0.1 and 0.2 lose their energy absorption capacity by about 2.7%. For the conical shells with mean thickness of 1.5 mm, their energy absorptions are reduced by 5.29% and 8.49% when the thickness is varied with *TR*=0.1 and *TR*=0.2, respectively. In case of conical shells with the mean thickness = 2 mm, their energy absorptions are reduced by 4.11% and 5.14% with *TR*=0.1 and *TR*=0.2, respectively.

IV. Conclusions and Remarks

This study has investigated the behavior of cylindrical and conical shells with thickness varying along the length. Their patterns of collapse were observed and found that the later folds are in slightly larger size than the previous folds. This is due to the thickness of wall that is increased downward along the length. In addition, the load-displacement curves of them were also investigated. It was observed that the load-displacement curves of cylindrical shells with varying thickness along the length tend to increase as the collapse progress. This indicates that the energy absorption capacity of varying thickness cylinder may be increased as the collapse progresses. Considering the energy absorption capacity, it was found that the cylindrical shells with thickness varying along their length can absorb more energy compared to constant thickness cylinder. In addition, their energy absorption capacities were observed to increase as the value to *TR* increased. However, this was in contrast for the conical shells. The energy absorption capacity of conical shells was found to decrease as the thickness varying along the length.

V. Acknowledgement

Authors wish to thank the Thailand Research Fund (TRF) for financial support to this research.

VI. Refferences

1) Pugsley A, Macaulay M. The large-scale crumpling of thin cylindrical columns. Quart J Mech and App Mech 1960;8(1):1-15.
2) Alexander JM. An approximate analysis of the collapse of thin cylindrical shells under axial loads. Quart J Mech and App Mech 1960;13:10-15.
3) Abramowicz W, Jones N. Dynamic axial crushing of circular tubes. Int J Impact Eng 1984;2:263-81.
4) Abramowicz W, Jones N. Dynamic progressive buckling of circular and square tubes. Int J Impact Eng 1986;4:243-70.
5) Wierzbicki T, Bhat SU, Abramowicz W, Brodikin D. A two folding element model of progressive crushing of tubes. Int J Solid Struct 1992;29(24):3269-88.
6) Singace AA, El-Sobky H, Reddy TY. On the eccentricity factor in the progressive crushing of tubes. Int J Solids Struct 1995;32(24):3585-602.
7) Singace AA, El-Sobky H. Further experimental investigation on the eccentricity factor in the progressive crushing tubes. Int J Solids Struct 1996;33(24):3517-38.
8) Singace AA, El-Sobky H. Influence of end radial constraints on the collapse of axially crushed tubes. Exper Mech 1998. p. 333-40.
9) Karagiozova D, Alves M, Jones N. Inertia effects in axisymetrically deformed cylindrical shells under axial impact. Int J Impact Eng 2000;24: 1083-115.
10) Karagiozova D, Jones N. Influence of stress waves on the dynamic progressive and dynamic plastic buckling of cylindrical shells. J Solids Struct 2001;38:6723-49.
11) Gupta NK, Venkatesh. A study of the influence of diameter and wall thickness of cylindrical tubes on their axial collapse. Thin Walled Struct 2006;44: 290-300.
12) Seide P. Axisymmetrical Buckling of circular cones under axial compression. Trans. ASME (J Appl. Mech) 1956. p. 625-8.
13) Singer J. Buckling of circular conical shells under axisymmetrical external pressure. J Mech Eng Sci 1961;3(4):330-9.
14) Weingarten VI, Morgan EJ, Seid P. Elastic stability of thin-walled cylindrical and conical shells under axial compression. AIAA 1965;3(3):500-5.
15) Esslinger M, Geier B. Buckling and postbuckling behaviour of conical shells subjected to axisymmetric loading and of cylinders subjected to bending. In: Koiter WT, Mikhalov BK, editors. Theory of Shells. Amsterdam: North Holland Publ, 1980. p. 263-88.
16) Mamalis AG, Johnson W. The quasi-static crumpling of thin-walled circular cylinder and frusta under axial compression. Int J Mech Sci 1983;25(9-10):713-32.
17) Mamalis AG, Johnson W, Viegelahn GL. The crumpling of steel thin-walled tubes and frusta under axial compression at elevated strain-rates: some experimental results. Int J Mech Sci 1984;26(11-12): 537-47.
18) Mamalis AG, Manolakos DE, Viegelahn GL, Vaxevanidis NM, Johnson W. On the inextensional axial collapse of thin PVC conical shells. Int J Mech Sci 1986;28(5):323-35.
19) Mamalis AG, Manolakos DE, Saigal S, Viegelahn G, Johnson W. Extensible plastic collapse of Thin-walled frusta as any absorbers. Int J Mech Sci 1986;28(4):219-29.

20) Xue P, Yu TX, Tao XM. Large deformation model of flat-topped conical shell under axial compression. Key Eng Materials 2000;177-180:745-50.
21) El-Sobky H, Singace AA, Petsios M. Mode of collapse and energy absorption characteristics of constrained frusta under axial impact loading. Int J Mech Sci 2000;43:743-57.
22) Gupta NK, Mohamed Sheriff N, Velmurugan R. A study on buckling of thin conical frusta under axial loads. Thin Walled Struct 2006;44:986-96.
23) Gupta NK, Venkatesh. Experimental and numerical studies of impact axial compression of thin-walled conical shells. Int J Impact Eng 2007;34: 708-20.
24) Koiter WT, Elishakov I, Lee YW, Starnes Jr. JH. Buckling of an axially compressed cylindrical shell of variable thickness. Int J Solid Struct 1994;31(6):797-805.
25) Li YW, Elishakov I, Starnes Jr. JH. Axial buckling of composite cylindrical shells with periodic thickness variation. Computers & Structures 1995;56(1):65-74.
26) Li YW, Elishakov I, Starnes Jr. JH, Bushnell D. Effect of the thickness variation and initial imperfection on buckling of composite cylindrical shells: asymptotic analysis and numerical results by BORSOR4 and PANDA2. Int J Solids Struct 1997;34(28):3755-67.
27) Aghajari S, Abedi K, Showkati H. Buckling and post-buckling behavior of thin-walled cylindrical steel shells with varying thickness subjected to uniform external pressure. Thin Walled Struct 2006;44:904-9.
28) Andrews KRF, England GL, Ghani E. Classification of the axial collapse of cylindrical tubes under quasi-static loading. Int J Mech Sci 1983;25:687-96.

A Novel Two Switches Based Dc-Dc Multilevel Voltage Multiplier

GJRE Classification (FOR)
GJRE: F, 090699

Julio C. Rosas-Caro, R. Salas-Cabrera, J. C. Mayo-Maldonado.

Abstract **– This paper proposes a novel dc-dc converter called the dc-dc multilevel voltage multiplier (mvm). In general, an nx mvm can be built by using two switches, 2n-2 diodes and 2n-2 capacitors, free of magnetic components. It is based on the multilevel converters principle and designed for unidirectional power transfer applications. Each device blocks one voltage level, therefore high voltage converters can be synthesized with low voltage devices. The main advantage of this topology is the reduced number of transistors and gate drives. Possible applications have a wide range from low power silicon-based voltage multipliers to medium power level dc links for multilevel inverters based distributed generation (dg) systems, where a capacitor's voltage balancing is a challenge for more than three levels. Experimental results prove the principle of such converters.Index terms – dc-dc converter, multilevel converter, voltage multiplier.**

I. INTRODUCTION

Multilevel converters have attracted interest in power conversion [1][8], being the main reason that the devices are exposed to low voltage stress, which means that high voltage converters can be developed using low voltage devices, which is important for high power applications [1][2]. Relative to conventional topologies, some additional advantages of multilevel converters are: (*i*) low harmonic distortion, (*ii*) low electromagnetic emission noise, (*iii*) low switching frequency, (*iv*) high efficiency, (*v*) able to operate without magnetic components [2][3][8]. Multilevel converters are one of the most important topics in power electronics, and industrial application research, the three main topologies are: (*i*) diode clamped, (*ii*) capacitor-clamped, and (*iii*) cascaded multi-cell. A generalized topology is proposed in [3], showing that all basic structures and new multilevel topologies can be derived from the generalized topology.It has been shown in [2] that in DC-DC applications the diode-clamped multilevel converter has a voltage capacitor‘s unbalance problem, because it cannot provide redundant switching states to control capacitors voltage, but the capacitor-clamped multilevel converter have been successfully used for DC-DC conversion in low power converters [2][5][6][10] and ultra low power silicon based converters [9] mainly as a voltage multiplier. Most of the multilevel converter applications are focused in high power motor drives, static VARs generation, and other utility applications [1][2][8]. They are also suitable for FACTS devices [4], low power DC-DC conversion, specially for automotive applications [6] [10], and renewable energy systems [4][5[7]. Initially proposed for DC-AC and AC-DC conversion, it has been shown in [2] that DC-DC converters generalized topology. They eliminate magnetic components, although they present drawbacks in the capacitor‘s voltage balancing, being this the main challenge.

About- Manuscript received July 14, 2010.

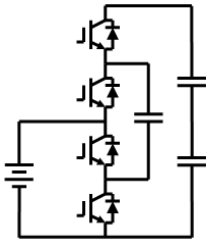

Fig. 1. Two-levels capacitor-clamped DC-DC multilevel converter.This paper proposes a new DC-DC converter, named *DC-DC Multilevel Voltage Multiplier* (MVM), based on two switches, 2N-2 diodes, and 2N-2 capacitors, for an Nx converter. It is a voltage multiplier able to maintain and balance the output voltage levels. The reduced number of switches saves valuable circuits in the gate drive. An additional advantage is that the number of levels can be increased by adding diodes and capacitors, and an entire converter can be built with several modules.This converter is based in the multilevel converters‘ principle; it is proposed for unidirectional power flow applications such as distributed generation to link the DC renewable energy system with a multilevel inverter, and ultra low power applications, such as silicon DC-DC-based converters, and for all applications where a voltage needs to be multiplied without magnetic components and several voltage levels need to be references to the same point. The topology is simulated and prototyped; experimental results are provided.

II. DC-DC MULTILEVEL VOLTAGE MULTIPLIER

Fig. 2 depicts the proposed topology, where the number of switches doesn‘t depend on the numbers of levels. To explain its operation principle, a 3x MVM is analyzed, simulated and prototyped.

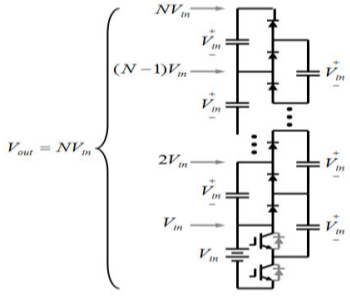

Fig. 2. Nx Multilevel Voltage Multiplier.

Fig. 3 shows the three-level MVM, based on four diodes, four capacitors, and two switches, implemented with IGBTs. The IGBT switches functioning in a complementary way, when switch S1 is turned on, switch S2 is turned off and vice versa with a fixed duty cycle of 0.5. The control is very simple, and it doesn't even need a microcontroller; an oscillator can provide the gate drive signals.

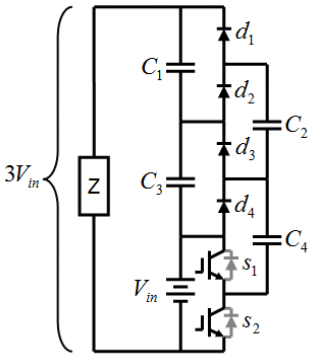

Fig. 3. 3x DC-DC Multilevel Voltage Multiplier.

The converter‘s operating principle is explained utilizing Fig. 3-5, where a duty cycle (D) equal to 0.5 is assumed. When S1 is *off* and S2 is *on*, C4 is charged to Vin, Fig. 4a. At the same time, C2 and C4 are connected to Vin and C3, Fig, 4b, while load is connected to Vin, C1, and C3, Fig. 4c. Then C4 is clamped to voltage Vin, and C2 is clamped to C3. Similarly, when S1 is *on* and S2 is *off*, C4 clamps to C3, Fig. 5a, and the voltage across C1 and C3 is clamped by the voltage across C2 and C4, Fig. 5b; the load Z is connected to Vin, C2, and C4, Fig. 5c. Thus, all capacitors are subjected to the same voltage Vin. From Fig. 4-5 all diodes and switches block just one voltage level, and a high voltage converter can be implemented with low voltage devices.

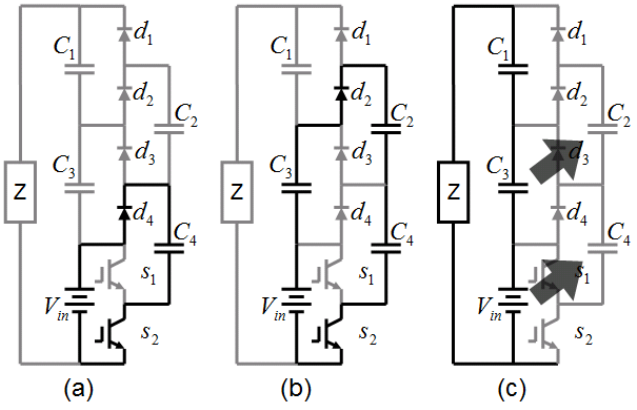

Fig. 4. S1 is *off* S2 is *on*.

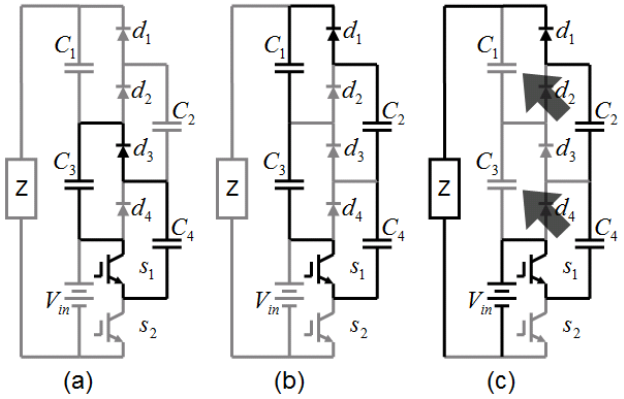

Fig. 5. S1 is *on* and S2 is *off*.

This strategy keeps all capacitors‘ voltage to Vin, and the number of gate drive circuits is limited to two. The number of levels can be increased in a modular way, adding diodes and capacitors, allowing a multistage structure. The self-balancing's voltage capacitor allows the MVM to feed neutral points multilevel inverters for more than three levels, where the neutral point topology cannot balance the capacitors' voltage by itself.

III. DIODE AND SWITCH VOLTAGE DROP LIMITATION

In actual implementations the switches' and diodes' voltage drop must be taken into account since it avoids capacitors to be charged to Vin, this effect is studied in the present section.The voltage drop in conventional IGBTs and power diodes are around 2 volts, and it can be ignored in medium and high power applications with several hundred volts, but in low voltage applications should be considered. For simplicity, the voltage drop in switches and diodes is assumed to be equal to Vd. From Fig. 4a and Fig 6 it can be seen that the actual voltage across C4 becomes:

$$V_{C4} = V_{in} - V_{switch} - V_{Diode} \qquad (1)$$

$$V_{C4} = V_{in} - 2V_d$$

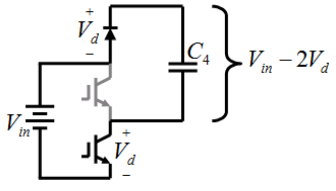

Fig. 6. Charging C4 with diode‘s and switch‘s voltage-drop.

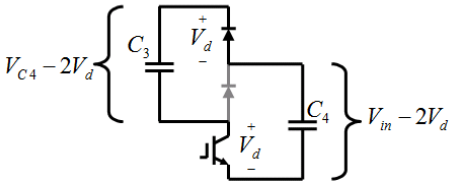

Fig. 7. Charging C3 with diode‘s and switch‘s voltage-drop.

From Fig. 5a, Fig 7, and (1), it can be written:

$$V_{C3} = V_{C4} - 2V_d = V_{in} - 4V_d \quad (2)$$

C2 is charged from Vin and C3 with C4 in series, as it is shown in Fig. 4b and Fig. 8. The voltage across C2 can be evaluated by:

$$V_{in} + V_{C3} - 2V_d = V_{C4} + V_{C2}$$
$$V_{in} + (V_{in} - 4V_d) - 2V_d = (V_{in} - 2V_d) + V_{C2}$$
$$V_{C2} = V_{in} - 4V_d \quad (3)$$

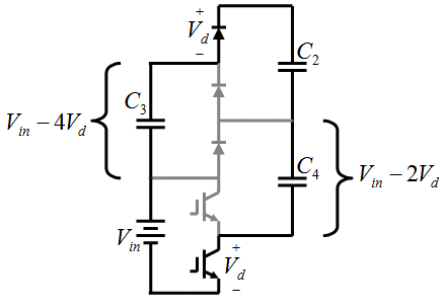

Fig.8. Charging C2 with diode‘s and switch‘s voltage-drop.

Likewise, C1 is charged in a similar way as it can be seen in Fig. 5b and Fig 9. Voltage across C1 can be expressed as:

$$V_{C4} + V_{C2} - 2V_d = V_{C3} + V_{C1}$$
$$(V_{in} - 2V_d) + (V_{in} - 4V_d) - 2V_d = (V_{in} - 4V_d) + V_{C1}$$
$$V_{C1} = V_{in} - 4V_d \quad (4)$$

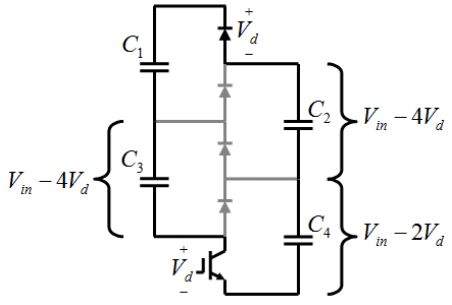

Fig.9. Charging C1 with diode‘s and switch‘s voltage-drop.

From (1)-(4), Fig. 3 becomes Fig 10, and the expression for the output voltage is as follows:

$$V_{out} = V_{in} - 8V_d \quad (5)$$

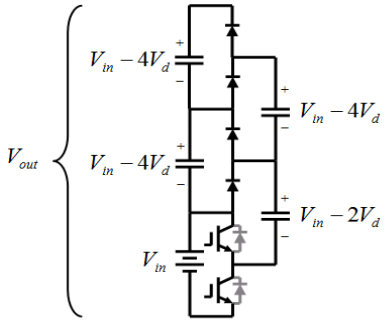

Fig.10. 3x MVM adding the diodes‘ and switches‘ voltage-drop.

Fig. 11 displays the equivalent to Fig. 2 including all the devices‘ forward voltage-drop. Finally, the general expression for the output voltage in an Nx multilevel voltage multiplier is shown in (6). This one must be considered to design an multilevel voltage multiplier:

$$V_{out} = NV_{in} - (N-1)4V_d \quad (6)$$

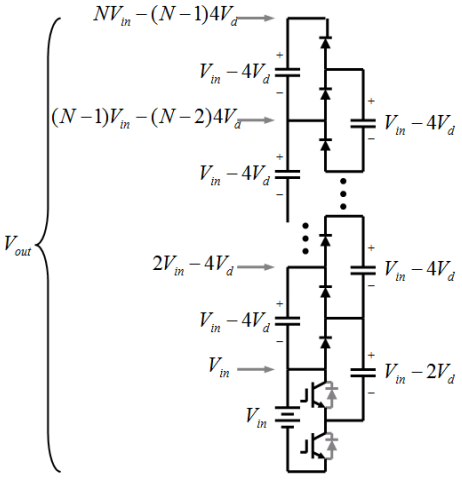

Fig.11. Nx MVM including diodes‘ and switches‘ voltage-drop.

The previous analysis indicates that the total output voltage is limited by the devices' forward voltage-drop, although the voltage capacitor keeps practically equal and constant, independent of the capacitor's level, except the lower one which exhibits a slight higher voltage. The load doesn't affect the multilevel operation, and all capacitors have a self-balanced voltage; this fact allows the MVM to feed multilevel inverters or loads with several voltage levels. A similar analysis can be done for all multilevel converters to get the actual output voltage taken into account the discrete devices' voltage-drop.

IV. Experimental Results

The circuit in Fig. 3 is simulated in ~~“~~*Saber*” and prototyped. Capacitors have a capacitance of C = 12000µF, Fig. 12.

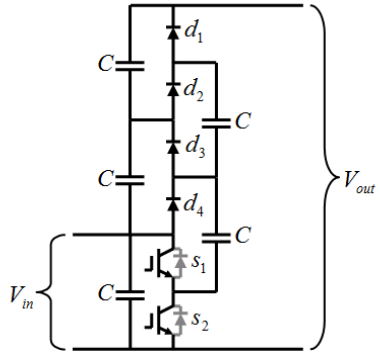

Fig. 12. MVM schematic prototype, C = 12000µF.

The two gate drive signals are provided by an eight bits Freescale microcontroller model MC68HC908QT4CP. Fig. 13 and Fig. 14 exhibit the test bench.

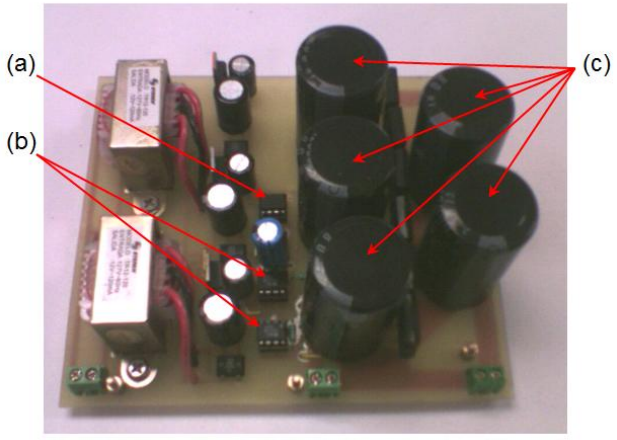

Fig. 13. (a) Microcontroller, (b) gate drives, (c) capacitors.

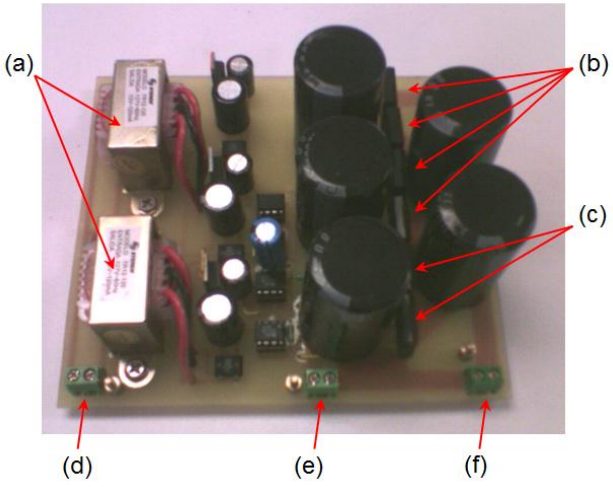

Fig. 14. (a) Isolated gate drives power supplies, (b) diodes, (c) IGBTs, (d) gate drives power input, (d) DC input voltage, (f) DC output voltage.

Fig. 15 illustrates the gate drive signals generated by the microcontroller at 5.7 kHz with a security dead-time.Several tests were done, Fig. 15-18 show the test waveforms. Fig. 15 shows the gate drive signals generated by the microcontroller, the duty cycle is 50%, and a dead-time was included. Fig. 16 displays the voltage across the lower device S2. Fig. 17-18 present the input and output voltage for two cases: (*i*) Vin = 20V, (*ii*) Vin = 30V.

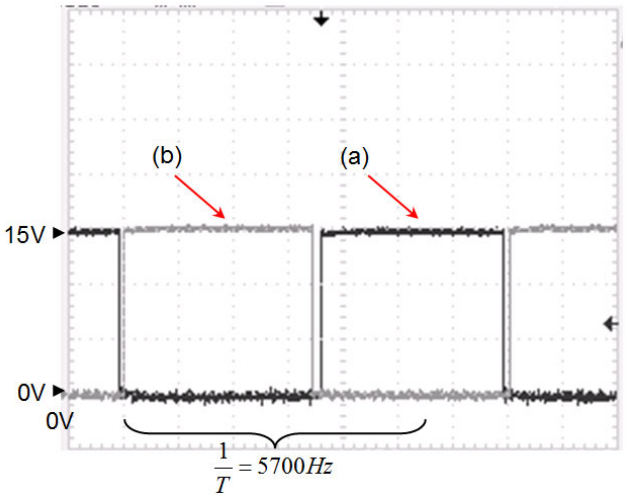

Fig. 15. (a) S1 gate signal, (b) S2 gate signals.

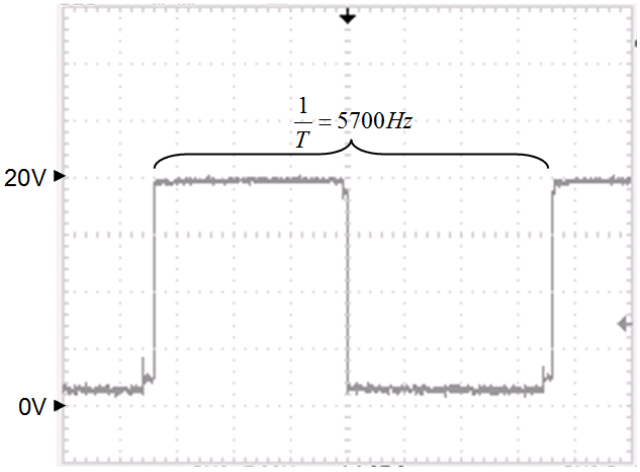

Fig.16. Voltage across S2 with an input voltage of 20V.

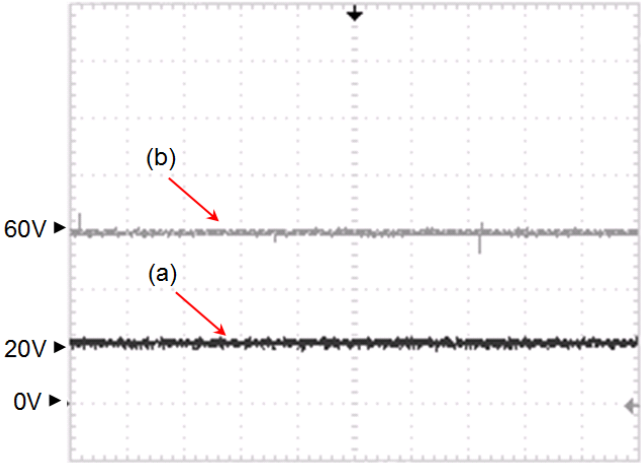

Fig. 17. (a) Input voltage, (b) output voltage.

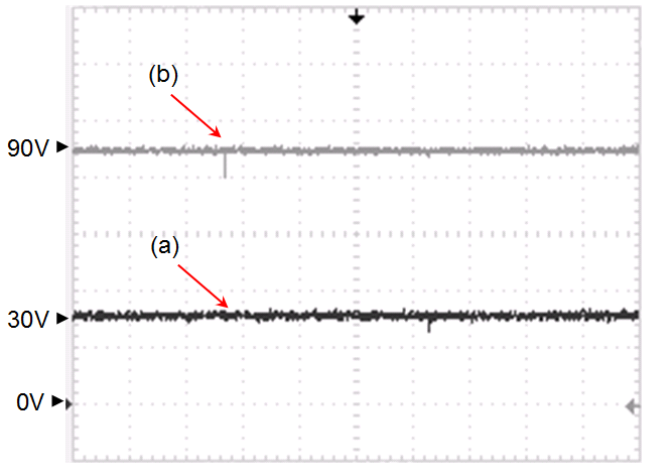

Fig. 18. (a) Input voltage, (b) output voltage.

V. Conclusion

A novel DC-DC Nx converter has been proposed, based on two switches, 2N-2 diodes and 2N-2 capacitor. It is a voltage multiplier able to maintain closely the same voltage level in all output levels. The effect of diodes' and switches' voltage-drop has been analyzed, and the output voltage expression has been corrected according to such analysis, which can be applied to all multilevel converters.The reduced number of switches saves valuable circuits in the gate drive, reducing the price in low power applications. The number of levels can be increased just adding diodes and capacitors achieving a modular topology. This converter is proposed for unidirectional power flow applications, such as distributed generation to link the DC renewable energy system with a multilevel inverter, or ultra low power application such as silicon based DC-DC converters, and for all applications where a DC voltage needs to be multiplied without magnetic components, the topology is simulated and prototyped; experimental results are provided.

VI. References

1) Rodriguez, J.; Jih-Sheng Lai; Fang Zheng Peng; Multilevel inverters: a survey of topologies, controls, and applications Industrial Electronics, IEEE Transactions on Volume 49, Issue 4, Aug. 2002 Page(s):724–738.
2) Fan Zhang; Peng, F.Z.; Zhaoming Qian; Study of the multilevel converters in DC-DC applications Power Electronics Specialists Conference, 2004. PESC 04. 2004 IEEE 35th Annual Volume 2, 20-25 June 2004 Page(s):1702 - 1706 Vol.2
3) Fang Zheng Peng; A generalized multilevel inverter topology with self voltage balancing Industry Applications, IEEE Transactions on Volume 37, Issue 2, March-April 2001 Page(s):611 – 618.
4) Tolbert, L.M.; Peng, F.Z.; Multilevel converters as a utility interface for renewable energy systems Power Engineering Society Summer Meeting, 2000. IEEE Volume 2, 16-20 July 2000 Page(s):1271-1274 vol. 2 .
5) Khan, F.H.; Tolbert, L.M.; A Multilevel Modular Capacitor-Clamped DC–DC Converter Industry Applications, IEEE Transactions on Volume 43, Issue 6, Nov.-dec. 2007 Page(s):1628 – 1638.
6) Fang Zheng Peng; Fan Zhang; Zhaoming Qian; A magnetic-less DC-DC converter for dual-voltage automotive systems Industry Applications, IEEE Transactions on Volume 39, Issue 2, March-April 2003 Page(s):511 – 518.
7) Walker, G.R.; Sernia, P.C.; Cascaded DC-DC converter connection of photovoltaic modules Power Electronics, IEEE Transactions on Volume 19, Issue 4, July 2004 Page(s):1130 – 1139.
8) Jih-Sheng Lai; Fang Zheng Peng; Multilevel converters-a new breed of power converters Industry Applications, IEEE Transactions on Volume 32, Issue 3, May-June 1996 Page(s):509 – 517.
9) Corona-Murguia, O.; Sandoval-Ibarra, F.; A Silicon-based Voltage Doubler: Preliminary Results Electrical and Electronics Engineering, 2006 3rd International Conference on Sept. 2006 Page(s):1 – 4.
10) Peng, F.Z.; Fan Zhang; Zhaoming Qian; A novel compact DC-DC converter for 42 V systems Power Electronics Specialist Conference, 2003. PESC '03. 2003 IEEE 34th Annual Volume 1, 15-19 June 2003 Page(s):33 - 38 vol.1.

Implementation of Quality Based Algorithm for Wimax Simulation Using SISO and SIMO Techniques

Bhavin S. Sedani [1] , Dr. G.R.Kulkarni[2]

***Abstract*-This paper presents the designing of more primitive algorithm of WiMAX (Worldwide Interoperability for Microwave Access) system simulation for lower Bit Error Rate Perspective. WiMAX is considered today the most interesting opportunity, able to provide radio coverage distances of almost 50 kilometers and data throughput up to 70 Mbps, and to complete wired network architectures, ensuring a flexible and cheap solution for the last-mile. In its mobile variant, WiMAX has the potential to replace cellular networks. In this way, the WiMAX may be seen as the fourth generation (4G) of mobile communications systems. The vital aspect of simulation of WiMAX system is to achieve the lower Bit Error Rates, higher Signal to Noise Ratio and there by higher system capacity.There is one fundamental aspects of wireless communication that make the problem challenging and interesting, that is the phenomenon of fading. The technique called diversity, can dramatically improve the performance over fading channels. The main objectie of this research paper is to achieve the greater reduction in bit error rate for wireless system by implementing antenna diversity principle like SIMO (Singe Input Multiple Outputs) and to compare the performance analysis of same.**

Keywords-AWGN, BER, SISO, SIMO and WiMAX

I. INTRODUCTION TO WIMAX

The experienced growth in the use of digital networks has led to the need for the design of new communication networks with higher capacity. The telecommunication industry is also changing, with a demand for a greater range of services, such as video conferences, or applications with multimedia contents. The increased reliance on computer networking and the Internet has resulted in a wider demand for connectivity to be provided "any where, any time", leading to a rise in the requirements for higher capacity and high reliability broadband wireless telecommunication systems. Wireless access to data networks is expected to be an area of rapid growth for mobile communication systems. The huge uptake rate of mobile phone technologies, WLANs and the exponential growth that is experiencing the use of the internet have resulted in an increased demand for new methods to obtain high capacity wireless networks. WiMAX methods to obtain high capacity wireless networks. WiMAX is considered today the most interesting opportunity, able to provide radio coverage distances of almost 50 kilometers and data trough-put up to 70 Mbps and to complete wired network architectures, ensuring a flexible and cheap solution for the last-mile. The interoperability is a very strategic issue, on which equipment cost and volume of sales will be based. Operators will not be bound to a unique equipment supplier, as the radio base stations will be able to interact with terminals produced by different suppliers. Operators can benefit of suppliers‘ competition in terms of costs and innovation. The existing technologies such as Wireless Fidelity (Wi-Fi), Digital Subscriber Line (DSL), Global System for Mobile communications (GSM), Integrated Services Digital Network (ISDN), and the relatively new 3G technologies have not been able to provide higher capacity along with high bit rate and wide coverage areas. WiMAX provides an appropriate solution to certain rural access zones that are today prevented from having access to broadband internet because of cost consideration.WiMAX has the potential to impact all forms of telecommunications. In a fixed wireless communication, WiMAX can replace the telephone company's copper wire networks, the cable TV's coaxial cable infrastructure while offering Internet Service Provider services. In its mobile variant, WiMAX has the potential to replace cellular networks. In this way, as shown in figure 1 the WiMAX may be seen as the fourth generation (4G) of mobile communications system as the convergence of cellular telephony, computing, internet access, and potentially many multimedia applications become a real fact. [4] In comparison with Wi-Fi and Cellular technology, Wi-Fi provides a high data rate, but only on a short range of distances and with a slow movement of the user. On the other hand, Cellular offers larger ranges and vehicular mobility, but instead, it provides lower data rates, and requires high investments for its deployment. WiMAX tries to balance this situation. WiMAX fills the gap between Wi-Fi and Cellular, thus providing vehicular mobility, and high service areas and data rates as shown in figure 2

About[1]-Kadi Sarva Vishwavidyalaya, Sector-15, NearKH - 5, Gandhinagar - 382 015.Gujarat – INDIA E-mail: bhavin_s_sedani@yahoo.com Ph: +91 9925041418

About[2]- Principal, C.U.Shah College of Engineering & Technology, Wadhwan - Gujarat, India E-mail: grkulkarni29264@rediffmail.com Ph: +91 9427665745

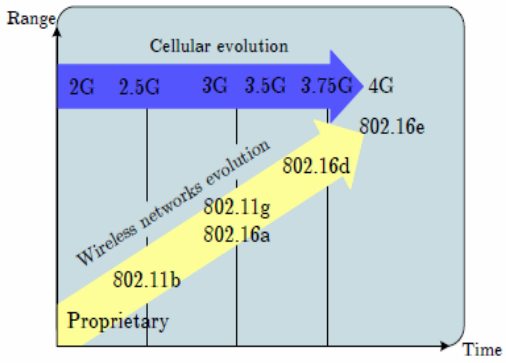

Figure 1 Cellular evolution Vs. Wireless network Evolution

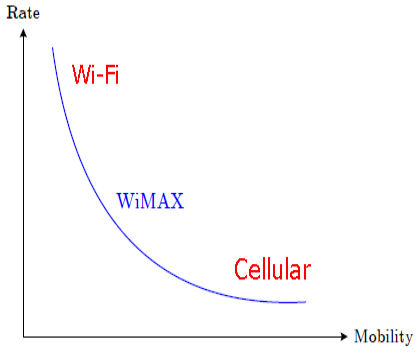

Figure 2 Data rate and Mobility

WiMAX is a standards based technology for wireless MANs conforming to parameters which enable interoperability. WiMAX developments have been moving forward at a rapid pace since the initial standardization efforts in IEEE 802.16. Standards for Fixed WiMAX (IEEE 802.16-2004) were announced as final in 2004, followed by Mobile WiMAX (IEEE 802.16e) in 2005. The WiMAX standards are mentioned in table 1.

WiMAX Standard	Definition Year	Frequency Band
802.16	2002	10-66 GHz
802.16(a)	2003	2-11 GHz
802.16(b)	2003	5-6GHz
802.16(c)	2003	10-66GHz
802.16(d)	2003	2-11GHz
802.16-2004	2004	2-66GHz
802.16(e)	2005	2-11GHz

Table 1 WiMAX Standards

In Europe, the standards for wireless MANs were formalized under the ETSI as HiperMANs. These were also based on IEEE 802.16 standards but did not initially use the same parameters (such as frequency or number of subcarriers). These were later harmonized with the WiMAX standards. The IEEE 802.16d standards provide for fixed and nomadic access, while the 802.16e standards also provide mobility up to speeds of 120 kilometers per hour.

II. Problem Domain

In 4G transmission system, link reliability and maximum data throughput is the need for transmitting real time data at high speed. However when the path is in a deep fade, any communication scheme will likely suffer from errors. The phenomenon of fading: that makes the time-variation of the channel strengths due to the small-scale effect of multi path fluctuation, as well as larger scale effects such as path loss via distance attenuation and shadowing by obstacles. Antenna diversity principle is one of the promising solutions for this. Traditionally the design of wireless systems has been focused on increasing the reliability of the air interface; in this context, fading and interference are viewed as nuisances that are to be countered. Recent focus has shifted more towards increasing the spectral efficiency; associated with this shift is a new point of view that **fading can be viewed as an opportunity** to be exploited. **The main objective of this work is to provide a unified treatment of wireless communication from both these points of view.** There are many ways to obtain diversity. Diversity over time can be obtained via coding and interleaving: information is coded and the coded symbols are dispersed over time in different coherence periods so that different parts of the code-words experience independent fades. Analogously, one can also exploit diversity over frequency if the channel is frequency-selective. In a channel with multiple transmit or receive antennas spaced sufficiently far enough, diversity can be obtained over space as well. In a 4G wireless network, macro-diversity can be exploited by the fact that the signal from a base station can be received by two receiving antennas at mobile station. This type of diversity is known as Single Input Multiple Outputs antenna diversity technique. Also diversity is such an important resource; a wireless system typically uses several types of diversity such as Multiple Inputs Single Output, Multiple Inputs Multiple Outputs etc.

III. Antenna Diversity Techniques

A natural solution to improve the performance of system in fading environment is to ensure that the information symbols pass through multiple signal paths, each of which fades independently, making sure that reliable communication is possible as long as one of the paths is strong. This technique is called **diversity**, and it can dramatically improve the performance over fading channels. Antenna diversity can be obtained by placing multiple antennas at the transmitter and/or the receiver

Single Input Single Output Antenna System (SISO)

The main fundamental behind advance antenna system implementation is the diversity. In the initially stages, the various modulation schemes like coherent BPSK, coherent

QPSK, coherent 4-PAM, coherent 16-QAM were in which error probability decay very slowly proportional to 1/SNR. [1]

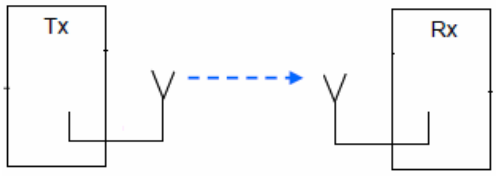

Figure 3 (a) Single Input Single Output Antenna System

Basically the above mention modulation techniques did not use diversity principle that is the single antenna system were used at transmitter and receiver in both the side as shown in figure 3 (a), anticipating lower poor spectral efficiency and lesser capacity. However in such a scenario, diversity can be obtained by implementing the OFDM technique i.e. frequency diversity during the transmission of symbols.

Single Input Multiple Output Antenna Diversity Technique

The first step toward using diversity is to use a single input multiple output configurations, e.g., one transmit and two receive antennas as shown in figure 3 (b). This configuration is called single input multiple output (SIMO). For example, a base station with one transmit and two receive antennas would be SIMO (1 X L system).

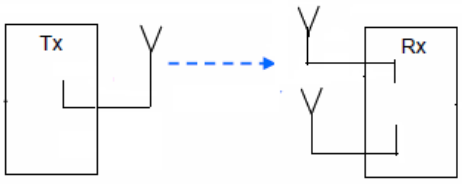

Figure 3 (b) Single Input Multiple Outputs Antenna System

In a flat fading channel with 1 transmit antenna and 2 (L) receive antennas, the channel model is as follows:
$y_l[m] = h_l[m]x[m] + w_l[m]$, Where $l = 1, \ldots, L$ The noise $w_l[m]$ independent across the antennas. We would like to detect $x[1]$ based on $y_1[1], \ldots, y_L[1]$. If the antennas are spaced sufficiently far apart, then we can assume that the gains $h_l[1]$ are independent Rayleigh, and we get a diversity gain of L.With receive diversity; there are actually two types of gain as we increase L. This can be seen by considering the expression for the error probability of BPSK conditioned on the channel gains: [1]

$$Q\left(\sqrt{2\|\mathbf{h}\|^2 \mathrm{SNR}}\right)$$

We can break up the total received SNR conditioned on the channel gains into a product of two terms:

$$\|\mathbf{h}\|^2 \mathrm{SNR} = L\mathrm{SNR} \cdot \frac{1}{L}\|\mathbf{h}\|^2$$

The first term corresponds to a power gain (also called array gain): by having multiple receive antennas and coherent combining at the receiver, the effective total received signal power increases linearly with L: doubling L yields a 3 dB power gain. The second term reflects the diversity gain and by averaging over multiple independent signal paths, the probability that the overall gain is small is decreased and BER is reduced. [1]

Muleiple Inputs Single Outputs Antenna Diversity Techniaue

The next step toward using diversity is to use a multiple input single output configurations, e.g., two transmit antennas and one receive antenna. This configuration is called multiple inputs single output (MISO) as shown in figure 3 (c). For example, a base station with two transmit and one receive antennas would be MISO (L X 1 system).

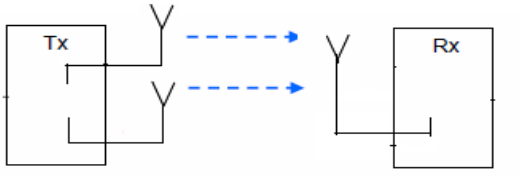

Figure 3 (c) Multiple Inputs Single Output Antenna System

Now consider the case when there are L transmits antennas and 1 receive antenna, the MISO channel. This is common in the downlink of a cellular system since it is often cheaper to have multiple antennas at the base station than to having multiple antennas at every handset. It is easy to get a diversity gain of L: simply transmit the same symbol over the L different antennas during L symbol times. Generally, any time block length L can be used on this transmit diversity system which simply use one antenna at a time and transmit the coded symbols of the time diversity code successively over the different antennas. This provides a coding gain over the repetition code. Coding scheme can also be designed for the transmit diversity system. Space Time Code is one of the most elegant, so-called Alamouti scheme. This is the transmit diversity scheme proposed in several third generation cellular standards.

Multiple Input Multiple Output Antenna Diversit Technique

MIMO involves the transmission of two streams using two or more than two spatially separated antennas. The streams are received at the receiver by using spatially separated antennas. The streams are then separated by using the space time processing, which forms the core of the MIMO technology as shown in figure 3 (d). A base station using two transmit antennas and two receive antennas is referred to as MIMO (n X n).

Figure 3 (d) Multiple Inputs Multiple Outputs Antenna System

In addition to provide diversity, MIMO channels also provide additional degree of freedom for communication. The main advantages of MIMO channels over SISO channels are the array gain, the diversity gain, and the multiplexing gain

IV. Implementation of Quality Based Algorithm for Wi-Max Simulation.

For the implementation of WiMAX simulation algorithm as shown in figure 4, MATLAB simulation is carried out strictly as per the IEEE standards 802.16d [8]. Also the resultant BER is calculated using WiMAX SISO (no diversity) and WIMAX SIMO (diversity method) techniques. Finally Comparative analysis is displayed for the performance evaluation of different WiMAX systems
Basically the simulation algorithm contains three major parts of WiMAX system.

1. Transmitter
2. Channel
3. Receiver

Users can input their own choice about the inclusion of diversity techniques by entering the number of receiving antennas i.e. 1 for SISO or 2 for SIMO. In the next step, rate_id and selection of cyclic prefix for Orthogonal Frequency Division Multiplexing Technique (OFDM) in the range of 1/4, 1/8, 1/16, 1/32 is defined as per IEEE standards 802.16. The BER performance is carried out with number of OFDM symbols for e.g. 50, 100,500, 1000, etc. User define input is required before the simulation process for the number of transmitting and receiving antennas i.e. the choice of diversity scheme.Randomly generated data stream by Pseudo Random Binary Sequence Generator is produced for the simulation process. FEC (Forward Error Correction) coding is applied to the randomized stream of data for coding Purpose. As an outer code Read Solomon coding is applied in the first phase for different rate_ids, using inbuilt function _RSENC' of MATLAB. The RS encoded data is applied to the convolutional coder for much transparency. Block interleaving is applied to the coded stream to protect the information from data loss errors.After that the modulation schemes like QPSK ¾ or 16 QAM ½ is applied to interleaved data. At last before the transmission of symbols through the wireless Additive channel, IFFT is performed on the stream to realize OFDM.

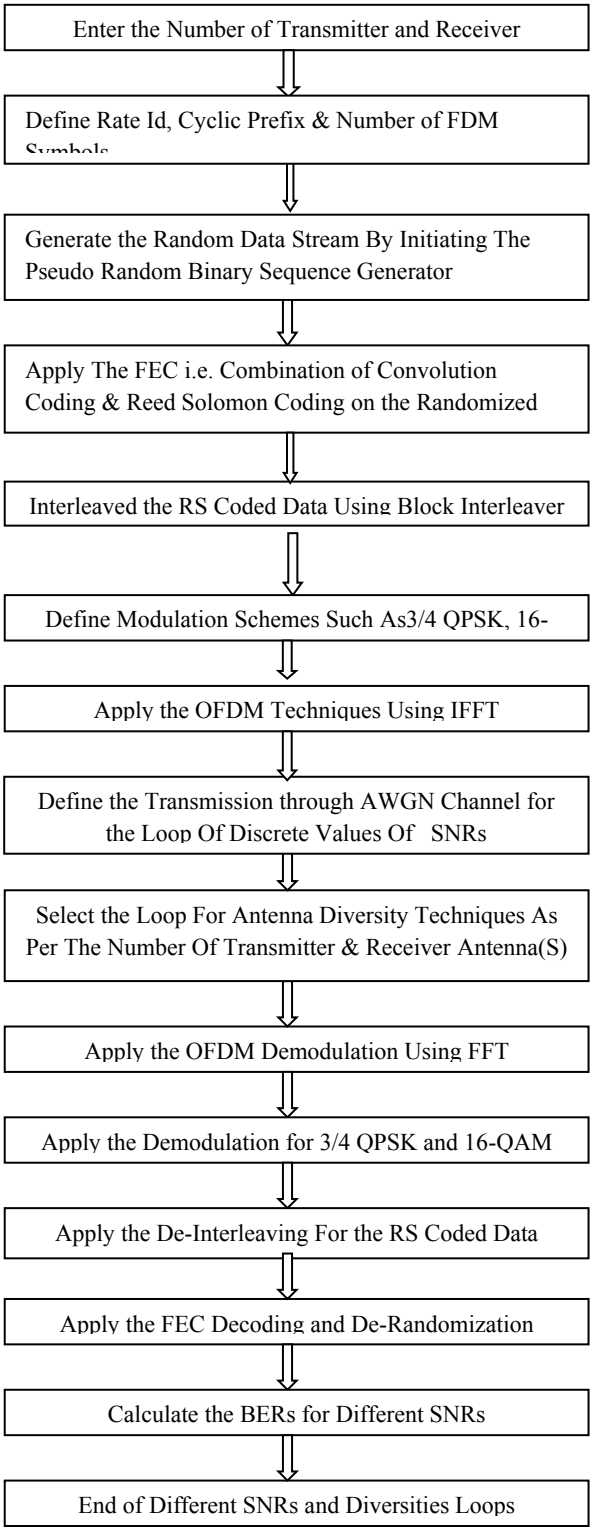

Figure 4 WiMAX Simulation Algorithm

In the next phase, AWGN (Additive White Gaussian Noise Channel) channel is defined as per the type of diversity scheme.For SISO scheme, single AWGN channel between one transmitting antenna and one receiving antenna is realized. For SIMO diversity technique, single AWGN channel and two noise matrixes are defined between one Transmitting antenna and two receiving antennas.At

receiving side, OFDM demodulation is carried out by taking FFT of the received data frame. After that the Demodulation and De-interleaving of the frequency domain symbols is carried out. At last FEC de-coding is performed to rearrange the data stream to the original fashion.In the final phase of simulation, the decoded data stream of last step will be compared with Original randomized data stream of the transmitter side and BER will be calculated by inbuilt MATLAB function _BITERR'. Also simulation graphs are plotted for SNRs v/s BER.

V. Simulation Results

The BER v/s SNR relationship for the WiMAX system with the Single Input Single Output Antenna technique is shown in figure 5 with the value of cyclic prefix = ¼ and QPSK ¾ as the modulation scheme.As can be seen from graph, in case of no diversity, i.e. using single transmitting and single receiving antenna, initially the BER can be obtained around **0.48** and at higher value of SNR, the achievable BER decreases around **0.009 for 8 dB SNR**. Also the values of BER are high as there is no implementation of numbers of antennas in either transmitter or receiver side and throughput of the system totally depends on the channel SNR.

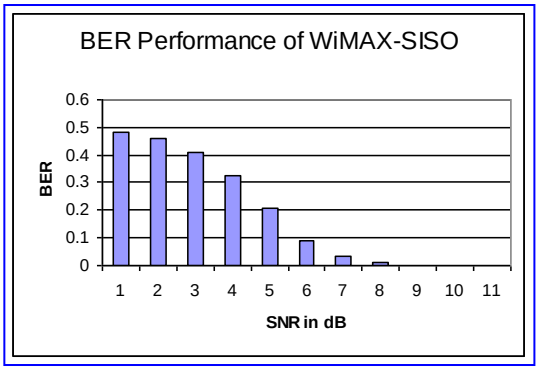

Figure 5 BER Performance of Single Input Single Output Antenna System

The BER v/s SNR relationship for the WiMAX system with the Single Input Multiple Output Antenna system is shown in figure-6 with the value of cyclic prefix = ¼ QPSK ¾ as the modulation scheme.

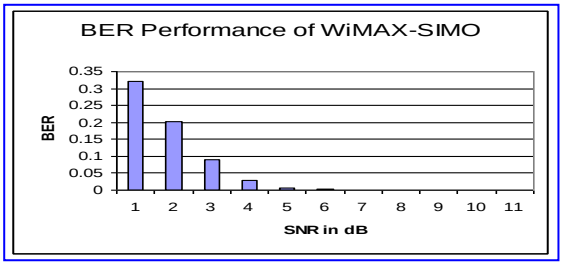

Figure 6 BER Performance of Single Input Multiple Outputs Antenna Diversity Technique

As can be seen from the graph, in case of receive diversity, i.e. using single transmitting and two receiving antennas, initially the BER can be obtained around 0.322 and at higher value of SNR, the achievable BER decreases around 0.00018 for 8 dB SNR.

Comparative Analysis

From the comparison of simulation results of WiMAX SISO and WiMAX SIMO, it can be observed that with the implementation of receiving diversity (SIMO), BER performance is improved compared to SISO antenna system. It is due to the fact that by averaging over multiple independent signal paths, the probability of error is decreased and BER is reduced for the same value of SNR. In this way, by using SIMO diversity technique, **the received signal quality gets enhanced by averaging over multiple independent signals.**

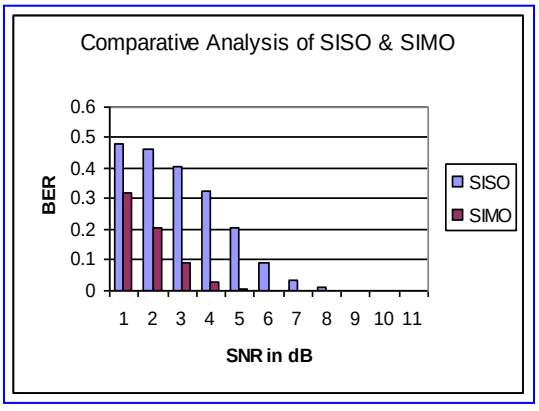

Figure 7 Comparisons between WiMAX SISO and WIMAX SIMO

VI. Simulation Results of Variation in Modulation Order

Figure 8 shows the BER performance of WiMAX system for 16-QAM ½ with cyclic prefix ¼. It can be observed that by changing the order of modulation scheme, the BER of the system is also affected. As the modulation order M increases, the BER of the system also increases.

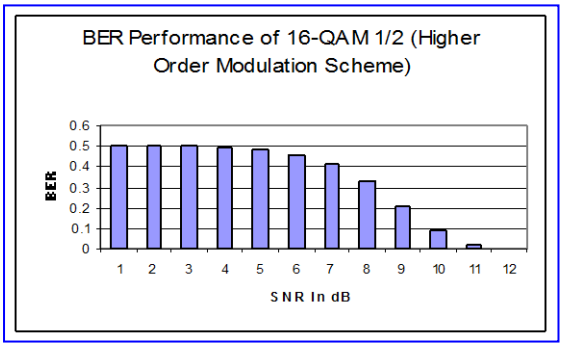

Figure 8 Effect of variation in modulation order

This is due to the fact that for fixed number of transmitting and receiving antennas, as the modulation order increases

i.e. in turn the no. of bits per symbol increases for that modulation scheme, due to the variation in their spatial position as well overlapping, the loss of bits will be encountered which is the main cause behind the degradation of BER. The degradation of BER can be more specifically observed by analyzing the comparison of BER performance of QPSK ¾ Vs. 16 QAM ½. The comparative analysis is shown in figure 9.

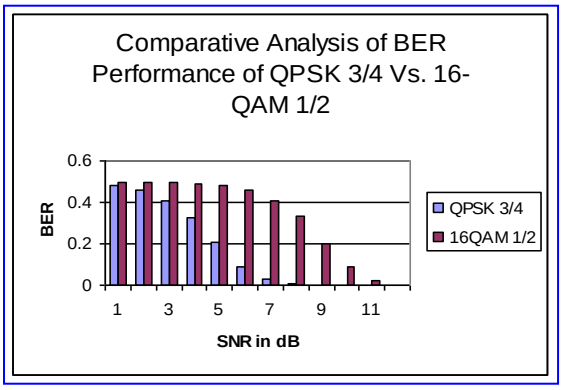

Figure 9 Comparative analysis of QPSK ¾ Vs. QAM ½

When the lower order modulation scheme QPSK ¾ has been applied, the BER is approximately 0.2048 at 5dB SNR and which is quite lower as compared to higher order modulation 16 QAM ½ for which BER = 0.4817 at the same value of 5dB SNR. In this way, it can be concluded that the diversity technique with lower order modulation also give the excellent throughput of the system. However when the order of modulation is low, it also causes the degradation in the data rates of the systems. So there is always trade-off in the selection of order of modulation and in practice, it totally depends on the application.

VII. Conclusion

WiMAX may be seen as the fourth generation of mobile communications systems as WiMAX is an evolving wireless networking standard for point to multipoint wireless networking which works for the _lastmile' connections. The key problem with the wireless channels is impairment of the channel by fading and interference. The major goal of this research paper is to develop the quality based algorithm for WiMAX system in antenna diversity environment for lower BER Perspective. Conventional single-antenna transmission techniques aiming at an optimal wireless system performance operate in the time domain and/or in the frequency domain. In particular, channel coding is typically employed, so as to overcome the detrimental effects of multipath fading. However, with regard to the ever-growing demands of wireless services, the time is now ripe for evolving the antenna part of the 4G radio system. In fact, when utilizing multiple antennas, the unused spatial domain can be exploited.Simulation of WiMAX along with the implementation of Antenna Diversity Technique (SIMO) achieves the drastic improvement in performance regarding to Bit Error Rates as compared to conventional antenna system. (SISO). For SISO WiMAX system, the attainable BER is 0.407 at 3dB SNR while for SIMO WiMAX system, the achievable BER is 0.089 at same value of SNR. Hence by averaging over multiple independent signal paths, the probability that the overall gain is small is decreased and BER of the system is enhanced.Also it can be observed that by increasing the modulation order M, BER of the system also increases for the same value of SNR. When the lower order modulation scheme has been applied, the BER is approximately 0.2048 at 5dB SNR, while for the higher order modulation scheme, BER = 0.4817 for the same value of SNR.More specifically, this paper examines the simulation of WiMAX system in antenna diversity environment on the platform of MATLAB 2007a.

VIII. Future Enhancement

In this research paper, the performance analysis and simulation results are presented using SIMO diversity technique. However in future a quality based algorithm can be implemented using MISO (Multiple Input Single Output) and MIMO (Multiple Input Multiple Output) diversity techniques for better system throughput. In such a case, two efficient wireless channels must be defined for the transmission of two independent information signals through two transmitting antennas. With MISO diversity technique, two independent channels are defined, signal fades independently; making sure that reliable communication is possible as long as one of the paths is strong and received signal quality will get enhanced

Also with the implementation of transmit diversity and received diversity i.e. MIMI, the lowest BERs can be achieved and performance can be dramatically improved compared to other system. It is due to the fact that MIMO technique exploits the advantages of MISO and SIMO diversity techniques.

IX. References

1) David Tse, University of California, Berkeley Pramod Viswanath, Fundamental of Wireless Communication,published by Cambridge University Press, 2004
2) H. Farhat, G. Grunfelder, A. Carcelen and G. El Zein," MIMO Channel Sounderat 3.5 GHz: Application to WiMAX System",JOURNAL COMMUNICATIONS, VOL. 3, NO. 5, OCTOBER 2008
3) Jelena Mi¡si and Vojislav B. Misic, Wireless Personal Area Networks Performance,Interconnections and Security with IEEE 802.15., John Wiley & Sons, Ltd
4) Amitabh Kumar, —Mobile Broadcasting with WiMAX: Principles, Technology, and Applications", Focal Press Media Technology Professional Elsevier-2008
5) Abdulrahman Yarali and Saifur Rahman,—WiMAX Broadband Wireless Access Technology: Services,

Architecture and Deployment Models", IEEE Transaction.

6) Hui Liu Guoqing Li ―OFDM-BasedBroadband Wireless Networks Design and Optimization", A John Wiley & Sons, Mc., Publication, 2005
7) Jelena Mi¡si and Vojislav B. Misic, ―Wireless Personal Area Networks Performance", Interconnections and Security with IEEE 802.15., John Wiley & Sons, Ltd.
8) 802.16™, IEEE Standard for Local and metropolitan area networks, Part 16: Air Interface for Fixed Broadband Wireless Access Systems, IEEE Computer Society and the IEEE Microwave Theory and Techniques Society.
9) Onsy Abdel Alim, Hiba S. Abdallah and Azza M. Elaskary. ―Simulation of WiMAX Systems", *IEEE Transaction.*

Converting Cassava (*Manihot spp)* Waste from Gari Processing Industry to Energy and Bio-Fertilizer

GJRE Classification (FOR)
GJRE: G, 1003

J.I. Eze

Abstract: **The high COD values associated with indiscriminate discharging of cassava peels and effluents during cassava processing to gari was studied. To challenge this problem, a 500-litre capacity batch-operated metal biogas digester was designed and constructed. Cassava roots were harvested, peeled and the pulp fermented for 4 days at ambient conditions. The resultant unwanted liquid and cassava peels were used to charge the biogas digester at a ratio of 3:1 (i.e. liquid waste to cassava peels) and allowed to ferment for 21 days. During the fermentation period, rate of biogas generation, pH of the digesting medium, both total and volatile solids were monitored using appropriate standard laboratory methods while the odour levels of the garri processing site was by sensory evaluation and stastical analyses. The fertility status of the biogas slurry was assessed by evaluating the percentage of the ammonium-nitrogen, potassium, and phosphorous contents both before and after fermentation. Results obtained show generation of a combustible gas (biogas) after 3 days of charging. A rich bio-fertilizer and a significant reduction of odour level within the gari processing vicinity (P<0.05) were also recorded.**

Keywords: Biogas, gari, acidogenes, methanogenes and cyanogenic glucoside

I. Introduction

Cassava (manihot spp) is one of the most staple roots that is being consumed in the different forms in Nigeria and other African countries. In Nigeria it is consumed either as foo foo or processed into garri. The technology of processing cassava roots into gari involves essentially, peeling, grating, fermenting, de-watering and frying. Basic processes such as soaking, grating and fermatation, increase qualities of cyanogenic glycosides and cassava waste products lost into the wash water used. This wash water that that has been reported to contain high BOD oncentration, can not be discharged directly into the environment; they need to be treated biologically before discharging (Chittendum, et. all, 1980).

Anaerobic digestion of the cassava waste water is an eco-friendly technology that can not only stabilize the cassava waste water but also produces biogas as an alternative to fuel wood needed for the light roasting of the mashed pulp in shallow metal vats placed on fire.

About: National Centre for Energy Research and Development (NCERD) University of Nigeria, Nsukka. Enugu State, Nigeria.
E-mail: ikejon55@yahoo.com
Phone : +2348063285864

The detoxified cassava waste water can also be used to supplement other local feed ingredients for animal production (Tewe, 2008). Besides the energy value of this conversion the pollution potential of the cassava waste water is also minimized within the environment this research was therefore, undertaken to scientifically explore the possible application of biological degradation of gari processing wastes in solving the energy and environmental pollution of garri processing sites in Nsukka, Nigeria. However, the specific objectives of this research include:

To assess odour level of the environment where garri is being processed and produced, before and after a production batch.

To assess the impart of cyanogenic glucoside in biogas generation from cassava-based wastes.

To evaluate the fertilizing value of the cassava digested slurry.

II. Literature Review

Reported study by Okoro (1986) and Okafor (1994) confirmed that in Nigeria, more than 60% of the rural population is engaged in cassava-based cottage industries. Millions of tons of this waste water from such industries cause environmental pollution. These wastes need to be managed and utilized in environmentally before final disposal. Anaerobic degradation of these complex materials to biogas and other by products of low molecular weight is eco-friendly technology. In the process, these complex wastes are degraded in the first instance, by the acid-forming bacteria that convert the waste to compounds of low molecular weight fatty acids. These are later converted in the second stage by methane-forming bacteria to biogas (methane), carbon dioxide and other products.

The biogas produced has wide range of applications including its use for lighting, driving automobiles, powering farm machinery heating, cooking. The successful operation of a digester relies on the correct balance between the acidogenic and methanogenic bacteria in the system and this occurs within a pH range of 6.5-7.6 ().The p.H is considered by the carbon dioxide/ bicarbonate buffer system; the bicarbonate being in equilibrium with ammonia generated from nitrogenous materials present in the waste.

The anaerobic digester effluent from the biomethanization process is commonly used as a liquid fertilizer. However, land applying anaerobic digester effluents often creates serious environmental problems. For instance, limitation of

farm lands can cause excessive accumulation of nutrients and the odour often bothers neighbouring residents as people expending into rural areas from crowded cities. Additionally, runoff after heavy rainfalls or storms can cause entrophication and pollution when these nutrients are carried to the run place or ground water (Filmax 2009).

III. Materials and Methods

A 500litre (0.5m3) capacity batch-operated metal biogas digester was designed and constructed at our mechanical workshop using a 2mm thick mild stainless steel metal. The inlet and outlet pipes are all made of metal. A 1mm rubber hose served as the biogas conveying system from the digester of the biogas burner or gas cylinder depending on the need. A 3/8 rod was used to construct the stirrer (Fig.1). Special rubber flanges were used to ensure leak-free joints during the coupling of the various digester components. There are two control values to regulate the flow of gas to the burner; one is located at the beginning of the joint between the top of the digester and the gas conveying-hose while the other valve is connected to the biogas burner. At the lower part of the digester, a circular slurry outlet that is closed with a thread plug for discharging off the slurry, is incorporated. This slurry outlet also serves as the sampling port for the collection of the digesting waste for intermittent analysis.

The wastes for charging the digester were cassava peels. The cassava roots were manually peeled with a knife to expose the pulp, washed in clean water and they were grated in a lister (6 AP) engine-powered grating machine made for that purpose. It was packed in jute bags and de-watered using local fabricating mechanical press. Pressure was applied to express the unwanted liquid from the mashed cassava pulp by tightening two big nuts fitted to the pressing machine. The cassava pulp was then left to ferment for four days at ambient conditions with occasional application of pressure to squeeze out unwanted fluid. It was this fluid (effluent) which has earlier been reported to contain high strength process effluent, with various COD values that was mixed with the cassava peels at a ratio of 2:1 (effluent to cassava peels) and used to charge the digester. The charged digester was monitored on daily basis with the following parameters:

1) Gas production rate was assessed by downward displacement of water using a 25l transparent and calibrated plastic gallon
2) The temperature of the experimental location was monitored with a thermometer while that of the digester slurry was recorded with a thermocouple.
3) The pH of the slurry was monitored with a Jeanway3020 pH meter and pressure was with a manometer.

The total solid and volatile acid contents were determined in the laboratory by standard methods as recorded by (Maynell, 1982).

1) Presence of hydrogen cyanide in biogas was determined by using draeger tubes sensitive in the range of 0-30ppm.
2) The fertilizing value of biogas slurry was through appropriate chemical analyses of the percentage of potassium (K), phosphorus (P) and nitrogen (N) of the wastes before and after fermentation, as recorded in AOAC (1990).
3) The odour level in the gari processing site was evaluated through interviews of some neighbours living at least 50meters away from the gari processing vicinity. A 7-point Hedonic scale sensory (odour/flavour) was also used to assess this parameter.

Plate 1: The Biogas Digester used For Experiment

IV. Results and Discussion

The results of some of the parameters such as Total solids and pressure measured during the period are presented in Table 1 while that of the digester and ambient temperatures are presented in Fig 2 respectively.. The maximum and minimum daily temperatures recorded were 36^{0}C and 26^{0}C respectively (Fig. 2). The optimum operating temperature range was 30 – 35^{0}C. Below 30^{0}C, digestion proceeded more slowly. Lower temperatures appeared to favour acid-forming bacteria and the system became more susceptible to a reduction in pH (Fig 4). There was no defined pattern of pressure change during the period. The internal pressure reached a maximum of 55 cm SWG*. This was evident when gas evolution was rapid and the internal pressure exceeded 50 cm SWG; causing effluent overflow and a great leak of biogas from an air-tight gas tank of the digester.

Gas production rate with daily temperature cycling of the system was observed to vary linearly with temperature (Fig. 3). This could be as a result of a combination of factors, improved mixing by convection, increased bacterial activity and degassing. The temperature differential between the ambient and digester temperatures was about ±2^{0}C and both were also observed to be linearly related.

* = Standard Water Gauge

Table 1: Changes in the digester pressure and total solids during fermentation

Times(days)	Pressure	TS(%)	Times(days)	Pressure	TS(%)
1	0.0	4.20	11	40.10	2.61
2	28.4	4.05	12	48.60	2.51
3	32.3	3.72	13	54.20	2.22
4	30.0	3.88	14	30.30	1.90
5	28.3	3.81	15	35.40	1.61
6	34.4	3.77	16	40.60	1.46
7	45.2	3.77	17	49.50	1.39
8	50.3	3.74	18	48.00	1.30
9	55.0	3.70	19	43.2	1.28
10	53.8	2.65	20	36.2	1.2
			21	20.2	1.19

T dig- Temperature of Digester, T amb- Ambient Temperature

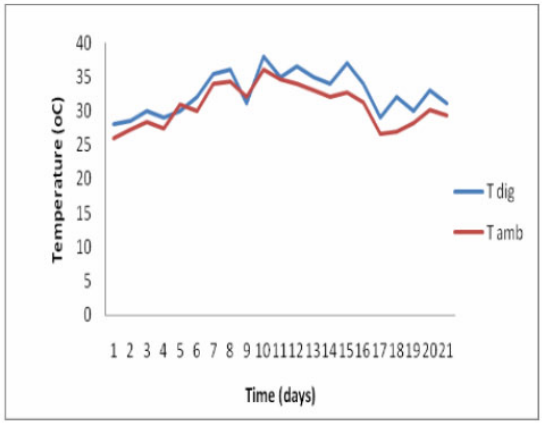

Fig. 2 Temperature Variations During Fermentation

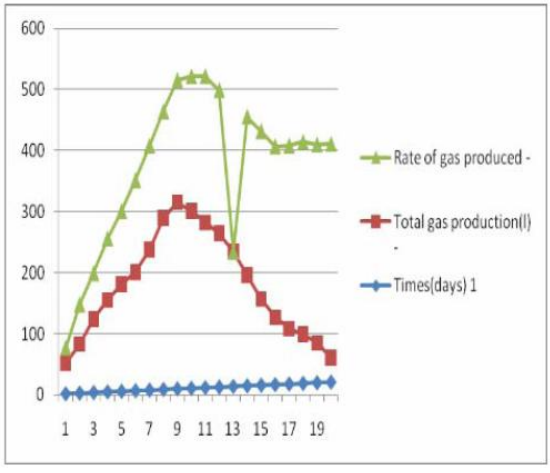

Fig.3 Gas Production during the study

Result of the pH of the digesting slurry shows an initial acidic medium which decreased linearly as the hydraulic retention time increased (Fig. 3). This was attributed to the activities of acidogenes that were initially concerned with the polymerization of organic substrates in the digester; hence, there was no biogas cassava contains cyanogenic glucosides which liberate cyanide under the influence of endogenous enzymes with the concentration of these glucosides in the peelings, test results for possible presence of hydrogen cyanide in the biogas from cassava peelings indicated that there was no cyanide in it. This result supports earlier claim by (Chittenden *et*. al.,1980) that hydrogen cyanide, if present, in biogas, was at a concentration of less than 1 ppm. The total solids of the fermenting medium diminished as hydraulic retention time increased. This is as a result of the conversion of the production in the initial stage of production. As the hydraulic retention time advanced, the acidogenes were displaced by the methanogenes, thereby increasing biogas production rate and yields. Decline in gas production was noted on the 11th day when the operational factors and conditions in the biogas digester changed against methanogenesis. Though polymers to monosaccharides and amino acids. These compounds were later converted to methane and ammonium compounds which turned the pH towards neutral that favoured methanogenesis (Eze, *et. al.*, 2008).

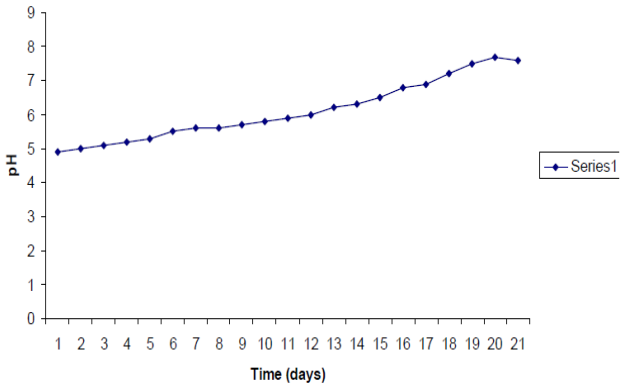

Fig. 4: Changes in pH During Fermentation

The chemical composition of the input materials loaded into the digester and the digested slurry out-put of the fermentation system as presented in Table 2 shows that organic matters are degraded during anaerobic fermentation to produce biogas, thereby making the percentage of Nitrogen in the slurry to rise compared with the solid content. The three fertilizer elements were therefore, conserved during anaerobic fermentation. This may crate an elusion of ―new" Nitrogen if only the Total Kledahl Nitrogen (TKN) is considered. Nitrogen can be lost only by reduction of nitrates to nitrogen gas and volatilization of ammonia into biogas.. Loss of nitrogen through volatilization of ammonia can occur from the slurry if not correctly handled. The volatile fatty acids which serve as primary sources of energy for the ruminants decrease during anaerobic digestion. This is because the process converts available energy into gas.

Table 2: Chemical composition of input materials and digested slurry

Parameters Determined	Input materials	Output materials
Total solid (%)	4.50+0.28	2.45+0.21
Volatile acids(acetic acid mg/l)	820+2.04	200+1.52
Nitrogen (%)	0.38+0.59	0.65+0.27
Phosphorus (%)	0.72+0.18	1.25+0.26
Potash (%)	0.55+0.13	0.97+0.28
Potassium (g/l)	4.94+0.23	5.80+0.28
Potassium (g/l)	4.94+0.23	5.80+0.28
Ammonia (g/l)	0.68+1.53	0.40+1.83
p.H	6.20+0.54	7.40+0.26

Table 3: Sensor Evaluation Result sheet for the Panels

Score	Odour	Sample A	Sample B
7	Extremely unobjectionable		
6	Moderately unobjectionable		
5	Slightly unobjectionable		
4	Neither objectionable or unobjectionable		
3	Slightly objectionable		
2	Moderately objectionable		
1	Extremely objectionable		

Sensory evaluation of the odour level of the gari processing site was carried out with sensory evaluation sheet as presented in Table 4. Results of the sensory panellists showed that 64 out of 81 residents within the gari processing site maintained that after anaerobic digestion of the gari processing wastes ,the prevailing odour level there was ―extremely unobjectionable" while 9 indicated that it was ―moderately unobjectionable" and the remaining 8 residents described the site as being ―slightly objectionable". Statisticaly, application of anaerobic fermentation in gari waste management has a significant impact in odour reduction ($P<0.05$) within the gari processing vicinity with a rich bio-fertilizer.

V. CONCLUSION

This research has demonstrated that anaerobic fermentation is an environmentally friendly technology that could be used to generate biogas. This biogas could be used as a reliable and an eco-friendly alternative energy to fuel wood needed for the various unit operations in gari processing industries in Nigeria. It was also noted that cyanide in cassava has no effect on biogas production from cassava wastes. Application of biogas technology as an alternative to fuel wood has the potential of addressing the pollution problems associated with the Nigerian gari processing industries. The associated slurry has been confirmed to conserve those fertilizer elements that have the potential to re-condition the soil and increase its fertility. The bio-fertilizer, i;e, the slurry, was observed to be relatively odourless; thereby enhancing the environmental sanitation of the gari processing vicinity. Besides, it is a home made technology.

VI. REFERENCES

1. AOAC (1990): Official Methods of Analysis of Assoc. of Analytical Chemistry, 14th edn, Arlinton, Virginia, 2209.
2. Chittenden, A.E, S.W. Head and B. breag (1990). Anaerobic digesters for small-acale vegetable processing Plants. Tropical Products Institute, London.
3. Eze, J.I, C.D Ogbonnia and E.O Uzodinma (2008). Application of Metallic digesters in Anaerobic digestion of Vegetable Wastes. Nigerian journal of Solar energy, Vol 19(2),20–4 .
4. Filmax (2009). The Biogas Digester Expert Pages. Http/www.rosneath.com.au/ipc6/copyr ight.html
5. Meynell,P.L (1982). Methane: Planning a digester. Prism Press.Stable Court, Chalmigton Dorsett.
6. Okafor I. T and L.m. Okafor (1986). Waste Water Engineering Management: Disposal and Re-Use MicGraw Hill book Co., New York.
7. Tewe,O.O (2008). Detoxification of Cassava Products and Effects of Residual Toxins on Consuming animals. FAO corporate document Repository, pp. 4 – 10.

Global Journals Guidelines Handbook 2010

www.GlobalJournals.org

FELLOW OF INTERNATIONAL CONGRESS OF ENGINEER (FICE)

- 'FICE' title will be awarded to the person/institution after approval of Editor-in-Chief and Editorial Board. The title 'FICE' can be added to name in the following manner
  e.g. **Dr. Andrew Knoll, Ph.D., FICE**
  Er. Pettar Jhone, M.E., FICE
- FICE can submit two papers every year for publication without any charges. The paper will be sent to two peer reviewers. The paper will be published after the acceptance of peer reviewers and Editorial Board.
- **Free unlimited Web-space** will be allotted to 'FICE 'along with subDomain to contribute and partake in our activities.
- A **professional email address** will be allotted free with unlimited email space.
- FICE will be authorized to receive e-Journals -GJRE for the Lifetime.
- FICE will be exempted from the registration fees of Seminar/Symposium/Conference/Workshop conducted internationally of GJRE (FREE of Charge).
- FICE will be Honorable Guest of any gathering held.

ASSOCIATE OF INTERNATIONAL CONGRESS OF ENGINEER (AICE)

- AICE title will be awarded to the person/institution after approval of Editor-in-Chef and Editorial Board. The title 'AICE' can be added to name in the following manner:
  eg. Dr. Thomas Herry, Ph.D., AICE
- AICE can submit one paper every year for publication without any charges. The paper will be sent to two peer reviewers. The paper will be published after the acceptance of peer reviewers and Editorial Board.
- Free twoGB Web-space will be allotted to 'FICE' along with subDomain to contribute and participate in our activities.
- A professional email address will be allotted with free 1GB email space.
- AICE will be authorized to receive e-Journal GJRE for lifetime.

ANNUAL MEMBER

- Annual Member will be authorized to receive e-Journal GJRE for one year (Journal Subscription for one year).
- The member will be allotted free 1 GB Web-space along with subDomain to contribute and participate in our activities.
- A professional email address will be allotted free 500 MB email space.

PAPER PUBLICATION

- The members can publish paper once. The paper will be sent to two-peer reviewer. The paper will be published after the acceptance of peer reviewers and Editorial Board.

The Area or field of specialization may or may not be of any category as mentioned in 'Scope of Journal' menu of the GlobalJournals.org website. There are 37 Research Journal categorized with six parental Journals GJCST, GJMR, GJRE, GJMBR, GJSFR, GJHSS. For Authors should prefer the mentioned categories. There are three widely used systems UDC, DDC and LCC. The details are available as 'Knowledge Abstract' at Home page. The major advantage of this coding is that, the research work will be exposed to and shared with all over the world as we are being abstracted and indexed worldwide.
The paper should be in proper format. The format can be downloaded from first page of 'Author Guideline' Menu. The Author is expected to follow the general rules as mentioned in this menu. The paper should be written in MS-Word Format (*.DOC,*.DOCX).
The Author can submit the paper either online or offline. The authors should prefer online submission.

Online Submission: There are three ways to submit your paper:

(A) (I) Register yourself using top right corner of Home page then Login from same place twice. If you are already registered, then login using your username and password.

(II) Choose corresponding Journal from "Research Journals" Menu.

(III) Click 'Submit Manuscript'. Fill required information and Upload the paper.

(B) If you are using Internet Explorer (Although Mozilla Firefox is preferred), then Direct Submission through Homepage is also available.

(C) If these two are not convenient, and then email the paper directly to dean@globaljournals.org as an attachment.

Offline Submission: Author can send the typed form of paper by Post. However, online submission should be preferred.

Preferred Author Guidelines

MANUSCRIPT STYLE INSTRUCTION (Must be strictly followed)

Page Size: 8.27" X 11'"

- Left Margin: 0.65
- Right Margin: 0.65
- Top Margin: 0.75
- Bottom Margin: 0.75
- Font type of all text should be Times New Roman.
- Paper Title should be of Font Size 24 with one Column section.
- Author Name in Font Size of 11 with one column as of Title.
- Abstract Font size of 9 Bold, "Abstract" word in Italic Bold.
- Main Text: Font size 10 with justified two columns section
- Two Column with Equal Column with of 3.38 and Gaping of .2
- First Character must be two lines Drop capped.
- Paragraph before Spacing of 1 pt and After of 0 pt.
- Line Spacing of 1 pt
- Large Images must be in One Column
- Numbering of First Main Headings (Heading 1) must be in Roman Letters, Capital Letter, and Font Size of 10.
- Numbering of Second Main Headings (Heading 2) must be in Alphabets, Italic, and Font Size of 10.

You can use your own standard format also.

Author Guidelines:

1. General,

2. Ethical Guidelines,

3. Submission of Manuscripts,

4. Manuscript's Category,

5. Structure and Format of Manuscript,

6. After Acceptance.

1. GENERAL

Before submitting your research paper, one is advised to go through the details as mentioned in following heads. It will be beneficial, while peer reviewer justify your paper for publication.

Scope

The Global Journals welcome the submission of original paper, review paper, survey article relevant to the all the streams of Philosophy and knowledge. The Global Journals is parental platform for Global Journal of Computer Science and Technology, Researches in Engineering, Medical Research, Science Frontier Research, Human Social Science, Management, and Business organization. The choice of

specific field can be done otherwise as following in Abstracting and Indexing Page on this Website. As the all Global Journals are being abstracted and indexed (in process) by most of the reputed organizations. Topics of only narrow interest will not be accepted unless they have wider potential or consequences.

2. ETHICAL GUIDELINES

Authors should follow the ethical guidelines as mentioned below for publication of research paper and research activities.

Papers are accepted on strict understanding that the material in whole or in part has not been, nor is being, considered for publication elsewhere. If the paper once accepted by Global Journals and Editorial Board, will become the *copyright of the Global Journals.*

Authorship: The authors and coauthors should have active contribution to conception design, analysis and interpretation of findings. They should critically review the contents and drafting of the paper. All should approve the final version of the paper before submission

The Global Journals follows the definition of authorship set up by the Global Academy of Research and Development. According to the Global Academy of R&D authorship, criteria must be based on:

1) Substantial contributions to conception and acquisition of data, analysis and interpretation of the findings.

2) Drafting the paper and revising it critically regarding important academic content.

3) Final approval of the version of the paper to be published.

All authors should have been credited according to their appropriate contribution in research activity and preparing paper. Contributors who do not match the criteria as authors may be mentioned under Acknowledgement.

Acknowledgements: Contributors to the research other than authors credited should be mentioned under acknowledgement. The specifications of the source of funding for the research if appropriate can be included. Suppliers of resources may be mentioned along with address.

Appeal of Decision: The Editorial Board's decision on publication of the paper is final and cannot be appealed elsewhere.

Permissions: It is the author's responsibility to have prior permission if all or parts of earlier published illustrations are used in this paper.

Please mention proper reference and appropriate acknowledgements wherever expected.

If all or parts of previously published illustrations are used, permission must be taken from the copyright holder concerned. It is the author's responsibility to take these in writing.

Approval for reproduction/modification of any information (including figures and tables) published elsewhere must be obtained by the authors/copyright holders before submission of the manuscript. Contributors (Authors) are responsible for any copyright fee involved.

3. SUBMISSION OF MANUSCRIPTS

Manuscripts should be uploaded via this online submission page. The online submission is most efficient method for submission of papers, as it enables rapid distribution of manuscripts and consequently speeds up the review procedure. It also enables authors to know the status of their own manuscripts by emailing us. Complete instructions for submitting a paper is available below.

Manuscript submission is a systematic procedure and little preparation is required beyond having all parts of your manuscript in a given format and a computer with an Internet connection and a Web browser. Full help and instructions are provided on-screen. As an author, you will be prompted for login and manuscript details as Field of Paper and then to upload your manuscript file(s) according to the instructions.

To avoid postal delays, all transaction is preferred by e-mail. A finished manuscript submission is confirmed by e-mail immediately and your paper enters the editorial process with no postal delays. When a conclusion is made about the publication of your paper by our Editorial Board, revisions can be submitted online with the same procedure, with an occasion to view and respond to all comments.

Complete support for both authors and co-author is provided.

4. MANUSCRIPT'S CATEGORY

Based on potential and nature, the manuscript can be categorized under the following heads: Original research paper: Such papers are reports of high-level significant original research work.

Review papers: These are concise, significant but helpful and decisive topics for young researchers.

Research articles: These are handled with small investigation and applications

Research letters: The letters are small and concise comments on previously published matters.

5. STRUCTURE AND FORMAT OF MANUSCRIPT

The recommended size of original research paper is less than seven thousand words, review papers fewer than seven thousands words also. Preparation of research paper or how to write research paper, are major hurdle, while writing manuscript. The research articles and research letters should be fewer than three thousand words, the structure original research paper; sometime review paper should be as follows:

Papers*:* These are reports of significant research (typically less than 7000 words equivalent, including tables, figures, references), and comprise:

(a)*Title* should be relevant and commensurate with the theme of the paper.

(b) A brief Summary, *"Abstract"* (less than 150 words) containing the major results and conclusions.

(c) Up to *ten keywords*, that precisely identifies the paper's subject, purpose, and focus.

(d) An *Introduction*, giving necessary background excluding subheadings; objectives must be clearly declared.

(e) Resources and techniques with sufficient complete experimental details (wherever possible by reference) to permit repetition; sources of information must be given and numerical methods must be specified by reference, unless non-standard.

(f) Results should be presented concisely, by well-designed tables and/or figures; the same data may not be used in both; suitable statistical data should be given. All data must be obtained with attention to numerical detail in the planning stage. As reproduced design has been recognized to be important to experiments for a considerable time, the Editor has decided that any paper that appears not to have adequate numerical treatments of the data will be returned un-refereed;

(g) Discussion should cover the implications and consequences, not just recapitulating the results; *conclusions* should be summarizing.

(h) Brief Acknowledgements.

(i) References in the proper form.

Authors should very cautiously consider the preparation of papers to ensure that they communicate efficiently. Papers are much more likely to be accepted, if they are cautiously designed and laid out, contain few or no errors, are summarizing, and be conventional to the approach and instructions. They will in addition, be published with much less delays than those that require much technical and editorial correction.

The Editorial Board reserves the right to make literary corrections and to make suggestions to improve briefness.

It is vital, that authors take care in submitting a manuscript that is written in simple language and adheres to published guidelines.

Format

Language: The language of publication is UK English. Authors, for whom English is a second language, must have their manuscript efficiently edited by an English-speaking person before submission to make sure that, the English is of high excellence. It is preferable, that manuscripts should be professionally edited.

Standard Usage, Abbreviations, and Units: Spelling and hyphenation should be conventional to The Concise Oxford English Dictionary. Statistics and measurements should at all times be given in figures, e.g. 16 min, except for when the number begins a sentence. When the number does not refer to a unit of measurement it should be spelt in full unless, it is 160 or greater.

Abbreviations supposed to be used carefully. The abbreviated name or expression is supposed to be cited in full at first usage, followed by the conventional abbreviation in parentheses.

Metric SI units are supposed to generally be used excluding where they conflict with current practice or are confusing. For illustration, 1.4 l rather than 1.4 × 10-3 m3, or 4 mm somewhat than 4 × 10-3 m. Chemical formula and solutions must identify the form used, e.g. anhydrous or hydrated, and the concentration must be in clearly defined units. Common species names should be followed by underlines at the first mention. For following use the generic name should be constricted to a single letter, if it is clear.

Structure

All manuscripts submitted to Global Journals, ought to include:

Title: The title page must carry an instructive title that reflects the content, a running title (less than 45 characters together with spaces), names of the authors and co-authors, and the place(s) wherever the work was carried out. The full postal address in addition with the e-mail address of related author must be given. Up to eleven keywords or very brief phrases have to be given to help data retrieval, mining and indexing.

Abstract, used in Original Papers and Reviews:

Optimizing Abstract for Search Engines

Many researchers searching for information online will use search engines such as Google, Yahoo or similar. By optimizing your paper for search engines, you will amplify the chance of someone finding it. This in turn will make it more likely to be viewed and/or cited in a further work. Global Journals have compiled these guidelines to facilitate you to maximize the web-friendliness of the most public part of your paper.

Key Words

A major linchpin in research work for the writing research paper is the keyword search, which one will employ to find both library and Internet resources.

One must be persistent and creative in using keywords. An effective keyword search requires a strategy and planning a list of possible keywords and phrases to try.

Search engines for most searches, use Boolean searching, which is somewhat different from Internet searches. The Boolean search uses "operators," words (and, or, not, and near) that enable you to expand or narrow your affords. Tips for research paper while preparing research paper are very helpful guideline of research paper.

Choice of key words is first tool of tips to write research paper. Research paper writing is an art.A few tips for deciding as strategically as possible about keyword search:

- One should start brainstorming lists of possible keywords before even begin searching. Think about the most important concepts related to research work. Ask, "What words would a source have to include to be truly valuable in research paper?" Then consider synonyms for the important words.
- It may take the discovery of only one relevant paper to let steer in the right keyword direction because in most databases, the keywords under which a research paper is abstracted are listed with the paper.
- One should avoid outdated words.

Keywords are the key that opens a door to research work sources. Keyword searching is an art in which researcher's skills are bound to improve with experience and time.

Numerical Methods: Numerical methods used should be clear and, where appropriate, supported by references.

Acknowledgements: Please make these as concise as possible.

References

References follow the *Harvard scheme* of referencing. References in the text should cite the authors' names followed by the time of their publication, unless there are three or more authors when simply the first author's name is quoted followed by et al. unpublished work has to only be cited where necessary, and only in the text. Copies of references in press in other journals have to be supplied with submitted typescripts. It is necessary that all citations and references be carefully checked before submission, as mistakes or omissions will cause delays.

References to information on the World Wide Web can be given, but only if the information is available without charge to readers on an official site. Wikipedia and Similar websites are not allowed where anyone can change the information. Authors will be asked to make available electronic copies of the cited information for inclusion on the Global Journals homepage at the judgment of the Editorial Board.

The Editorial Board and Global Journals recommend that, citation of online-published papers and other material should be done via a DOI (digital object identifier). If an author cites anything, which does not have a DOI, they run the risk of the cited material not being noticeable.

The Editorial Board and Global Journals recommend the use of a tool such as Reference Manager for reference management and formatting.

Tables, Figures and Figure Legends

Tables: Tables should be few in number, cautiously designed, uncrowned, and include only essential data. Each must have an Arabic number, e.g. Table 4, a self-explanatory caption and be on a separate sheet. Vertical lines should not be used.

Figures: Figures are supposed to be submitted as separate files. Always take in a citation in the text for each figure using Arabic numbers, e.g. Fig. 4. Artwork must be submitted online in electronic form by e-mailing them.

Preparation of Electronic Figures for Publication

Even though low quality images are sufficient for review purposes, print publication requires high quality images to prevent the final product being blurred or fuzzy. Submit (or e-mail) EPS (line art) or TIFF (halftone/photographs) files only. MS PowerPoint and Word Graphics are unsuitable for printed pictures. Do not use pixel-oriented software. Scans (TIFF only) should have a resolution of at least 350 dpi (halftone) or 700 to 1100 dpi (line drawings) in relation to the imitation size. Please give the data for figures in black and white or submit a Color Work Agreement Form. EPS files must be saved with fonts embedded (and with a TIFF preview, if possible).

For scanned images, the scanning resolution (at final image size) ought to be as follows to ensure good reproduction: line art: >650 dpi; halftones (including gel photographs) : >350 dpi; figures containing both halftone and line images: >650 dpi.

Color Charges: It is the rule of the Global Journals for authors to pay the full cost for the reproduction of their color artwork. Hence, please note that, if there is color artwork in your manuscript when it is accepted for publication, we would require you to complete and return a color work agreement form before your paper can be published.

Figure Legends: Self-explanatory legends of all figures should be incorporated separately under the heading 'Legends to Figures'. In the full-text online edition of the journal, figure legends may possibly be truncated in abbreviated links to the full screen version. Therefore, the first 100 characters of any legend should notify the reader, about the key aspects of the figure.

6. AFTER ACCEPTANCE

Upon approval of a paper for publication, the manuscript will be forwarded to the dean, who is responsible for the publication of the Global Journals.

6.1 Proof Corrections

The corresponding author will receive an e-mail alert containing a link to a website or will be attached. A working e-mail address must therefore be provided for the related author.

Acrobat Reader will be required in order to read this file. This software can be downloaded

(Free of charge) from the following website:

www.adobe.com/products/acrobat/readstep2.html. This will facilitate the file to be opened, read on screen, and printed out in order for any corrections to be added. Further instructions will be sent with the proof.

Proofs must be returned to the dean at dean@globaljournals.org within three days of receipt.

As changes to proofs are costly, we inquire that you only correct typesetting errors. All illustrations are retained by the publisher. Please note that the authors are responsible for all statements made in their work, including changes made by the copy editor.

6.2 Early View of Global Journals (Publication Prior to Print)

The Global Journals are enclosed by our publishing's Early View service. Early View articles are complete full-text articles sent in advance of their publication. Early View articles are absolute and final. They have been completely reviewed, revised and edited for publication, and the authors' final corrections have been incorporated. Because they are in final form, no changes can be made after sending them. The nature of Early View articles means that they do not yet have volume, issue or page numbers, so Early View articles cannot be cited in the conventional way.

6.3 Author Services

Online production tracking is available for your article through Author Services. Author Services enables authors to track their article - once it has been accepted - through the production process to publication online and in print. Authors can check the status of their articles online and choose to receive automated e-mails at key stages of production. The authors will receive an e-mail with a unique link that enables them to register and have their article automatically added to the system. Please ensure that a complete e-mail address is provided when submitting the manuscript.

6.4 Author Material Archive Policy

Please note that if not specifically requested, publisher will dispose off hardcopy & electronic information submitted, after the two months of publication. If you require the return of any information submitted, please inform the Editorial Board or dean as soon as possible.

6.5 Offprint and Extra Copies

A PDF offprint of the online-published article will be provided free of charge to the related author, and may be distributed according to the Publisher's terms and conditions. Additional paper offprint may be ordered by emailing us at: editor@globaljournals.org .

Informal Tips for writing a Engineering Research Paper to increase readability and citation

Before start writing a good quality Engineering Research Paper, let us first understand what is Engineering Research Paper? So Engineering Research Paper is the paper which is written by professionals, engineers or scientists who are associated to the field of engineering from all over the world. If you are novel to this field then you can consult about this field from your supervisor or guide.

Techniques for writing a good quality Engineering Research Paper:

1. Choosing the topic- In most cases, the topic is searched by the interest of author but it can be also suggested by the guides. You can have several topics and then you can judge that in which topic or subject you are finding yourself most comfortable. This can be done by asking several questions to yourself, like Will I be able to carry our search in this area? Will I find all necessary recourses to accomplish the search? Will I be able to find all information in this field area? If the answer of these types of questions will be "Yes" then you can choose that topic. In most of the cases, you may have to conduct the surveys and have to visit several places because this field is related to the field of Engineering. Also, you may have to do a lot of work to find all rise and falls regarding the various data of that subject. Sometimes, detailed information plays a vital role, instead of short information.

2. Evaluators are human: First thing to remember that evaluators are also human being. They are not only meant for rejecting a paper. They are here to evaluate your paper. So, present your Best.

3. Think Like Evaluators: If you are in a confusion or getting demotivated that your paper will be accepted by evaluators or not, then think and try to evaluate your paper like an Evaluator. Try to understand that what an evaluator wants in your research paper and automatically you will have your answer.

4. Make blueprints of paper: The outline is the plan or framework that will help you to arrange your thoughts. It will make your paper logical. But remember that all points of your outline must be related to the topic you have chosen.

5. Ask your Guides: If you are having any difficulty in your research, then do not hesitate to share your difficulty to your guide (if you have any). They will surely help you out and resolve your doubts. If you can't clarify what exactly you require for your work then ask the supervisor to help you with the alternative. He might also provide you the list of essential readings.

6. Use of computer is recommended: At a first glance, this point looks obvious but it is first recommendation that to write a quality research paper of any area, first draft your paper in Microsoft Word. By using MS Word, you can easily catch your grammatical mistakes and spelling errors.

7. Use right software: Always use good quality software packages. If you are not capable to judge good software then you can lose quality of your paper unknowingly. There are various software programs available to help you, which you can get through Internet.

8. Use the Internet for help: An excellent start for your paper can be by using the Google. It is an excellent search engine, where you can have your doubts resolved. You may also read some answers for the frequent question how to write my research paper or find model research paper. From the internet library you can download books. If you have all required books make important reading selecting and analyzing the specified information. Then put together research paper sketch out.

9. Use and get big pictures: Always use encyclopedias, Wikipedia to get pictures so that you can go into the depth.

10. Bookmarks are useful: When you read any book or magazine, you generally use bookmarks, right! It is a good habit, which helps to not to lose your continuity. You should always use bookmarks while searching on Internet also, which will make your search easier.

11. Revise what you wrote: When you write anything, always read it, summarize it and then finalize it.

12. Make all efforts: Make all efforts to mention what you are going to write in your paper. That means always have a good start. Try to mention everything in introduction, that what is the need of a particular research paper. Polish your work by good skill of writing and

always give an evaluator, what he wants.

13. Have backups: When you are going to do any important thing like making research paper, you should always have backup copies of it either in your computer or in paper. This will help you to not to lose any of your important.

14. Produce good diagrams of your own: Always try to include good charts or diagrams in your paper to improve quality. Using several and unnecessary diagrams will degrade the quality of your paper by creating "hotchpotch." So always, try to make and include those diagrams, which are made by your own to improve readability and understandability of your paper.

15. Use of direct quotes: When you do research relevant to literature, history or current affairs then use of quotes become essential but if study is relevant to science then use of quotes is not preferable.

16. Use proper verb tense: Use proper verb tenses in your paper. Use past tense, to present those events that happened. Use present tense to indicate events that are going on. Use future tense to indicate future happening events. Use of improper and wrong tenses will confuse the evaluator. Avoid the sentences that are incomplete.

17. Never use online paper: If you are getting any paper on Internet, then never use it as your research paper because it might be possible that evaluator has already seen it or maybe it is outdated version.

18. **Pick a good study spot:** To do your research studies always try to pick a spot, which is quiet. Every spot is not for studies. Spot that suits you choose it and proceed further.

19. Know what you know: Always try to know, what you know by making objectives. Else, you will be confused and cannot achieve your target.

20. Use good quality grammar: Always use a good quality grammar and use words that will throw positive impact on evaluator. Use of good quality grammar does not mean to use tough words, that for each word the evaluator has to go through dictionary. Do not start sentence with a conjunction. Do not fragment sentences. Eliminate one-word sentences. Ignore passive voice. Do not ever use a big word when a diminutive one would suffice. Verbs have to be in agreement with their subjects. Prepositions are not expressions to finish sentences with. It is incorrect to ever divide an infinitive. Avoid clichés like the disease. Also, always shun irritating alliteration. Use language that is simple and straight forward. put together a neat summary.

21. Arrangement of information: Each section of the main body should start with an opening sentence and there should be a changeover at the end of the section. Give only valid and powerful arguments to your topic. You may also maintain your arguments with records.

22. Never start in last minute: Always start at right time and give enough time to research work. Leaving everything to the last minute will degrade your paper and spoil your work.

23. Multitasking in research is not good: Doing several things at the same time proves bad habit in case of research activity. Research is an area, where everything has a particular time slot. Divide your research work in parts and do particular part in particular time slot.

24. Never copy others' work: Never copy others' work and give it your name because if evaluator has seen it anywhere you will be in trouble.

25. Take proper rest and food: No matter how many hours you spend for your research activity, if you are not taking care of your health then all your efforts will be in vain. For a quality research, study is must, and this can be done by taking proper rest and food.

26. Go for seminars: Attend seminars if the topic is relevant to your research area. Utilize all your resources.

27. Refresh your mind after intervals: Try to give rest to your mind by listening to soft music or by sleeping in intervals. This will also improve your memory.

28. Make colleagues: Always try to make colleagues. No matter how sharper or intelligent you are, if you make colleagues you can have several ideas, which will be helpful for your research.

29. **Think technically:** Always think technically. If anything happens, then search its reasons, its benefits, and demerits.

30. Think and then print: When you will go to print your paper, notice that tables are not be split, headings are not detached from their descriptions, and page sequence is maintained.

31. Adding unnecessary information: Do not add unnecessary information, like, I have used MS Excel to draw graph. Do not add irrelevant and inappropriate material. These all will create superfluous. Foreign terminology and phrases are not apropos. One should NEVER take a broad view. Analogy in script is like feathers on a snake. Not at all use a large word when a very small one would be sufficient. Use words properly, regardless of how others use them. Remove quotations. Puns are for kids, not grunt readers. Amplification is a billion times of inferior quality than sarcasm.

32. Never oversimplify everything: To add material in your research paper, never go for oversimplification. This will definitely irritate the evaluator. Be more or less specific. Also too, by no means, ever use rhythmic redundancies. Contractions aren't essential and shouldn't be there used. Comparisons are as terrible as clichés. Give up ampersands and abbreviations, and so on. Remove commas, that are, not necessary. Parenthetical words however should be together with this in commas. Understatement is all the time the complete best way to put onward earth-shaking thoughts. Give a detailed literary review.

33. Report concluded results: Use concluded results. From raw data, filter the results and then conclude your studies based on measurements and observations taken. Significant figures and appropriate number of decimal places should be used. Parenthetical remarks are prohibitive. Proofread carefully at final stage. In the end give outline to your arguments. Spot out perspectives of further study of this subject. Justify your conclusion by at the bottom of them with sufficient justifications and examples.

34. After conclusion: Once you have concluded your research, the next most important step is to present your findings. Presentation is extremely important as it is the definite medium though which your research is going to be in print to the rest of the crowd. Care should be taken to categorize your thoughts well and present them in a logical and neat manner. A good quality research paper format is essential because it serves to highlight your research paper and bring to light all necessary aspects in your research.

Informal Guidelines of Research Paper Writing

Key points to remember:

- Submit all work in its final form.
- Write your paper in the form, which is presented in the guidelines using the template.
- Please note the criterion for grading the final paper by peer-reviewers.

Final Points:

A purpose of organizing a research paper is to let people to interpret your effort selectively. The journal requires the following sections, submitted in the order listed, each section to start on a new page.

The introduction will be compiled from reference matter and will reflect the design processes or outline of basis that direct you to make study. As you will carry out the process of study, the method and process section will be constructed as like that. The result segment will show related statistics in nearly sequential order and will direct the reviewers next to the similar intellectual paths throughout the data that you took to carry out your study. The discussion section will provide understanding of the data and projections as to the implication of the results. The use of good quality references all through the paper will give the effort trustworthiness by representing an alertness

of prior workings.

Writing a research paper is not an easy job no matter how trouble-free the actual research or concept. Practice, excellent preparation, and controlled record keeping are the only means to make straightforward the progression.

General style:

Specific editorial column necessities for compliance of a manuscript will always take over from directions in these general guidelines.

To make a paper clear

· Adhere to recommended page limits

Mistakes to evade

- Insertion a title at the foot of a page with the subsequent text on the next page
- Separating a table/chart or figure - impound each figure/table to a single page
- Submitting a manuscript with pages out of sequence

In every sections of your document

· Use standard writing style including articles ("a", "the," etc.)

· Keep on paying attention on the research topic of the paper

· Use paragraphs to split each significant point (excluding for the abstract)

· Align the primary line of each section

· Present your points in sound order

· Use present tense to report well accepted

· Use past tense to describe specific results

· Shun familiar wording, don't address the reviewer directly, and don't use slang, slang language, or superlatives

· Shun use of extra pictures - include only those figures essential to presenting results

Title Page:

Choose a revealing title. It should be short. It should not have non-standard acronyms or abbreviations. It should not exceed two printed lines. It should include the name(s) and address (es) of all authors.

Abstract:

The summary should be two hundred words or less. It should briefly and clearly explain the key findings reported in the manuscript--must have precise statistics. It should not have abnormal acronyms or abbreviations. It should be logical in itself. Shun citing references at this point.

An abstract is a brief distinct paragraph summary of finished work or work in development. In a minute or less a reviewer can be taught the foundation behind the study, common approach to the problem, relevant results, and significant conclusions or new questions.

Write your summary when your paper is completed because how can you write the summary of anything which is not yet written? Wealth of terminology is very essential in abstract. Yet, use comprehensive sentences and do not let go readability for briefness. You can maintain it succinct by phrasing sentences so that they provide more than lone rationale. The author can at this moment go straight to shortening the outcome. Sum up the study, with the subsequent elements in any summary. Try to maintain the initial two items to no more than one ruling each.

- Reason of the study - theory, overall issue, purpose
- Fundamental goal
- To the point depiction of the research
- Consequences, including definite statistics - if the consequences are quantitative in nature, account quantitative data; results of any numerical analysis should be reported
- Significant conclusions or questions that track from the research(es)

Approach:

- Single section, and succinct
- As a outline of job done, it is always written in past tense
- A conceptual should situate on its own, and not submit to any other part of the paper such as a form or table
- Center on shortening results - bound background information to a verdict or two, if completely necessary
- What you account in an conceptual must be regular with what you reported in the manuscript
- Exact spelling, clearness of sentences and phrases, and appropriate reporting of quantities (proper units, important statistics) are just as significant in an abstract as they are anywhere else

Introduction:

The **Introduction** should "introduce" the manuscript. The reviewer should be presented with sufficient background information to be capable to comprehend and calculate the purpose of your study without having to submit to other works. The basis for the study should be offered. Give most important references but shun difficult to make a comprehensive appraisal of the topic. In the introduction, describe the problem visibly. If the problem is not acknowledged in a logical, reasonable way, the reviewer will have no attention in your result. Speak in common terms about techniques used to explain the problem, if needed, but do not present any particulars about the protocols here. Following approach can create a valuable beginning:

- Explain the value (significance) of the study
- Shield the model - why did you employ this particular system or method? What is its compensation? You strength remark on its appropriateness from a abstract point of vision as well as point out sensible reasons for using it.
- Present a justification. Status your particular theory (es) or aim(s), and describe the logic that led you to choose them.
- Very for a short time explain the tentative propose and how it skilled the declared objectives.

Approach:

- Use past tense except for when referring to recognized facts. After all, the manuscript will be submitted after the entire job is done.
- Sort out your thoughts; manufacture one key point with every section. If you make the four points listed above, you will need a least of four paragraphs.
- Present surroundings information only as desirable in order hold up a situation. The reviewer does not desire to read the whole thing you know about a topic.

- Shape the theory/purpose specifically - do not take a broad view.
- As always, give awareness to spelling, simplicity and correctness of sentences and phrases.

Procedures (Methods and Materials):

This part is supposed to be the easiest to carve if you have good skills. A sound written Procedures segment allows a capable scientist to replacement your results. Present precise information about your supplies. The suppliers and clarity of reagents can be helpful bits of information. Present methods in sequential order but linked methodologies can be grouped as a segment. Be concise when relating the protocols. Attempt for the least amount of information that would permit another capable scientist to spare your outcome but be cautious that vital information is integrated. The use of subheadings is suggested and ought to be synchronized with the results section. When a technique is used that has been well described in another object, mention the specific item describing a way but draw the basic principle while stating the situation. The purpose is to text all particular resources and broad procedures, so that another person may use some or all of the methods in one more study or referee the scientific value of your work. It is not to be a step by step report of the whole thing you did, nor is a methods section a set of orders.

Materials:

- Explain materials individually only if the study is so complex that it saves liberty this way.
- Embrace particular materials, and any tools or provisions that are not frequently found in laboratories.
- Do not take in frequently found.
- If use of a definite type of tools.
- Materials may be reported in a part section or else they may be recognized along with your measures.

Methods:

- Report the method (not particulars of each process that engaged the same methodology)
- Describe the method entirely
- To be succinct, present methods under headings dedicated to specific dealings or groups of measures
- Simplify - details how procedures were completed not how they were exclusively performed on a particular day.
- If well known procedures were used, account the procedure by name, possibly with reference, and that's all.

Approach:

- It is embarrassed or not possible to use vigorous voice when documenting methods with no using first person, which would focus the reviewer's interest on the researcher rather than the job. As a result when script up the methods most authors use third person passive voice.
- Use standard style in this and in every other part of the paper - avoid familiar lists, and use full sentences.

What to keep away from

- Resources and methods are not a set of information.
- Skip all descriptive information and surroundings - save it for the argument.
- Leave out information that is immaterial to a third party.

Results:

The principle of a results segment is to present and demonstrate your conclusion. Create this part a entirely objective details of the outcome, and save all understanding for the discussion.

The page length of this segment is set by the sum and types of data to be reported. Carry on to be to the point, by means of statistics and tables, if suitable, to present consequences most efficiently.

You must obviously differentiate material that would usually be incorporated in a study editorial from any unprocessed data or additional appendix matter that would not be available. In fact, such matter should not be submitted at all except requested by the instructor.

Content

- Sum up your conclusion in text and demonstrate them, if suitable, with figures and tables.
- In manuscript, explain each of your consequences, point the reader to remarks that are most appropriate.
- Present a background, such as by describing the question that was addressed by creation an exacting study.
- Explain results of control experiments and comprise remarks that are not accessible in a prescribed figure or table, if appropriate.
- Examine your data, then prepare the analyzed (transformed) data in the form of a figure (graph), table, or in manuscript form.

What to stay away from

- Do not discuss or infer your outcome, report surroundings information, or try to explain anything.
- Not at all take in raw data or intermediate calculations in a research manuscript.
- Do not present the similar data more than once.
- Manuscript should complement any figures or tables, not duplicate the identical information.
- Never confuse figures with tables - there is a difference.

Approach

- As forever, use past tense when you submit to your results, and put the whole thing in a reasonable order.
- Put figures and tables, appropriately numbered, in order at the end of the report
- If you desire, you may place your figures and tables properly within the text of your results part.

Figures and tables

- If you put figures and tables at the end of the details, make certain that they are visibly distinguished from any attach appendix materials, such as raw facts
- Despite of position, each figure must be numbered one after the other and complete with subtitle
- In spite of position, each table must be titled, numbered one after the other and complete with heading
- All figure and table must be adequately complete that it could situate on its own, divide from text

Discussion:

The Discussion is expected the trickiest segment to write and describe. A lot of papers submitted for journal are discarded based on problems with the Discussion. There is no head of state for how long a argument should be. Position your understanding of the outcome visibly to lead the reviewer through your conclusions, and then finish the paper with a summing up of the implication of the study. The purpose here is to offer an understanding of your results and hold up for all of your conclusions, using facts from your research and generally accepted information, if suitable. The implication of result should be visibly described.
Infer your data in the conversation in suitable depth. This means that when you clarify an observable fact you must explain mechanisms that may account for the observation. If your results vary from your prospect, make clear why that may have happened. If your results agree, then explain the theory that the proof supported. It is never suitable to just state that the data approved with prospect, and let it drop at that.

- Make a decision if each premise is supported, discarded, or if you cannot make a conclusion with assurance. Do not just dismiss a study or part of a study as "uncertain."
- Research papers are not acknowledged if the work is imperfect. Draw what conclusions you can based upon the results that you have, and take care of the study as a finished work
- You may propose future guidelines, such as how the experiment might be personalized to accomplish a new idea.
- Give details all of your remarks as much as possible, focus on mechanisms.
- Make a decision if the tentative design sufficiently addressed the theory, and whether or not it was correctly restricted.
- Try to present substitute explanations if sensible alternatives be present.
- One research will not counter an overall question, so maintain the large picture in mind, where do you go next? The best studies unlock new avenues of study. What questions remain?
- Recommendations for detailed papers will offer supplementary suggestions.

Approach:

- When you refer to information, differentiate data generated by your own studies from available information
- Submit to work done by specific persons (including you) in past tense.
- Submit to generally acknowledged facts and main beliefs in present tense.

Administration Rules Listed Before Submitting Your Research Paper to Global Journals

Please carefully note down following rules and regulation before submitting your Research Paper to Global Journals:

Segment Draft and Final Research Paper: You have to strictly follow the template of research paper. If it is not done your paper may get rejected.

- The **major constraint** is that you must independently make all content, tables, graphs, and facts that are offered in the paper. You must write each part of the paper wholly on your own. The Peer-reviewers need to identify your own perceptive of the concepts in your own terms. NEVER extract straight from any foundation, and never rephrase someone else's analysis.
- Do not give permission to anyone else to "PROOFREAD" your manuscript.

Written Material: You may discuss with your guides and key sources.

- Do not copy or imitate anyone else paper. (Various Methods to avoid Plagiarism is applied by us on every paper, if found guilty, you will be blacklisted by all of our collaborated research groups, your institution will be informed for this and strict legal actions will be taken immediately.)
- To guard yourself and others from possible illegal use please do not permit anyone right to use to your paper and files.

Criterion for Grading a Research Paper *(Compilation)* by Global Journals

Please note that following table is only a Grading of "Paper Compilation" and not on "Performed/Stated Research" whose grading solely depends on Individual Assigned Peer Reviewer and Editorial Board Member. These can be available only on request and after decision of Paper. This report will be the property of Global Journals.

Topics	Grades		
	A-B	**C-D**	**E-F**
Abstract	Clear and concise with appropriate content, Correct format. 200 words or below	Unclear summary and no specific data, Incorrect form Above 200 words	No specific data with ambiguous information Above 250 words
Introduction	Containing all background details with clear goal and appropriate details, flow specification, no grammar and spelling mistake, well organized sentence and paragraph, reference cited	Unclear and confusing data, appropriate format, grammar and spelling errors with unorganized matter	Out of place depth and content, hazy format
Methods and Procedures	Clear and to the point with well arranged paragraph, precision and accuracy of facts and figures, well organized subheads	Difficult to comprehend with embarrassed text, too much explanation but completed	Incorrect and unorganized structure with hazy meaning
Result	Well organized, Clear and specific, Correct units with precision, correct data, well structuring of paragraph, no grammar and spelling mistake	Complete and embarrassed text, difficult to comprehend	Irregular format with wrong facts and figures
Discussion	Well organized, meaningful specification, sound conclusion, logical and concise explanation, highly structured paragraph reference cited	Wordy, unclear conclusion, spurious	Conclusion is not cited, unorganized, difficult to comprehend
References	Complete and correct format, well organized	Beside the point, Incomplete	Wrong format and structuring

Index

E

F

G

H

I

K

L

M

N

O

P

Q

R

S

T

U

V

W

Z

Global Journal of Researches in Engineering

Visit us on the Web at www.GlobalJournals.org | www.ComputerResearch.org
or email us at helpdesk@globaljournals.org

ISSN 9755861